ROCKETDYNE • A DIVISION OF NORTH AMERICAN AVIATION, INC.

NASA-CR-72176
Rocketdyne-R-6838-1

FINAL REPORT

EVALUATION AND DEMONSTRATION OF THE USE OF CRYOGENIC PROPELLANTS (O_2-H_2) FOR REACTION CONTROL SYSTEMS

VOLUME I

CONCEPTUAL DESIGN AND ANALYTICAL EVALUATION

by

G. Falkenstein, D. Grubman, A. Liebman
and N. Rodewald

Prepared for

NATIONAL AERONAUTICS AND SPACE ADMINISTRATION

June 1967

Contract NAS3-7941

ROCKETDYNE
A Division of North American Aviation, Inc.
6633 Canoga Avenue, Canoga Park, California

NASA-CR-72176
Rocketdyne-R-6838-1

FINAL REPORT

EVALUATION AND DEMONSTRATION OF THE USE OF CRYOGENIC PROPELLANTS (O_2-H_2) FOR REACTION CONTROL SYSTEMS
VOLUME I
CONCEPTUAL DESIGN AND ANALYTICAL EVALUATION

by

G. Falkenstein, D. Grubman, A. Liebman
and N. Rodewald

prepared for

NATIONAL AERONAUTICS AND SPACE ADMINISTRATION

Contract NAS3-7941

Technical Management
NASA Lewis Research Center
Cleveland, Ohio
Advanced Rocket Technology Branch
Paul Herr

ROCKETDYNE
A Division of North American Aviation, Inc.
6633 Canoga Avenue, Canoga Park, California

ROCKETDYNE • A DIVISION OF NORTH AMERICAN AVIATION, INC.

EVALUATION AND DEMONSTRATION OF THE USE OF CRYOGENIC PROPELLANTS (O_2-H_2) FOR REACTION CONTROL SYSTEMS

Technically Reviewed and Approved by:

G. L. Falkenstein
Principal Scientist
Propulsion Processes

T. A. Coultas
Manager
Propulsion Physics, Processes and Applications

Release Approval

R. B. Lawhead
Manager
Physical and Engineering Sciences

ROCKETDYNE
A Division of North American Aviation, Inc.
6633 Canoga Avenue, Canoga Park, California

Contract NAS 3-7941
National Aeronautics and Space Administration
Lewis Research Center
Cleveland, Ohio

FOREWORD

This report was prepared for the NASA Lewis Research Center, Cleveland, Ohio, by Rocketdyne, A Division of North American Aviation, Inc., Canoga Park, California. The effort described herein was conducted under Contract NAS3-7941.

ACKNOWLEDGEMENTS

The accomplishments described in this report were conducted by the Research and Small Engines Divisions of Rocketdyne under the program management of R. B. Lawhead and E. V. Zettle of the Research Division. Mr. P. Herr was the NASA Project Manager; his technical efforts in support of this initial study are especially acknowledged. The authors also wish to acknowledge the efforts and support of R. Rollins of the NASA Office of Advanced Research and Technology.

The technical effort and preparation of this report was augmented by the enthusiastic participation of the following personnel.

H. Burge
C. Cunningham
D. Dermody
D. Dougherty
T. Mills
E. Prono
T. Sloat

ABSTRACT

The results and evaluations of an investigation of the feasibility of a cryogenic (O_2-H_2) reaction control system are presented. This volume presents the analytical, conceptual design, and system analysis results from the program. Possible applications of such a reaction control system include propellant settling engines, attitude control, and secondary propulsion for upper stages, spacecraft, and orbital tankers. Two types of systems representative of a system integrated with the tankage for a pump-fed main propulsion system (chamber pressure of 10 psia) and a system fed from separate tankage (chamber pressure of 100 psia) were investigated. Theoretical combustion performance and temperature characteristics were evaluated. The thrustors for such a system and a temperature and pressure conditioning subsystem were examined from a component standpoint. Conceptual designs were prepared and evaluated, and past work was reviewed from a design analysis standpoint. Candidate system design concepts were evaluated from the standpoints of weight, volume, reliability, technical state-of-the-art, etc., and one concept selected for further investigation. The selected system was modeled and the resulting equations programmed for a digital computer. This program was used to simulate system and thrustor operation and thus, to evaluate operating characteristics and the type of control required. Experimental evaluation of the system is reported in Volume II of this report.

CONTENTS

ILLUSTRATIONS

TABLES

SUMMARY

The use of the cryogenic propellants, hydrogen-oxygen, in upper stage rocket propulsion systems is desirable due to the higher energy release of such propellants. To date, cryogenic-propellant reaction control system development has not kept pace with the larger cryogenic propellant propulsion systems, thereby creating a technological void in the reaction control spectrum. The development and use of a cryogenic reaction control system would reduce the number of propellant combinations required on board a vehicle utilizing cryogenic propellants, thereby decreasing overall vehicle complexity and increasing reliability. The cryogenic reaction control system approach, however, could magnify some of the presently known technical problem areas or introduce new problem areas, such as: ignition techniques, multiple start requirements, propellant conditioning and control, and thrustor durability.

In particular, since the hydrogen and oxygen propellants utilized in a reaction control thrustor may be drawn from the main propellant tanks in the gaseous state (i.e., as vent gases with the possibility of small quantities of liquid propellant or gaseous pressurant intermixed) or from separate independent tankage in the liquid state (with subsequent vaporization and two-phase flow in the propellant lines), difficulty in controlling thrustor inlet conditions and mixture ratio may be encountered. Therefore this problem was expected to dominate thrustor design and control design, and would necessitate use of propellant conditioning equipment to control the state of the injected gaseous propellants.

The basic purpose of this program was to investigate the above problem areas and thereby ascertain the feasibility of a cryogenic reaction control system for spacecraft applications, and to generate basic system design data that could be utilized during the ultimate development of an operational system. Accordingly, a 16-month program has been conducted to evaluate the potential for a reaction control system utilizing the cryogenic oxygen-hydrogen propellant combinations. Analysis and concept design are reported herein (Volume I). Component design and experimental results are reported in Volume II.

Illustrative system applications were compiled to supplement the generalized operating and design goals established for this program and to identify possible operating constraints. Possible applications were identified as: propellant settling engines, stage recovery power, attitude control, and secondary propulsion for orbital tankers. The most useful range of thrust was found to be from 20 to 100 pounds, and chamber pressure levels were indicated to be either 10 psia or 100 psia.

Existing computer programs were used to calculate the theoretical performance in terms of the thermodynamic state and compositions of the exhaust products, and obtain estimates of probable compositional freezing during the expansion process. The 10 psia pressure oxygen-hydrogen performance characteristics differ from those at the 100 psia level in a significant manner. One effect is that performance optimizes at different mixture ratios. This leads to optimized performance for the 10 psia level with substantially lower combustion temperatures.

The cryogenic RCS was divided into two distinct component subsystems such that the experimental study would be consistent with the very general nature of the program goals. One subsystem was defined to

condition the propellants to a given thermodynamic state regardless of the inlet state; the other subsystem consisted of the thrustors.

Based on the overall RCS application analysis the low pressure (10 psia) system was selected for experimental investigation in this program chiefly because of the total lack of existing technology at this pressure level for both the conditioner and thrustor. Analysis of the conditioner operations showed pressure control to be critical in maintaining the thrustor catalyst bed temperature in a range which prevents bed burnout. However, even a small relaxation in the pressure requirement (i.e., increasing maximum thrustor operating pressures oy a few psia) may markedly alter the criticality of the control problems. Three types of pressure control were analytically evaluated; (1) a pressure sensor operating an on-off valve, (2) a regulating device, and (3) a bellows-bladder device connecting these two propellant flow systems. Since suitable off-the-shelf control components were not available for the experimental program, modified components were utilized in a best-effort approach. A "hot tube" heat exchanger system with O_2-H_2 combustion product feed back was chosen for the conditioner subsystem with the entire subsystem pneumatically decoupled from the thrustors.

The thrustor design concepts study resulted in the selection of a cylindrical chamber with a simple conical nozzle and an in-line catalyst bed which would be designed to operate at a mixture ratio of 1. Downstream injection of additional oxygen would be employed to raise the overall thrustor M.R. to a design value of 2.5. The thrustor propellant inlet feed temperature of 200 R was selected as the design point in order to assure reliable ignition without oxygen freezing. To prevent freezing requires both propellants to be in excess of about 115 R.

Mathematical models of the conditioner and thrustor were developed and programmed for computer solution. The resulting dynamic simulation was used to examine the operation and response characteristics of the system and to determine the key operating and design parameters.

Analysis presented herein served as the basis for detailed design of components to be used in the experimental program reported in Volume II of this report. Design concepts and alternatives are analyzed and evaluated.

INTRODUCTION

The application of cryogenics (O_2/H_2) as the main propellants in advanced upper stages, and manned and unmanned spacecraft also opens the possibility of utilizing a cryogenic reaction control system (RCS) in these vehicles. To date, only cold gas, liquid monopropellant, and storable bipropellant systems have been utilized for reaction control. All of these systems suffer some disadvantages when applied to advanced vehicles. The cold gas systems (chiefly nitrogen systems) have a low specific impulse, a low density impulse, and heavy tankage requirements. The monopropellant systems (hydrogen peroxide and hydrazine) are characterized by fairly low impulses ($\sim$ 250 seconds) and propellant freezing difficulties when located in a cryogenic vehicle. The storable bipropellants have higher specific impulses, but again the system must be insulated and/or heated to eliminate the possibility of propellant freezing. A new approach to advanced reaction control systems by utilizing cryogenic propellants would seem to offer a way to circumvent many of these problems. Further, a low pressure system might also utilize the boiloff propellants during long duration coast periods, thus minimizing tankage complexity. A higher pressure system, although not possessing the latter advantage, could take advantage of the temperature compatibility for storage purposes.

The use of the oxygen-hydrogen propellant combination does introduce the additional problem of ignition since the combination is not hypergolic. For this case of a multiple engine system, catalytic ignition offers a simple, reliable approach. However, this approach does require that the temperature of the hydrogen fed to the thrustors be sufficiently high to avoid the formation of solid oxygen upon propellant mixing. The formation of solid oxygen has been shown to result in unreliable and in some cases, destructive ignition. Hence, some method of increasing the propellant temperature is necessary.

The thermodynamic state of the inlet propellants to the thrustor will directly affect propellant flow control. To simplify the control requirements, the conditioning system should deliver propellants at controlled conditions. Also, in the case of the low pressure system, if the system is to utilize main tankage propellants, then the RCS must be able to accept the propellants in various thermodynamic states from liquid at the normal boiling point to gas at elevated temperatures and with varying amount of helium diluent. The propellant must then be conditioned to a given state to aid in the overall control of the thrust level and propellant mixture ratio. The control requirements for the high pressure system should be less severe, since the propellants leaving the storage tanks will remain at a relatively static thermodynamic state.

This report covers the initial phases of a 16-month applied research program which evaluated a cryogenic RCS utilizing the oxygen-hydrogen propellant combination. The overall program objectives included the exploration of possible problem areas in such a system as well as demonstrating the feasibility of such a system. For conceptual purposes, the RCS was divided into two subsystems; (1) the thrustors, and (2) a conditioner to adjust and control the thermodynamic state of the propellants. The program consisted of six tasks as follows:

I. Thrustor analysis and Conceptual Design
II. Conditioner Analysis and Conceptual Design
III. Thrustor Design and Fabrication
IV. Conditioner Design and Fabrication
V. Thrustor Evaluation Tests
VI. Conditioner Evaluation Tests

The initial efforts, which are reported herein, consisted of initial conceptual design, concept analysis, design criteria analysis, and concept evaluation efforts. The objectives of these efforts were to evaluate a

number of subsystem concepts and select the most promising as well as a chamber pressure level (10 or 100 psia) for the remainder of the program. The final effort wasthen aimed at defining the subsystem designs, experimentally evaluating subsystem components, analytically evaluating the results with respect to the establishment of clearly defined design criteria, and demonstrating the feasibility of the subsystems.

A number of basic design parameter and operating goals were defined prior to initiation of this program:

Thrust (each thrustor)	20 lb_f
Expansion Area Ratio	50:1
Mixture Ratio (O/F)	from 0.5 to 6.0
Duration	60 minutes
Minimum Impulse Bit	1 lb_f-sec.
Ignition Delay (maximum)	10 milliseconds
Mission Time	1 hour to 220 days

The program is to initially consider two chamber pressure levels, 10 psia as representative for main tank propellant utilization and 100 psia as representative of separate cryogen tankage. Further, the system design should be based on supplied propellants at the following compositions and thermodynamic states:

Hydrogen Thermodynamic State - 37R liquid to 500R gas, in single and mixed phases

Oxygen Thermodynamic State - 163R liquid to 500R gas, in single or mixed phases

Propellant Composition - propellants containing 0 to 50 percent helium pressurant at the 10 psia chamber pressure level, pure propellant at the 100 psia pressure level

Supply Pressures - 20 ± 5 for 10 psia chamber pressure, 175 ± 5 psia for 100 psia chamber pressure.

The analytical efforts are divided into six areas for reporting purposes; Applications Review, Theoretical Performance, Component Analysis-Thrustor, Component Analysis-Conditioner, Overall System Characteristics and Comparisons, and System Analysis and Simulation.

APPLICATIONS REVIEW

Possible system applications were compiled to supplement the operating and design goals established in the program work statement and to more clearly define typical applications for a cryogenic RCS. Meetings were held with several government vehicle contractors in which ideas and information pertinent to cryogenic RCS applications were exchanged. Also, the available literature dealing with the propulsion requirements for future stages and vehicles. The results as they affect the focus of the subject program are discussed below.

UTILIZATION OF CRYOGENIC REACTION CONTROL SYSTEMS

The applications of a cryogenic RCS have been divided into four general areas; propellant settling, attitude control, orbital tanker maneuvering, and residual propellant utilization for extra ΔV or spent stage maneuvering (recovery). To present the results in a concise form, the application requirements and typical operating conditions are summarized in Table 1. These are discussed in greater detail below.

Propellant Settling

The substitution of cryogenic propellant settling engines for existing monopropellant or storable bipropellant engines offers the advantage of appreciable gains in specific impulse with commensurate decreases in weight. The thrust range of applicability is from 10 to 80 pounds-thrust, with the greatest interest in the 50 to 80 pound-thrust range. Since a typical settling engine application is a single steady-state firing for

a 1 to 60 minute time period, rapid response is not a requirement. However, for the longer duration applications an appreciable savings in total RCS weight could be realized with the use of a high impulse propellant such as oxygen/hydrogen.

The use of cryogenic (O_2/H_2) settling engines on future spacecraft with cryogenic main propulsion systems offers compatible storage and high performance. In addition, the possibility of utilizing propellants drawn from the main propellant tanks offers a more simplified storage requirement. Because fast response is not a requirement and start transients will be only a minor portion of the rather extended run duration, it is expected that a design for this application will be considerably different than for the remaining applications. In particular, a boot-strapping, integrated thrustor-conditioner engine with regenerative conditioning is thought most attractive from a conceptual standpoint.

Attitude Control

Cryogen reaction control systems are attractive possibilities for attitude control in future cryogenic spacecraft and upper stages. Two factors are favorable, the increased performance of such a system when compared to cold gas, monopropellant, and storable bipropellant systems and much improved storage temperature compatibility. The attitude control functions for these advanced vehicles include limit cycle control during long-term coast periods, vehicle orientation for course correction, and reorientation and control during deceleration manuevers. Typical advanced spacecraft where a cryogenic RCS might be used in an attitude control function include cryogenic kick stages, nuclear kick stages, and cryogenic logistics vehicles. These would typically be aimed at planetary or lunar missions.

The attitude control requirements accompanying an application in a kick stage on a Mars mission (0.2 to 60 pound-thrust range) are listed below:

Usage Time After Launch	Function	Firing Mode
10 minutes	Separation Stabilization (pitch, yaw, roll)	Variable: minimum bit to 50 seconds continuous
10 minutes to 220 days	Attitude Control Limit Cycle (pitch, yaw, roll)	Minimum impulse bit, 5-hour cycle period for each axis
3 days to 194 days	Vehicle Reorientation (180 degrees maximum in each axis)	10 seconds continuous per thrustor

The use of the hydrogen boiloff as a cold-gas propellant for attitude control during interplanetary coast has been considered. The boiloff rate during this phase of the mission would be substantially greater than the hydrogen supply needed for the cold-gas propulsor. Thus the same thrust chamber might be used in a cold-gas operational mode for small impulse bit requirements and in a bipropellant mode for the higher impulse requirements. Such a scheme would conserve oxygen which has the low boiloff rate and would seem most applicable with the low pressure system utilizing only propellants supplied from the main propellant tankage.

The thrustor usage requirements of a cryogenic propulsion module to be used on a lunar logistic mission (4 to 8 pound-thrust range) include the following:

Usage Time After Launch	Function	Firing Mode
1.5 hours	Separation Stabilization (pitch, yaw, roll)	Variable: minimum bit to 50 seconds continuous
1.5 hours to 8 days	Attitude Control Limit Cycle (pitch, yaw, roll)	Minimum bit, 5-hour period each axis
14 to 140 hours	Vehicle Reorientation (180 degrees maximum in 2 axes)	10 seconds for yaw and roll

Specific information is not available concerning the secondary oxygen-hydrogen propulsion requirements for a nuclear spacecraft for a manned Mars mission. A probable thrust level would be from 75 to 300 pounds with both pulsing and steady state operational modes. These engines typically would be used for a transfer from a parking to assembly orbit, docking and assembly, earth departure, Mars breaking, Mars departure, and attitude control during coast.

In general, the attitude control application requires a rapid response. Although the specifics with respect to response times are not defined, time to 90 percent thrust of 50 milliseconds are thought to be near the upper limit. Because of the heat sink attributes of a packed catalytic bed, such a response with an initial cold bed is not expected. Thus, for an application demanding a low usage rate over an extended time period, the system would seem to have disadvantages. Conversely, for an application with a high usage over a short time period, such a factor would not be significant since the bed would remain at an elevated temperature.

Typical attitude control functions require a number of RCS modules placed at opposing points on the vehicle. With such an arrangement, it is not clear, a priori, whether separate propellant tankage for the RCS system or whether propellant feed from the main tankage represents the more favorable arrangement. Both must be considered.

Orbital Tanker Manuevering

Advanced vehicles to accomplish a cryogenic propellant supply function are presently under study. The use of a cryogenic RCS as a secondary propulsion system for such an unmanned vehicle would seem to merit consideration.

The thrustor usage requirements for the secondary propulsion system of an orbital tanker utilizing 150- and 300-pound-thrust engines are thought to be:

Function	Operational Mode	Maximum Number of Starts
Transfer Midcourse Correction	Steady State	1
Injection at Assembly Orbit Stabilization	Steady State	1
Station Keeping	Pulsing	25
Rendezvous Stabilization	Pulsing	20
Closure Maneuver	Steady State	4
Docking	Pulsing	50

Performance of the engines was not considered to be of importance for any of the above functions except the closure maneuver and docking since these two functions should consume essentially all of the propellants required for propulsion. Since these maneuvers take place over a short time period during which the catalytic bed will remain at temperature, pulse-performance should be high with negligible enthalpy loss. However, pulse repeatability for several of the other maneuvers which may occur over a longer time period is a factor which must be evaluated.

Thermal compatibility of the cryogenic RCS system with the main propellant tankage would seem an advantage for this application. Again, a priori selection of either separate propellant tankage or a propellant feed from the main tankage is not possible.

Utilization of Residual Propellants in Spent Stages

Cryogenic RCS technology might be applied to a secondary propulsion system directed at utilizing residual propellant to obtain additional ΔV or to accomplish stage maneuvering prior to spent stage recovery. A wide mixture ratio capability of from 0.5 to 6.0 would probably be necessary to insure efficient utilization of the residuals. It is noted that the relative quantities of the residual propellants is not exactly predetermined, but is dependent on mainstage propellant utilization. Firing durations of up to one hour are thought applicable. Response for such an application should not be a prime requirement and the operational concept for this application might well be similar to that of a settling engine.

The RCS system for such a system would necessarily utilize propellants fed from the main tankage. The main tankage pressures might initially be in the range of 20 - 40 psia with tankage pressure maintained via heat leakage to the tankage. Pressure control restraints for such a system which would determine the RCS operational pressure range are not presently defined.

APPLICATIONS SUMMARY

This effort has shown a number of possible applications for a cryogenic reaction control system; propellant settling engines for stages and spacecraft, cryogenic stage recovery, attitude control for stages and spacecraft, and secondary propulsion for orbital tankers. Although the possible thrust level ran from 0.2- to 1000-pounds-thrust, the range of greatest interest is from 20- to 100-pounds. Both steady-stage and pulse mode operation are of importance, with pulse reproducibility being of greatest importance in the latter operational mode. Two chamber pressure levels are of interest, 10 psia and 100 psia. The low pressure systems offer intriguing possibilities for integrating the secondary propulsion systems with the main propellant tankage and so, are quite attractive to the vehicle designer.

It is also significant that, in the cases of main tankage propellant utilization, the oxygen is generally available at higher pressure than the hydrogen--typically, 30 psia as opposed to 20 psia. However, the 10 psia chamber pressure level initially selected would seem to be approximately correct. Also, in general, helium dilution of the hydrogen is generally thought of in terms of small percentages, whereas substantial dilution of the oxygen is thought probable.

The high pressure system (100 psia) on the other hand, can be considered to be more directly competitive with currently existing storable systems. As such it would have to compete on the basis of impulse performance, total system weight, response characteristics, etc. The relative advantage trade-offs for the several systems will require a very careful study to enable the designer to optimize the vehicle. Further, it will be necessary to have in hand sufficient experimental design technology related to the cryogenic systems to enable a complete comparison of the various systems for the selection of an optimized vehicle design for any one application.

TABLE 1

MISSION APPLICATIONS

Application	Thrust Range	Maximum Steady-State Duration	Minimum Impulse Bit	Diluent Present In Main Tankage	Other Considerations
Propellant Settling	10 to 80 lb_f	1 to 60 minutes	-	helium for some vehicles	-
Attitude Control	0.2 to 150 lb_f	50 to 5 minutes	10 milliseconds	helium up to 50 percent	Modular for Reliability
Orbital Tanker Maneuvering	20 to 1000 lb_f	to 8 hours	10 milliseconds	helium for some vehicles	-
Spent Stage Recovery	20 to 100 lb_f	to 8 hours	-	helium in small amounts	-

SYSTEM THEORETICAL PERFORMANCE ANALYSIS

The theoretical performance establishes a basis for the design and evaluation of the reaction control system and for the selection of the thrustor and conditioner operating conditions. In addition, the theoretically computed physical properties of O_2-H_2 reacted mixtures were used for the design of the thrustor and conditioner subsystems. Existing Rocketdyne computer programs were used to calculate the thermo-chemical properties of the reaction products and the theoretical performance limits. The performance limits were calculated for gas expansion with full shifting flow and with frozen chemical compositions. A modified Bray analysis computer program was used to estimate the compositional freezing point in the expansion to allow interpretation of the performance results.

The reaction control system was first considered as a single adiabatic system (no heat loss or gain), the internal processes of propellant conditioning and thrustor performance not being considered. Thus, the system was treated as a black box in which it was assumed that:

1) all the necessary conditioning processes are fulfilled,
2) all of these processes are accomplished with no losses,
3) no materials, geometric, cooling, or other limitation prevents the system from responding according to the thermo-chemical dictates.

Specific impulse was the performance parameter that was evaluated with the overall system approach.

To approach a more relaistic evaluation of actual system performance, the overall system was subdivided into thrustor and conditioner subsystems. These were considered as black-box subsystems for the purpose of calculating theoretical performance. Idealizations similar to those

considered above for the overall system were again applied to these subsystems. The results of the overall system analysis are also applicable to the theoretical component analyses. Following this effort, each subsystem was evaluated with respect to realistic configurations and real losses due to inefficiencies. These component performance analyses are presented in later sections of the report.

OVERALL SYSTEM PERFORMANCE

From an overall, idealized system standpoint, the reaction control can be considered as a black box; i.e., an isolated system with no losses. Propellants are fed to the system and thrust is delivered. The specific enthalpy and composition of the combined propellants delivered from tankage determine the operation of the system. Several parameters were explicitly examined in the overall system performance evaluation:

1) The thermodynamic state of the entering propellants; specifically, the inlet propellant temperature and degree of helium dilution (for the 10 psia system)

2) Mixture ratio

3) Recombination rates during expansion and recombination effects on performance

The theoretical performance level and its dependence on mixture ratio, propellant inlet temperature and state, chamber pressure, and expansion area ratio are shown generally in Figs. 1 through 12. Figures 1 through 6 show specific impulse at a chamber pressure of 100 psia for full-shifting and full-frozen flow, and expansion area ratios of 50, 30, and 10; Figs. 7 through 12 show the specific impulse for the same conditions but at a chamber pressure of 10 psia. Mixture ratio is varied from 0.5 to 6.0, and the inlet propellant thermodynamic states considered are gases at 500R, 200R, and the normal boiling points of the propellants (163R for O_2 and 37R for H_2) and liquids at their normal boiling points. The impulse maxima at an expansion ratio of 50 are in the range of 465 seconds for full-shifting flow and 450 seconds for full-frozen flow (propellants supplied at 200 R).

Performance - Effect of Propellant Inlet Conditions

The inlet thermodynamic state of the propellants has a direct effect on performance inasmuch as the enthalpy (or temperature) level of the reacted mixture is affected. Because the hydrogen has such a high heat capacity (on a weight basis), the mix enthalpy is more sensitive to the hydrogen inlet temperature than to the oxygen temperature. Figure 13 illustrates this effect by showing the propellant mix temperature at a mixture ratio of unity as a function of the hydrogen temperature.

The first-order effect of the inlet temperature on performance is illustrated in Figure 1, a plot of theoretical specific impulse as a function of mixture ratio at four inlet conditions. The impulse is shown

to be decreased with lowered inlet temperatures or enthalpy potential of the propellants.

There are other, second-order effects of the inlet conditions on performance; specifically the position of the performance peak with mixture ratio, the degree of recombination at a given mixture ratio, and water condensation characteristics. These will be discussed under each individual topic.

Performance - Effect of Chamber Pressure

Chamber pressure has no significant effect on performance (< 2 seconds) at the low mixture ratios (~ 2.0); whereas at higher mixture ratios, the specific impulse is increased with increasing chamber pressure. Figure 14 shows the difference in specific impulse between the 100 and 10 psia chamber pressure cases as a function of mixture ratio for both full-shifting and full-frozen expansions. Significant chamber pressure effects on performance only appear at mixture ratios greater than 2.0 for full-frozen flow and 4.5 for full-shifting flow. At a mixture ratio of 2.5, the performance difference is less than 3 seconds for full-frozen flow. The maximum difference is 18 seconds for full-frozen flow at a mixture ratio of 6.0.

Performance - Effect of Mixture Ratio

Maximum specific impulse as shown in Figs. 1 through 12 occurs at a mixture ratio between 2 and 3 for full-frozen flow and at about 3.5 for a shifting expansion. This is in contrast to density impulse

(based on liquids at their normal boiling points) which maximizes at a higher mixture ratio as shown in Fig. 15. However, the density impulse curve is fairly insensitive to mixture ratio over a quite large range.

Operation of the thrust system at lower mixture ratios results in lower combustion temperatures and, consequently, less severe cooling requirements in the thrust chamber and nozzle. Thus, the question of the degree of chemical recombination during expansion becomes extremely important in determining the operating parameters of the system. Likewise, the relative importance of density impulse and specific impulse for specific applications is also significant. This report will weigh the specific impulse characteristics as most important because:

1. most cryogenic applications are specific impulse oriented (weight limited)
2. the density impulse is quite insensitive to mixture ratio.

Chemical Recombination Kinetics

The previously presented data showed the importance of chemical recombination to both the mixture ratio for maximum specific impulse and the level of specific impulse achieved. Therefore, the estimation of the recombination kinetic effects becomes important when designing and evaluating the system. Such an estimation will also serve as a basis for fluid dynamics calculations of the nozzle flow field and frictional drag losses when estimating the system thrust performance.

The determination of the point at which the chemical composition freezes during a given nozzle expansion case utilized an existing Rocketdyne computer program based on a generalized Bray criteria. The approach

utilized follows the method developed by L. C. Francicus and E. A. Legberg (Ref. 1), a "partial equilibrium" concept wherein the freezing point is established by equalizing the rate of compositional change due to pressure and temperature decay during expansion and the sum of the three-body recombination reaction rates. The three-body reactions are assumed to be the rate-limiting chemical step. Of the three significant three-body reactions

$$H + H + M \longrightarrow H_2 + M$$
$$H + OH + M \longrightarrow H_2O + M$$
$$O + H + M \longrightarrow OH + M$$

the second was assumed dominant, based on both the existing free radical concentrations and the heat of reaction. The freezing point calculation was based on the rate of this reaction. This is a conservative approach in the sense that if other reaction rates are also important, freezing will occur earlier in the expansion.

Two methods of defining the expansion geometry were considered for the calculations,

(1) a specification of a contraction angle α, an expansion angle B, and the ratio of the radius connecting α with B to the throat radius (known as analytical method)

(2) a point-by-point contour specification in this case based on four radii for expansion to the throat.

The second method is used when the chamber-to-throat region geometry is somewhat complicated; however, if freezing occurs upstream of the first point specified on the contour, the program will not give a solution.

The freezing point results are listed in Table 2. In all cases at the 10 psia chamber pressure level, the freezing point occurred at

contraction ratios larger than would be utilized in a real thrustor. The case listed in the table represents a severe case, the high mixture ratio leads to a high temperature and relatively large concentrations of free radicals. These conditions result in high recombination rates (on a relative basis), but still the freezing point is at a contraction ratio of approximately 15. Thus, full-frozen flow is predicted at the 10 psia chamber pressure level.

The predicted freezing point at a chamber pressure of 100 psia was found to vary from contraction ratios greater than 15 for low mixture ratios to just greater than 1 for mixture ratios of approximately 4.0. At low mixture ratios of $\sim$ 1.0, and a chamber pressure of 100 psia, the expansion process can again be considered as completely frozen. At the higher mixture ratio of 4.0, some chemical composition change will occur. However, this has a fairly small effect on performance as shown in Fig. 16 and 17. The direct effect on performance is indicated by the impulse curve which only shows a divergence of the shifting and frozen impulse curves at expansion area ratios greater than approximately . Shifting flow in the contraction section could have a second, indirect effect on performance via a change in gas properties which would affect the subsequent expansion process. The plots of gamma (C_p/C_v) for shifting flow in Fig. 18 and 19 indicate that this effect is negligible, however. Hence, for all practical purposes the expansion processes can be considered as occurring in a full-frozen manner for the system under consideration. The occurrence of aforeconcluded type of expansion has a significant effect on the choice of the mixture ratio operating point as shown in Fig. 1 - 12 and previously discussed. This is beneficial in the sense that operation in the maximum frozen specific impulse range of MR = 2 to 3 will result in lower combustion temperatures and less severe oxidation atmospheres. Cooling and material requirements could then be considerably less restrictive.

Performance - Effect of Expansion Area Ratio

The dependence of the impulse performance on expansion area ratio as balanced against additional frictional drag loss is a key factor in determining a nozzle design point, the others being weight and size considerations. This dependence is graphically depicted in Figs. 20 through 23 for two chamber pressure levels and mixture ratios. Both full-shifting and full-frozen performance values are depicted. Performance becomes quite insensitive to area ratio at area ratios greater than 30:1, making detailed trade-off quite necessary prior to a final application design.

The divergence of the performance curves (full-shifting from full-frozen) at a mixture ratio of 1.0 and area ratios greater than approximately 25:1 to 30:1 is caused by the theoretical condensation of water in the full-shifting case. Conversely, no water condenses at an area ratio of less than 50:1 for a mixture ratio of 2.5. In the latter case, the divergence of the two curves is caused by recombination effects.

In any case, it is evident that area ratios greater than 50:1 would be only marginally attractive, if at all, from an increased performance standpoint.

HELIUM DILUTION

Propellant supplied to the RCS from the main vehicle tankage, one of the two cases under consideration, may contain appreciable quantities of helium diluent. The helium would be present as residual pressurant. Depending on the method of pressurizing the tanks, normal boiloff and venting will tend to reduce the quantity of helium present and thus minimize the effect of the diluent.

Figures 24 through 35 show the effects of helium dilution of the incoming propellants on theoretical specific impulse at the 10 psia chamber pressure level. The comparisons are based on a definition of mixture ratio as the ratio of weight flows with the diluent included

$$MR = \frac{\text{oxygen plus oxygen diluent}}{\text{hydrogen plus hydrogen diluent}}$$

The dilution of the oxygen and to both propellants simultaneously results in reduced specific impulse, with very little difference in the performance between these two cases. The major effect is one of removing a reactant species (O_2) for an inert one (He).

When the helium dilutes the hydrogen, at the 50 weight percent level, specific impulse is nearly the same as the undiluted propellants at low mixture ratios. At mixture ratios greater than 1.5 to 2.0, specific impulse drops off severely. The latter is chiefly caused by the substitution of the inert helium for reactive hydrogen above a mixture of four (for 50% dilution). The effects of smaller degrees of hydrogen dilution will be significant only at higher mixture ratios.

COMBUSTION TEMPERATURE CHARACTERISTICS

The combustion temperature characteristics of the hydrogen-oxygen propellant combination have significance in two areas, control of the propellant mixture ratio fed to the catalyst bed and selection of a thrustor design based on materials compatibility and feasible modes of thrustor cooling. The former consideration is imposed because present state-of-the-art catalysts for low temperature (100 to 200R) service are limited to an approximate maximum operating temperature of 1500F. This limit was defined in a previous NASA program (Ref. 2) as that necessary to prevent damage to alumina substrate of the catalyst. Also, a catalyst bed exit temperature of at least 1000F is necessary in those engine designs which utilize the injection of additional oxygen downstream of the catalyst bed.

The effects of propellant inlet conditions and mixture ratio on theoretical combustion temperature are shown in Figs. 36 and 37. The 1500R temperature is seen to occur at mixture ratios from 0.75 to 1.25, depending on the inlet propellant temperature. The combustion temperature varies from 3000 to 4000R in the mixture ratio range from 2.0 to 3.0, corresponding to the maximum full-frozen flow specific impulse. Operation in this range of temperature leads to a significant reduction in the temperature environment over that experienced at the more normal large engine operating point of MR = ~5.2 (temperature of 5000 to 5500R).

The addition of helium diluent to the propellants for the 10 psia chamber pressure case can substantially change the combustion temperature as shown in Figs. 38 through 40 . The presence of 50% diluent in the hydrogen is seen to raise the combustion temperature by approximately 700R at mixture ratios near 1.0. This is caused by the lower

heat capacity of the helium as compared with the unreacted hydrogen it replaces. The impulse effects of 50% dilution of the hydrogen showed an almost negligible effect in this mixture ratio range, because of the increased temperature is accompanied by a similar increase in molecular weight. Since this increase is important to the reliable control of the thrustor, the dependence of the temperature on the percentage of helium dilution is shown in Fig. 41. Small amounts of helium are shown to have relatively small effects on the temperature. Figure 41 also shows a similar effect at a higher mixture ratio of 2.5. However, at higher mixture ratios, the percentage temperature difference decreases for two reasons;

(1) water absorbs a higher percentage of the energy
(2) the hydrogen is completely consumed at a mixture ratio of approximately 4.0 (for 50% dilution).

The effect of helium diluting the oxygen is one of removing combustable oxygen with a resultant decrease in temperature. This was the cause of the impulse degradation discussed above.

SUMMARY OF THEORETICAL PERFORMANCE CHARACTERISTICS

The low pressure hydrogen/oxygen performance characteristics differ from those at high pressure in a significant manner. The low operating pressure leads to frozen expansion of the chamber gases at the higher mixture ratios. This in turn results in a maximum specific impulse over the mixture ratio range of 2.75 to 3.25 for a 100 psia chamber pressure (specific impulse of ~475 seconds) and of 2.50 to 3.0 for a 10 psia chamber pressure (specific impulse of ~466 seconds). These mixture ratios, as opposed to higher values found at higher chamber pressures, result in substantially lowered combustion temperatures in the range of 3500F to 4500F. Such temperatures present a substantial reduction in the severity of the chamber environment.

The presence of helium diluent in the two propellants has a different effect depending on the propellant which is contaminated. With helium in the oxygen, the amount of combustible material in this fuel-rich mixture is decreased. This lowers the combustion temperature and specific impulse. With the hydrogen contaminated the combustion temperature is increased because of the lower heat capacity of the helium as compared with hydrogen. However, the specific impulse is changed only slightly because of a compensating effect of increased molecular weight.

TABLE 2

RESULTS FOR BRAY CRITERIA ANALYSIS OF
COMPOSITION FREEZING POINT DURING
COMBUSTION GAS EXPANSION

				Expansion Contour Specification Methods								
				Analytical			Point-by-Point Contour				Freezing Point Contraction Ratio	
P_c, psia	MR	T_{inlet} (R)	D_t, inches	Approach Angle ( ), degrees	R/R_t	Expansion Angle ( ), degrees	R_c, inches	R_d, inches	R_a, inches	R_b, inches	Analytical Nozzle	Contour Nozzle
100	1.0	200	0.38	45	0.392	15					15.228 (approx.)	
100	3.5	200	0.38	45	0.392	15	0.50	0.20	0.28	0.07	1.355	1.198
100	3.5	500	0.38				0.50	0.20	0.28	0.07		1.134
10	3.5	200	1.19				1.50	0.44	0.89	0.24		14.702 (approx.)

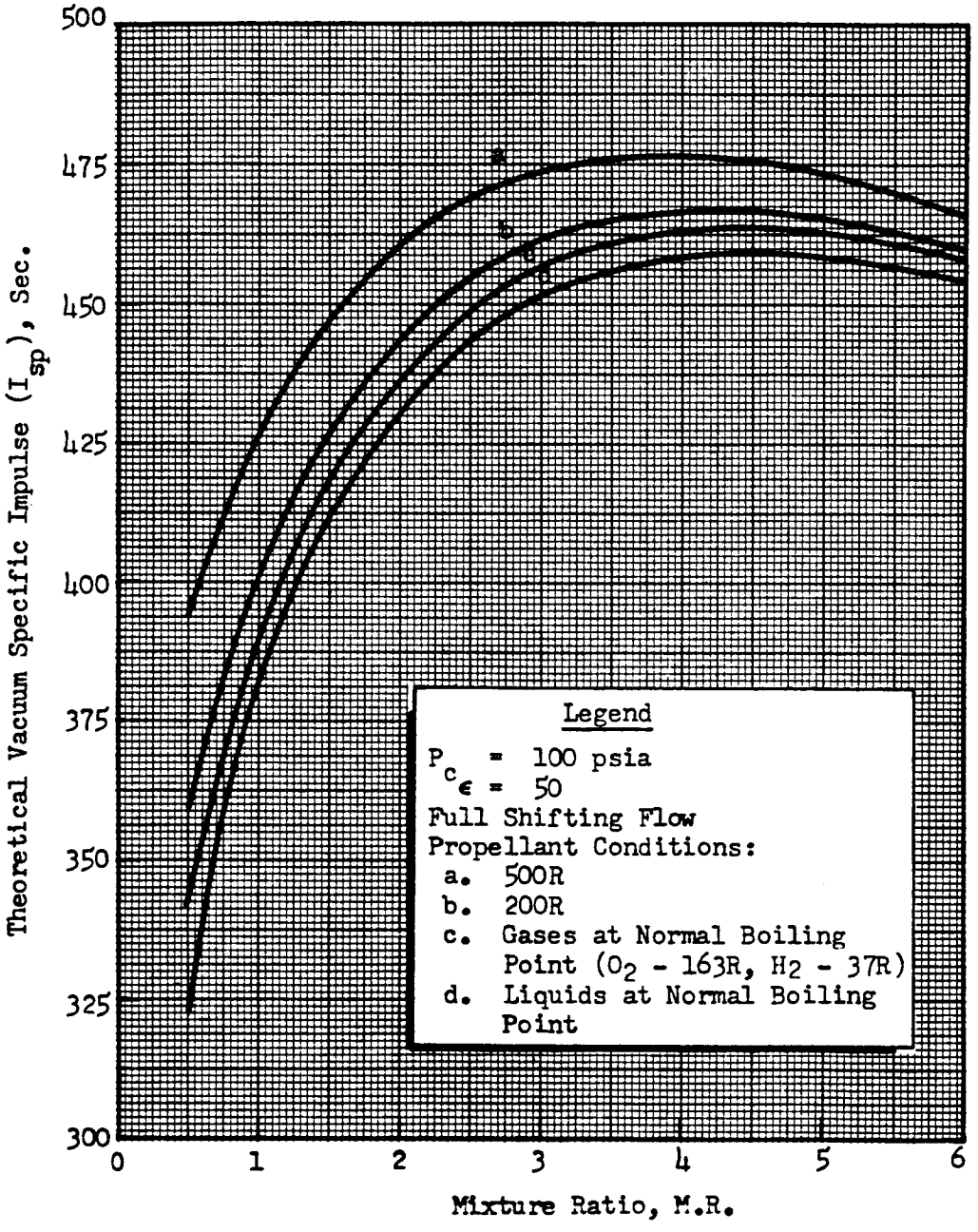

Figure 1. Theoretical Vacuum Specific Impulse as a Function of Mixture Ratio for Four Propellant Conditions (P_c = 100 psia, ϵ = 50, Full Shifting Flow)

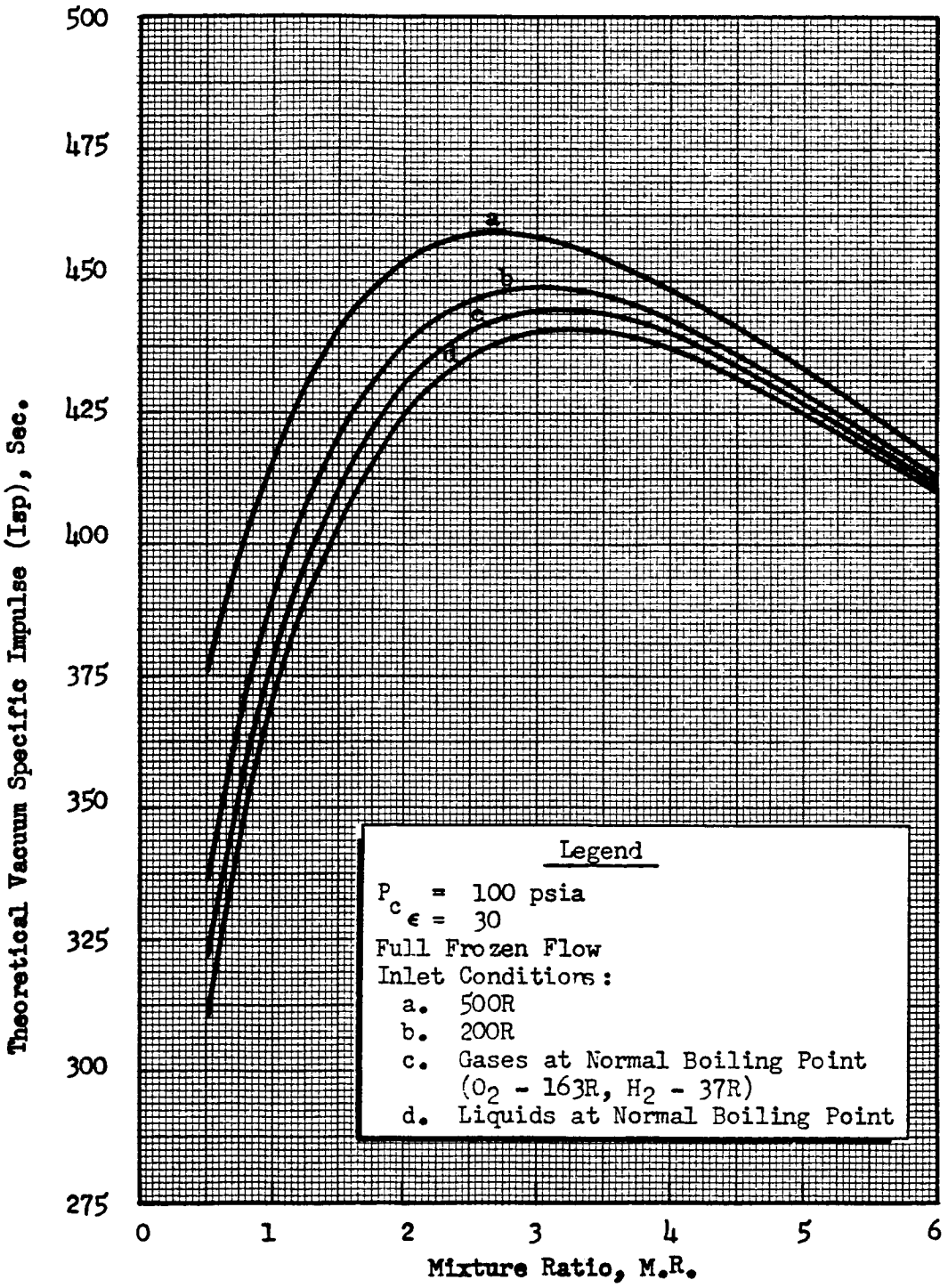

Figure 4. Theoretical Vacuum Specific Impulse as a Function of Mixture Ratio for Four Propellant Conditions (P_c = 100 psia, ϵ = 30, Full Frozen Flow)

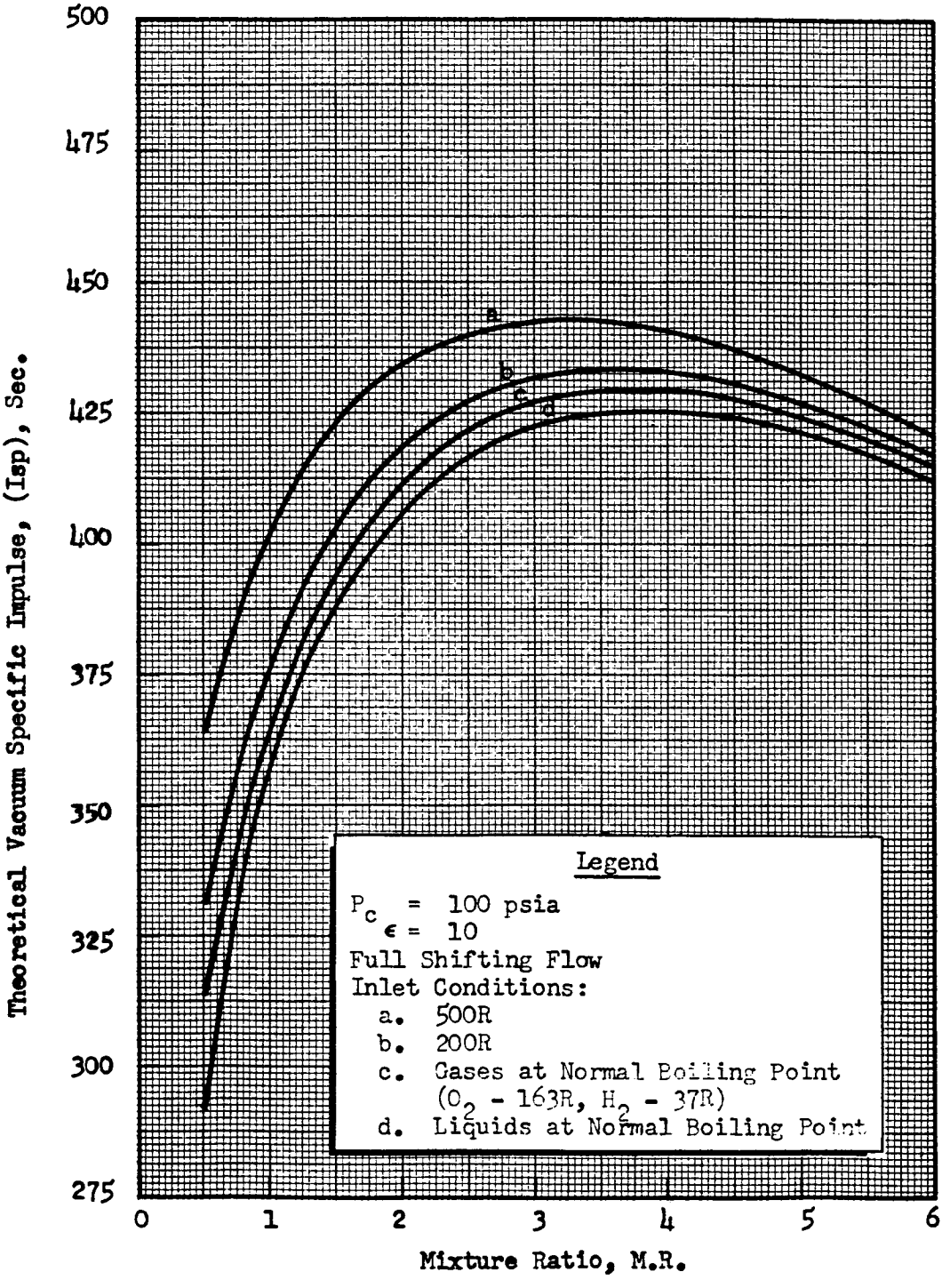

Figure 5. Theoretical Vacuum Specific Impulse as a Function of Mixture Ratio for Four Propellant Conditions (P_c = 100 psia, ϵ = 10, Full Shifting Flow)

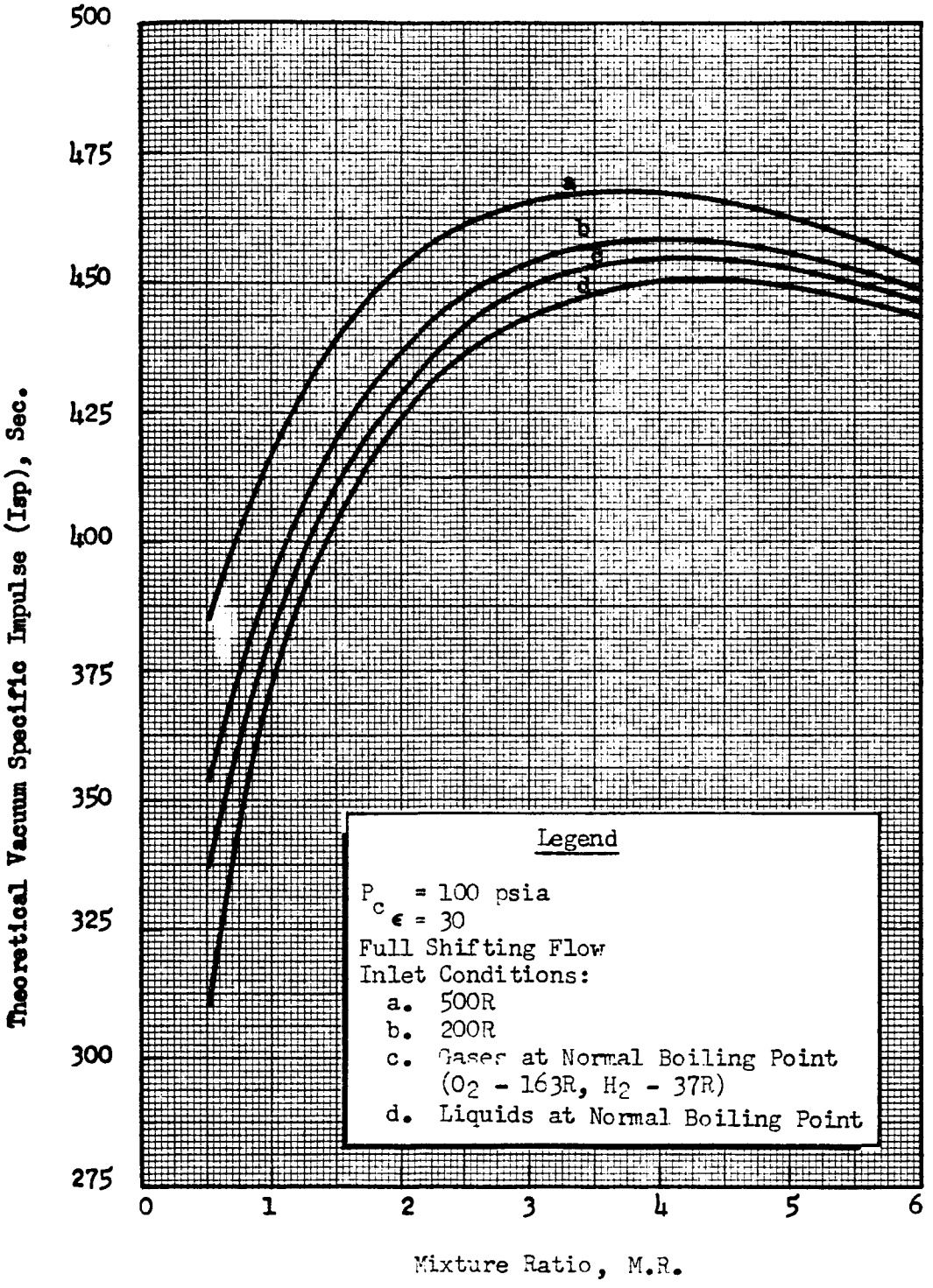

Figure 3. Theoretical Vacuum Specific Impulse as a Function of Mixture Ratio for Four Propellant Conditions (P_c = 100 psia, ϵ = 30, Full Shifting Flow)

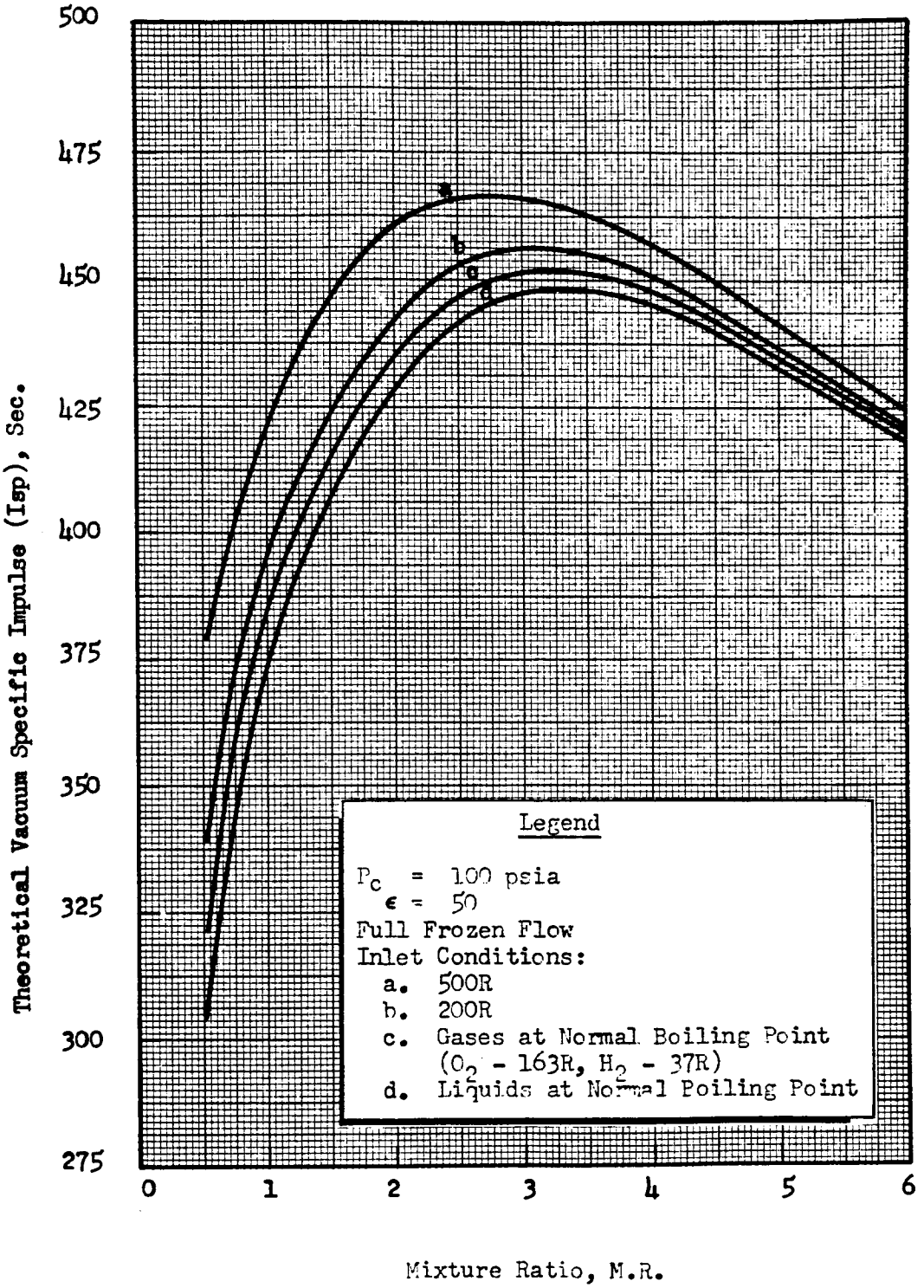

Figure 2. Theoretical Vacuum Specific Impulse as a Function of Mixture Ratio for Four Propellant Conditions (P_c = 100 psia, ϵ = 50, Full Frozen Flow)

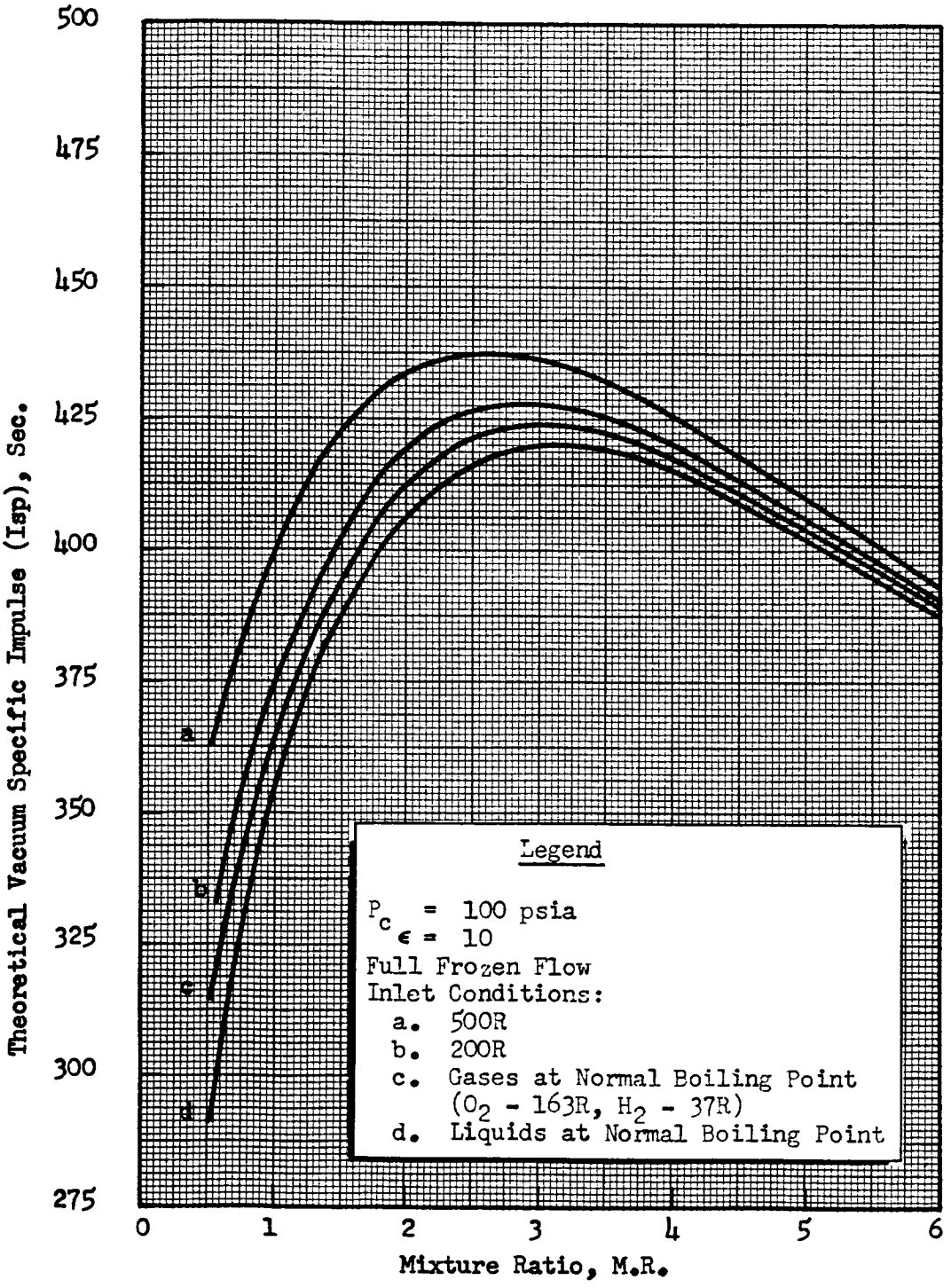

Figure 6. Theoretical Vacuum Specific Impulse as a Function of Mixture Ratio for Four Propellant Conditions (P_c = 100 psia, ϵ = 10, Full Frozen Flow)

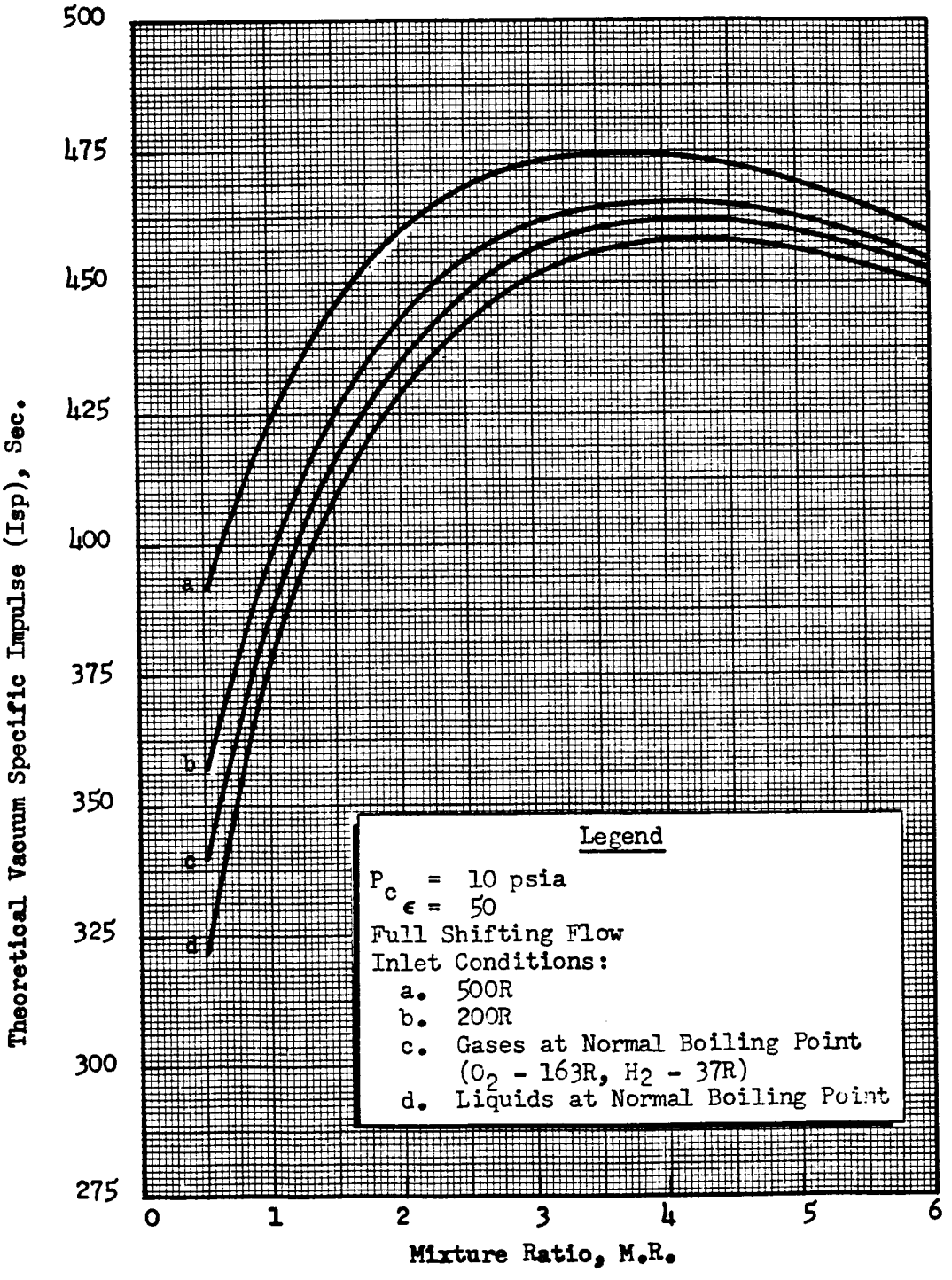

Figure 7. Theoretical Vacuum Specific Impulse as a Function of Mixture Ratio for Four Propellant Conditions (P_c = 10 psia, ϵ = 50, Full Shifting Flow)

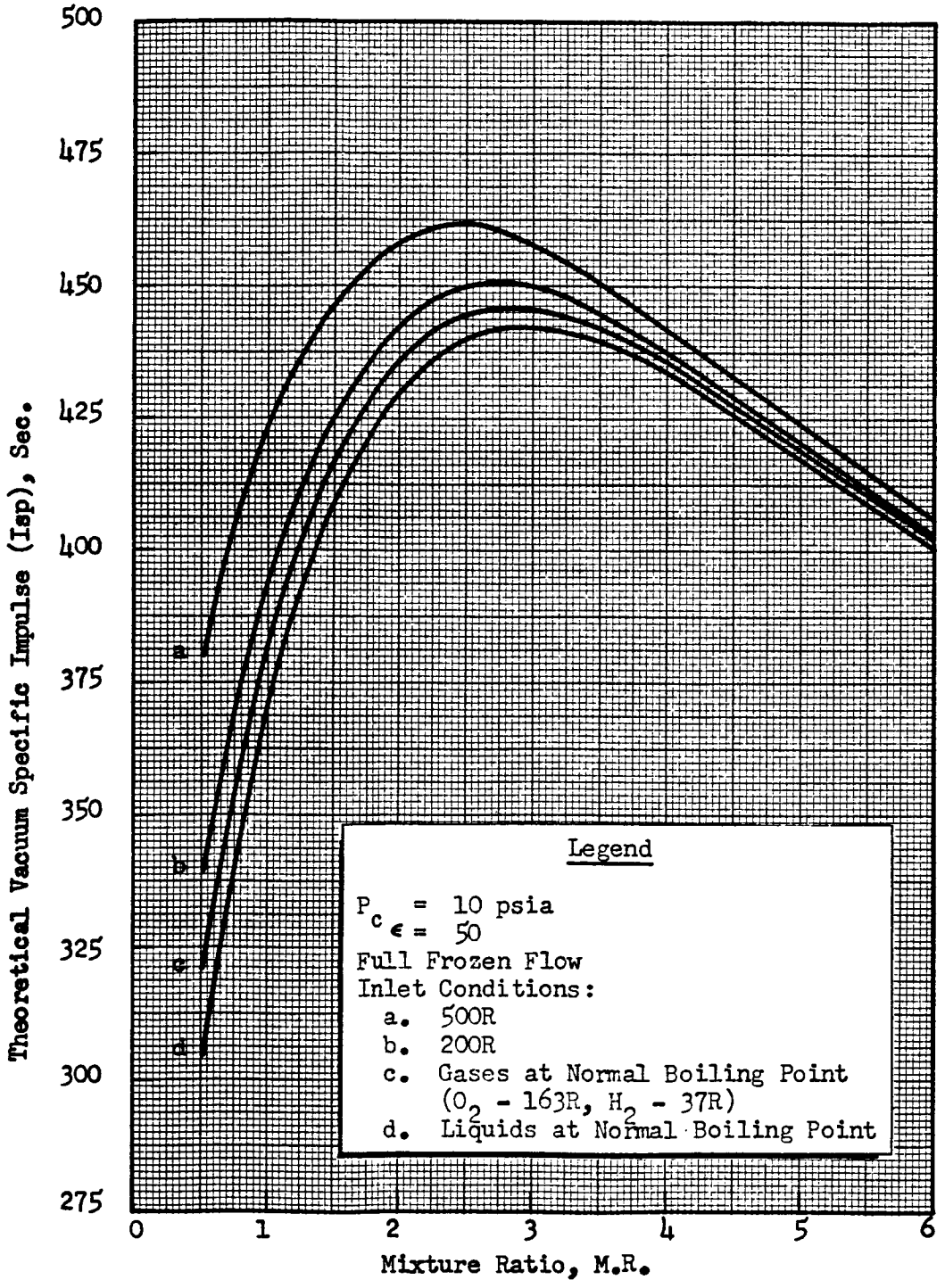

Figure 8. Theoretical Vacuum Specific Impulse as a Function of Mixture Ratio for Four Propellant Conditions (P_c = 10 psia, ϵ = 50, Full Frozen Flow)

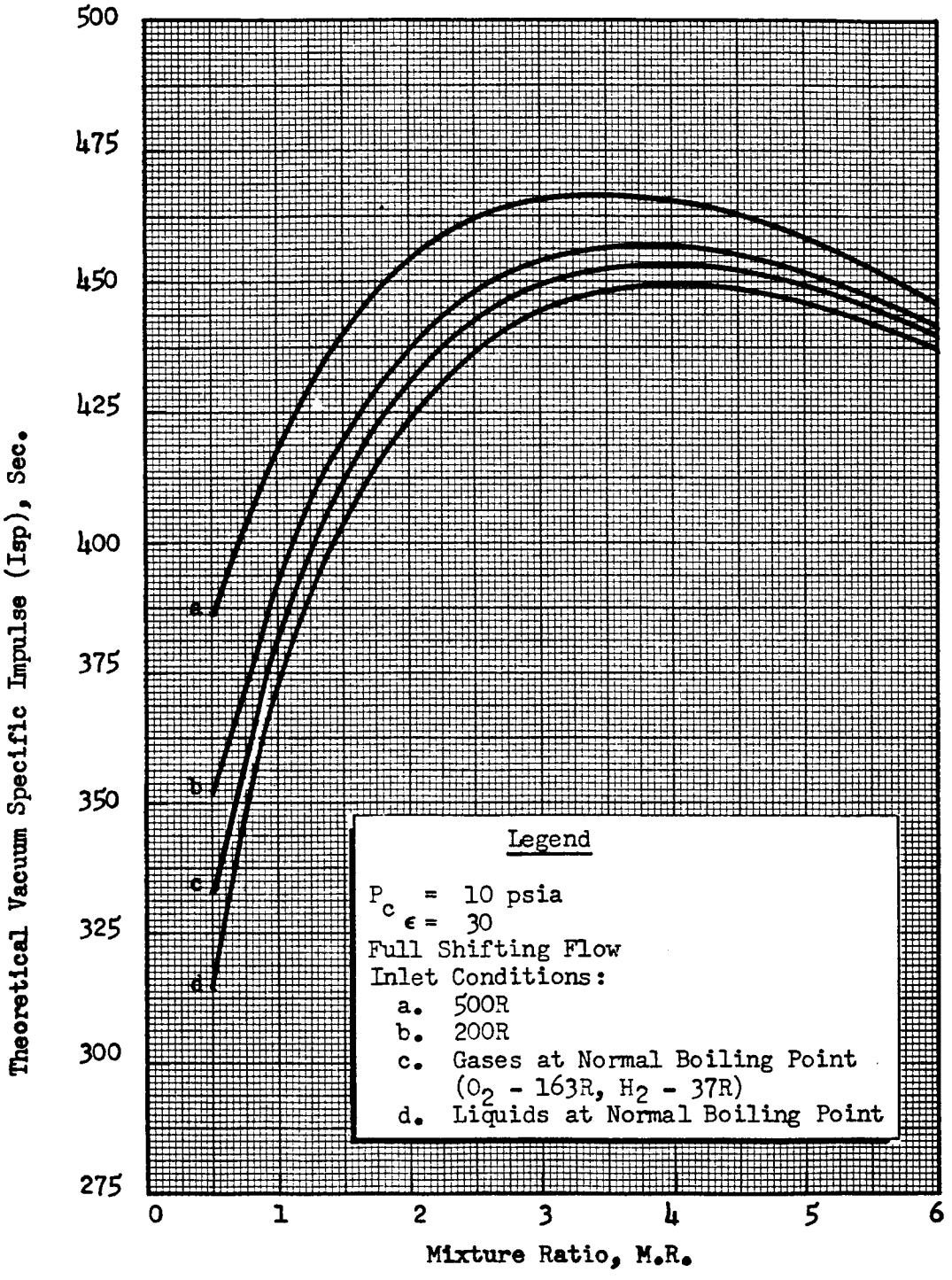

Figure 9. Theoretical Vacuum Specific Impulse as a Function of Mixture Ratio for Four Propellant Conditions (P_c = 10 psia, ϵ = 30, Full Shifting Flow)

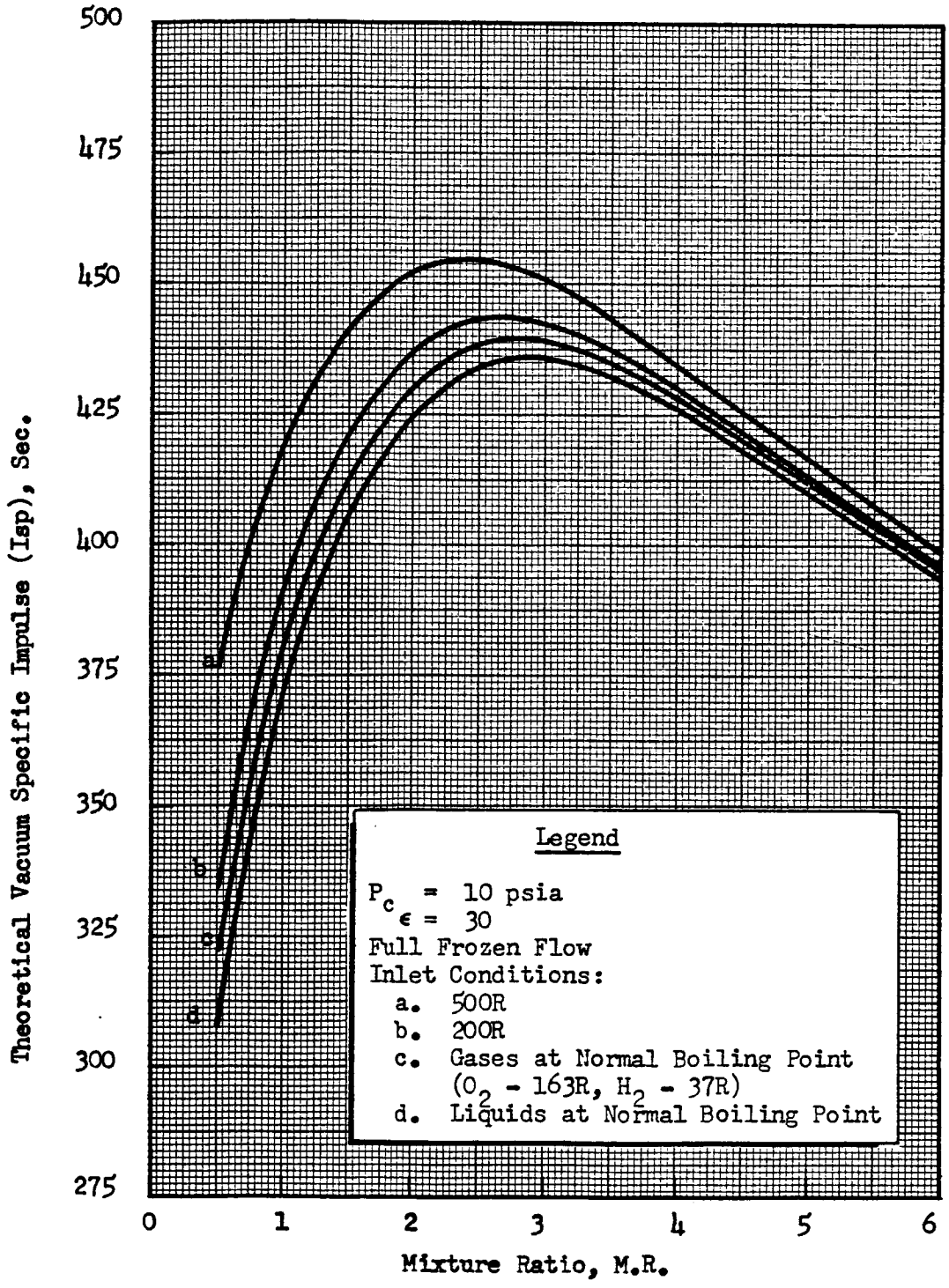

Figure 10. Theoretical Vacuum Specific Impulse as a Function of Mixture Ratio for Four Propellant Conditions (P_c = 10 psia, ϵ = 30, Full Frozen Flow)

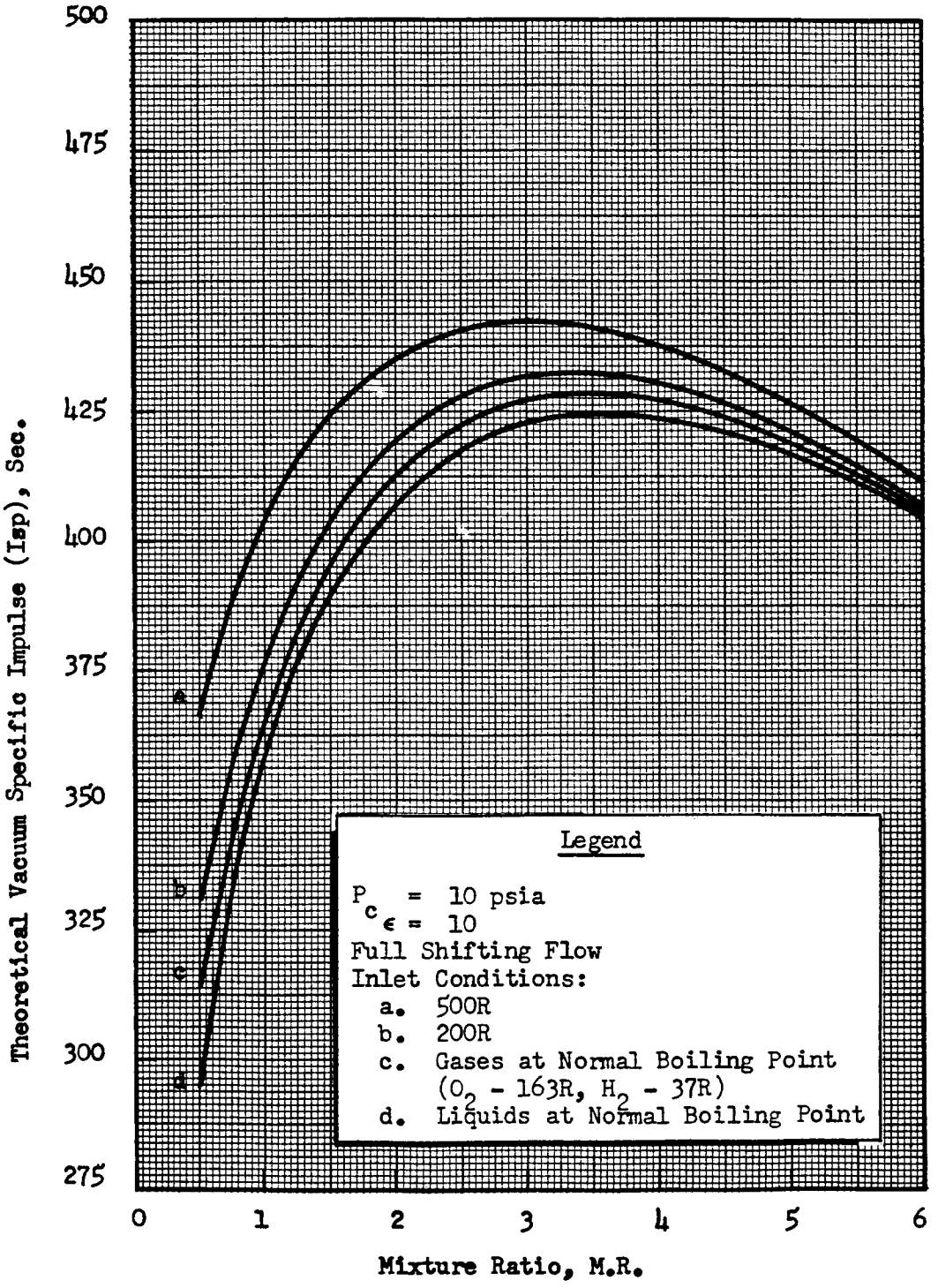

Figure 11. Theoretical Vacuum Specific Impulse as a Function of Mixture Ratio for Four Propellant Conditions (P_c = 10 psia, ϵ = 10, Full Shifting Flow)

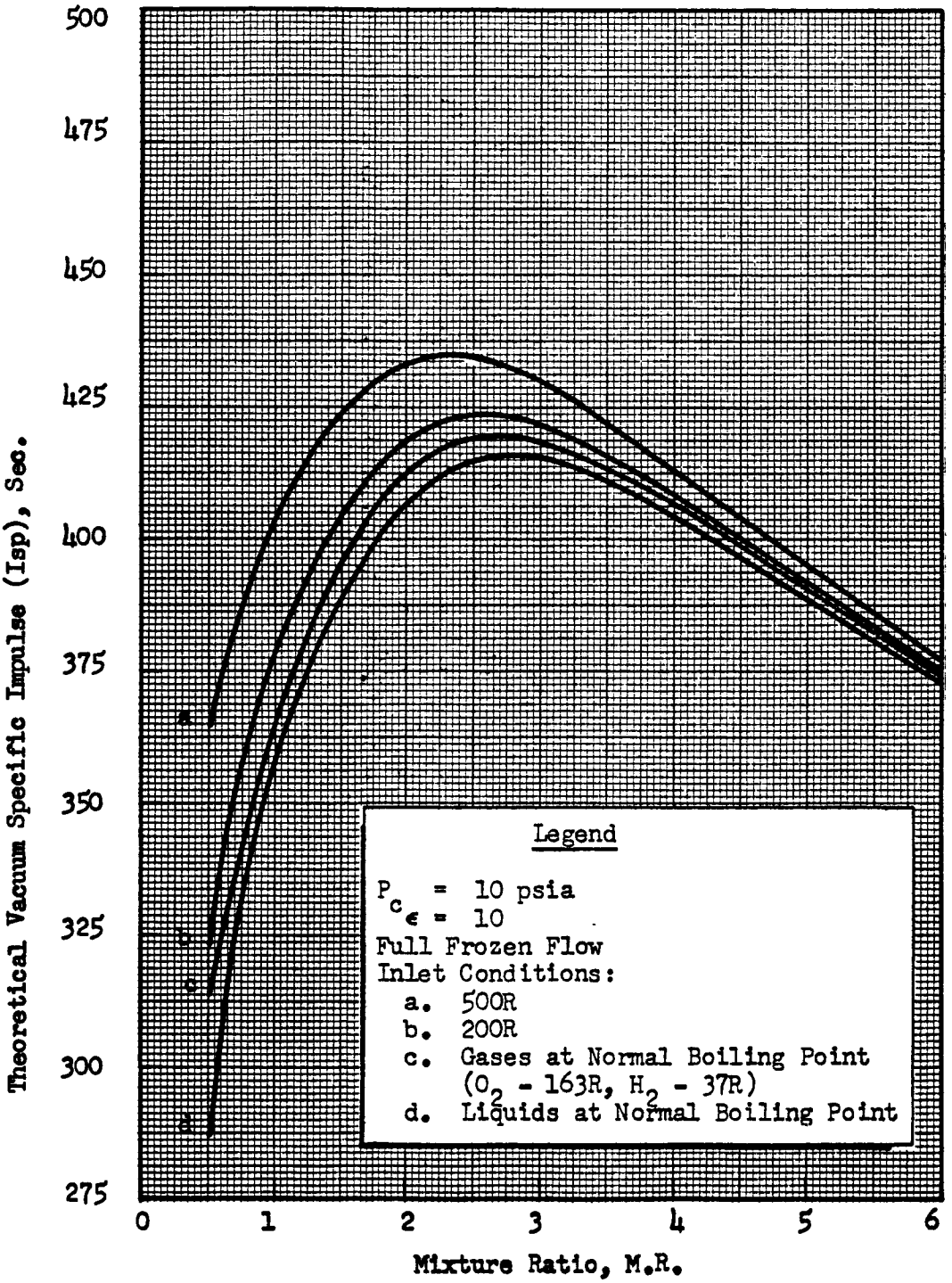

Figure 12. Theoretical Vacuum Specific Impulse as a Function of Mixture Ratio for Four Propellant Conditions (P_c = 10 psia, ϵ = 10, Full Frozen Flow)

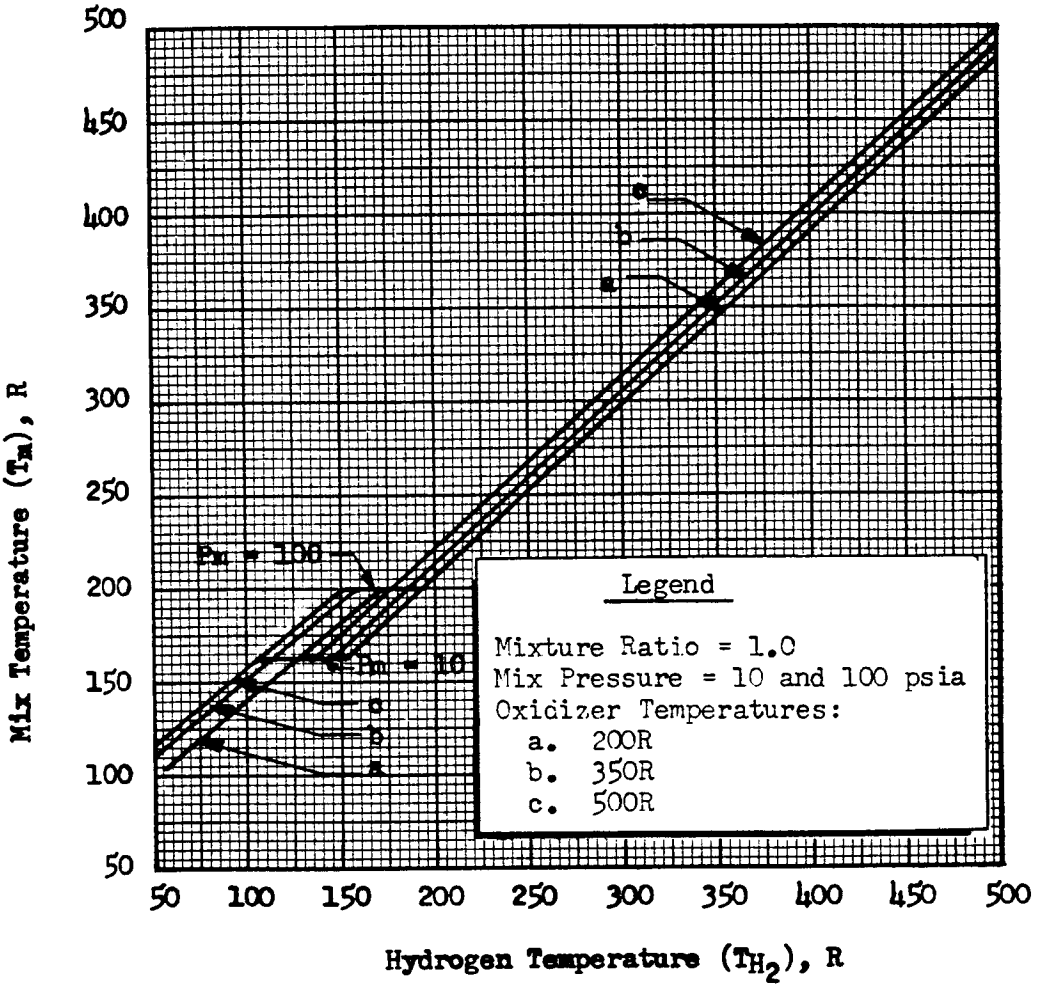

Figure 13. Resulting Mixture Temperature for Various Hydrogen and Oxygen Inlet Temperatures

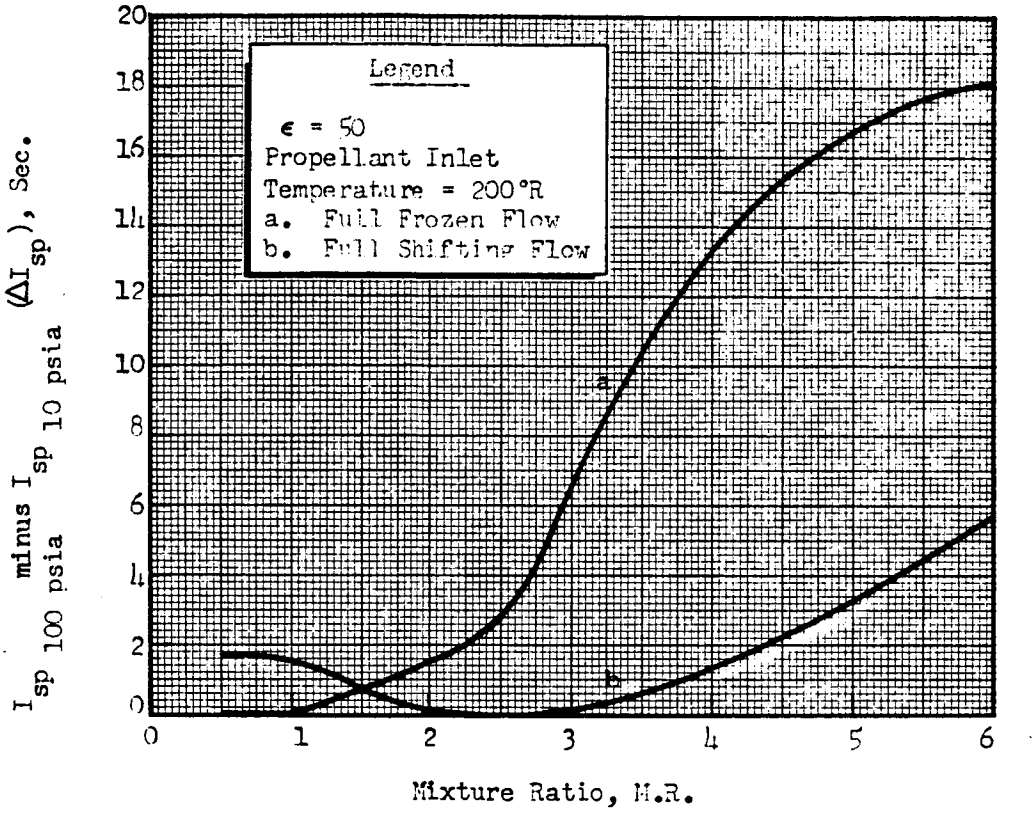

Figure 14. Difference Between Theoretical Specific Impulse at 100 psia and 10 psia Chamber Pressures for Shifting and Frozen Expansion

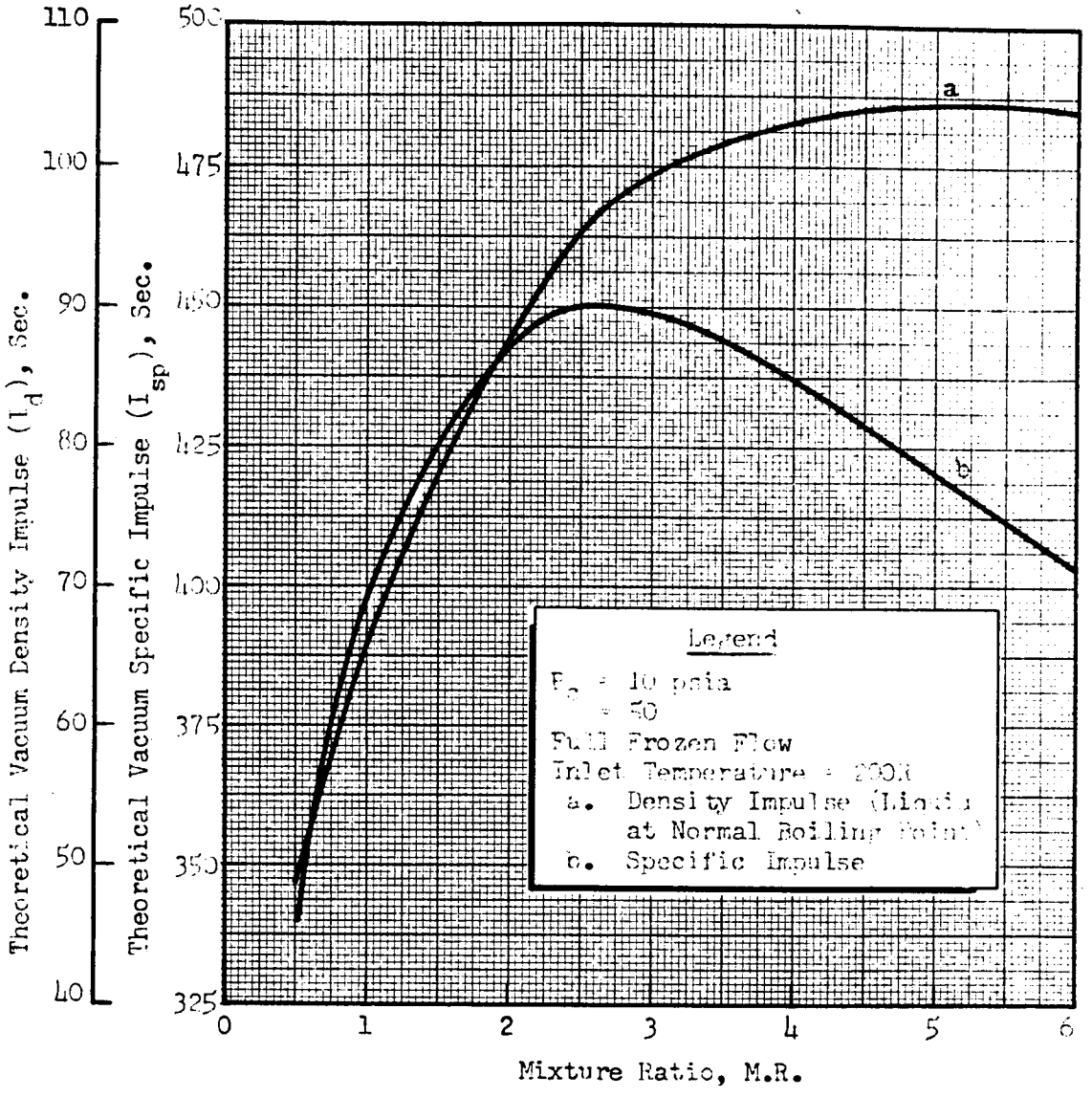

Figure 15. Theoretical Vacuum Density and Specific Impulse as a Function of Mixture Ratio

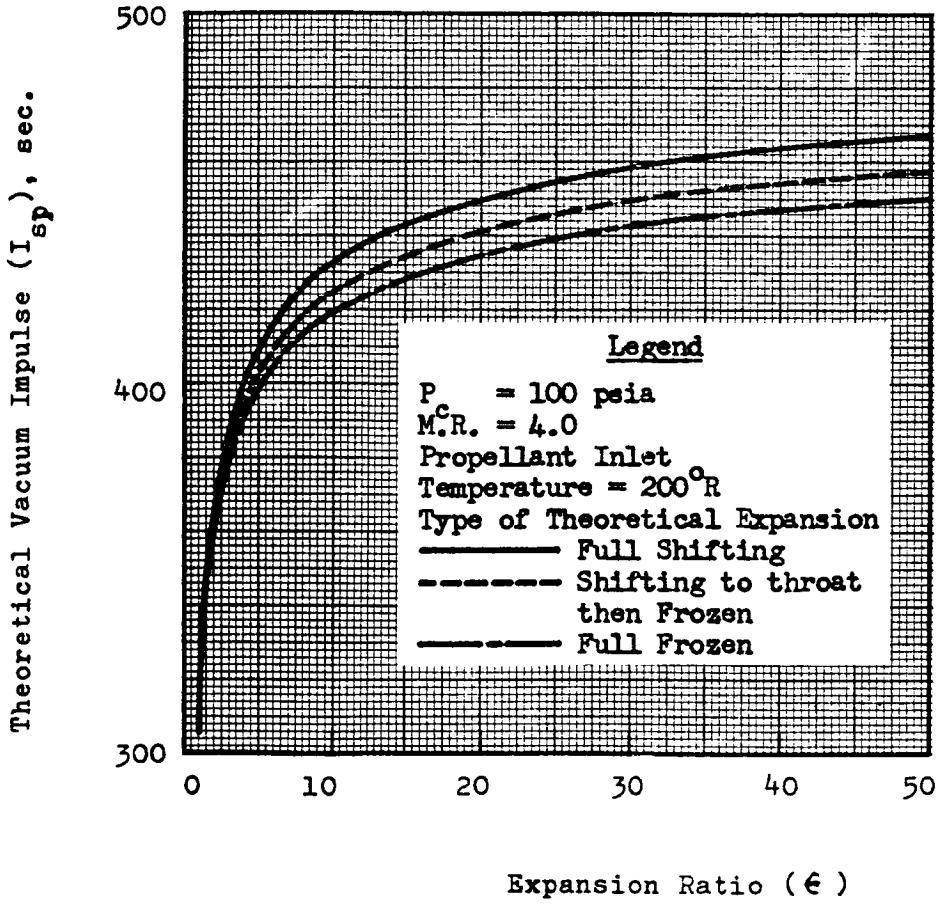

Figure 16. Theoretical Vacuum Specific Impulse as a Function of Expansion Ratio at a Mixture Ratio of 4.0 and Inlet Temperature of 200 R

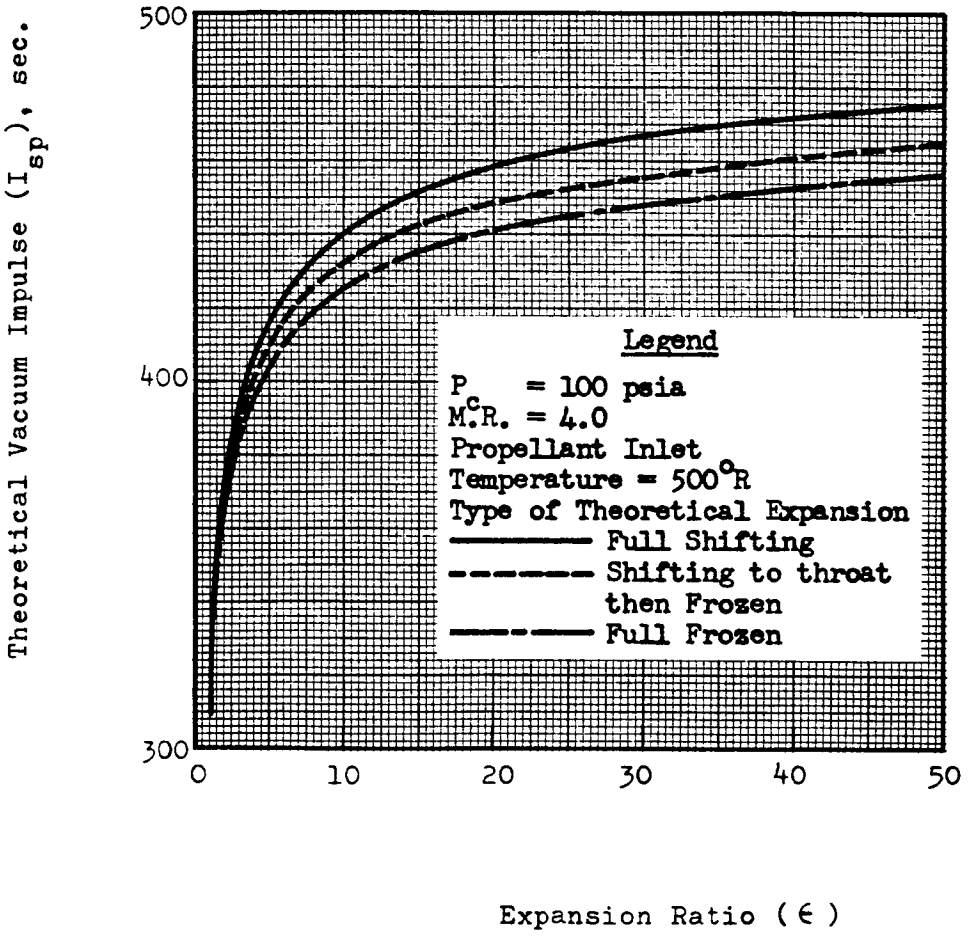

Figure 17. Theoretical Vacuum Specific Impulse as a Function of Expansion Ratio at a Mixture Ratio of 4.0 and Inlet Temperature of 500 R

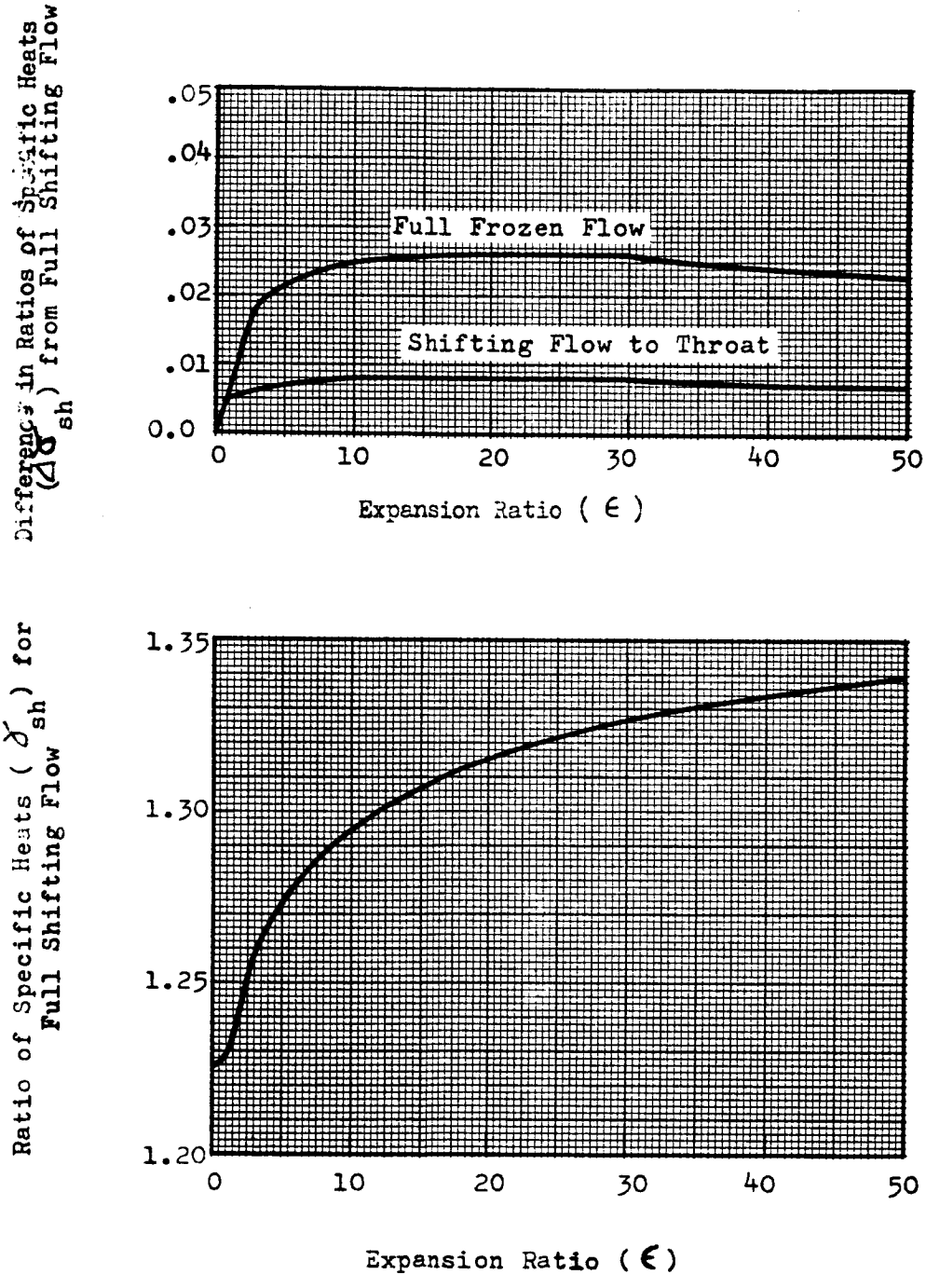

Figure 18. Ratio of Specific Heats (γ) as a Function of Expansion Ratio at a Mixture Ratio of 4.0 and Inlet Temperature of 200 R

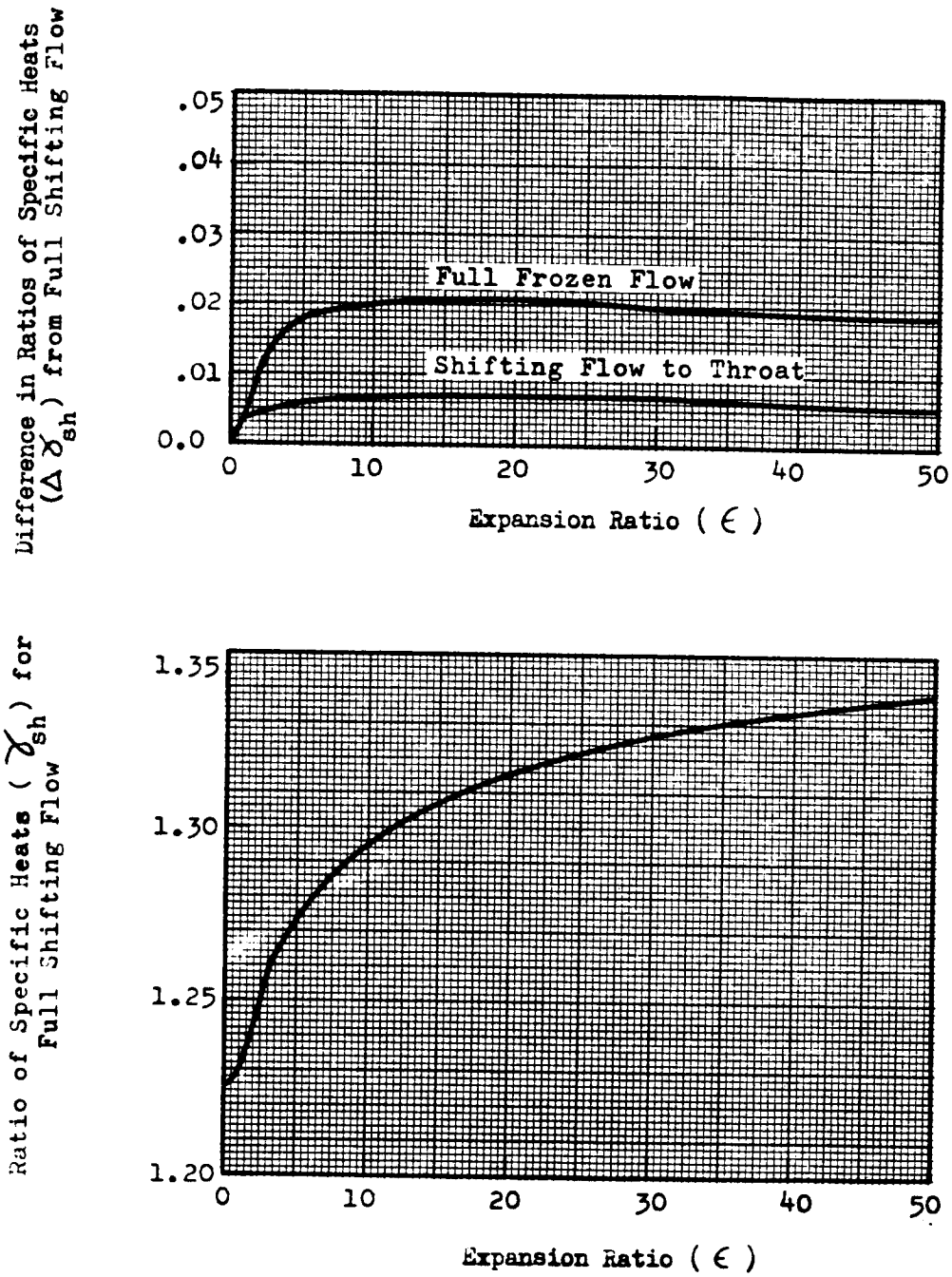

Figure 19. Ratio of Specific Heats (γ) as a Function of Expansion Ratio at a Mixture Ratio of 4.0 and Inlet Temperature of 500 R.

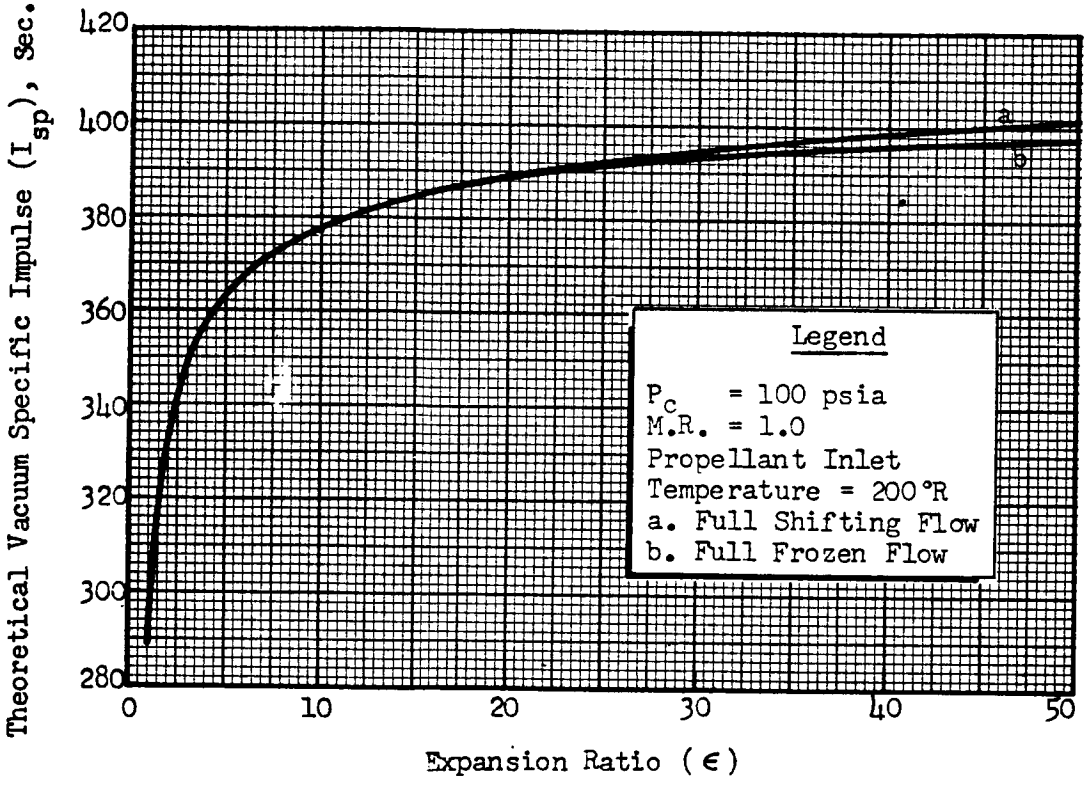

Figure 20. Theoretical Vacuum Specific Impulse as a Function of Expansion Ratio (P_c = 100 psia, M. R. = 1.0)

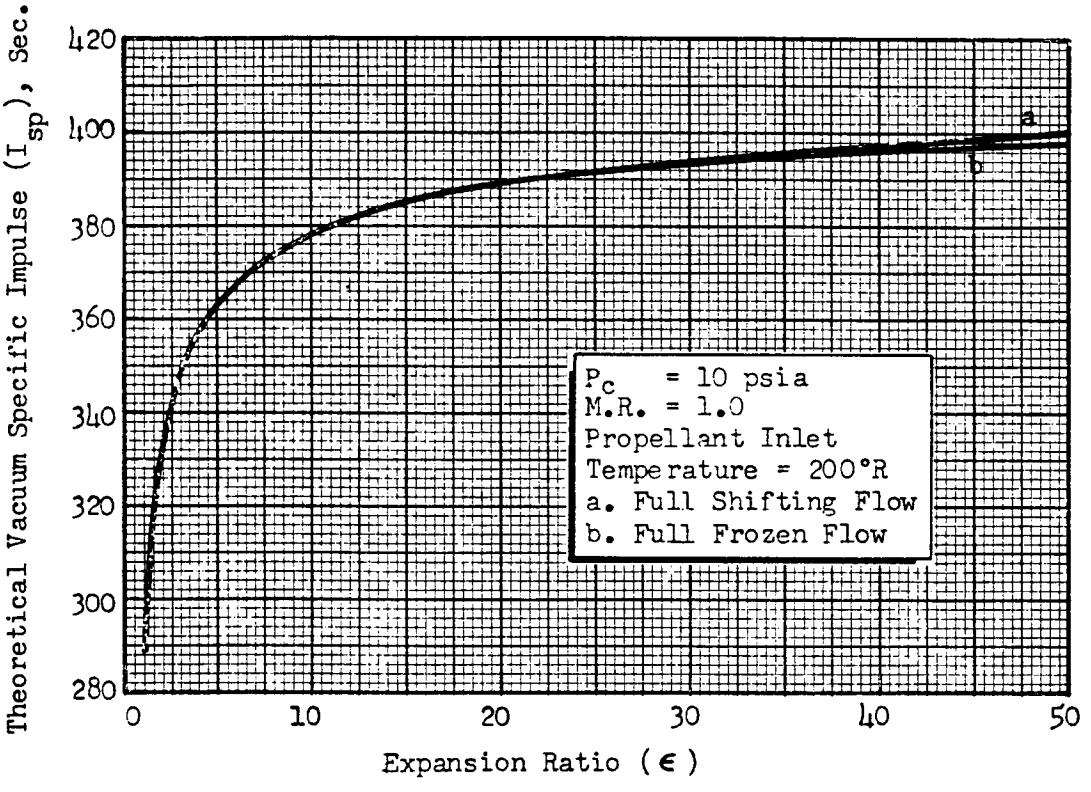

Figure 21. Theoretical Vacuum Specific Impulse as a Function of Expansion Ratio (P_c = 10 psia, M. R. = 1.0)

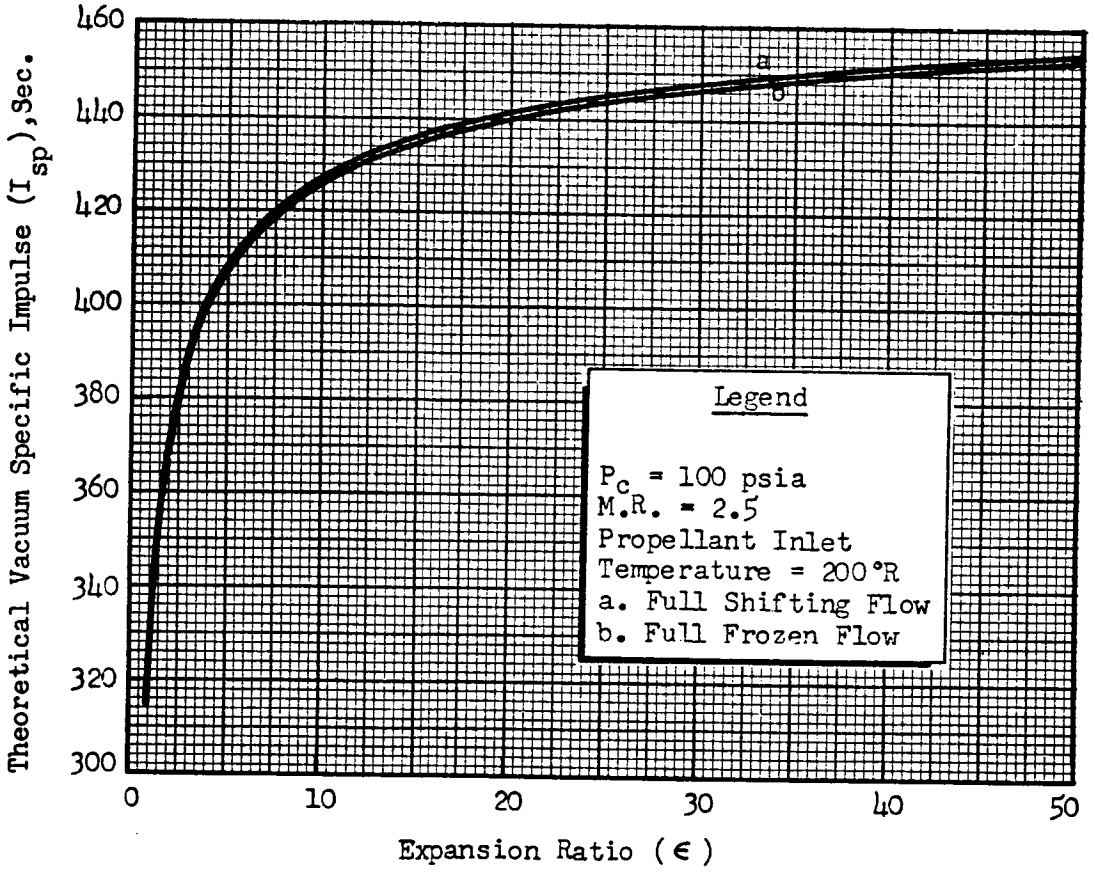

Figure 22. Theoretical Vacuum Specific Impulse as a Function of Expansion Ratio (P_c = 100 psia, M. R. = 2.5)

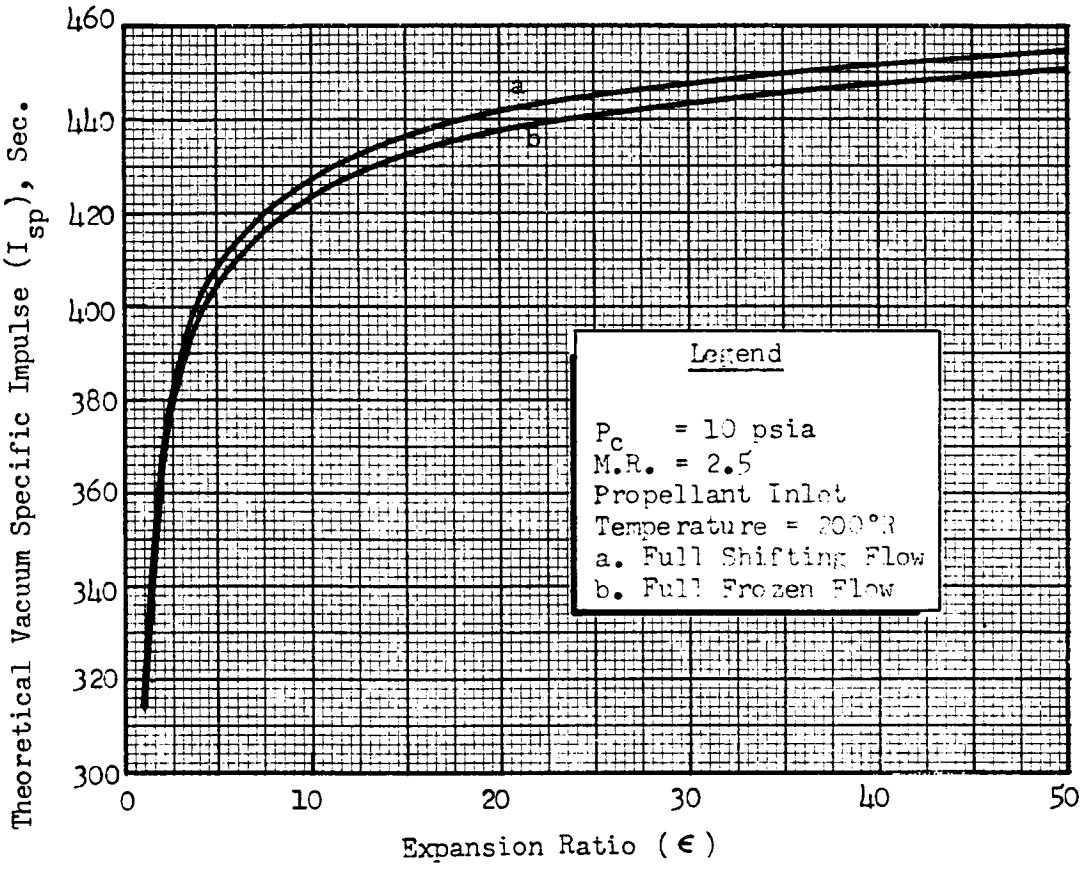

Figure 23. Theoretical Vacuum Specific Impulse as a Function of Expansion Ratio (P_c = 10 psia, M.R. = 2.5)

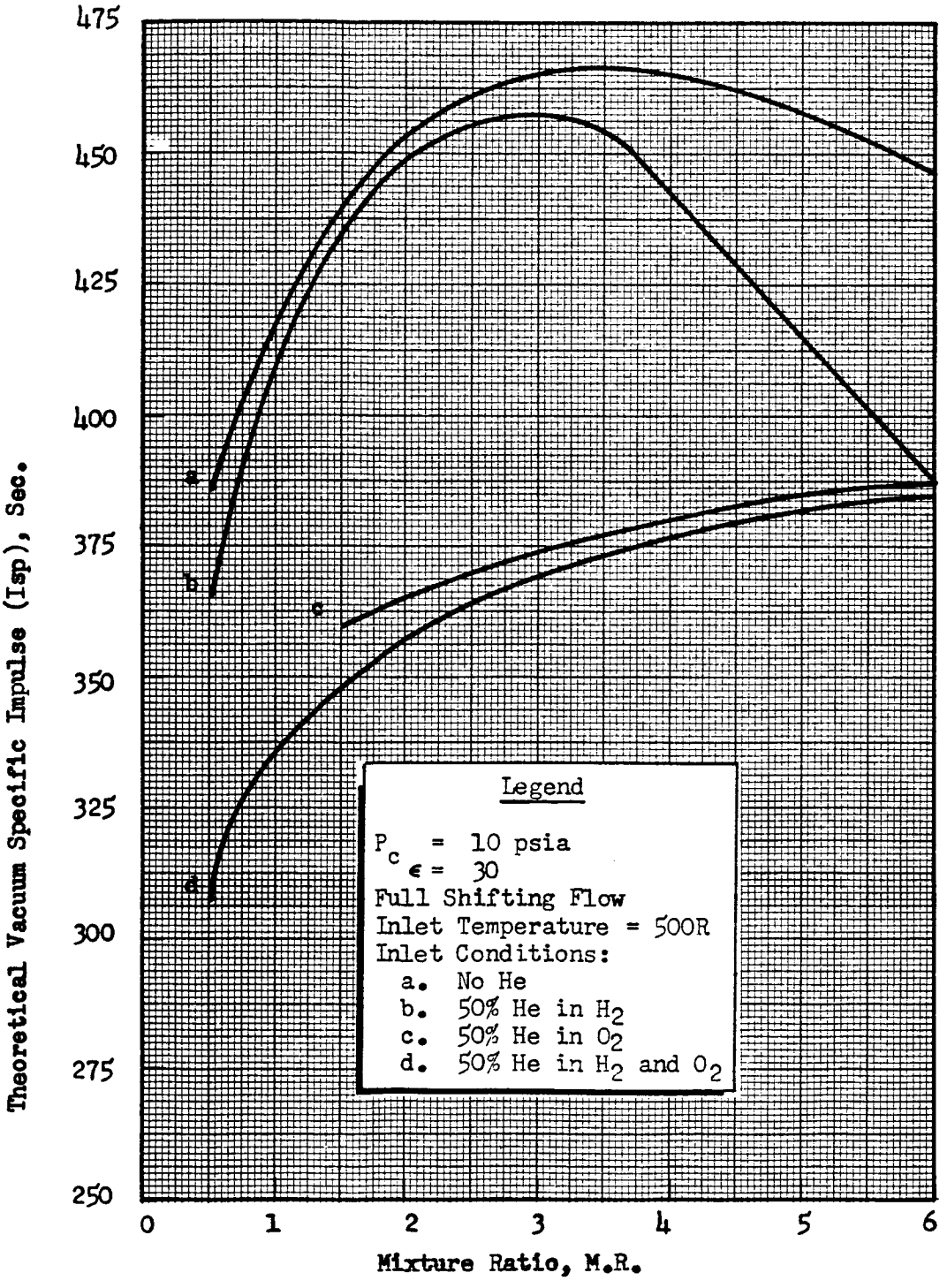

Figure 24. Theoretical Vacuum Specific Impulse as a Function of Mixture Ratio for Four Propellant Conditions with Helium Diluent (P_c = 10 psia, ϵ = 30, Full Shifting Flow)

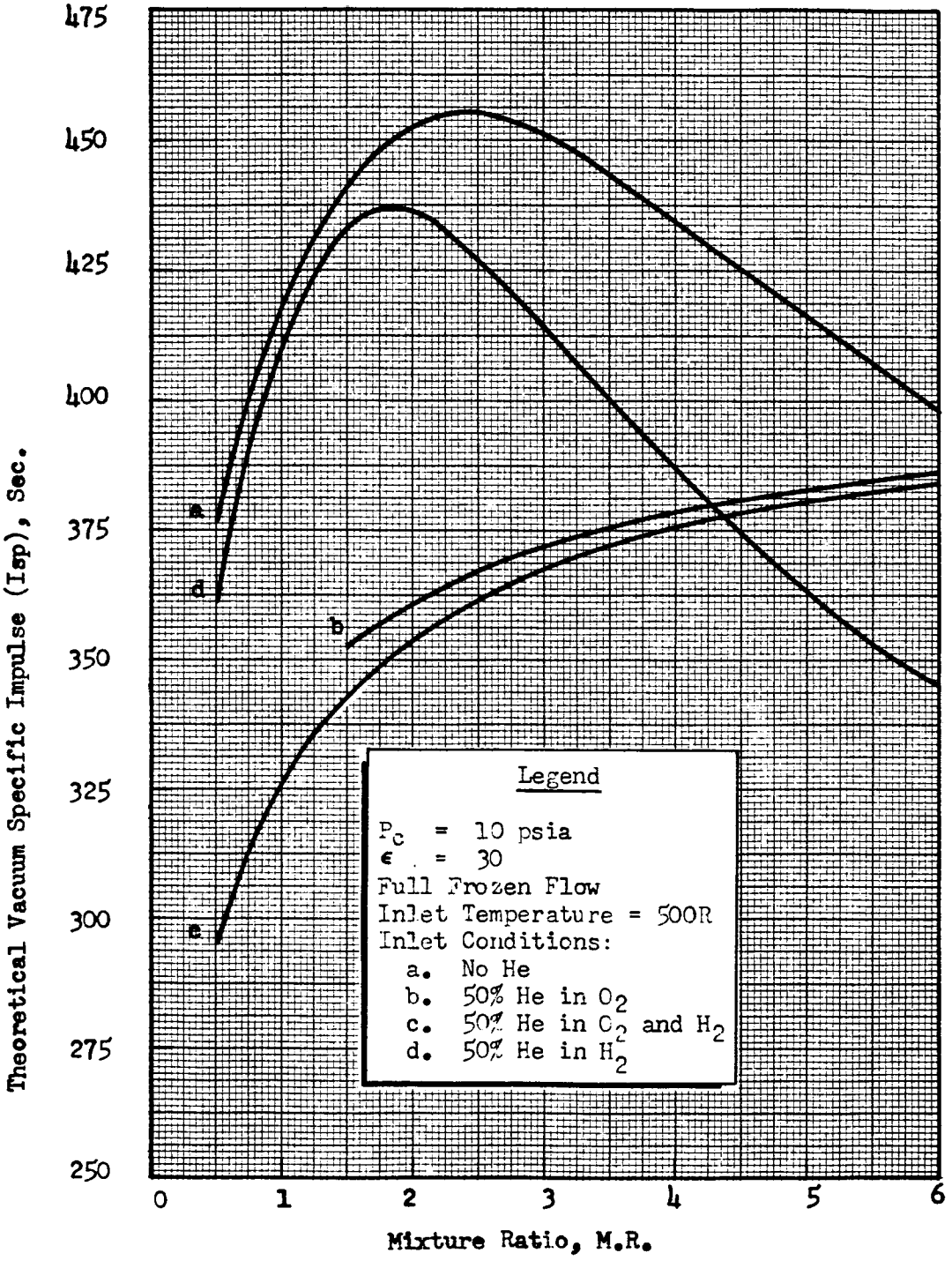

Figure 25. Theoretical Vacuum Specific Impulse as a Function of Mixture Ratio for Four Propellant Conditions with Helium Diluent (P_c = 10 psia, ϵ = 30, Full Frozen Flow)

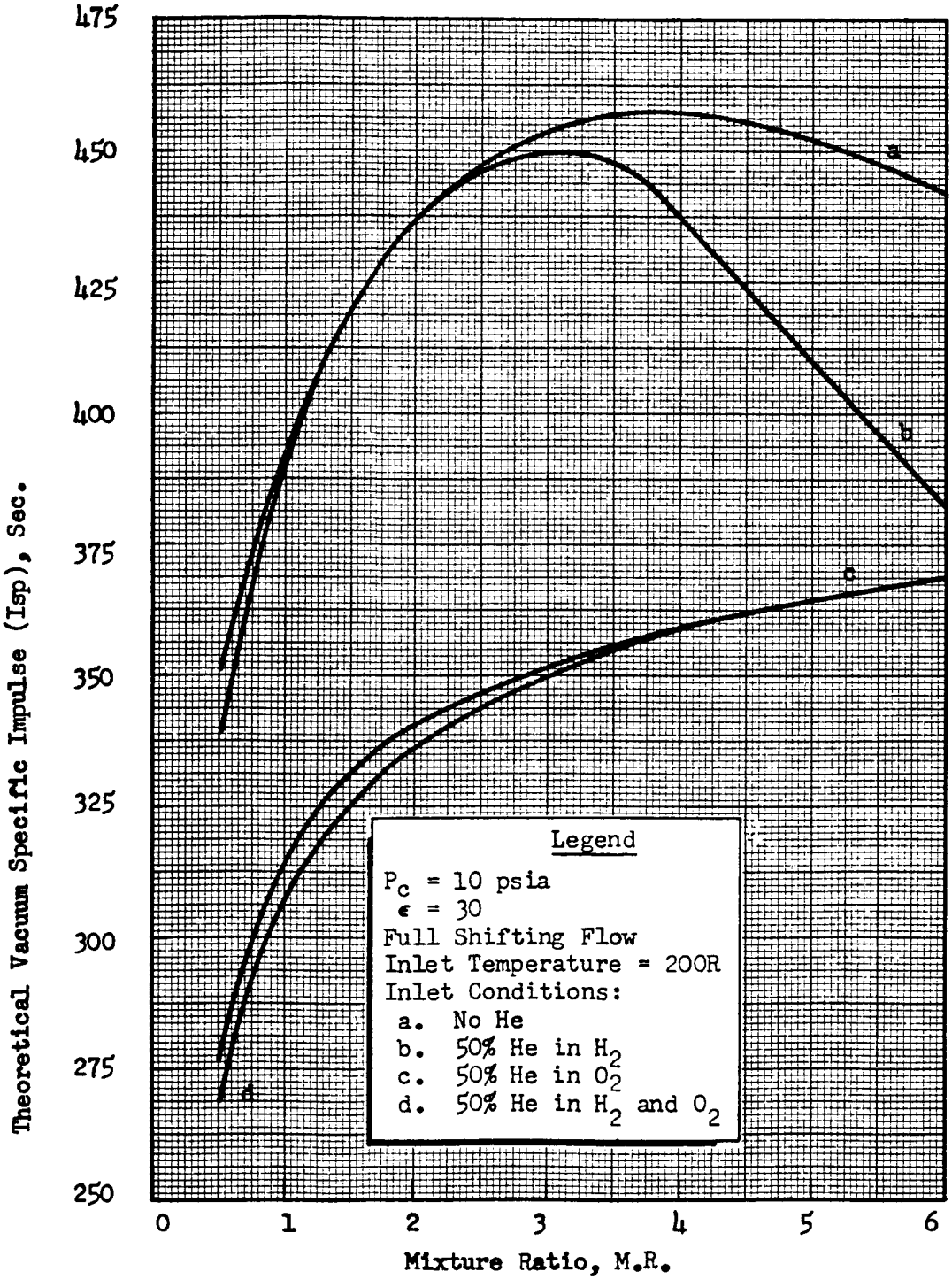

Figure 26. Theoretical Vacuum Specific Impulse as a Function of Mixture Ratio for Four Propellant Conditions with Helium Diluent (P_c = 10 psia, ϵ = 30, Full Shifting Flow)

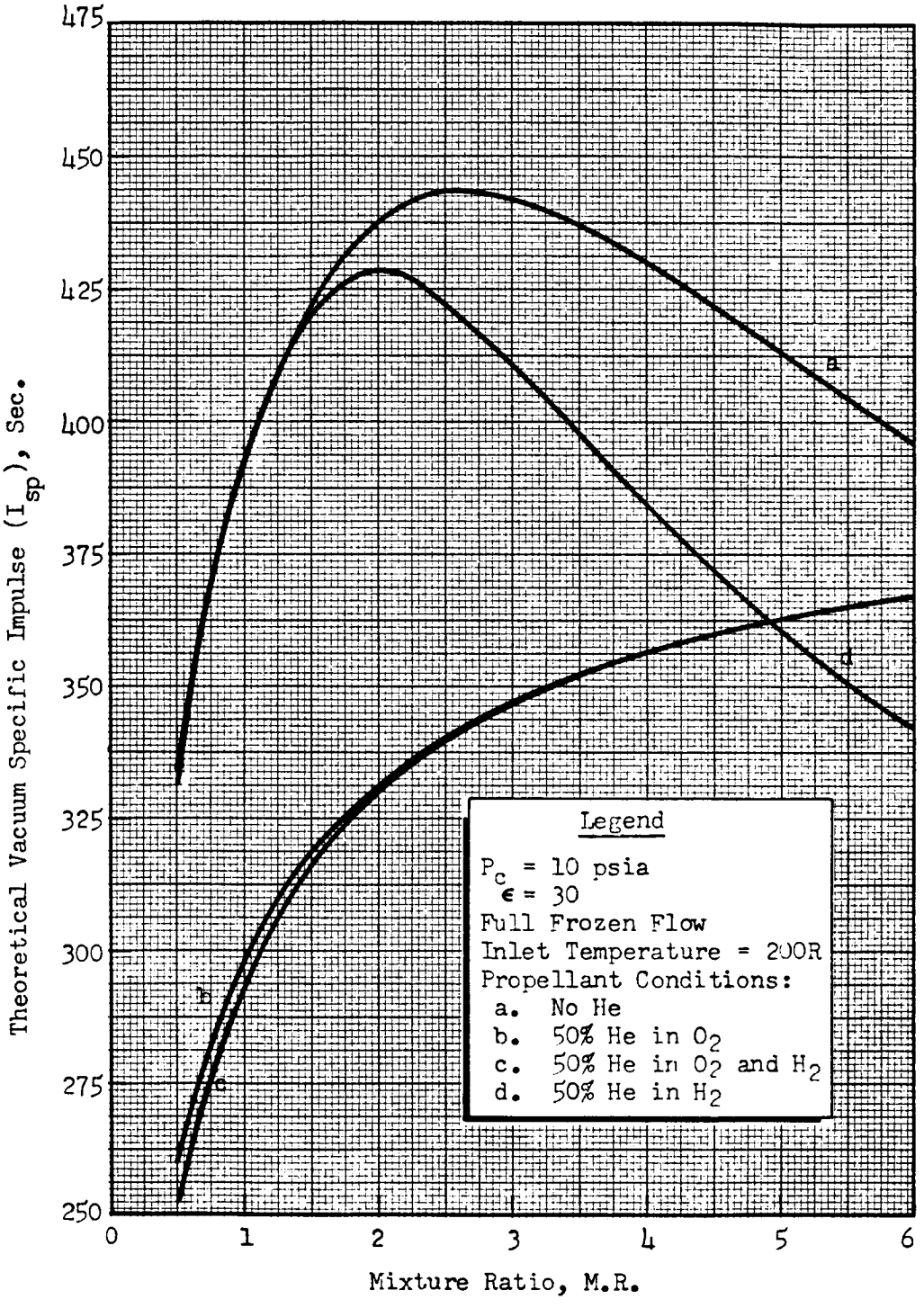

Figure 27. Theoretical Vacuum Specific Impulse as a Function of Mixture Ratio for Four Propellant Conditions with Helium Diluent (P_c = 10 psia, ϵ = 30, Full Frozen Flow)

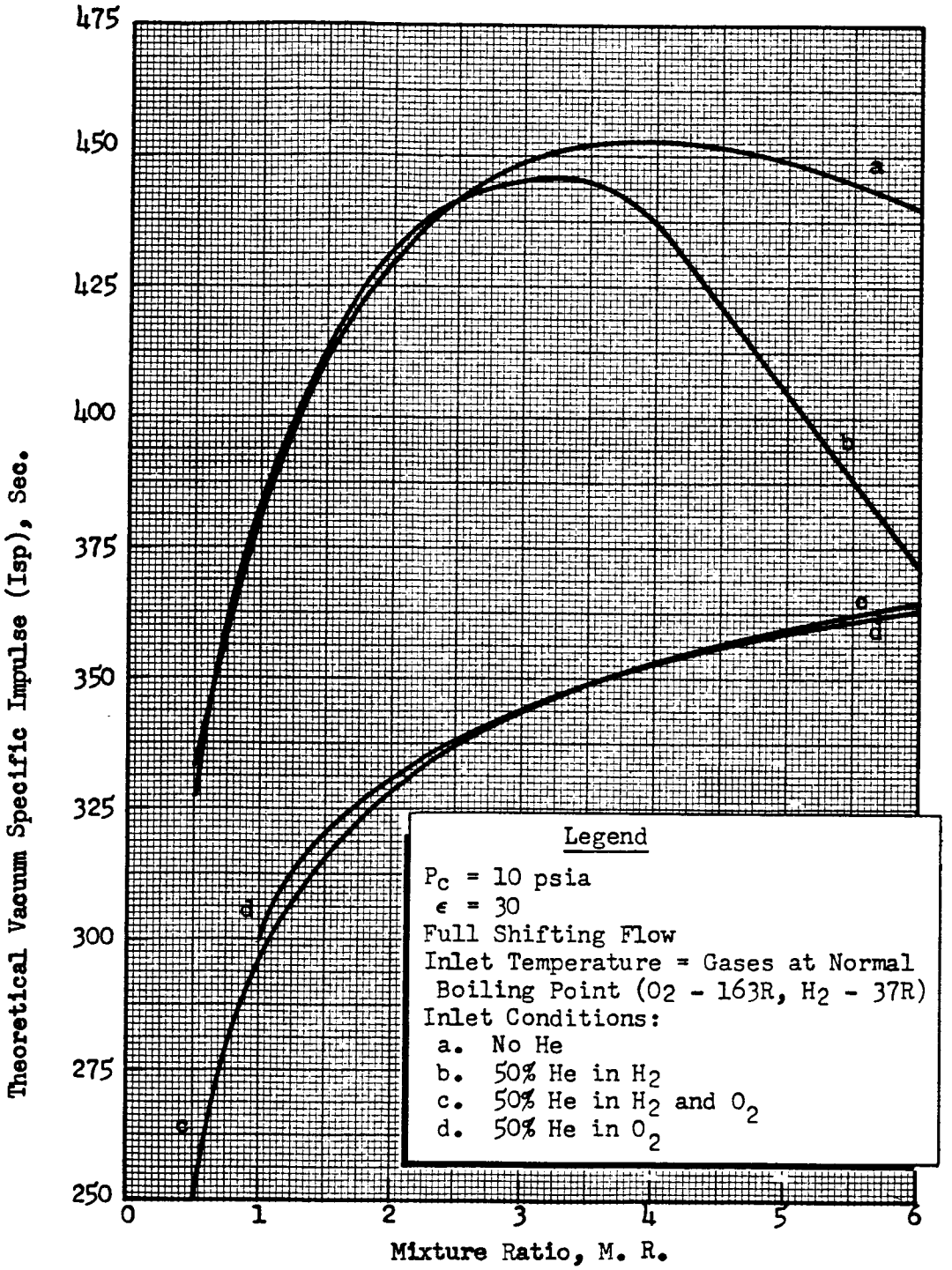

Figure 28. Theoretical Vacuum Specific Impulse as a Function of Mixture Ratio for Four Propellant Conditions with Helium Diluent (P_c = 10 psia, ϵ = 30, Full Shifting Flow)

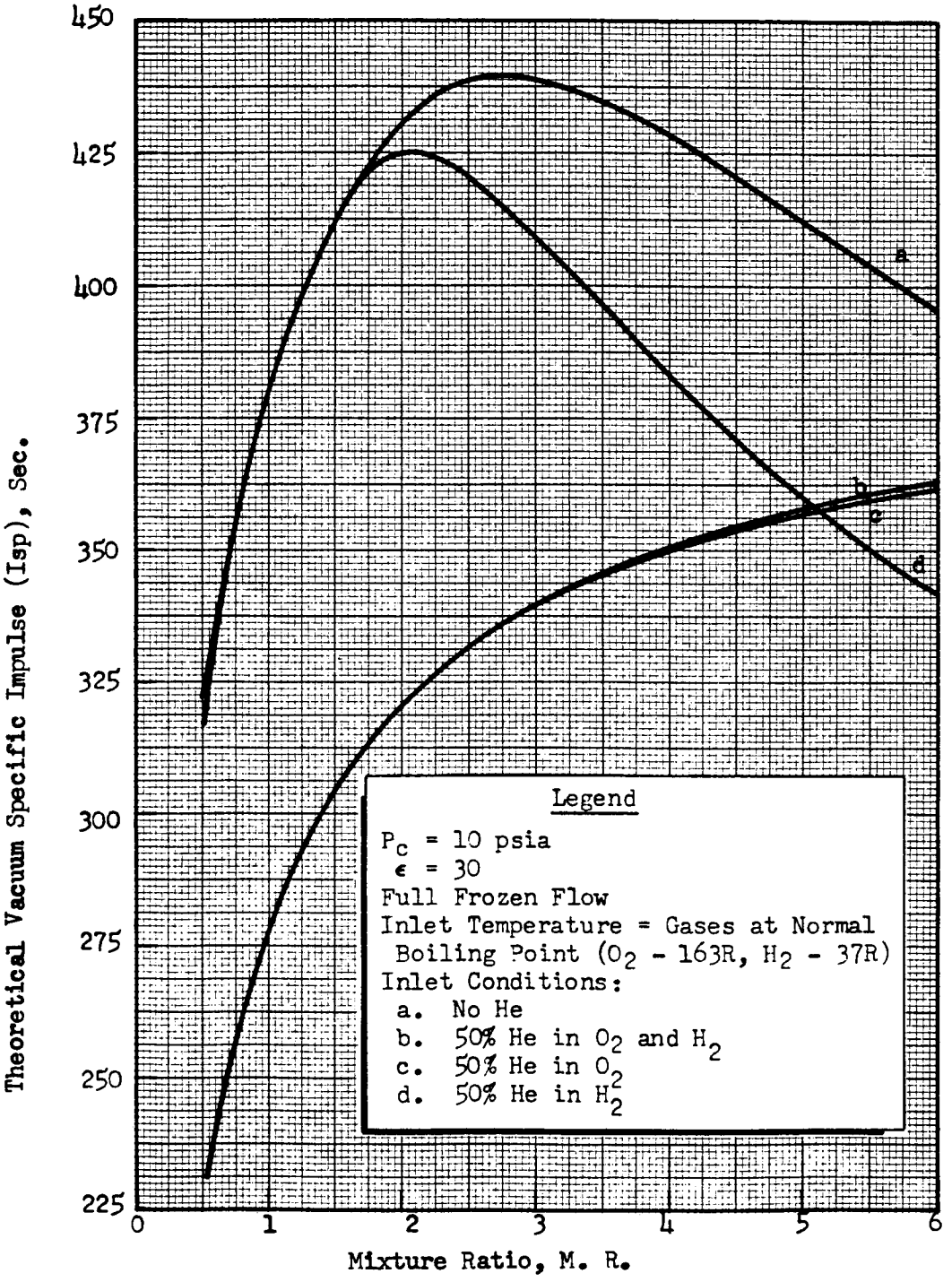

Figure 29. Theoretical Vacuum Specific Impulse as a Function of Mixture Ratio for Four Propellant Conditions with Helium Diluent (P_c = 10 psia, ϵ = 30, Full Frozen Flow)

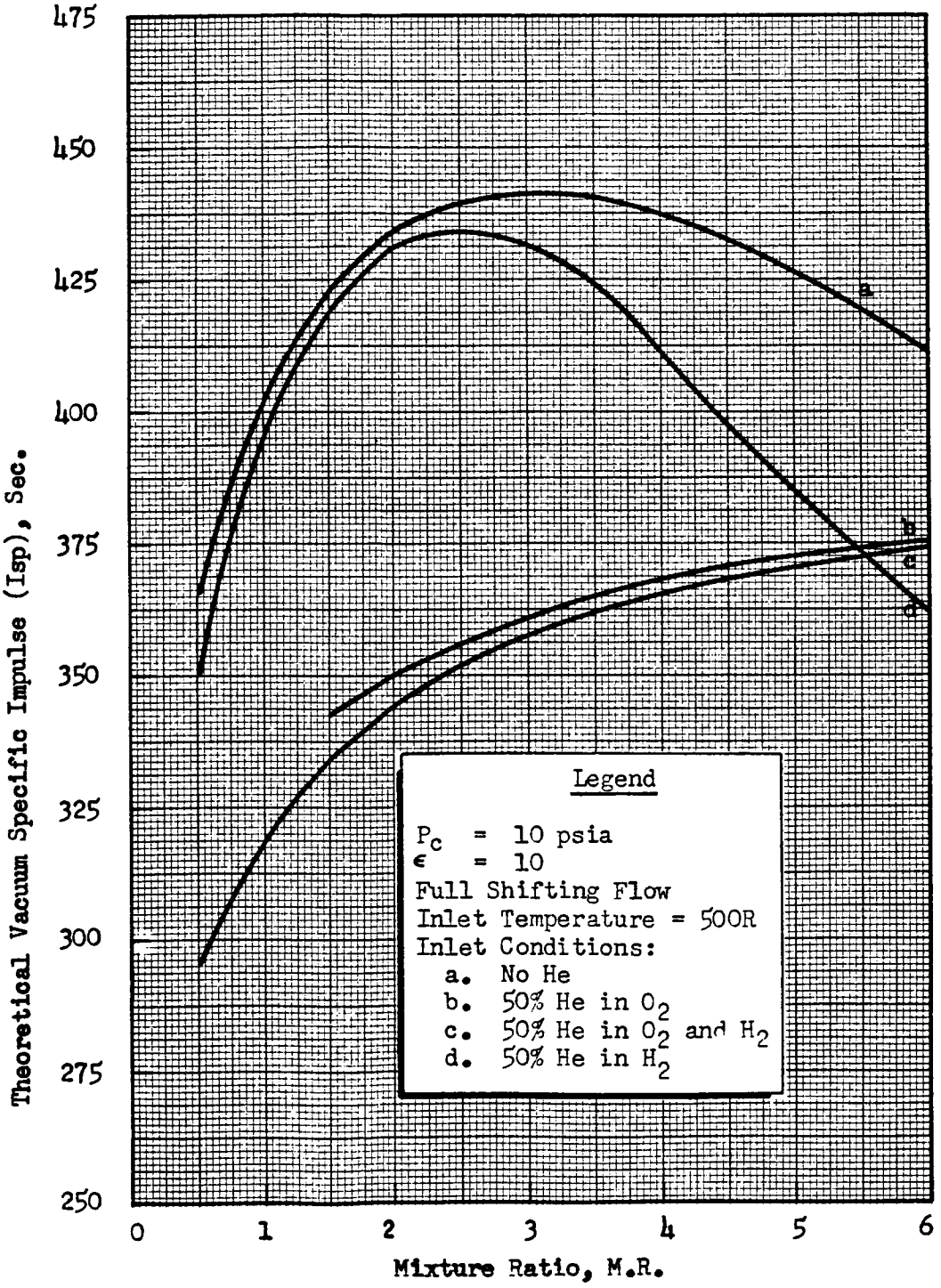

Figure 30. Theoretical Vacuum Specific Impulse as a Function of Mixture Ratio for Four Propellant Conditions with Helium Diluent (P_c = 10 psia, ϵ = 10, Full Shifting Flow)

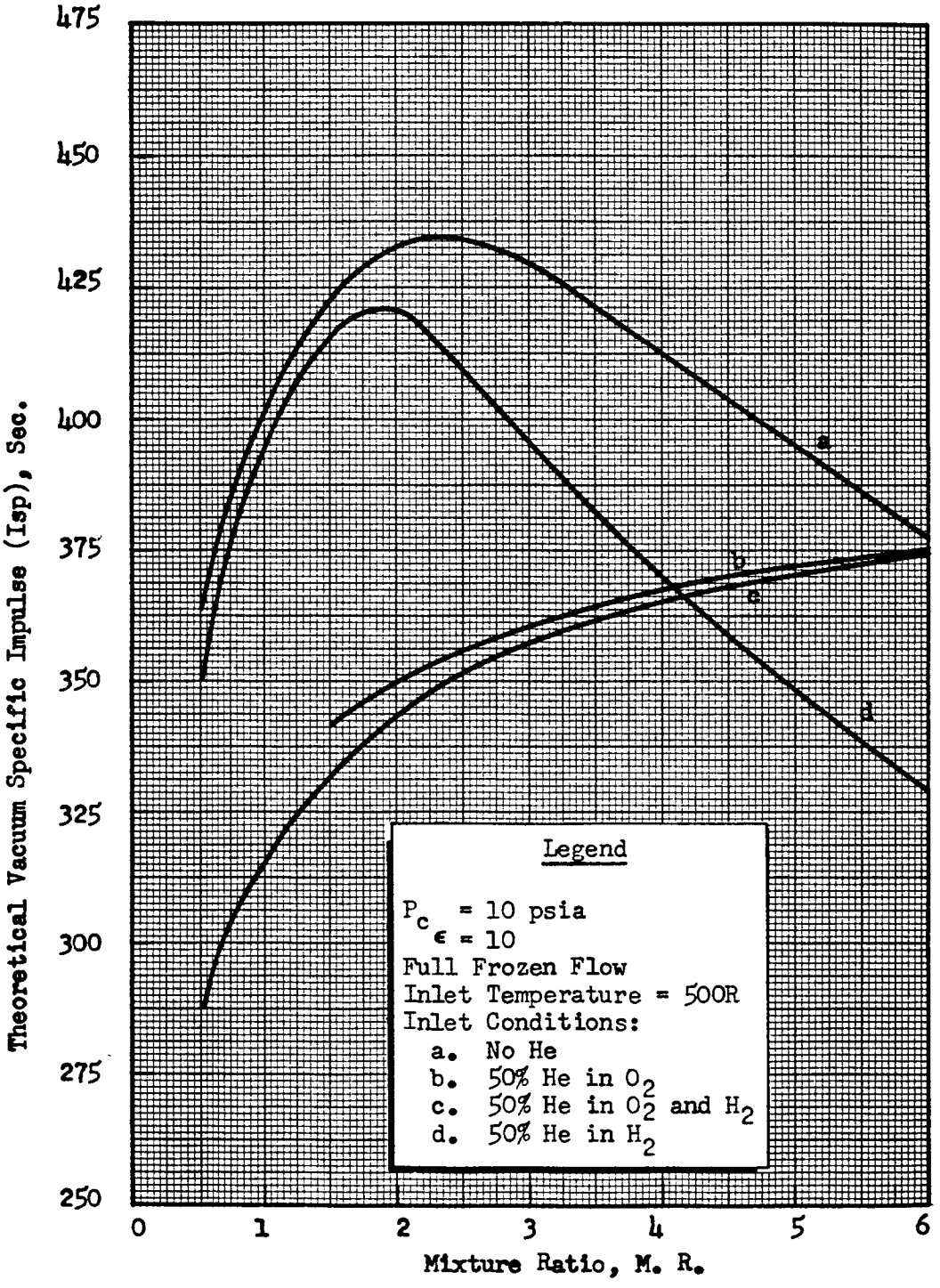

Figure 31. Theoretical Vacuum Specific Impulse as a Function of Mixture Ratio for Four Propellant Conditions with Helium Diluent (P_c = 10 psia, ϵ = 10, Full Frozen Flow)

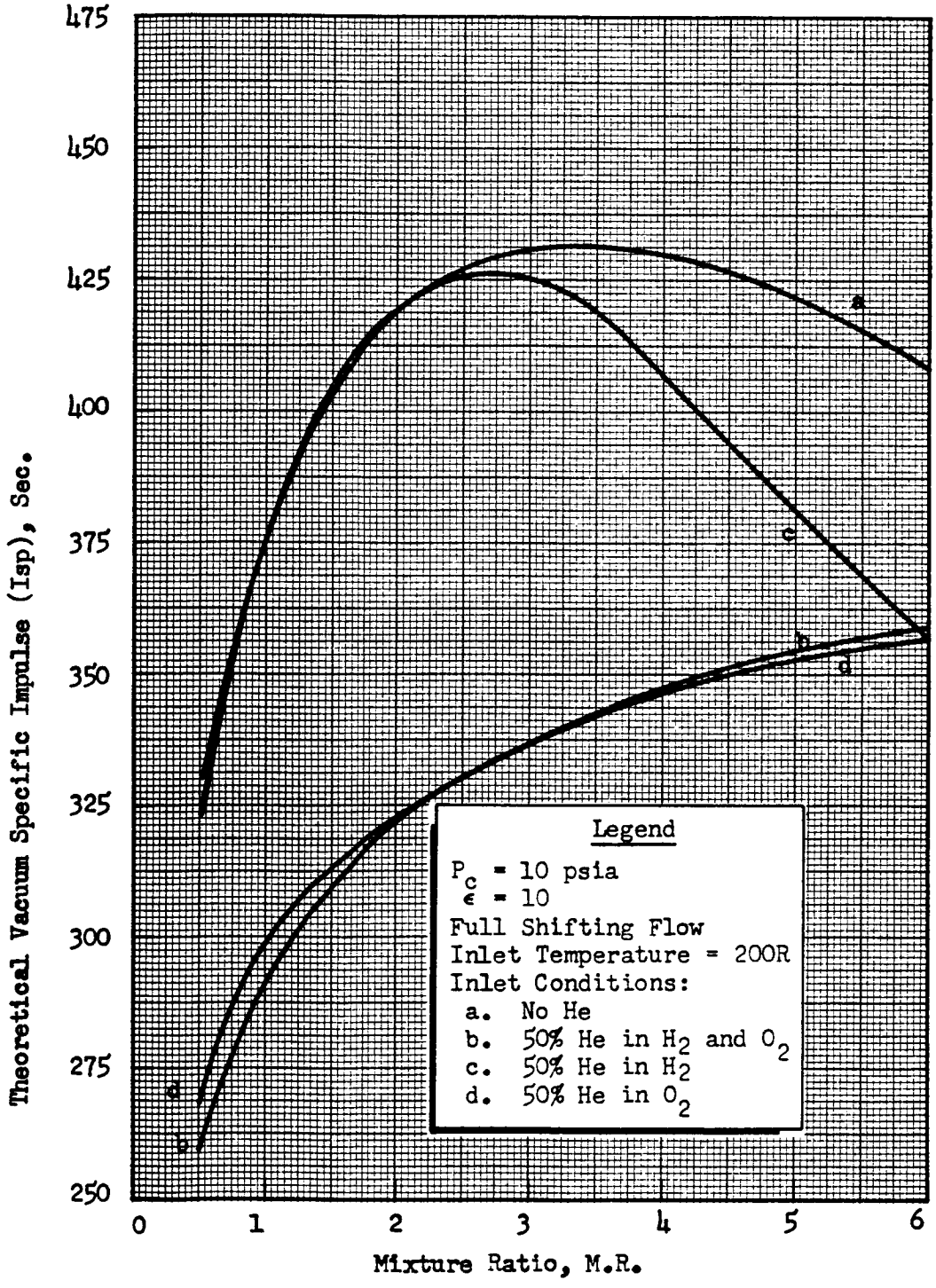

Figure 32. Theoretical Vacuum Specific Impulse as a Function of Mixture Ratio for Four Propellant Conditions with Helium Diluent (P_c = 10 psia, ϵ = 10, Full Shifting Flow)

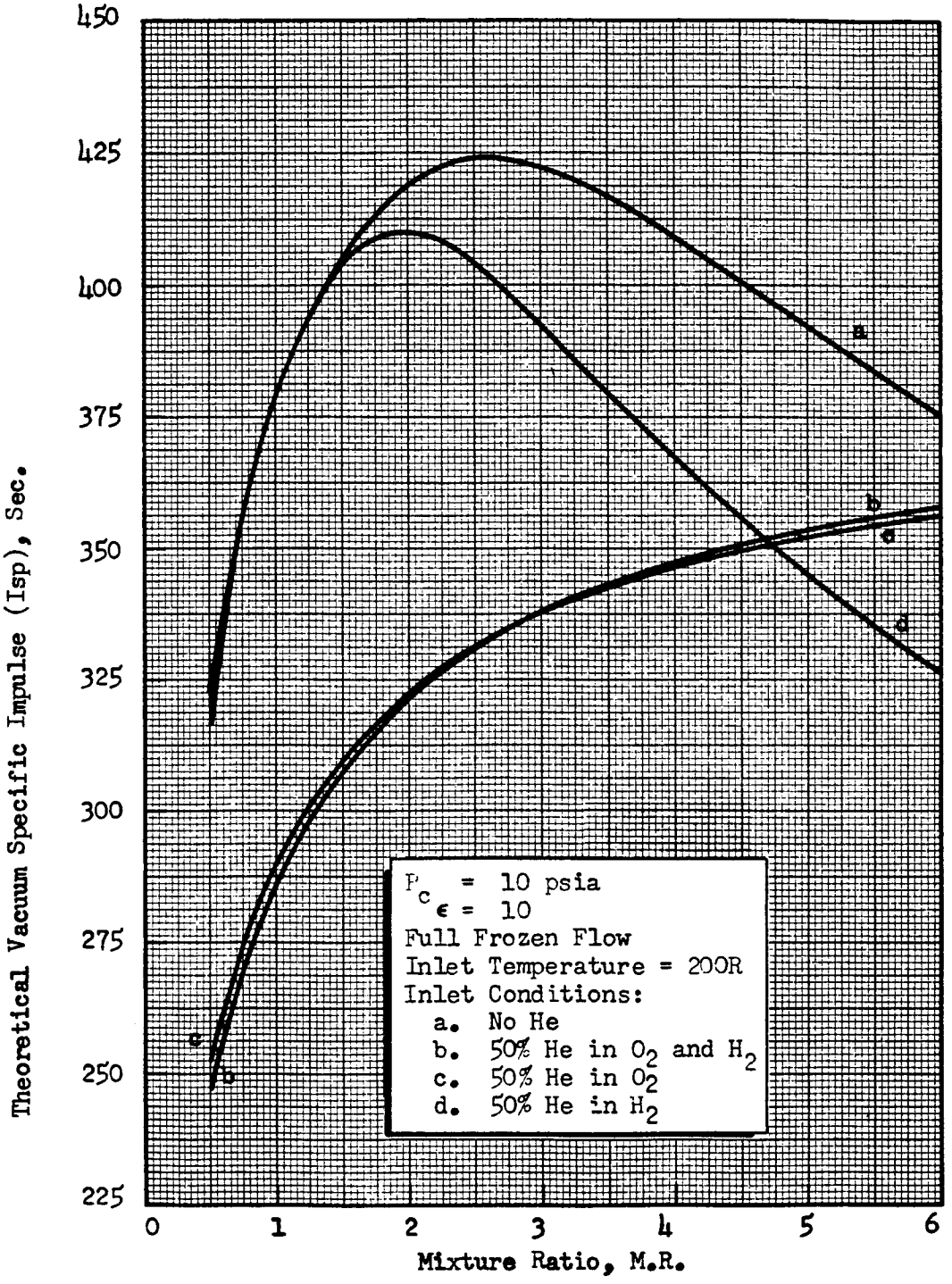

Figure 33. Theoretical Vacuum Specific Impulse as a Function of Mixture Ratio for Four Propellant Conditions with Helium Diluent (P_c = 10 psia, ϵ = 10, Full Frozen Flow)

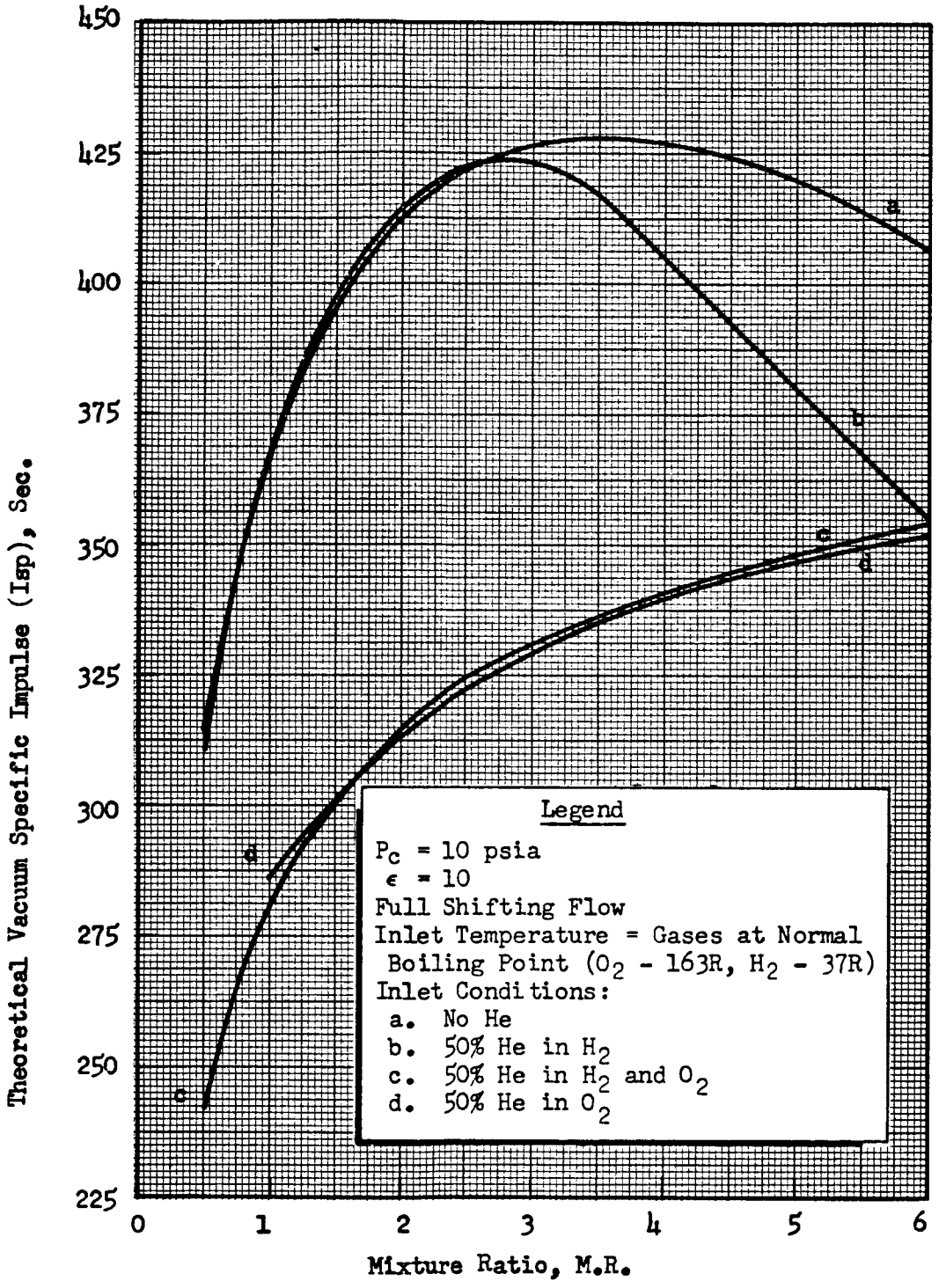

Figure 34. Theoretical Vacuum Specific Impulse as a Function of Mixture Ratio for Four Propellant Conditions with Helium Diluent (P_c = 10 psia, ϵ = 10, Full Shifting Flow)

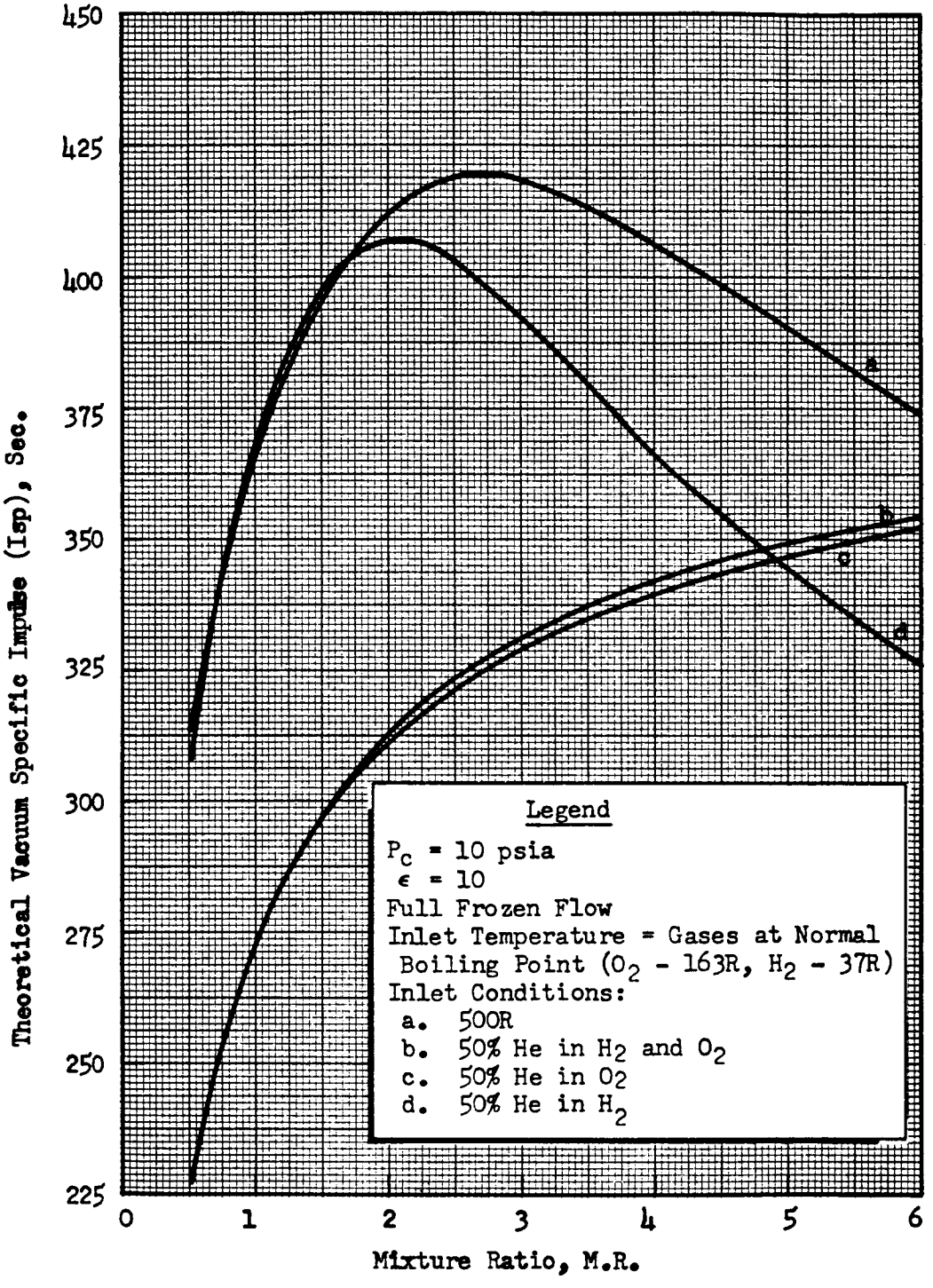

Figure 35 Theoretical Vacuum Specific Impulse as a Function of Mixture Ratio for Four Propellant Conditions with Helium Diluent (P_c = 10 psia, ϵ = 10, Full Frozen Flow)

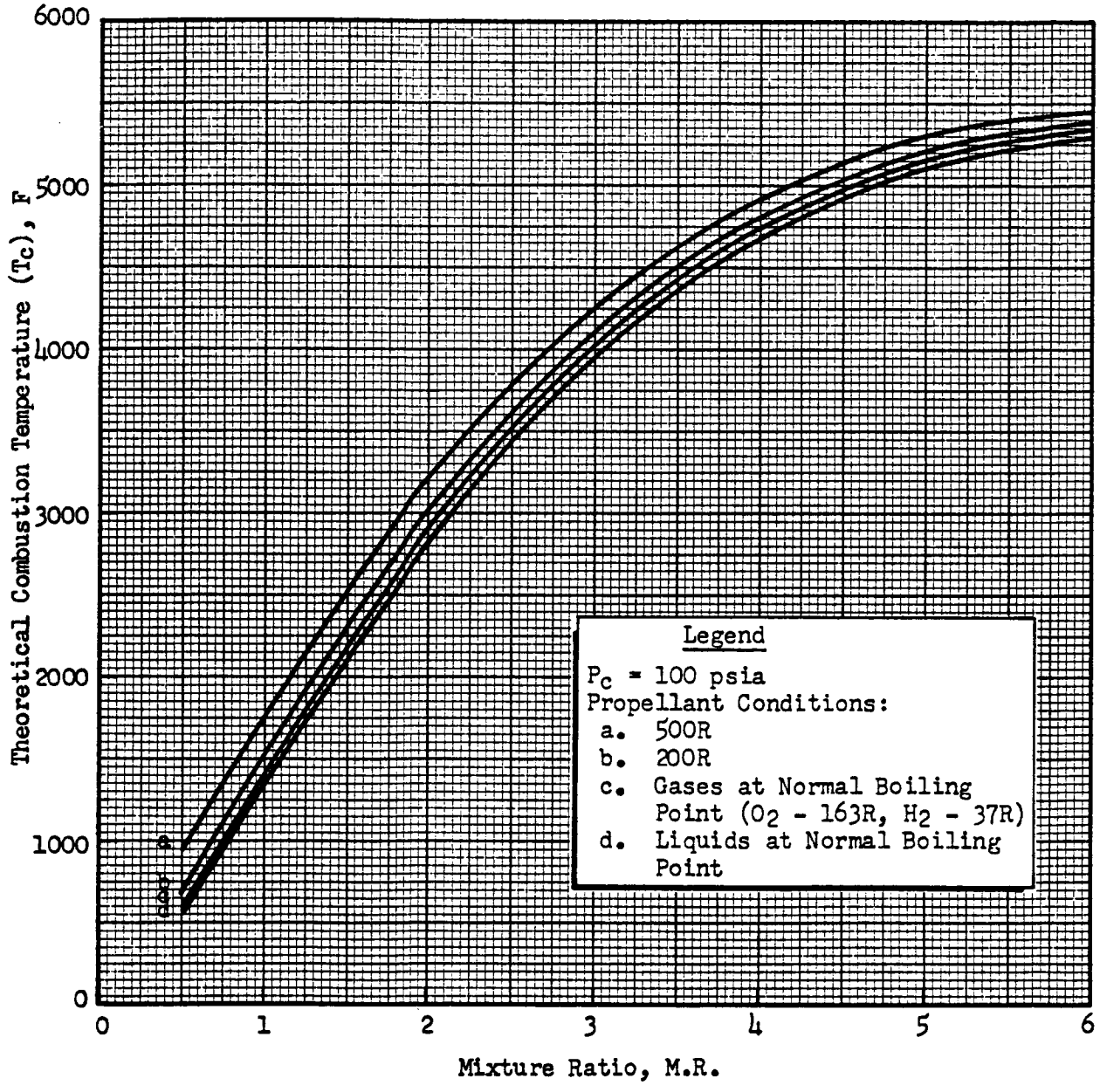

Figure 36. Theoretical Combustion Temperature as a Function of Mixture Ratio for Four Propellant Conditions (P_c = 100 psia)

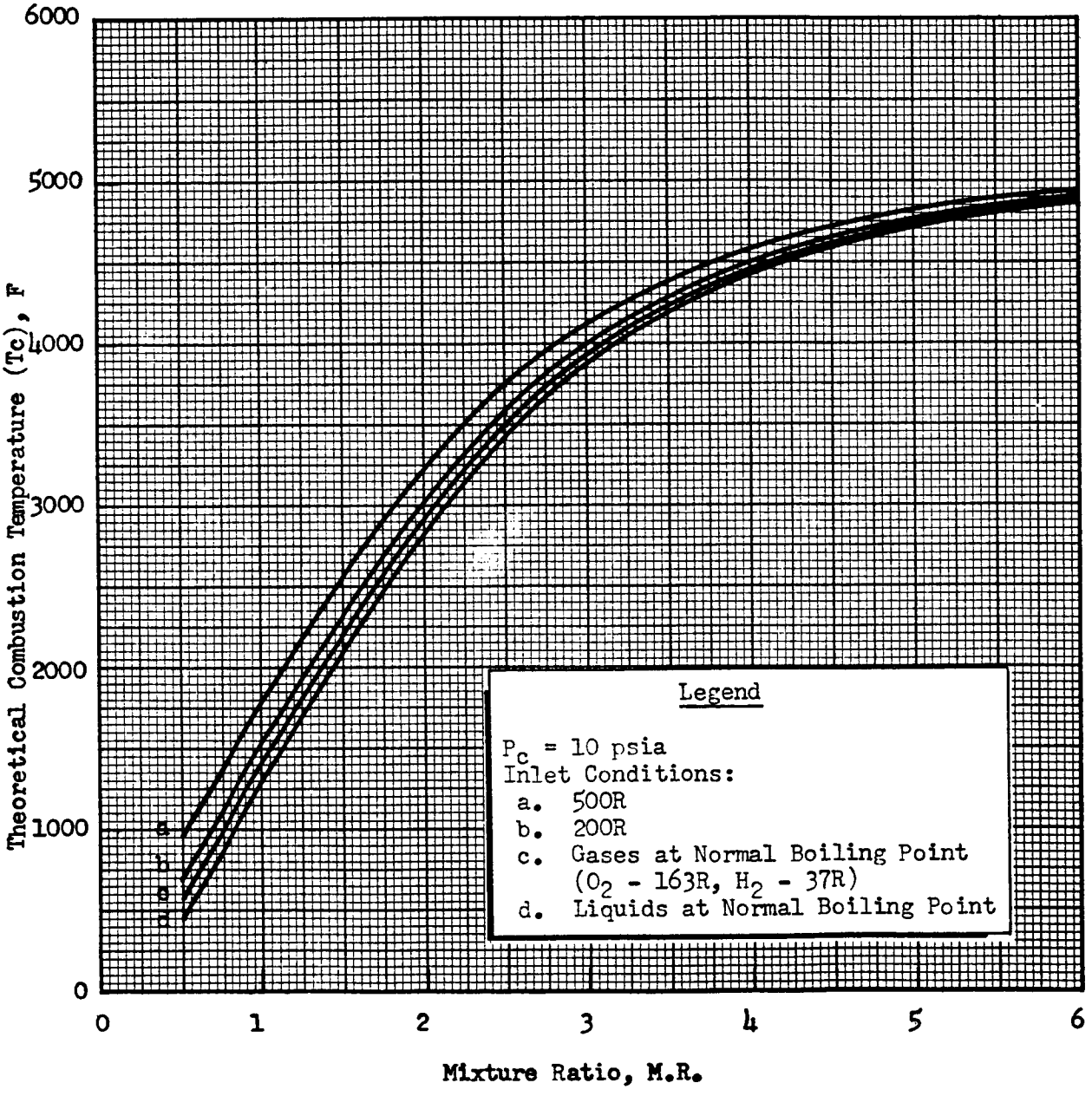

Figure 37. Theoretical Combustion Temperature as a Function of Mixture Ratio for Four Propellant Conditions (P_c = 10 psia)

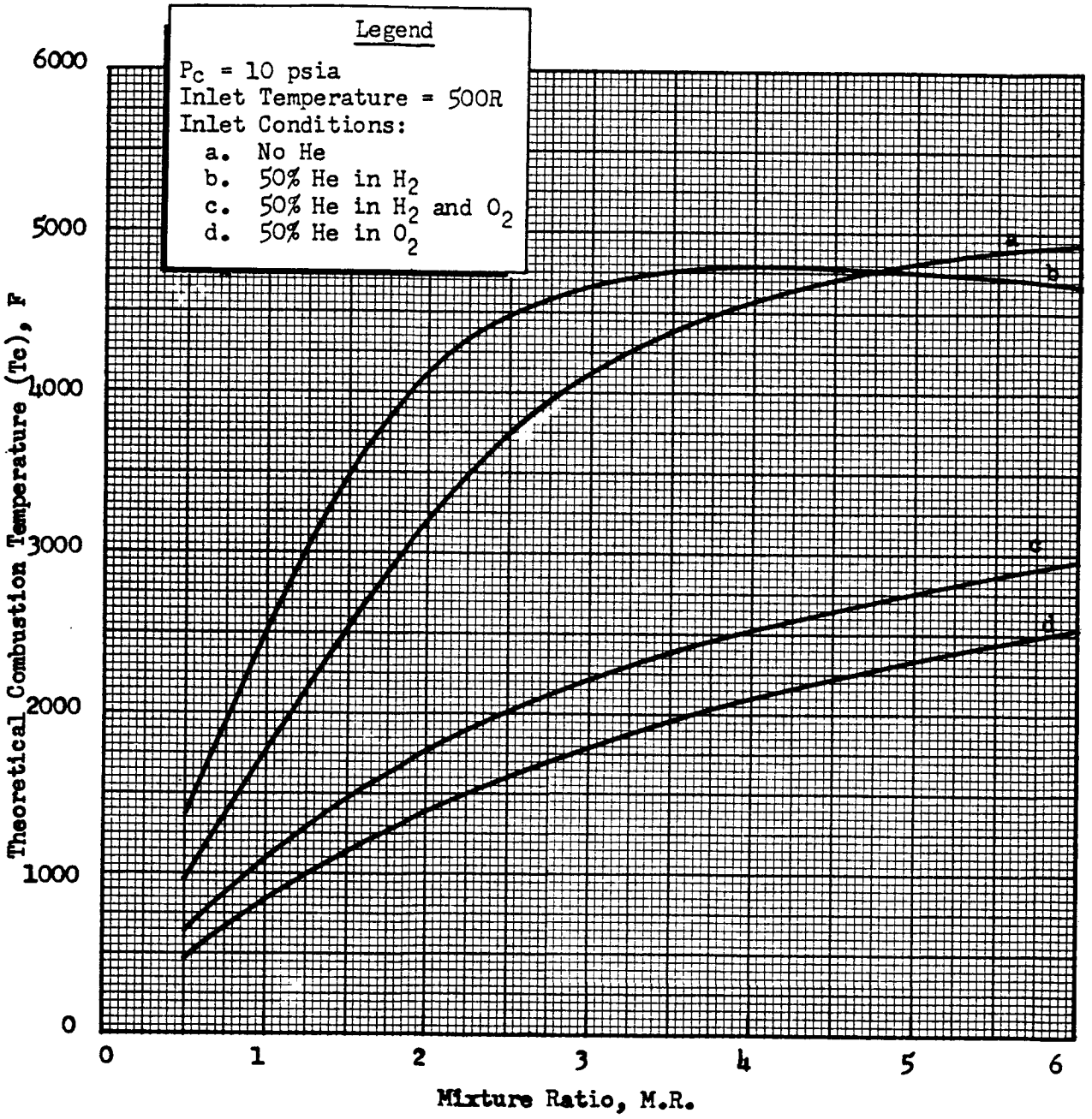

Figure 38. Theoretical Combustion Temperature as a Function of Mixture Ratio for Four Propellant Conditions with Helium Diluent (P_c = 10 psia, Propellant Temperature = 500R)

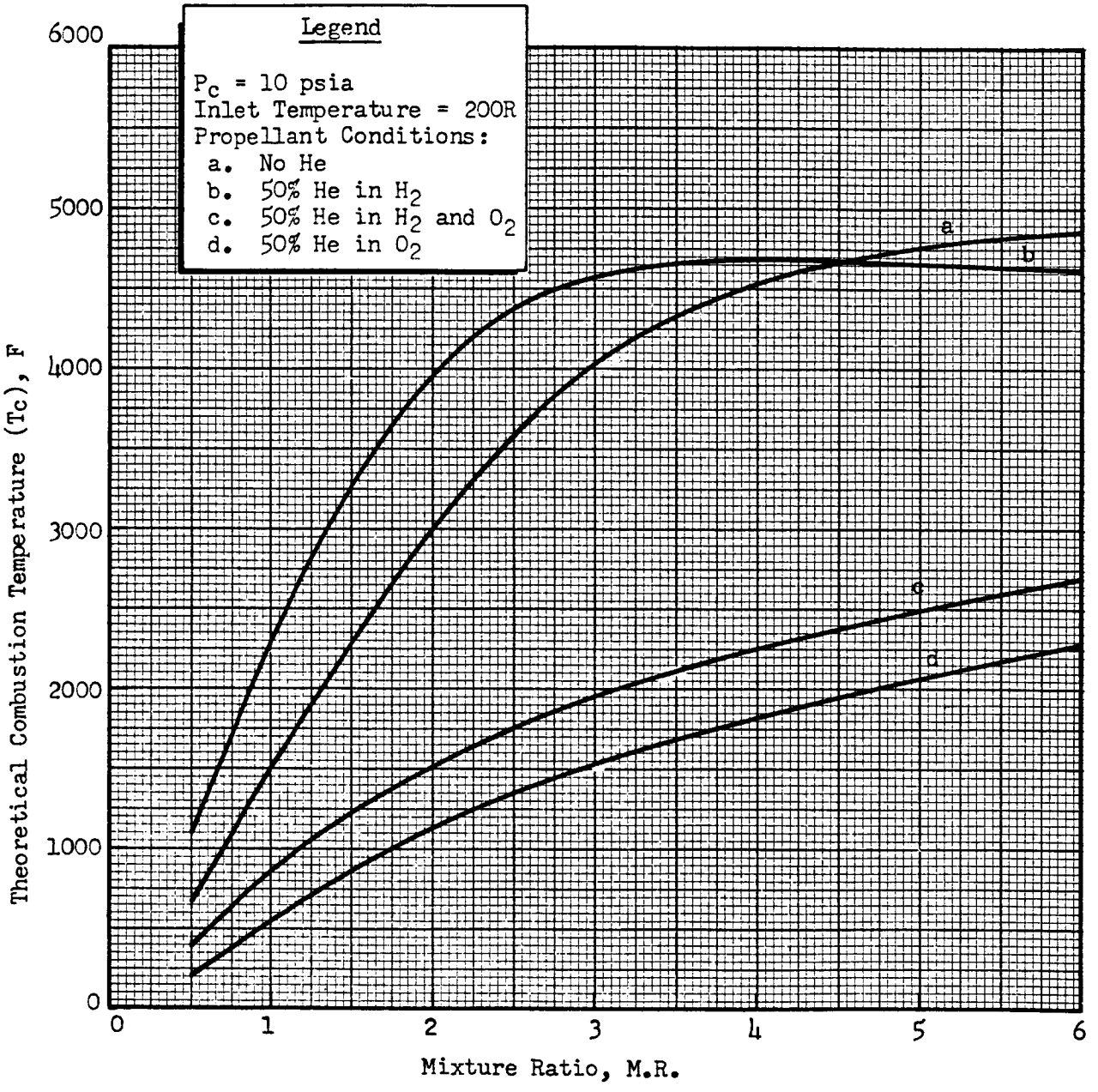

Figure 39. Theoretical Combustion Temperature as a Function of Mixture Ratio for Four Propellant Conditions with Helium Diluent (P_c = 10 psia, Propellant Temperature = 200R)

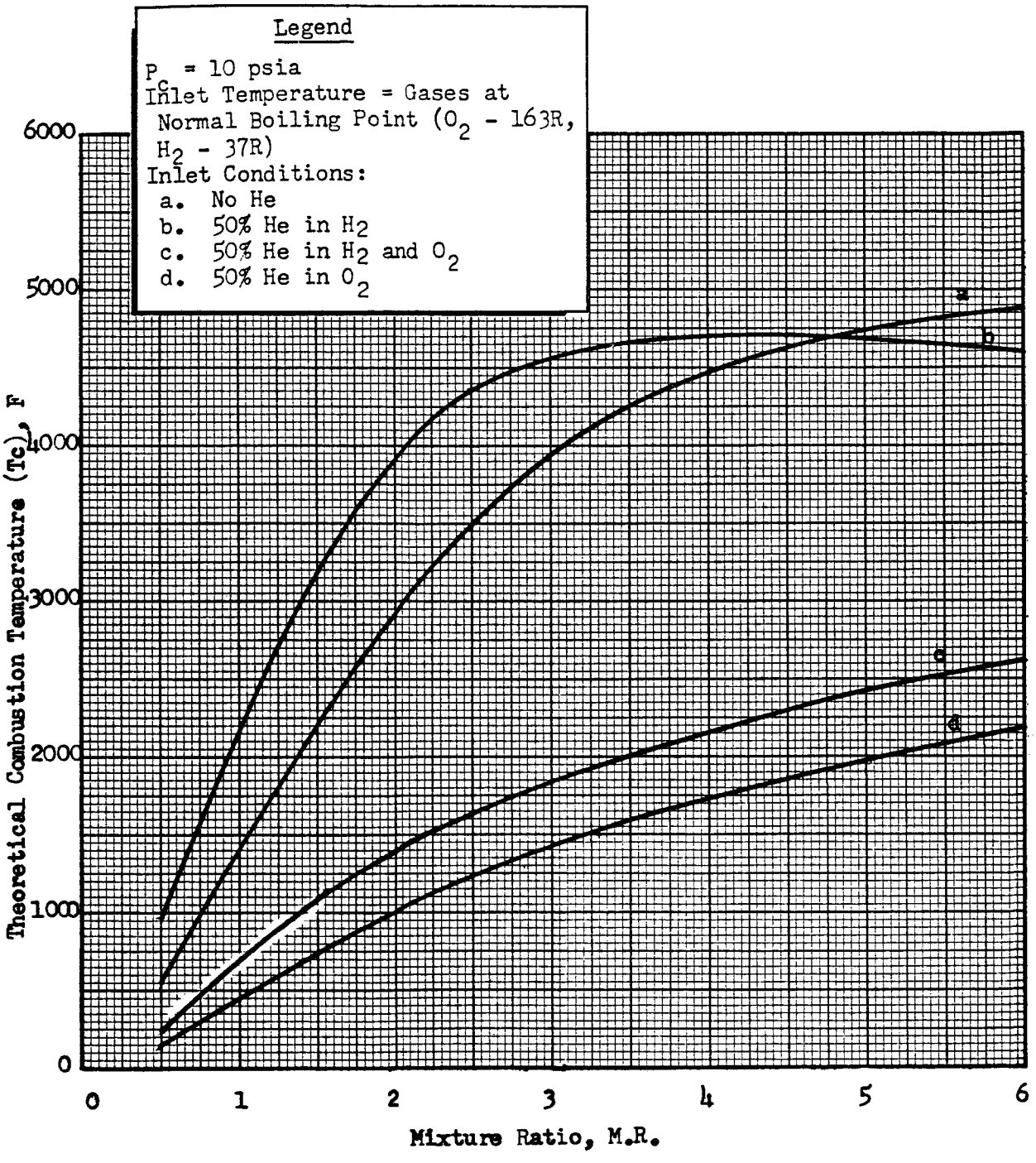

Figure 40. Theoretical Combustion Temperature as a Function of Mixture Ratio for Four Propellant Conditions with Helium Diluent (P_c = 10 psia, Propellant Temperature: Gases at Normal Boiling Point (O_2 - 163R, H_2 - 37R)

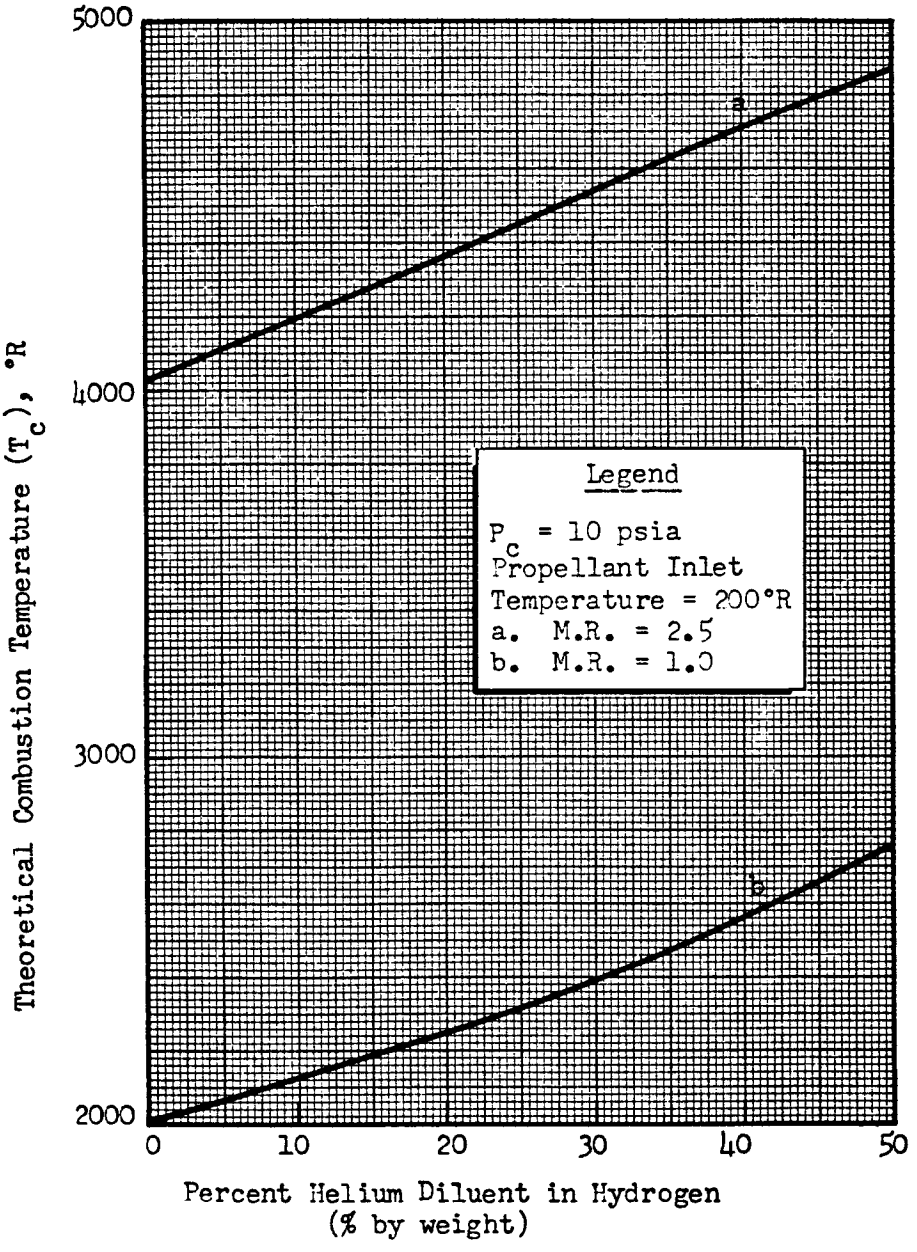

Figure 41. Theoretical Combustion Temperature as a Function of Helium Diluent in the Hydrogen

COMPONENT ANALYSIS - THRUSTOR

The thrustors in the subject cryogenic RCS must represent several significant departures from current small engines. These unique features include:

(1) Use of the cryogenic O_2-H_2 propellant combination

(2) Utilization of packed beds of catalyst pellets to induce reaction of the propellants

(3) Bipropellants fed as gases at chamber pressures of 100 and 10 psia.

The lack of existing design criteria and/or experience with such engines made necessary an initial, analytical design evaluation effort which included:

(1) Conceptual design evaluations at the 20 and 100 pound-thrust levels and the two chamber pressures of interest

(2) Review and reconsideration of past experimental results from catalytic bed studies and recently derived bed design criteria with emphasis on extrapolation to low pressure operation

(3) Consideration of injector-mixer designs for the introduction and mixing of the bipropellant gases

(4) Evaluations of engine performance and operating characteristics

At the conclusion of these efforts, a single thrustor concept was chosen, in conjunction with the conditioner concept selection, for further evaluation. Further analysis of the thrustor operation was accomplished. A model was formulated and programmed for use on a digital computer. The resulting simulated thrustor was utilized to determine expected operating characteristics and the effect of changing key design variables.

The aforementioned technical efforts are discussed in this section. This work is to serve as a basis for the remaining program efforts, which are to include experimental evaluations of the thrustor concept and comparisons of the experimental results with those predicted using the simulated thrustor.

The basic design parameter and operating goals for the thrustor subsystem were initially defined as:

Chamber Pressure Level	10 and 100 psia
Thrust (each thrustor)	20 lb_f
Expansion Area Ratio	50:1
Mixture Ratio (o/f)	from 0.5 to 6.0
Duration	60 minutes
Minimum Impulse Bit	1 lb_f - sec
Ignition Delay (maximum)	10 milliseconds
Mission Time	1 hour to 220 days

The theoretical performance analysis showed the most attractive mixture ratio range to be from $\sim$ 0.75 to $\sim$ 3.0, representing allowable packed bed flow conditions to the maximum expected specific impulse point. This effort will consider the mixture ratio range up to a value of 2.5. The latter represents a condition with a combustion temperature of less than 4000F and with a negligible decrease of specific impulse as compared with the full-frozen impulse maximum.

Two propellant feed temperatures, 200R and 500R, were selected as representative for system comparison purposes. Previous studies at relatively high pressures had indicated reliable ignition to 210R and below (Ref. 3). A temperature of 200 R was selected as representative of the minimum temperature to achieve reliable ignition. Further,

the assumption that the temperature limits for ignition are not significantly affected by pressure may not be true. This should not prevent the relative comparisons among the system concepts.

The feed temperature of 500 R was selected because one of the conditioner concepts, direct heating, must employ a temperature higher than the melting point of water.

THRUSTOR CONCEPTUAL DESIGNS

Nozzle and Chamber Concepts

The normally utilized chamber and nozzle design concept features a cylindrical chamber with either a bell or conical nozzle. Conical nozzles, the most simple, offer relatively good performance. The bell nozzle, a more complex contour, represents an improvement over conical nozzle performance and compactness. The basic thrustor dimensions for the two chamber pressures (10 and 100 psia) and thrust levels (20 and 100 lb_f) of interest are given in Table 3 . Three of these configurations are shown schematically in Figs. 42 , 43 , and 44 . The sizes of the 100 psia thrustors are similar to the sizes of present-day reaction control systems. However, the 10 psia engine are much larger and may present vehicle packaging problems, especially at the 100 lb-thrust level. To circumvent this disadvantage, advanced nozzle configurations were considered. A number of isentropic plugs and spike nozzles were sized. The resulting dimensions are shown in Table 4 . A schematic of one such design, a 10 psia, 100 lb-thrust chamber is shown in Fig. 45 . These designs are seen to be quite attractive from a compactness standpoint.

In comparing the cone, bell, and plug nozzles sized for 20 pounds thrust, 10 psia chamber pressure, and 50:1 exit area ratio, it can be

concluded that the plug nozzle would be less likely to present a vehicle packaging integration problem since it is much more compact. The geometrical advantages of the truncated plug are even greater at the 100 pound-thrust, 10 psia level. Truncated plug nozzles with design exit area ratios of 10 are shown for the 100 pound-thrust cases to indicate compactness practicability. Assuming the smaller exit area ratio reduces the theoretical specific by approximately 30 seconds, but does result in substantially reduced engine sizes.

Conical Nozzle Design. The 17.5 degree half angle was chosen for the conical nozzle design over the more conventional 15 degree half angle to minimize flow field nonisentropic shock phenomena which can occur in high area ratio nozzles. Such phenomena are reported in Ref. 4 and may represent sizeable losses in performance. In fact, similar phenomena were found to occur in the flow fields for the 17.5 degree designs from the results of method of characteristic calculations. However, in this case such phenomena, which are detected when characteristic surfaces of the same family intersect, were found to occur outside of the 50:1 design area ratio. Thus, the wall isentropic pressure distributions for the current designs should not be affected.

Bell Nozzle Design. Experience has shown that the length of a 15 degree half angle conventional conical nozzle can be reduced 80%, and equivalent or better performance can still be realized if a bell nozzle of equivalent area ratio is used with an optimum contour as based on the methods of Rao. Coordinates of a nominal Rao contour are given in Table 5 for the 80% bell nozzles considered for 50:1 exit area ratio applications herein. The Rao contour is termed nominal, since it was calculated assuming a constant ratio of specific heats,

$\gamma = 1.3$. Actually, for thrustor operations between the previously mentioned mixture ratio range, $1.0 \leq MR \leq 2.5$, one-dimensional frozen and shifting equilibrium analyses indicate that γ may range from 1.2 to 1.4; however, the variation between the Rao contours within this range should be negligible with respect of manufacturing tolerances.

Plug Nozzle Designs. Previous experiments with truncated spike (plug) nozzles have shown that a substantial portion of the thrust theoretically lost by truncation is recovered as a base pressure thrust on the plug (Ref. 5). A 70 percent recovery of the thrust lost by truncation was obtained with a 30:1 area ratio nozzle truncated from 6 to 33 percent of its isentropic length. These results were utilized in preparing the plug nozzle designs. Design contours for the plug nozzles considered herein are presented in Tables 7 & 7. In Table 6 the contour corresponds to an exit area ratio $\epsilon = 50:1$. In Table 7 the contour corresponds to an exit area ratio $\epsilon = 10:1$. Again, the contours were calculated assuming a value of $\epsilon = 1.3$. Regarding the contour variation over the thrustor mixture ratio range, considerations similar to that applied for the bell nozzle contour can be again applied. The contours in Tables 6 & 7 are considered optimum since they were calculated by the method of characteristics for axisymmetric flow.

Catalyst Bed Design Concepts

The catalyst bed design concepts considered for cylindrical chambers consist essentially of four basic types: (1) in-line bed, (2) in-line bed with downstream injection, (3) annular beds, and (4) pilot beds. Each of these concepts is depicted in Fig. 46. The in-line bed concept is the simplest and represents the design with the most experimental background information. The temperature of the exit gas is

limited by the temperature stability of the catalyst. Although low-temperature active catalysts are limited to approximately 1500R, a suitably designed admix of this catalyst with higher-temperature-stable metal oxide catalysts may allow a more versatile use of the concept. However, all of the propellant must pass through the bed which will result in an excessive pressure drop.

The in-line bed with downstream oxygen injection is a variation of the in-line concept, but with the advantage of an easily accomplished mixture ratio and performance increase to optimum values. At present only limited data are available on the experimental performance of such a concept. The annular bed concept is a design with several advantages. First, the pressure drop will be considerably less for the annular bed than for the in-line bed. Second, it provides a means of protecting the chamber walls with no penalty in performance. In terms of disadvantages, it requires a somewhat more complicated propellant manifold design than for the conventional chamber.

A truncated spike nozzle requires an annular engine, thereby presenting a new bed design problem. Several of many possible bed design concepts for such an engine are shown in Fig. 47. Since detailed experience with such an engine concept at the conditions of interest does not exist at present, it has not been afforded primary attention. Rather, it is viewed as a logical growth extension. The related bed concepts have not been treated in great detail. The first concept shown in Fig. 47, with the annular bed fed from central axis and with radial downstream injection, has been used for general evaluation purposes.

Injector-Mixer Concepts

In the basic hydrogen-oxygen catalytic thrustor concept, the propellants are premixed and then flowed through a catalytic fixed-bed reactor. Obtaining a uniform mixture is important; nonuniform mixtures lead to lowered performance and, more importantly, local high mixture ratio zones which could cause bed burnout and engine failure.

The injector mixer and mixing zone must be designed to promote homogeneous mixing of the propellants in as short a length as possible with a minimum of pressure drop. As indicated later in this report, the pressure inventory available for low-pressure engines is such that only about 2 to 3 psi are available to achieve such mixing in this region of the overall reactor. As far as the injector-mixer section of the reactor is concerned, there does not exist any well-founded theory or empirical results which provide for a clear-cut optimum choice to accomplish the mixing of two unlike gaseous propellant streams under conditions of low pressure drop.

Four general types of injector-mixers were considered and are shown schematically in Figure 48. The first type, termed "conventional", utilizes unlike impinging streams to utilize available pressure drop followed by an open mixing zone of sufficient length to achieve a high degree of mixing. The second type, "Diffusion Bed", has a diffusion bed substituted for the open mixing zone. The bed is to promote the turbulent flow of the propellants and thus, the mixing in a shorter length. The third concept, "Swirler-Diffuser Bed", offers a change in the impingement method from impinging streams to impinging sheets with an opposing angular momentum. The jet pump-diffusion bed is aimed at applications where hydrogen pressure drop is at a premium such as a regeneratively cooled chamber operating at a 10 psia chamber pressure.

THRUSTOR DESIGN CRITERIA

Injector-Mixer Design Criteria

Criteria for Fluid Impingement Design. Well-founded theoretical or empirical relationships for the design of any of the injector-mixer concepts for mixing two unlike gaseous propellant streams under conditions of low-pressure do not exist at present. However, it is known for liquid propellants that homogeneous mixture ratio distribution can be more nearly made to occur when the momenta of impinging two streams are properly adjusted. Such studies have been extensively carried out by Rocketdyne Research (Ref. 6 through 9) and the Jet Propulsion Laboratory (Ref. 10 through 12). A first analytical interpretation of the mixing problem for gases also suggests that the momentum criteria similar to those found in the above references, may be applicable to the gaseous mixing problems.

In general, the optimum mixing for liquids occur for unlike doublets when the following relationship is obeyed:

$$\frac{\rho_1 v_1^2 D_1}{\rho_2 v_2^2 D_2} = K, \text{ where K is close to 1.0} \qquad (1)$$

Since the stream momentum, M, is equal to the product of velocity head and orifice area, A, and the area is proportional to the square of the diameter, it can be shown that if Eq. 1 is satisfied with K equal to 1.0, the two stream momenta are related by:

$$\frac{M_1}{M_2} = \frac{\rho_1 v_1^2 D_1^2}{\rho_2 v_2 D_2^2} = \frac{D_1}{D_2} \quad . \qquad (2)$$

In terms of overall mixture ratio the relation may be reduced further to

$$\frac{D_1}{D_2} = \frac{\dot{w}_1^2 \ \rho_2 \ D_2^2}{\dot{w}_2^2 \ \rho_1 \ D_1^2} \tag{3}$$

or in terms of mixture ratio

$$MR = \left[\frac{\rho_o}{\rho_f} \left(\frac{D_o}{D_f} \right)^3 \right]^{1/2} \tag{4}$$

For other elemental injector designs the results can be reduced to the following:

two-on-two element

$$MR = \left[K' \frac{\rho_o}{\rho_f} \left(\frac{D_o}{D_f} \right)^3 \right]^{1/2} \tag{5}$$

two-on-one element

$$MR = \left[K'' \frac{\rho_1}{\rho_2} \left(\frac{2A_1}{A_2} \right)^n \right]^{1/2} \tag{6}$$

four-on-one element

$$MR = \left[K'' \frac{\rho_1}{\rho_2} \left(\frac{4A_1}{A_2} \right)^m \right]^{1/2} \tag{7}$$

In general, liquid propellant injector performance optimization, which is a measure of mixing optimization is found to follow curves as shown below:

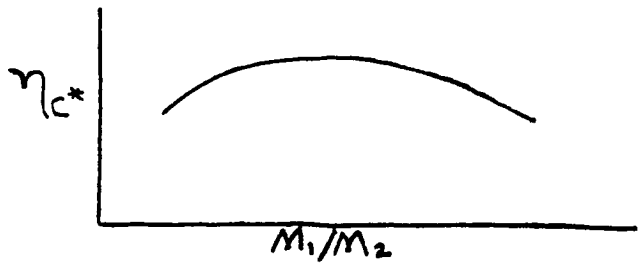

Assuming that such criteria again apply here, there would be optimum M_1/M_2 ratios for best mixing in a given mixing length. However, because of the expanding nature of gases the results may not be nearly as clear as for liquids. Further, criteria for determining the required mixing length, even with an optimized injector, are not known.

Mixing Zone Criteria. Within the mixing zone, the final propellant mixing must occur prior to the propellant mix entering the catalyst bed. This final mixing is necessary to remove concentration inhomogencities in the gas which could lead to flashback and performance degradation. It has been observed in previous catalytic ignition program efforts (Ref. 2, 3, 13, and 14) that occasionally flashback through the catalyst bed to the injector-mixer may occur, resulting in both catalyst bed and injector-mixer damage. In Ref. 2 it was hypothesized that this condition could be prevented if the mean local velocities exceeded the local mixture flame velocity. In Ref. 2 this hypothesis was further analytically pursued to provide a basis for design. A literature search showed the maximum observed turbulent and laminar flame velocities for ambient temperature premixed H_2/O_2 propellants at various pressures to be best represented by the data shown in Fig. 49. By methods presented in Ref. 2 these data were extrapolated to lower environmental temperatures as shown in Fig. 50. Design curves for the sizing of this section with no auxiliary mixing zone additions are shown in Fig. 51 and 52 for both 10- and 100-psia reactors with inlet environmental temperatures of 200 and 500R. However, the experimental proof of these criteria has not been demonstrated. As is seen from these curves, the flashback abatement will be more of a problem for higher pressures than at 10 psia. The flow areas in a typical 10 psia reactor design are, in general, considerably smaller than the limiting values presented in Fig. 51 .

The addition of mixing devices to the zone between the injector face and the catalyst bed offers a further improvement in flashback abatement. Such devices as inert pellets, metal shot, screens, etc. greatly increase the available surface for quenching as well as promote additional mixing of the gases.

Catalytic Bed Design Criteria

The correct design of the catalytic bed is a key factor in the successful demonstration of an oxygen-hydrogen catalytic thrustor. Available data on the catalytic ignition of these gaseous bipropellants were reviewed in Ref. 2 and 3 . These and subsequently obtained data were reviewed in the Task I effort with the purpose of presenting a design summary for oxygen-hydrogen catalytic reactors in this report.

The primary design factors for applying the packed bed H_2/O_2 catalytic reactor to attitude control thrustors are associated with the following: (1) catalyst bed sizing and flowrates, (2) catalyst temperature limitations, (3) effects of catalyst sizing and shape, (4) effects of varying catalytic chemical activity, and (5) resulting pressure drop effects for a given catalytic reactor design. Each of these areas is discussed below.

Catalyst Bed Sizing. The theoretical, and empirically substantiated basis for sizing the catalytic bed for igniter purposes is presented in Ref. 2 . The data which served as the basis for the model were obtained at reactor conditions associated with chamber pressures above 100 psia. The model is based on oxygen diffusion to the catalytic surface as the rate-limiting step in the reaction process. The

resulting theoretical required length of a catalytic reactor for H_2/O_2 gaseous propellants using spherical pellets is given by

$$x = 4.92 \frac{\bar{R}\bar{T}}{\alpha \bar{P}_T a} \bar{F} \left(\frac{G_o}{a \mu_f \psi} \right)^{0.41} Pr^{2.3} \qquad (8)$$

In this relation it is seen that the bed length requirement is dependent upon the mass rate velocity to the 0.41 power and inversely to a measure of the pellet size as similar to the 1.41 power. In addition, the average total pressure of the gases flowing in the bed enters the relation inversely to the first power. However, the local density enters in as a first-power direct effect.

In the original derivation (Ref. 2) the density and local total pressure were included as variables in x, the distance along the bed. If the two can be taken as appropriate local values, Eq. 8 can be reduced to:

$$x = \frac{4.92}{\alpha a} \left(\frac{G_o}{a \mu_f \psi} \right)^{0.41} Pr^{2/3} \qquad (9)$$

Comparing the theoretical results to experimental data shows that the relationship must be modified by an entrance length to

$$x = x_o + \frac{4.92}{\alpha a} \left(\frac{G_o}{a \mu_f \psi} \right)^{0.41} Pr^{2/3} \qquad (10)$$

Catalytic activity enters the relationship in an inverse manner and is given herein as α. For the 1/8-inch spherical MFSS and MFSA catalysts found to be the best H_2/O_2 catalyst available to date (Ref. 2), x_o is $\sim$0.3 inch. It is seen that the value of a, the surface area per unit volume, also influences the length requirement in an inverse manner, and the smaller the pellet size the less catalyst bed length is

required. The 1/8-inch MFSA catalyst data of Ref. 2 have been examined in detail to determine the effective value of α by comparing the theoretical values of x with the experimental values. In this manner, α was determined to be 0.147.

The overall reactor diameter is recommended to be such that

$$\frac{D_R}{D_P} > 8 \qquad (11)$$

to prevent fluid flow channeling in the reactor. Bed friction measurements have confirmed this relationship for a large number of packed-bed configurations used in the chemical processing industry, although it has not been verified in the H_2/O_2 catalytic work. The bed length requirements for H_2/O_2 igniters using 1/8-inch spherical MFSS or MFSA catalysts and satisfying Eq. 10 are given in Ref. 2 . The data in this reference were obtained at pressures ranging from 70 to 150 psia in a 1-inch-diameter reactor. As such the data should be directly applicable to 100-psia thrustors using 1/8-inch MFSA or MFSS catalysts.

A more generalized design procedure for both the 10- and 100-psia thrustors may be developed by developing curves in terms of G_o, the mass flowrate. This has been done for the cases of 1/8- and 1/16-inch catalyst assuming that α for 1/16-inch catalysts is also 0.147. The results are shown in Fig. 53 . In general, it is recommended that extrapolation procedure be based on Eq. 10 .

A catalyst development program (Ref. 15) recently completed by the Shell Development Corporation has led to a model of ignition which differs than that formulated above. The Shell effort was accomplished in laboratory apparatus at a total pressure of 14.7 psia with the hydrogen/oxygen combination diluted with helium and the active specie

partial pressures varied from approximately 0.5 to approximately 7 psia. The resolution between these two modeling approaches was not within the scope of this program, but differences in operating conditions (pressure and flow velocities) for the two types of experiments are probably responsible. Further experimental work over a wide pressure range was necessary.

Catalyst Temperature Limitations. The currently available catalysts recommended for H_2/O_2 ignition at low temperatures are MFSA and MFSS 1/8-inch spherical catalysts (Ref. 2). These catalysts are fuel-type catalysts, and as such are best operated in fuel-rich service. Previous experimental results have shown that these catalysts will operate at a maximum temperature of 1500F corresponding to a mixture ratio of ~1:1 with low temperature propellants (200R) without undergoing damage. For the admix concept presented above, a metal oxide catalyst will undoubtedly be necessary for use in the high temperature portions of the bed. Although very little data exists in the literature on the application of such catalysts to oxygen-hydrogen service, it is not expected that an extremely high catalytic activity would be required. Rather, high temperature durability would be requisite.

Catalyst Sizing and Shape Variations. In early O_2-H_2 catalytic work, Rocketdyne determined that spherical catalyst pellets offered the most repeatable ignition results. Further, based on analytical results presented above, the catalyst size would be as small as possible for minimum bed length. However, until only recently the smallest available MFSS- or MFSA-type catalysts were the 1/8-inch spheroids. A small quantity of 1/16-inch catalyst was made available to Rocketdyne for in-house studies. However, although the smaller catalyst provides a higher surface area-volume relation, a, it also results in a higher pressure drop for a given mass rate. This is not particularly critical at 100

psia, but it is quite critical at 10 psia. A substantial body of data is available for the 1/8-inch material at the 100-psia range, but no data exist at the 10-psia point. With the exception of the small amount of 1/16-inch data gathered in in-house studies and used to semi-quantitatively verify the scaling relationships, no data are available for the 1/16-inch catalyst pellets.

Varying Catalytic Activity. It is known with the type of catalyst being considered for this program, that the catalytic activity is temperature dependent as follows:

$$\propto \_ T^n \; C_1 \quad \exp^{(E/RT)} \tag{12}$$

This relation shows that the activity, which is a measure of conversion efficiency, falls off at reduced temperature. Consequently, it is expected that the length of the bed will be increased for a cold, initial temperature propellant mix over that of an ambient propellant.

Previous work at Rocketdyne has not indicated a low temperature activity limit on ignition. However, the low temperature results were obtained at relatively high preignition pressures and an extrapolation of this conclusion to low pressures may not be valid.

Pressure Drop. In this program, an extensive study of the pressure drop characteristics of packed beds in which reaction is occurring has been carried out for both the 1/8-inch catalyst results obtained in previous programs and for the 1/16-inch catalyst results obtained in recent in-house experiments. These results have been found to correlate quite well with the Ergun equation:

$$\frac{\Delta P}{G_o^2}\frac{\bar{\rho}}{L}\frac{D}{}\left(\frac{\epsilon^3}{1-\epsilon}\right) = 150\,\frac{(1-\epsilon)}{\frac{D\ G_o}{\mu_f}} + 1.75 \qquad (13)$$

This expression can be rewritten for use in analyzing results for reacting mixtures as

$$P(x)\frac{dP}{dx} = \left[150\,\frac{(1-\epsilon)}{\frac{D\ G_o}{\mu_f}} + 1.75\right]\frac{G_o}{D}\ RT(x) \qquad (14)$$

If the temperature distribution is known, and if the void fraction is taken as 0.31 for a random-packed bed, the pressure drop may be obtained by numerical integration of Eq. 14 .

If the average density, $\bar{\rho}$, in the bed is used, a series of approximate design curves may be derived to predict pressure drop in an H_2/O_2 catalytic reactor bed. Such curves are given in Fig. 54 and 55 for both the 10- and 100-psia cases.

Thrustor Response

The thrust response of the system to a demand signal is of prime importance. The subject thrustors differ from present-day thrustors chiefly by the inclusion of the catalytic bed and the dependence upon a catalytic initiation of the non-hypergolic reaction of the two propellants. These factors will be of prime importance in the reactor response characteristics. The first step in modeling the thrustor operational characteristics is an order of magnitude comparison with the purpose of defining the rate limiting steps. This is presented below.

Catalytic Reactor Response Comparisons. Previous Rocketdyne Research H_2/O_2 catalytic reactor studies have shown that the response characteristics of this type of reactor can be approximately determined by a consideration of three factors in an independent manner: (1) chemical response, (2) pneumatic response, and (3) thermal response. Each is discussed below.

Consideration of the heterogeneous catalytic reaction process shows that chemical reaction rates are primarily influenced by diffusion rates. In the case of interest herein, H_2 and O_2 species diffuse to the catalytic surface, and H_2O species diffuse away. Since diffusion velocities are inversely proportional to the square root of the species molecular weight, it is seen that the O_2 species diffusion is the controlling species in the reaction. Considering the diffusion to occur over as many as a hundred mean free molecular paths, it is found that the transit time is still less than a millisecond. Therefore, this response time attributable to diffusion is negligible. Further, experimental measurements of this type of response has shown it to correspond to the above time scale (Ref. 2).

Pneumatic response is associated with the transient fluid buildup within the catalytic reactor. The response associated with this filling was theoretically examined in Ref. 2 by considering a control volume containing a catalyst bed, mixing zone, and downstream volume and a sonic filling orifice and a sonic expelling orifice. The time to 90 percent pressure buildup in this model of the catalytic reactor is given by

$$\tau_{90} \approx 3\left(\frac{L^{*2}}{\bar{M}_g T_g}\right)^{1/2} \quad \text{ms} \qquad (15)$$

when the L* is determined by considering the entire free volume of the reactor. The value of $\bar{M}_g$ and T_g are average values in this analysis.

The major contributor to catalytic reactor response is associated with the catalytic reactor bed thermal absorption characteristics. For a given propellant mass rate and mixture ratio in the bed there is a maximum chemical energy release rate corresponding to complete reaction. The bed serves as a heat sink for this energy. An energy balance around the bed assuming the bed to be at a uniform temperature (infinite conductivity) gives:

Bed Energy Absorption = Energy Loss from Gas

$$M_B c_B \frac{dT}{dt} = \dot{W}_g c_g (T_{rg} - T) \tag{16}$$

with the boundary conditions

$$T(0) = T_0 \tag{16-a}$$

$$T(t) = T \tag{16-b}$$

The solution to this system of equations is given by

$$\frac{T_{rg}-T}{T_{rg}-T_o} = \exp\left\{-\frac{\dot{W}_g c_g}{M_b c_b} t\right\} \tag{17}$$

The 90 percent response point is given by

$$\tau_{90} = 3000 \frac{M_B c_B}{\dot{w}_g c_g} \text{ milliseconds} \tag{18}$$

These response results have been shown to be qualitative correct in a number of studies (Refs. 2 and 3) and are suggested as reliable indicators for predicting response. The generalized design curves are shown in Figs. 56 and 57 for the pneumatic and thermal response, respectively. The given times are for optimized bed design, i.e., minimum length vs G_o as predicted by the analysis of Ref. 2 .

As comparison of Figs. 56 and 57 shows, the thermal response is the predominant response characteristic to be considered. The times are long when pulse-mode operation is considered, and they emphasize the desirability of minimizing heat loss in the catalytic reactor itself. The effect of the large time constants if reflected primarily in startup of the reactor. Once the reactor is hot the time constant is not significant to the pulse-mode operation.

THRUSTOR PERFORMANCE AND OPERATION

Overall Thrustor Performance

The overall thrustor performance is best characterized by the value of actual specific impulse delivered. This value is degraded from the theoretical by a number of interacting, individual processes. However, for present purposes, the inefficiencies will be assumed independent--a good assumption of small inefficiencies. The actual specific impulse can then be written as

$$I_{sp} = \eta_{c^*} c^*_{theor.} \eta_{C_F} C_{F_{theor.}} \qquad (19)$$

where $c^*_{theor.}$ and $C_{F_{theor.}}$ are the theoretical values of characteristic exhaust velocity and thrust coefficient, respectively. The degradation

effects of incomplete combustion are contained in the value of c* efficiency, η_{c^*}. The thrust coefficient efficiency is assumed to express the effects of the remainder of the impulse losses. Those included are:

1) kinetic losses
2) divergence
3) frictional drag
4) heat transfer losses
5) condensation effects

Such a procedure implicitly assumes that the nozzle contour and surfaces are such that internal or oblique shock waves do not further reduce the performance. The estimated efficiency factors for each of these processes are applied to each concept are listed in Table XV. These factors do not include losses associated with the conditioning system, those were caused by feed back of hot gas for conditioning processes.

Combustion Efficiency. A very limited quantity of data exist concerning the combustion efficiency of packed bed reactors. The brief experimental effort reported in Ref. 16 obtained the results shown in Fig. 78 for in-line reactor configuration at a mixture ratio of 1.0. It is expected that improved combustion performance can be obtained at effort at optimization. However, for purposes of this evaluation, a combustion efficiency (η_{c^*}) of 98 percent was chosen, corresponding to a characteristic chamber length, L* = 35 inches. This value was assumed constant for all configurations evaluated.

It is recognized, however, that design criteria for downstream injection of additional oxygen have not been formulated. The achievement of high combustion efficiencies with this type of chamber may require the generation of detailed criteria for injection and mixing of the additional oxidizer.

Kinetic Losses. Kinetic losses arise from a nonequilibrium expansion of the combustion chamber gases. As discussed in the Theoretical Performance Section of this report, the oxygen-hydrogen combustion products should expand at the pressure levels of interest without significant recombination occurring. The kinetic efficiencies which evaluate the performance as compared with the equilibrium expansion specific impulse, were calculated as:

$$\eta_K = \frac{I_{sp} - I_{sp_F}}{I_{sp}} \qquad (20)$$

where I_{sp} and I_{sp_F} are the full-shifting and full-frozen values of vacuum specific impulse to an expansion area ratio of 50:1. The only difference in these values for the configurations of interest is one of operating mixture ratio, since the full-shifting and full-frozen impulse values are functions of mixture ratio.

Divergence. Divergence losses arise due to nonuniform nozzle flow as depicted in the sketches below.

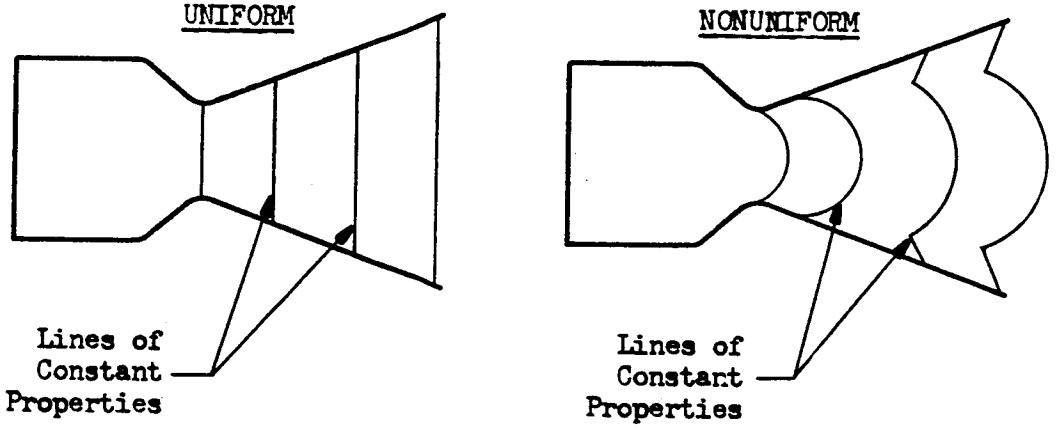

The sum of the actual divergence and kinetic losses were computed from the relation:

$$\eta_D = \frac{C_F - C_{F_D}}{C_F} \qquad (21)$$

in which C_F is the vacuum thrust coefficient assuming full shifting equilibrium flow and C_{F_D} is the corresponding value assuming nonuniform axisymmetric flow. Values of C_F were obtained in conjunction with the theoretical performance results.

In the nonuniform full-frozen flow case, values of C_{F_D} were calculated assuming axisymmetric, irrotational (or isentropic) flow at constant γ. From the kinetic analysis it was found by examination of γ variations in the initial nozzle region over the design mixture ratio range $1.0 \leq (MR) \leq 2.5$, that a representative value of $\gamma = 1.3$ with a minimum loss in accuracy. With these assumptions, and for $\gamma = 1.3$, the flow fields of all thirteen configurations were calculated utilizing existing Rocketdyne digital computer programs. The kinetic loss was subtracted from the combined loss, leaving the effect of divergence only.

Frictional Drag. Frictional drag losses occur from the viscous drag forces on the engine wall opposing the thrust force. The degree of impulse degradation caused by such a phenomenon was calculated assuming a fully developed, axisymmetric turbulent boundary layer from the chamber through the nozzle. The results of these calculations are presented in Table 8 .

Heat Transfer. The transfer of thermal energy from the combustion gases and its subsequent rejection to the surroundings will cause a loss in specific impulse performance. The magnitude of the loss is dependent on the cooling method and the duty cycle imposed on the engine. If regenerative cooling is used, the performance loss is negligible. The employment of radiation cooling will mean a larger, but still small loss, especially at the 10 psia chamber pressure level.

To confirm conclusions concerning heat flux levels, the heat transfer coefficients in the nozzle and chamber were estimated and heat losses calculated for two representative cases. These were calculated on operating mixture ratio of 3.5 and chamber pressures of 10 and 100 psia. The method used to estimate the heat transfer coefficients was similar to that of Elliot, Bartz, and Silver (Ref. 17) Plots of the heat transfer coefficient along the chamber axis for two cases are presented in Fig. 59 and 60.

The peak heat fluxes for the above causes were calculated based on a wall temperature of 1000 F. The resulting values (assuming the theoretical flame temperature of 4700 R) were 0.45 and 3.5 BTU/in^2-sec. for the 10 and 100 psia cases, respectively. These values should be approximately 10 to 13 percent lower at a mixture ratio of 2.5. The heat transfer coefficient at the 10 psia pressure level was also used to calculate steady-state temperatures for a radiation cooled wall. These were in the range of 2000 F to 2500 F over the mixture ratio range from 2.5 to 3.5 for a 100 percent combustion efficiency (theoretical flame temperature) and an emissivity of 1.0. This indicates that radiation cooling is quite feasible.

It is realized that the heat transfer coefficient calculations are based on a number of idealized assumptions. Actual measurements of the heat transfer characteristics are required for further evaluation.

Condensation of Water in the Nozzle. The theoretical full-shifting performance calculations were based on complete equilibrium in the gas stream during nozzle expansion. This included the formation of condensate when equilibrium considerations dictate, a process which from a purely thermodynamic view will increase performance due to the release of the enthalpy of condensation. However, the physical processes associated with the flow of two phases in the nozzle can cause a loss in thrust performance. These losses can be viewed as casued by an effective decrease in gas specific volume as mass is transferred to the relatively dense liquid phase and be viscous kinetic energy dissapation due to drag force of the gas on the condensed droplets. The severity of any of these effects is dependent on the relative quantity of condensate formed, the position in the nozzle at which condensation occurs, and the effective particle size of the condensate.

Examination of the theoretical performance characteristics show condensation to be predicted by equilibrium considerations only at large expansion area ratios and fairly low mixture ratios for the configurations under consideration. Because of this, the effects of condensation are relatively minor. The effects of the condensation enthalpy release

only affects an impulse gain on the order of 1.5 percent at a mixture ratio of 1.0. Likewise, it is expected that the frictional drag losses caused by two phase flow will be of the same magnitude or smaller. Since the actual, as opposed to the equilibrium, quantity of condensate formed cannot be predetermined, the performance effects must be estimated. For present purposes, the two above effects were assumed to balance and a maximum loss calculated as based on the equilibrium removal of mass from the gas to zero velocity condensate.

Performance Summary. In general, the results indicate that the thrustor subsystem should deliver specific impulse efficiencies in the range from 90 to 95 percent of full shifting. This corresponds to specific impulses in the 350 to 375 lb_f-sec per lb_m for mixture ratios of approximately 1.0 and 425 lb_f-sec per lb_m for mixture ratios of approximately 2.5.

CONCEPT SELECTION

Following the analysis efforts described above, it was necessary to choose a basic concept for further study. A cylindrical chamber with a conical nozzle, an in-line catalyst bed, and downstream injection of oxygen were selected for the thrustor design. Selection of the conical nozzle design over a bell design was based on ease of fabrication. More advanced designs directed at a minimization of thrustor weight, e.g., truncated spike configurations, should be considered in future programs. Selection of an operating chamber pressure in conjunction with a conditioner subsystem concept resulted in a value of 10 psia. The lack of existing data at this pressure level was the strongest thrustor-oriented reason for such a choice. A mixture ratio of 2.5 (O/F) was selected for the thrustor operation. Since the available low temperature catalysts will only withstand the temperatures produced by a mixture ratio of approximately unity, the additional oxygen is to be injected downstream of the catalyst bed. Predicted heat flux levels

at the relatively low flame temperatures involved (~4000 F) are expected to be sufficiently low to allow radiation cooled engines.

SUMMARY OF THRUSTOR DESIGN AND ANALYSIS CONSIDERATIONS

Evaluation of thrustor design concepts resulted in the selection of a cylindrical chamber with a conical nozzle, an in-line catalyst bed subjected to propellant at an approximate mixture ratio (O/F) of 1, and downstream injection of additional oxygen to raise the overall mixture ratio to 2.5, a value near the frozen specific impulse maximum. The choice of operating chamber pressure made in conjunction with a conditioner concept selection resulted in a 10 psia value. The chief thrustor-oriented reason for such a choice was the lack of existing technology at this pressure level. The combination of low chamber pressure and a relatively low mixture is expected to result in steady-state wall temperatures for a radiation-cooled thrustor of from 2000 to 2800 F.

The choice of a radiation cooled thrustor with no internal regenerative heating of the incoming propellants resulted from the general objectives of the experimental program. The inclusion of internal heat transfer could only serve to decrease the response of the thrustor. However, for those applications where quick response is irrelevant, or of minor consideration, increased overall system impulse could be obtained by partial regenerative heating of the propellants as is discussed in a previous section.

Previous investigations at pressure levels of 100 to 250 psia revealed that catalytic ignition could only be reliably obtained at inlet propellant temperatures sufficiently high to prevent oxygen freezing.

This requires the temperatures of both propellants to be in excess of approximately 115R. In addition, effective mixing of the two propellants prior to catalytic reaction can best be guaranteed by maintaining the mixed propellant temperature above the dew point of oxygen. Further, flow control of both propellants in the thrustor can most easily be maintained with gaseous propellants. Based on these considerations a propellant feed temperature of 200 R was selected as the design point for the experimental effort. It was recognized that with the conditioner system concept utilized, lower overall system impulse would result from increases in this temperature because an increasing fraction of the propellant would be diverted for conditioning purposes.

TABLE 3

O_2/H_2 ATTITUDE CONTROL CONICAL AND BELL NOZZLE DESIGNS

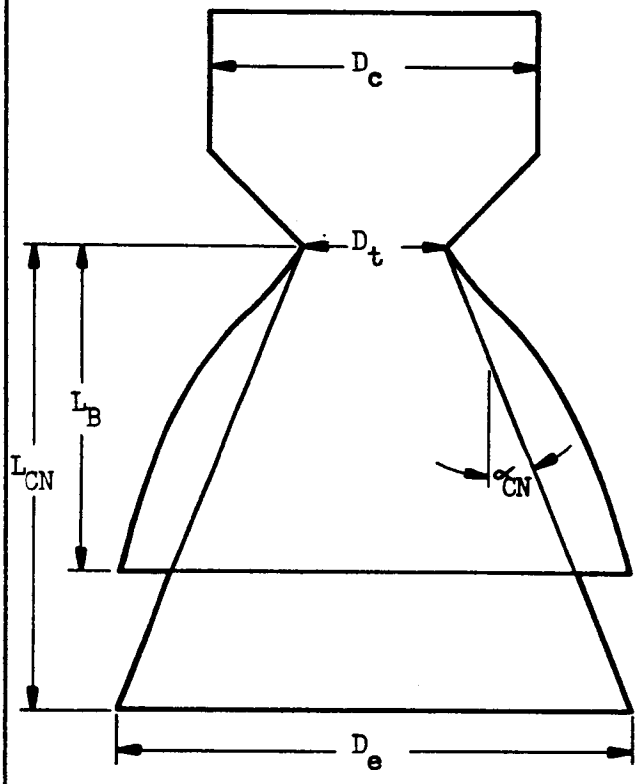

Nomenclature

L_B - bell nozzle length
L_{CN} - conical nozzle length
α_{CN} - cone half angle
D_c - chamber diameter
D_t - nozzle throat diameter
D_e - nozzle exit diameter
F - thrust
P_c - chamber pressure
ϵ - area ratio

REFERENCE DATA			PRELIMINARY DIMENSIONS					
F (lb)	P_c (psia)	ϵ	L_B (in)	L_{CN} (in)	α_{CN} (degrees)	D_c (in)	D_t (in)	D_e (in)
20	10	50	9.14	11.42	17.5	3.00	1.19	8.41
100	10	50	20.43	25.52	17.5	7.00	2.66	18.78
20	100	50	2.92	3.66	17.5	1.00	0.38	2.69
100	100	50	6.53	8.18	17.5	2.00	0.85	6.02

TABLE 4

O_2H_2 ATTITUDE CONTROL SPIKE NOZZLE DESIGNS

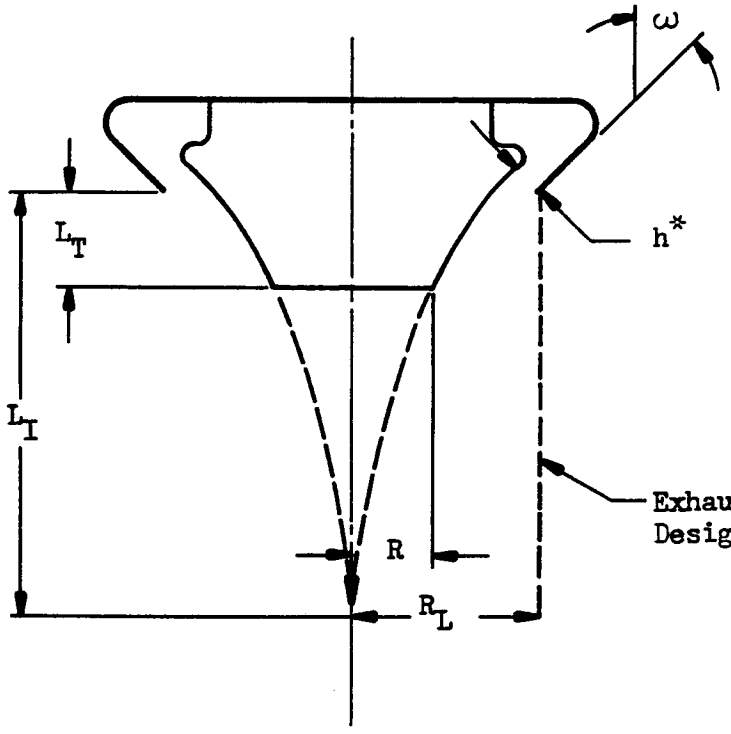

Nomenclature

ω - cowl lip slope
h^* - gap width
R_L - cowl lip radius
R - base radius
L_I - isentropic spike length
L_T - truncated spike length
F - thrust
P_c - chamber pressure
Exhaust Streamtube for Design Point
ϵ - area ratio

REFERENCE DATA			PRELIMINARY DIMENSIONS					
F (lb)	P_c (psia)	ϵ	L_T (in)	L_T (in)	h^* (in)	ω (degrees)	R_L (in)	R (in)
20	10	50	24.60	2.46	0.04	84.1	4.26	2.98
100	10	10	10.30	1.03	0.22	64.7	4.39	3.07
20	100	50	7.60	0.76	0.01	84.1	1.32	0.92
100	100	10	3.24	0.32	0.07	64.7	1.38	0.97

TABLE 5

BELL CONTOUR FOR O_2/H_2 ATTITUDE CONTROL ENGINES

X/R_t	Y/R_t	X/R_t	Y/R_t	X/R_t	Y/R_t
0.202	1.056	2.010	2.187	5.953	4.057
0.205	1.058	2.149	2.267	6.315	4.194
0.208	1.060	2.290	2.348	6.690	4.332
0.312	1.125	2.435	2.429	7.079	4.470
0.426	1.198	2.582	2.510	7.483	4.609
0.540	1.271	2.733	2.592	7.903	4.748
0.653	1.344	2.886	2.673	8.341	4.888
0.767	1.418	3.041	2.755	8.797	5.029
0.882	1.492	3.199	2.836	9.273	5.170
0.999	1.567	3.344	2.909	10.288	5.455
1.117	1.642	3.669	3.070	11.398	5.742
1.237	1.718	3.978	3.218	12.613	6.030
1.360	1.795	4.292	3.362	13.948	6.319
1.484	1.872	4.609	3.504	15.417	6.606
1.612	1.950	4.932	3.643	17.036	6.891
1.742	2.028	5.262	3.782	18.167	7.071
1.874	2.107	5.602	3.919		

Coordinate System

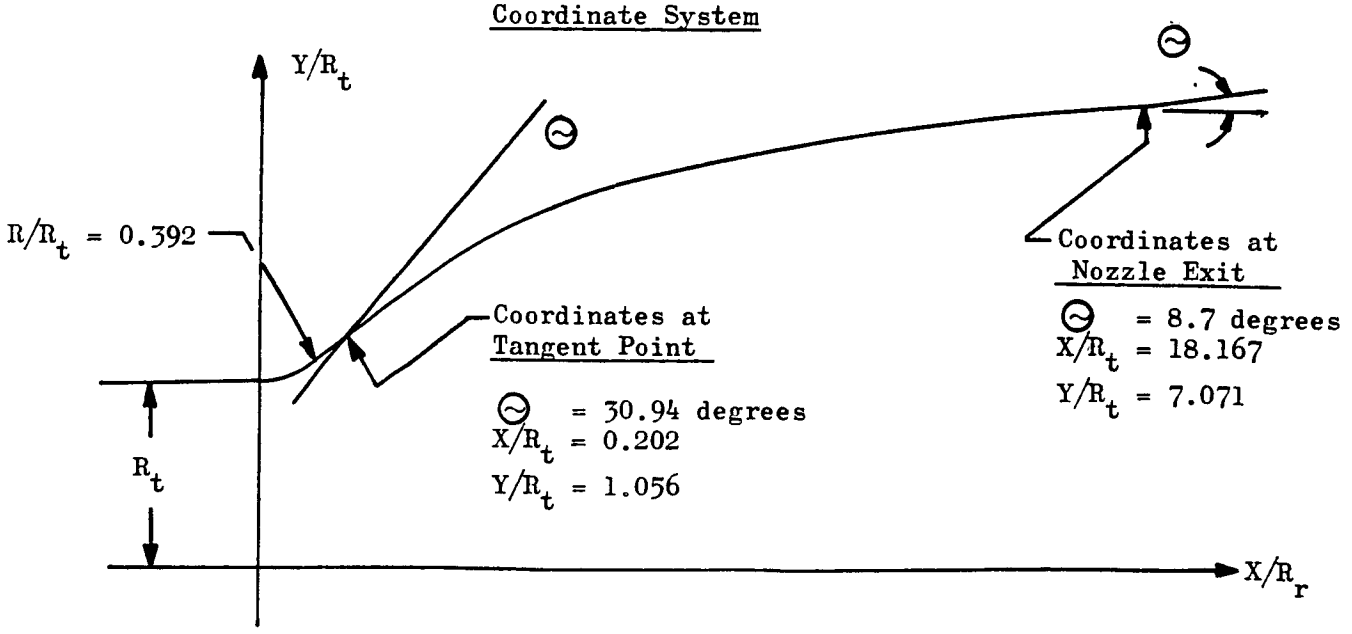

TABLE 6

PLUG CONTOUR FOR O_2/H_2 ATTITUDE CONTROL ENGINES.

(ϵ = 50:1)

X/R_L	Y/R_L	ω	X/R_L	Y/R_L	ω
2.341	0.225	9.64	-0.006	0.966	63.39
1.380	0.405	12.61	-0.008	0.970	65.63
0.885	0.529	16.04	-0.010	0.974	67.81
0.595	0.621	19.43	-0.011	0.977	69.94
0.413	0.691	22.69	-0.012	0.980	72.02
0.293	0.744	25.90	-0.013	0.983	74.03
0.216	0.787	29.01	-0.014	0.985	75.99
0.154	0.820	32.05	-0.014	0.987	77.88
0.113	0.848	34.99	-0.014	0.989	79.70
0.083	0.870	37.89	-0.015	0.991	81.46
0.061	0.888	40.72	-0.015	0.993	83.13
0.044	0.903	43.48	-0.015	0.994	84.73
0.031	0.916	46.17	-0.015	0.996	86.23
0.021	0.927	48.80	00.015	0.997	87.62
0.014	0.936	51.36	-0.015	0.999	88.90
0.007	0.944	53.88	-0.015	1.000	90.03
0.003	0.951	56.34	-0.015	1.001	90.98
-0.001	0.957	58.75	-0.015	1.002	91.68
-0.004	0.962	61.10			

Coordinate System

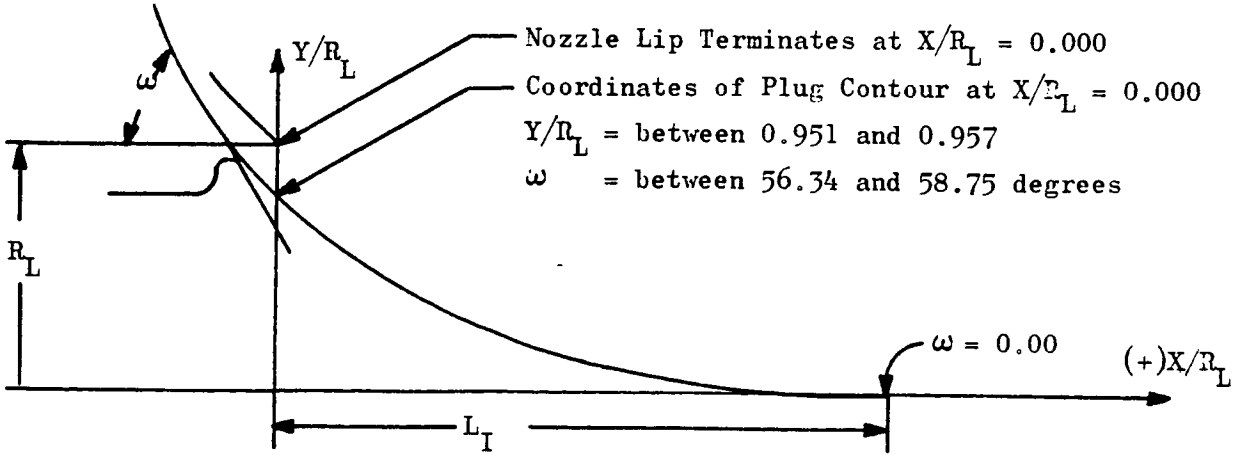

TABLE 7

PLUG CONTOUR FOR O_2/H_2 ATTITUDE CONTROL ENGINES
(ϵ = 10:1)

X/R_L	Y/R_L	ω	X/R_L	Y/R_L	ω
			0.029	0.846	47.44
2.110	0.132	10.84	0.017	0.860	49.52
1.461	0.261	12.78	0.007	0.872	51.55
1.064	0.360	15.66	-0.001	0.883	53.52
0.798	0.441	18.46	-0.008	0.893	55.44
0.609	0.509	21.19	-0.014	0.902	57.30
0.471	0.566	23.84	-0.020	0.911	59.10
0.368	0.614	26.43	-0.024	0.919	60.83
0.288	0.656	28.94	-0.028	0.926	62.48
0.226	0.692	31.40	-0.032	0.933	64.06
0.178	0.723	33.81	-0.035	0.940	65.55
0.139	0.750	36.20	-0.038	0.946	66.93
0.107	0.774	38.92	-0.040	0.952	68.21
0.082	0.796	41.33	-0.042	0.958	69.34
0.061	0.815	43.23	-0.045	0.965	70.28
0.044	0.831	45.32	-0.048	0.973	70.98

Coordinate System

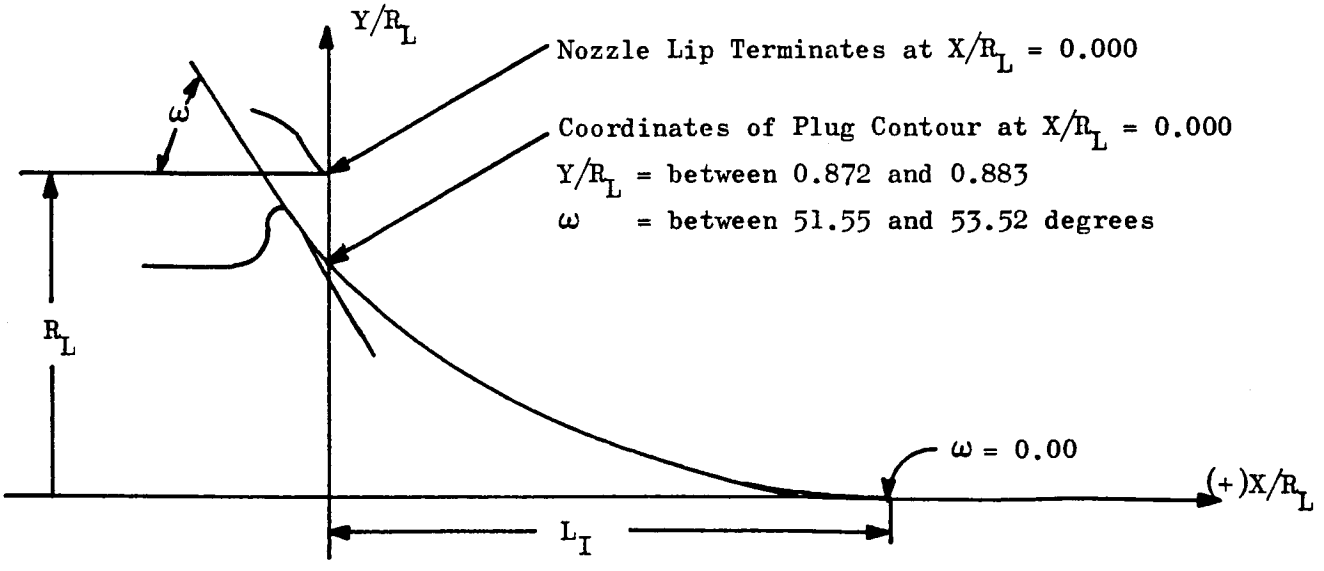

TABLE 8

PERFORMANCE AND HEAT TRANSFER RESULTS FOR TYPICAL CATALYTIC O_2/H_2 THRUSTORS

Nozzle Type	F (lbs)	P_c (psia)	D	$(MR)_D$ (o/f)	$I_{SP_{VAC}}$ (sec)	Thrust Inefficiencies, percent					Total Eff. %	$I_{SP_{ACT}}$ (sec)
						c*	D	F	K	c		
LOW CHAMBER PRESSURE APPLICATIONS												
Cone	20	10	50	1.0	400	2.0	4.6	2.9	0.5	0.5	.898	359
Bell	20	10	50	1.0	400	2.0	2.2	2.9	0.5	0.5	.920	368
Bell	100	10	50	1.0	400	2.0	2.2	2.3	0.5	0.5	.926	370
HIGH CHAMBER PRESSURE APPLICATIONS												
Bell	30	100	50	1.0	402	2.0	2.2	2.3	1.0	1.2	.916	368
Bell	100	100	50	1.0	402	2.0	2.2	1.7	1.0	1.2	.931	374
HIGH MIXTURE RATIO												
Cone	20	10	50	2.5	455	2.0	2.2	2.2	1.1	None	.927	422

Definitions

- c* - combustion efficiency
- D - divergence
- F - friction
- K - kinetic
- c - condensation (maximum)

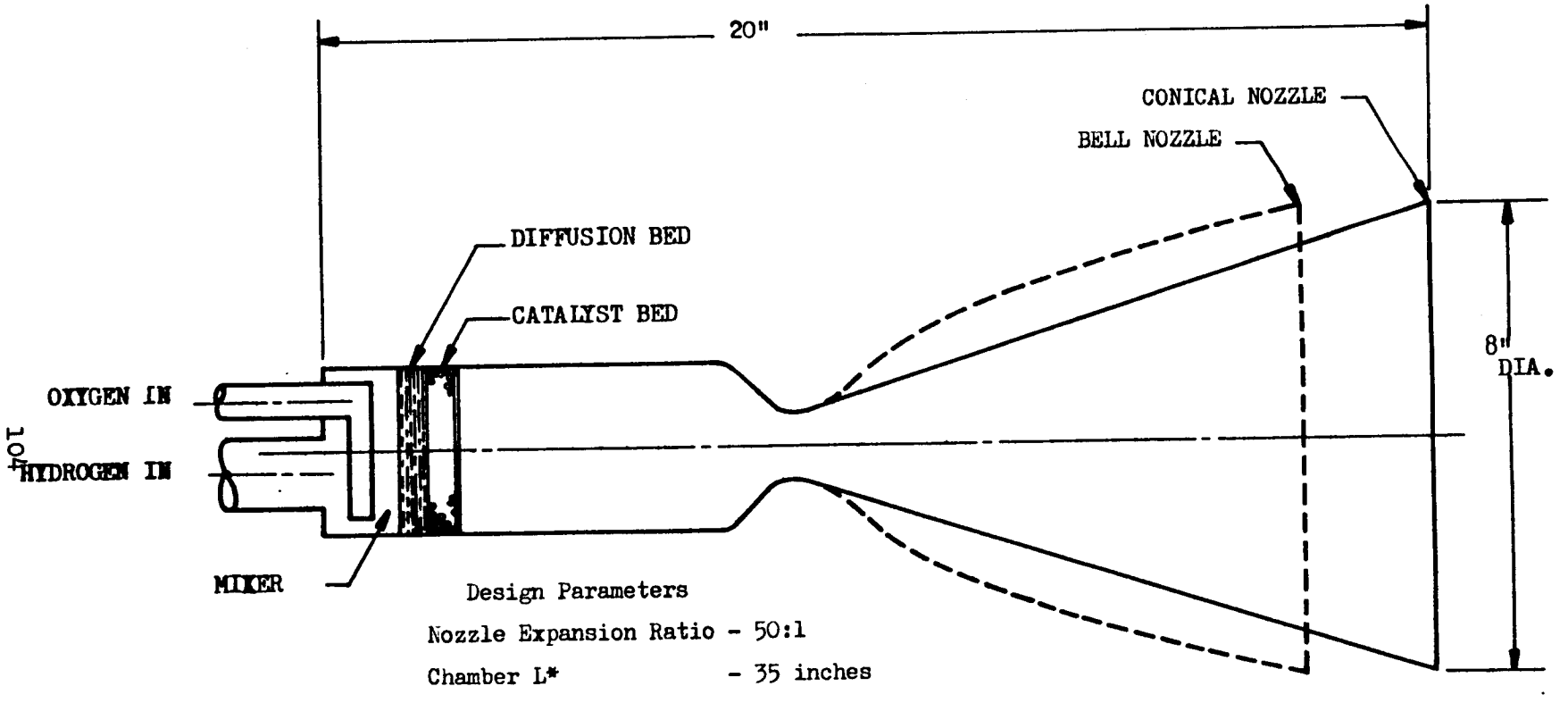

Figure 42. Conceptual Schematic of 20 Pound-Thrust, 10 Psia Full-Flow Thrustor

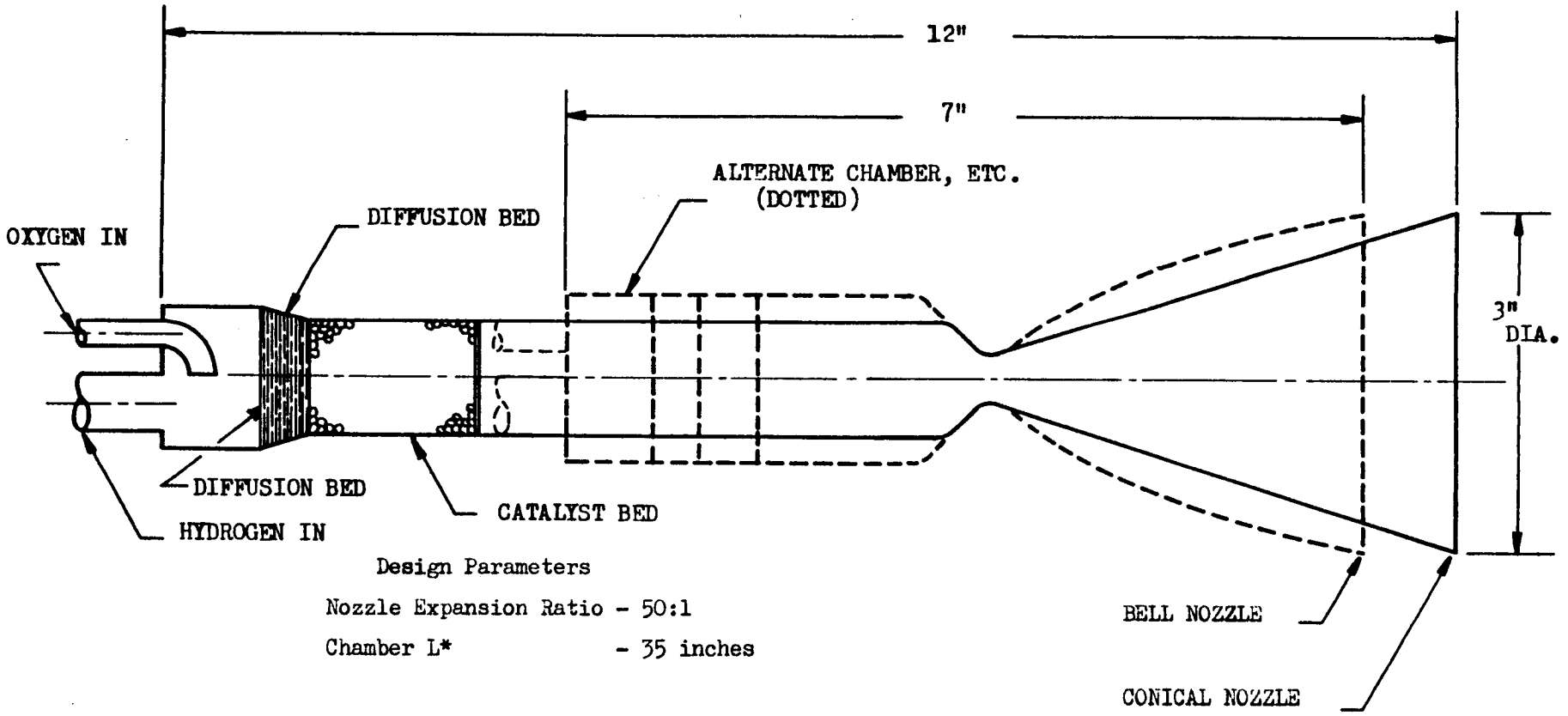

Figure 43. Conceptual Schematic of 20 Pound-Thrust, 100 Psia Full-Flow Thrustor

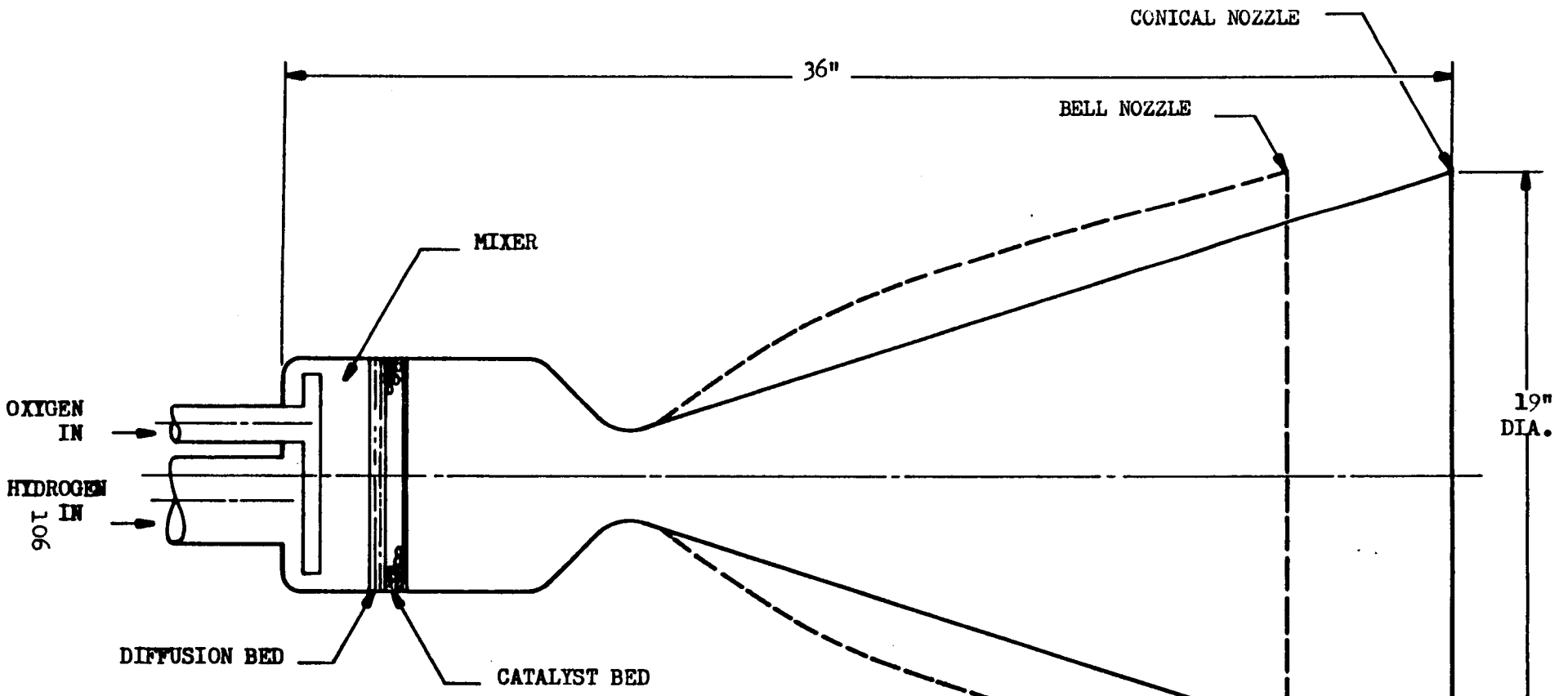

Figure 44. Conceptual Schematic of 100 Pound-Thrust, 10 Psia Full-Flow Thrustor

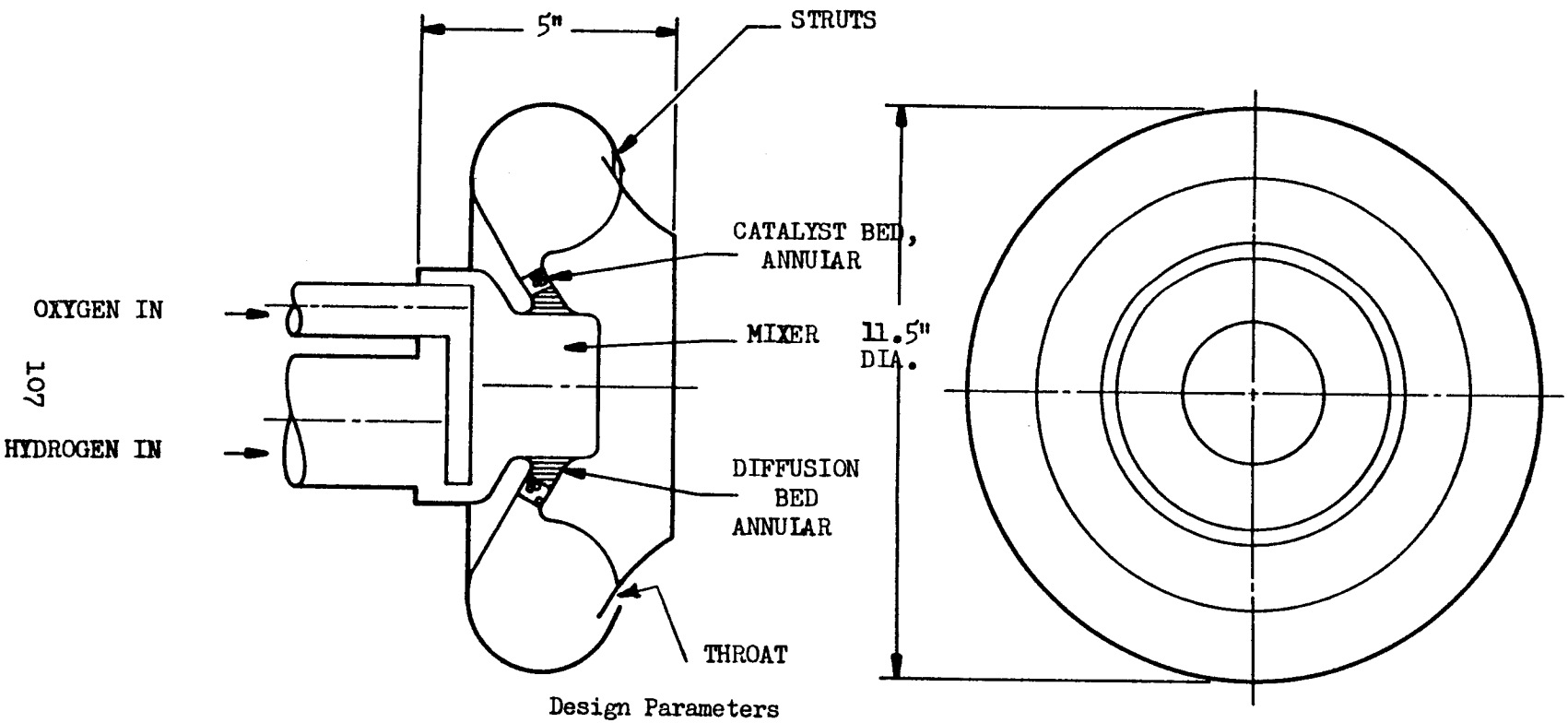

Figure 45. Conceptual Schematic of 100 Pound-Thrust, 10 Psia Truncated Spike Thrustor

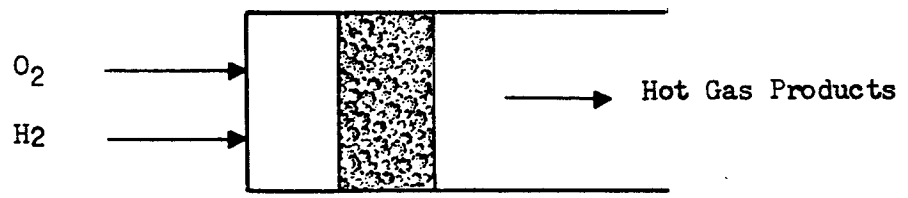

INLINE BED

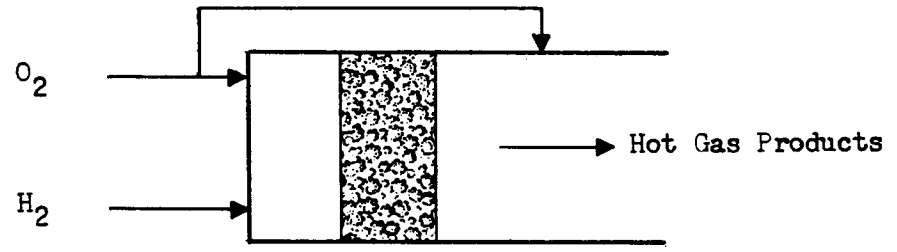

INLINE BED
WITH DOWNSTREAM INJECTION

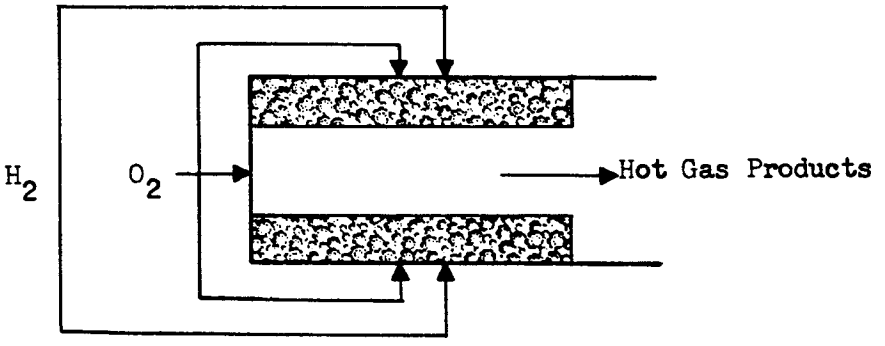

ANNULAR BED

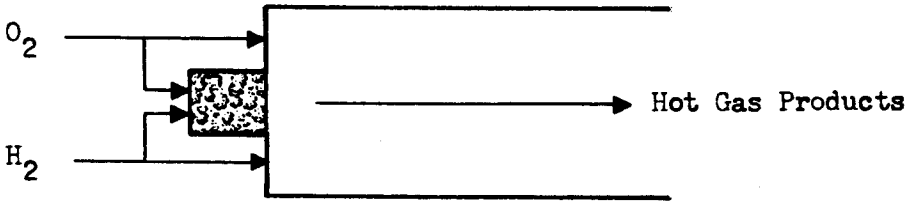

PILOT BED

Figure 46. Catalyst Bed Design Concepts

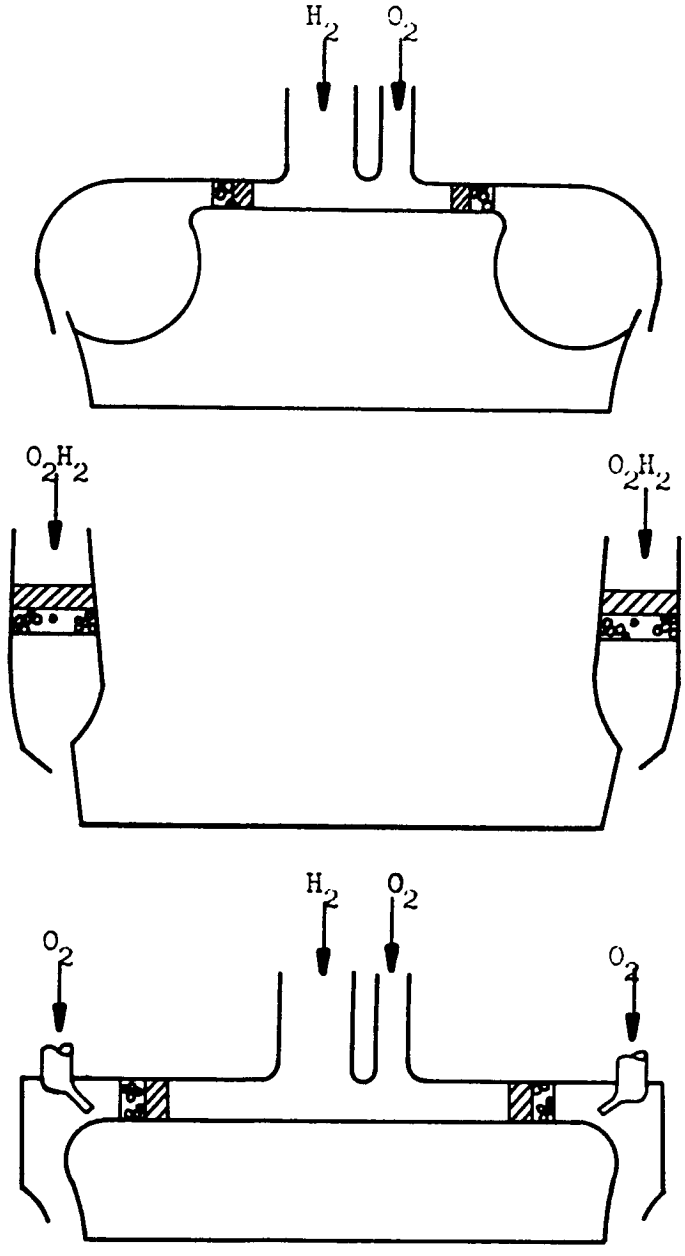

Figure 47. Truncated Spike Catalyst Bed Design Concepts

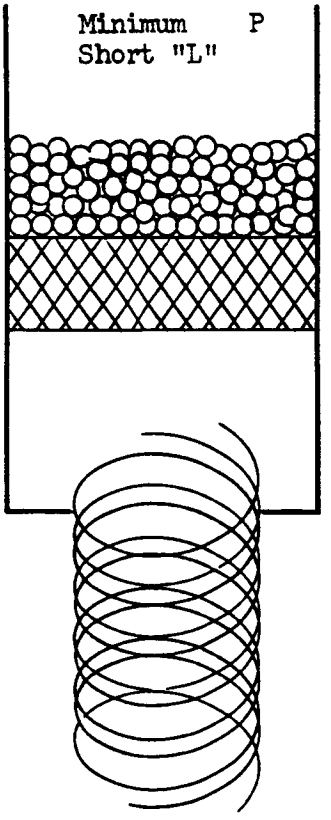

SWIRLER-DIFFUSION BED

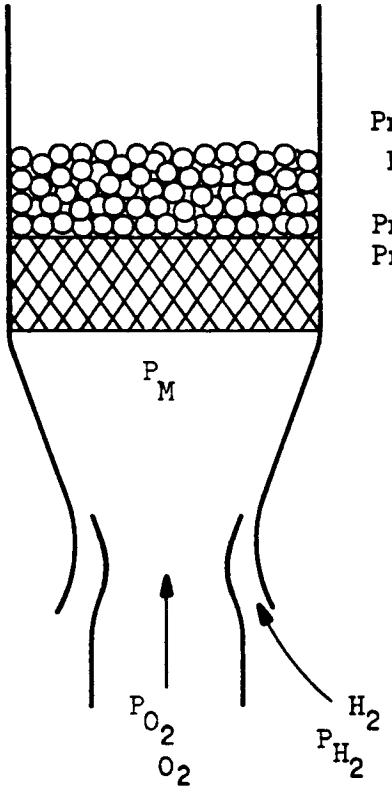

Pressure Balance
P_{O_2} P_M P_{H_2}
Provide Max. Pressure Recovery

JET PUMP-DIFFUSION BED

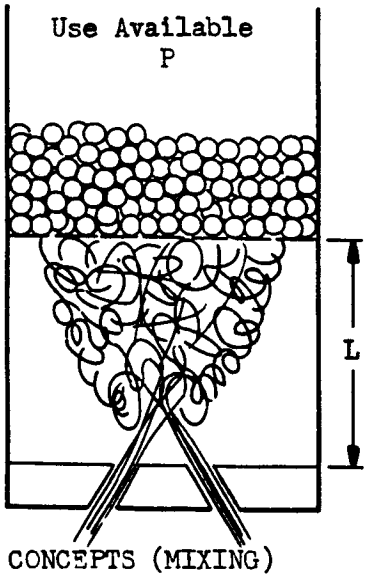

CONCEPTS (MIXING)
CONVENTIONAL

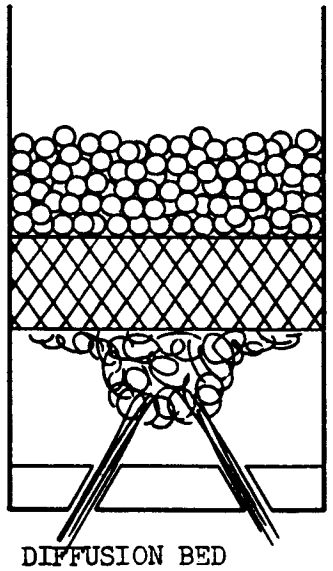

DIFFUSION BED

Couple with Jets
Provide Final Homogeneous Mixing, Shorten L.

Figure 48. Low Pressure Injector-Mixer Concepts

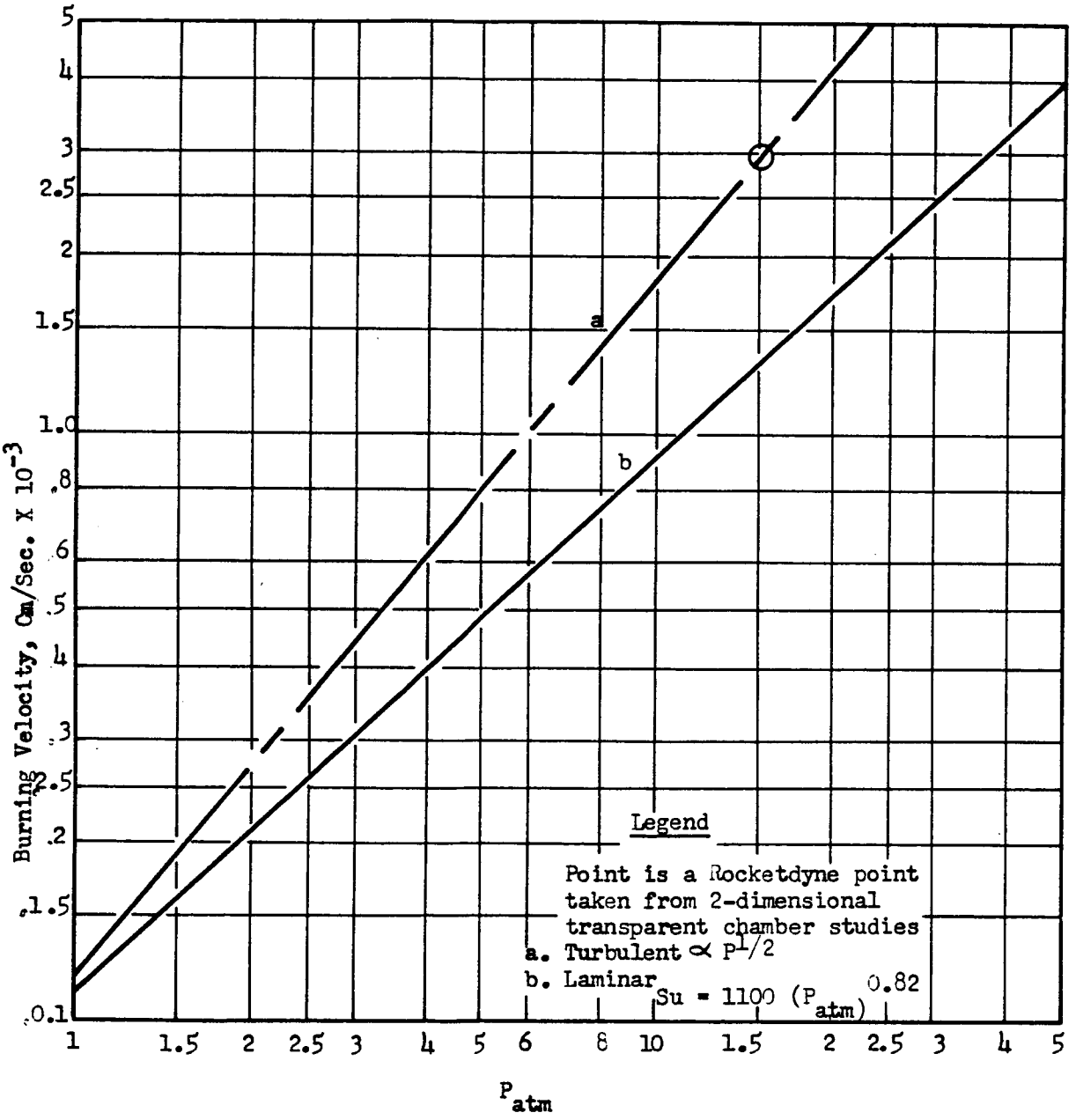

Figure 49. Flame Velocity Data Available from Literature

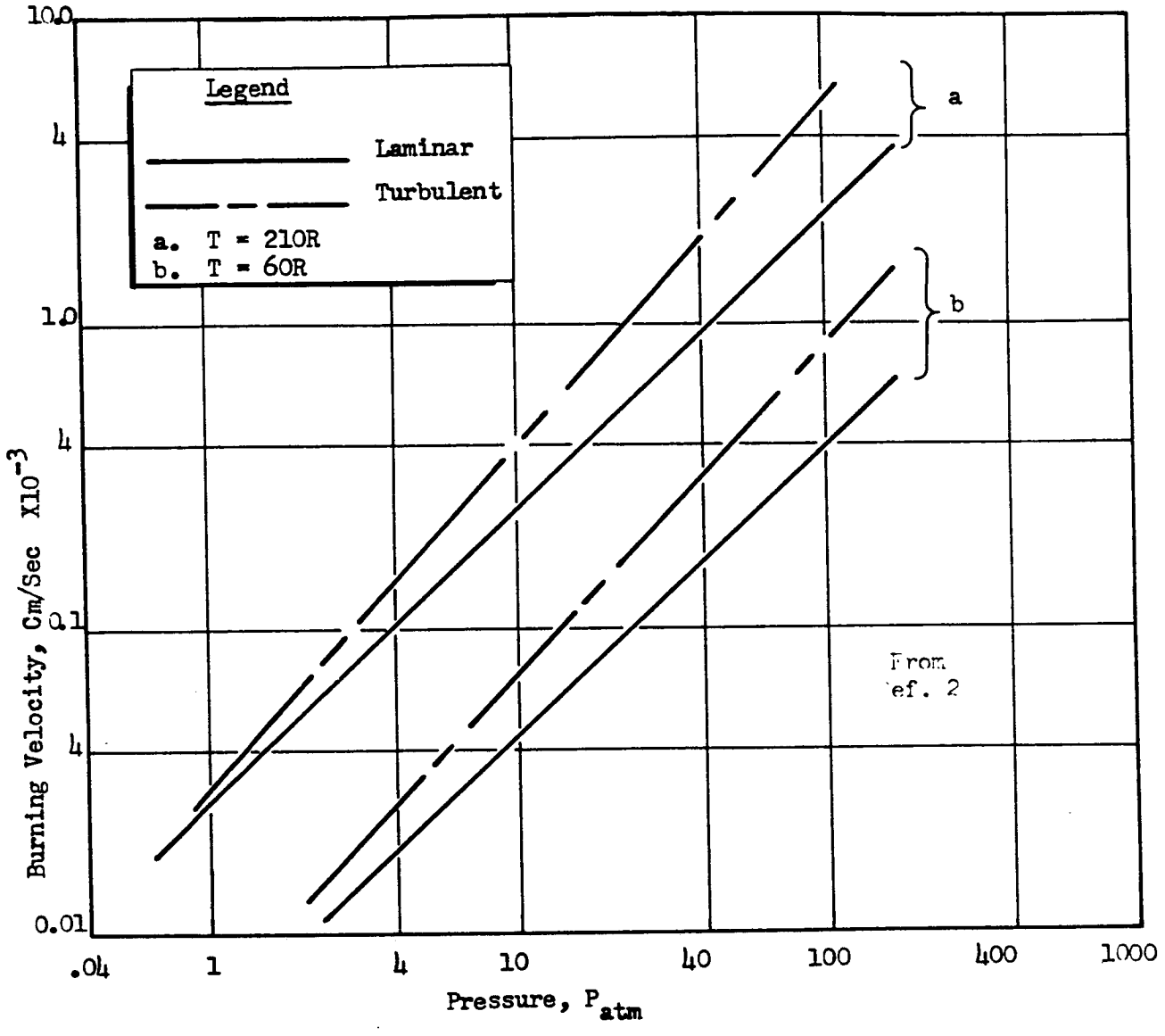

Figure 50. Flame Velocity Extrapolated Data to 60R and 210R for Turbulent and Laminar Flames

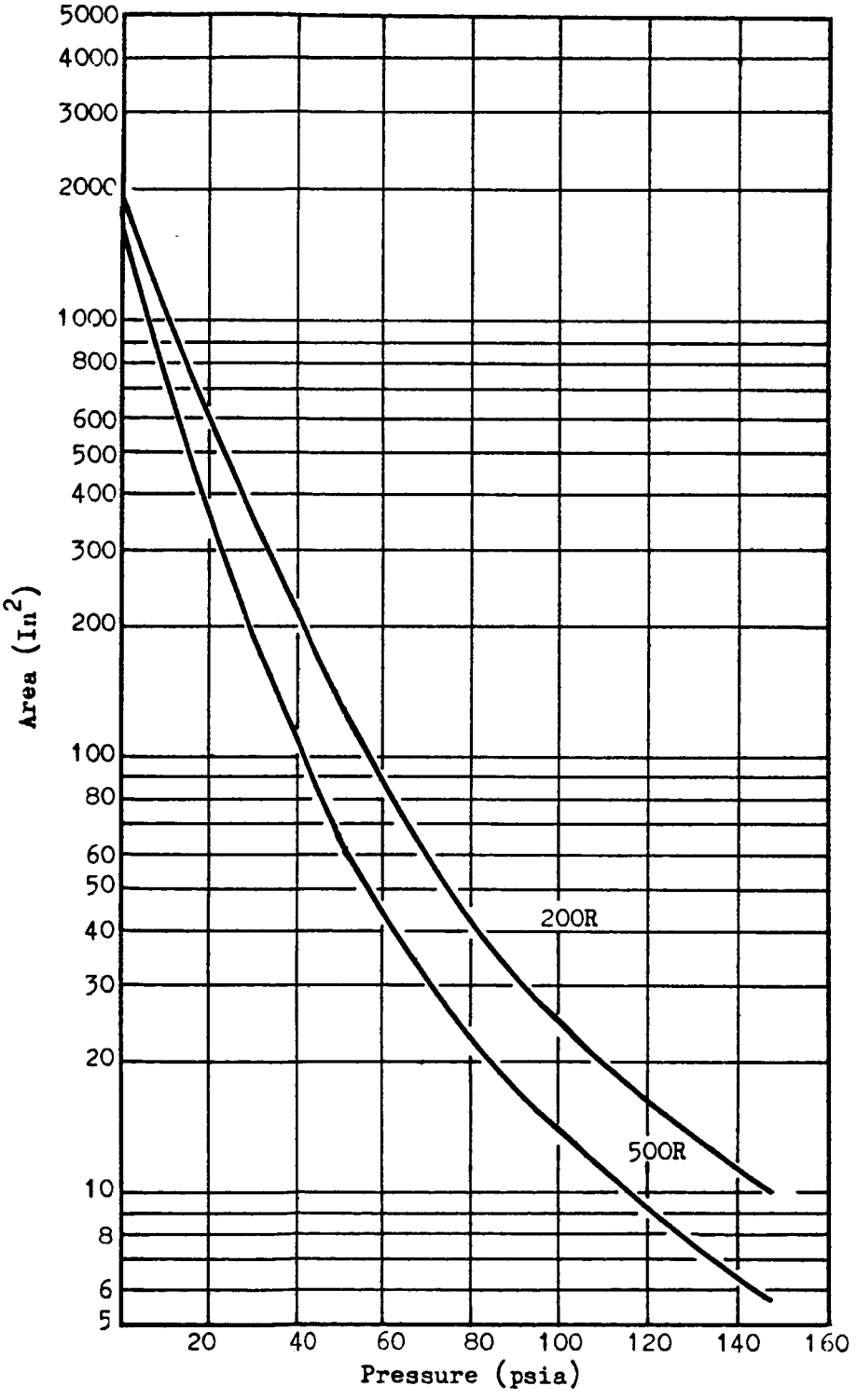

Fig.51. Maximum Reactor Bed Flow Area for Flashback Prevention as a Function of Upstream Pressure in a 20 lbf. Thrustor

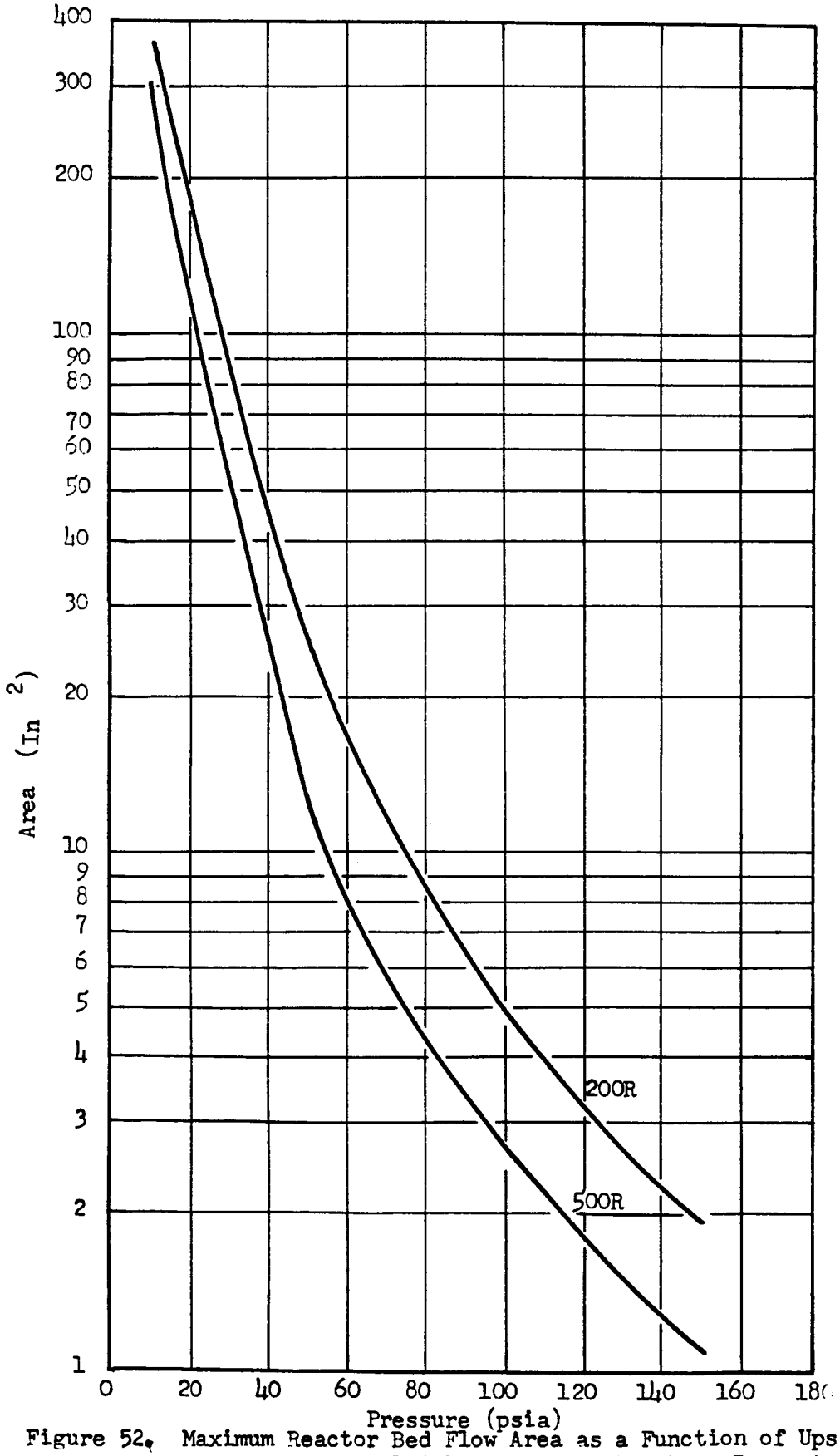

Figure 52. Maximum Reactor Bed Flow Area as a Function of Upstream Bed Pressure at 100 lb_f. Thrust Level to Prevent Flashback for two Propellant Inlet Temperatures.

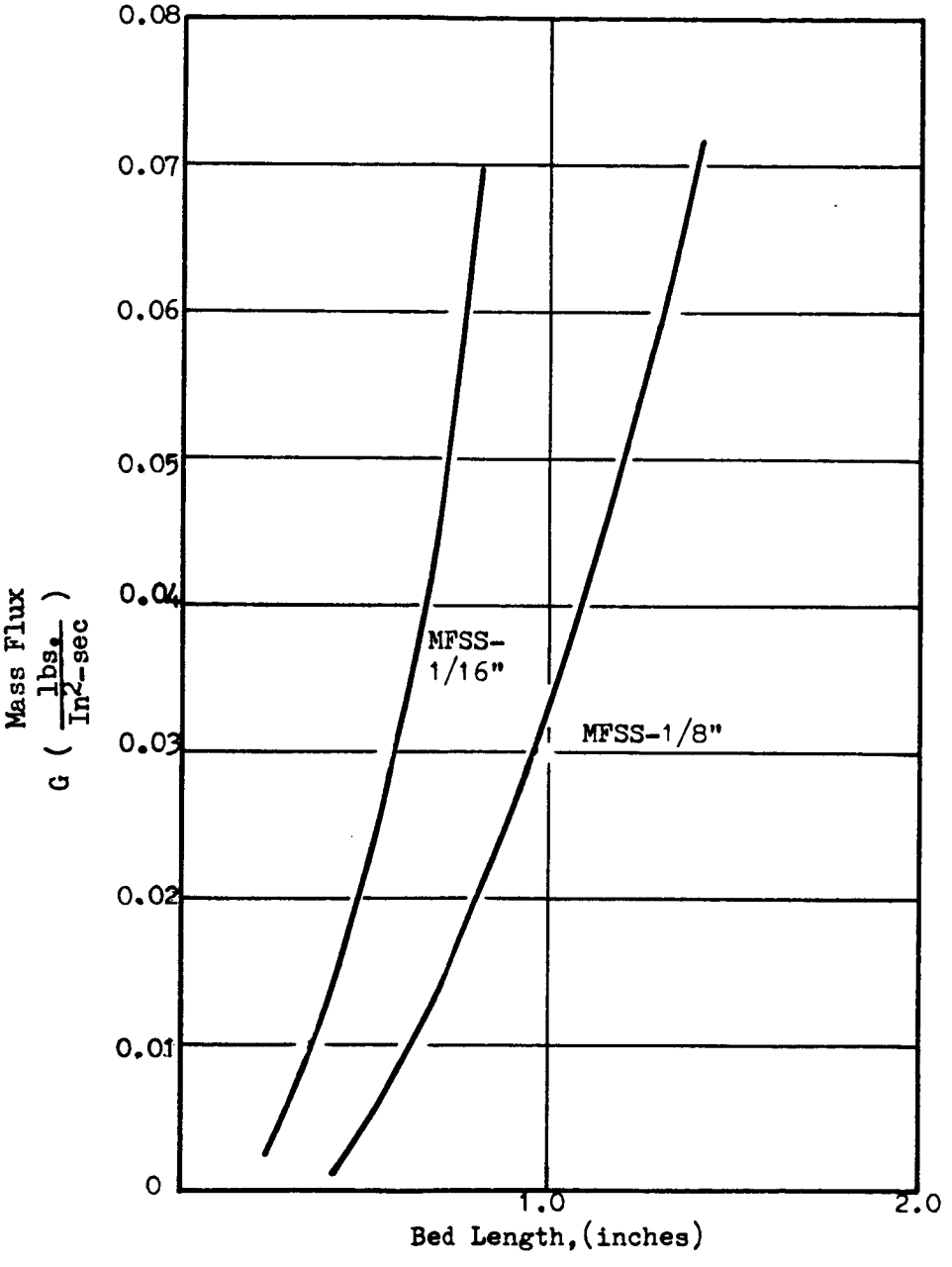

Figure 53. Theoretical Minimum Reactor Bed Length Required for Complete Reaction (H_2/O_2) as a Function of Superficial Mass Flux for two Catalyst Types

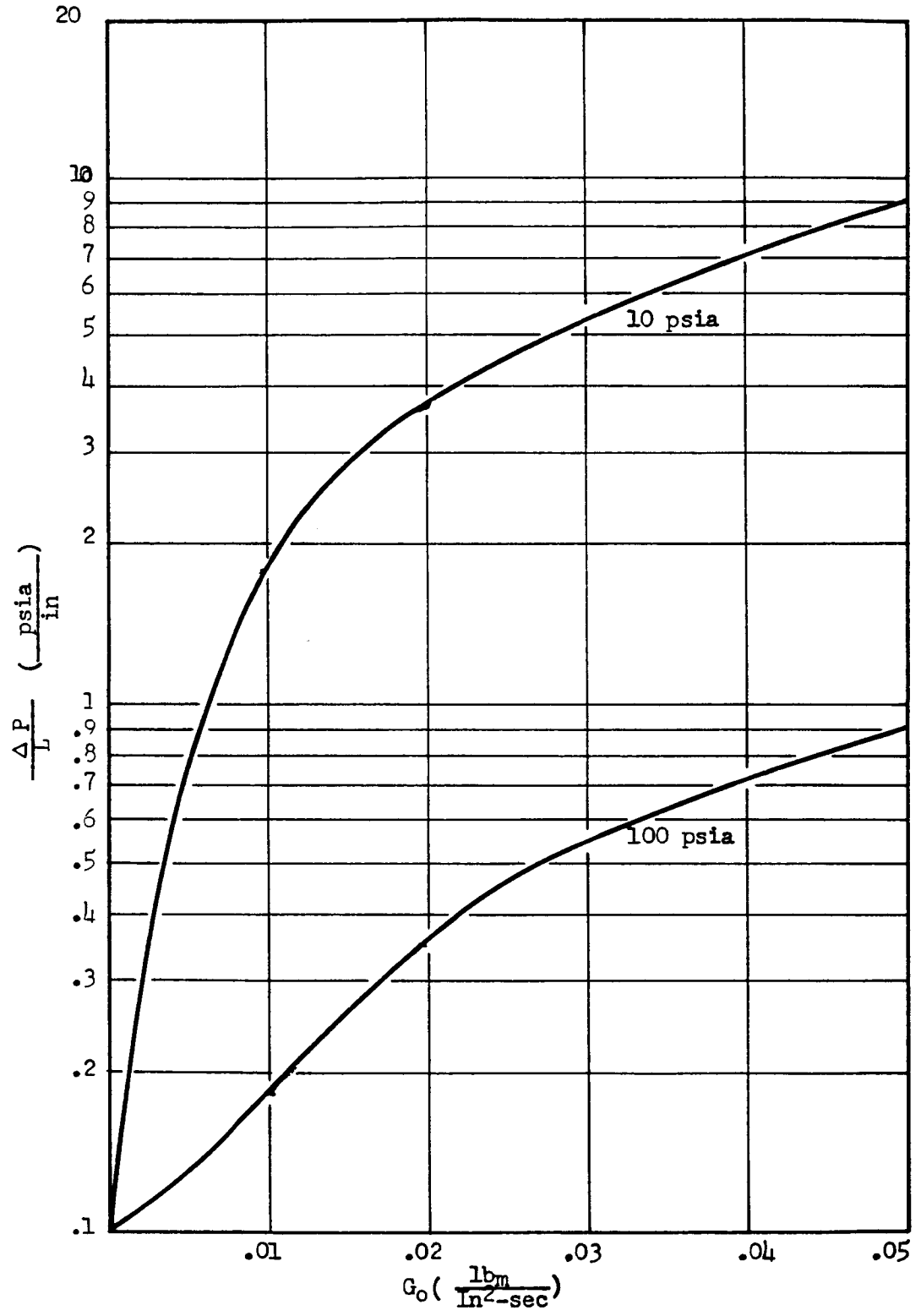

Figure 54. Theoretical Pressure Drop Per Unit Length of a Reactor Bed Composed of MFSA-1/8 Catalyst As a Function of Superficial Mass Flux for Nominal Bed Pressures of 100 and 10 psia

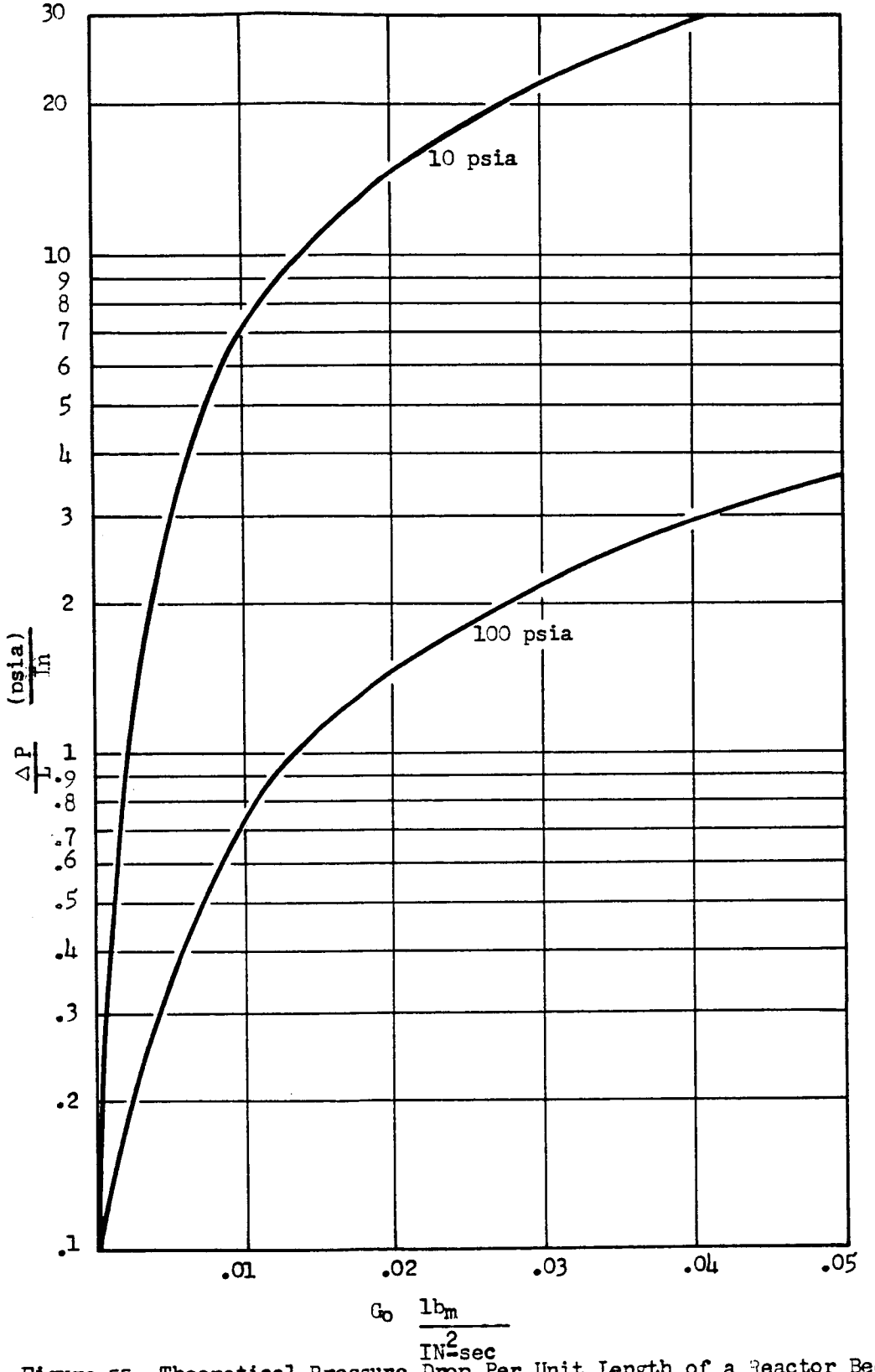

Figure 55. Theoretical Pressure Drop Per Unit Length of a Reactor Bed Composed of MFSA-1/16 Catalyst as a Function of Superficial Mass Flux for Nominal Bed Pressures of 100 and 10 psia.

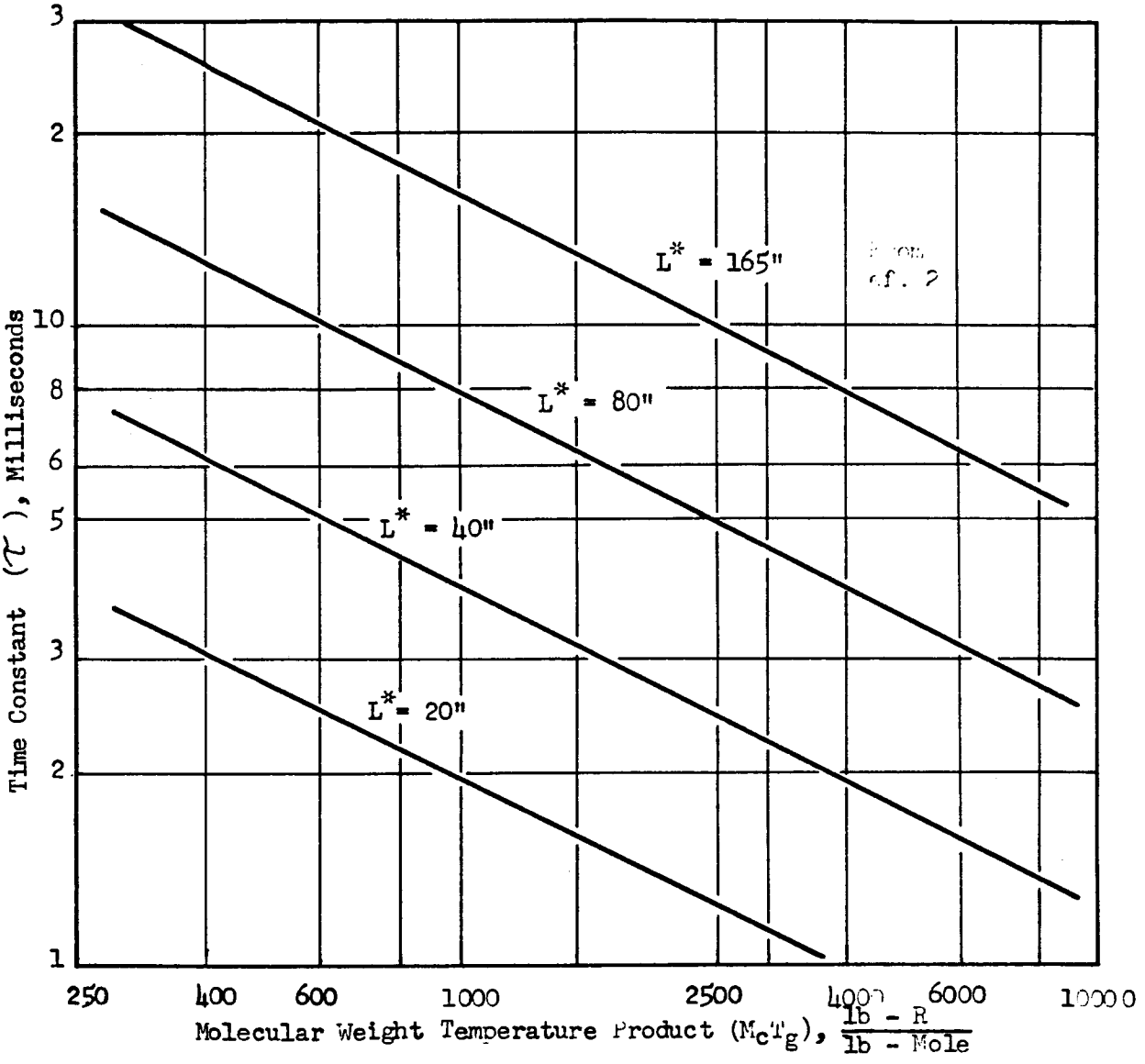

Figure 56. Pneumatic filling constant to 95% steady state Pressure for Various assumed Sizes of Reactor and Steady State Temperatures

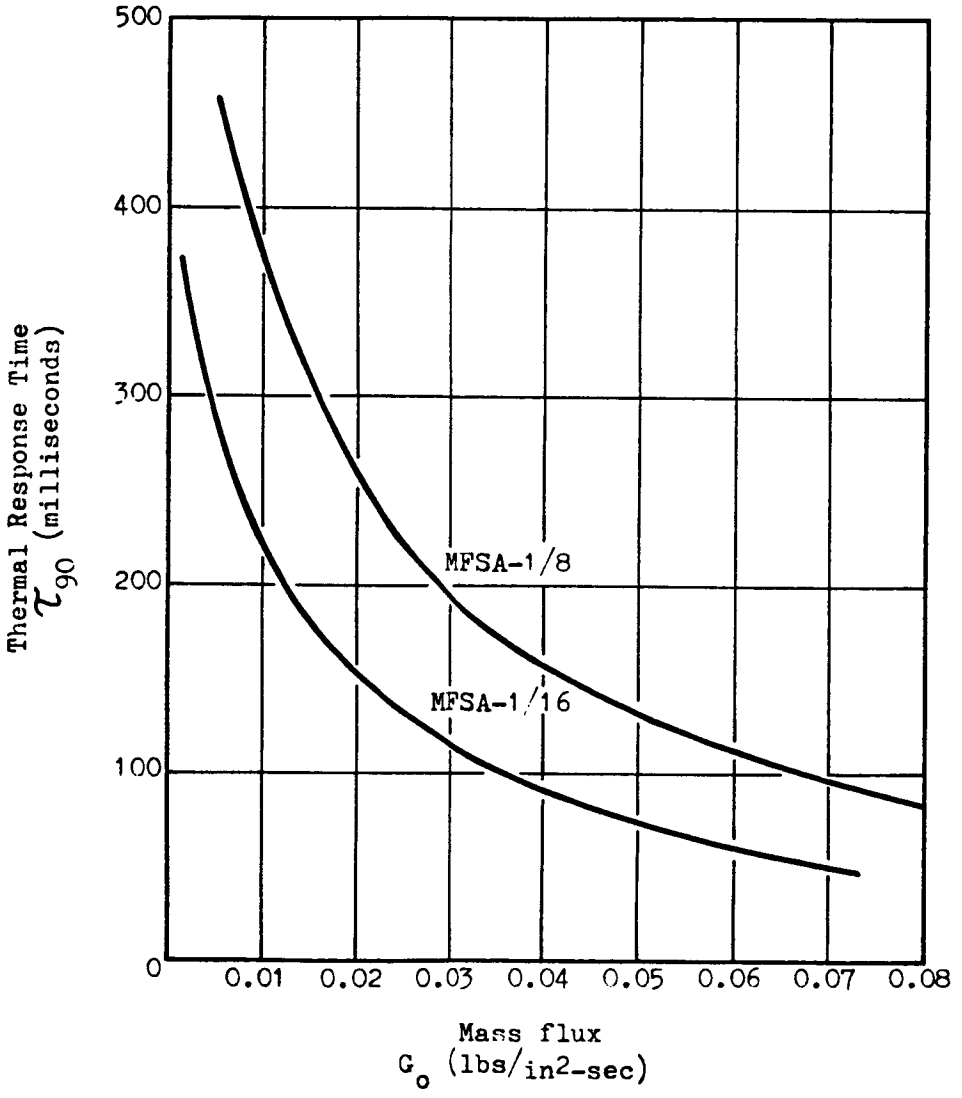

Figure 57. Thermal Response (time to 90% of Steady-State Reacted Gas Temperature) for MFSA-1/8" and MFSA 1/16" Catalyst as a Function of Superficial Mass Flux at the Optimum Bed Length.

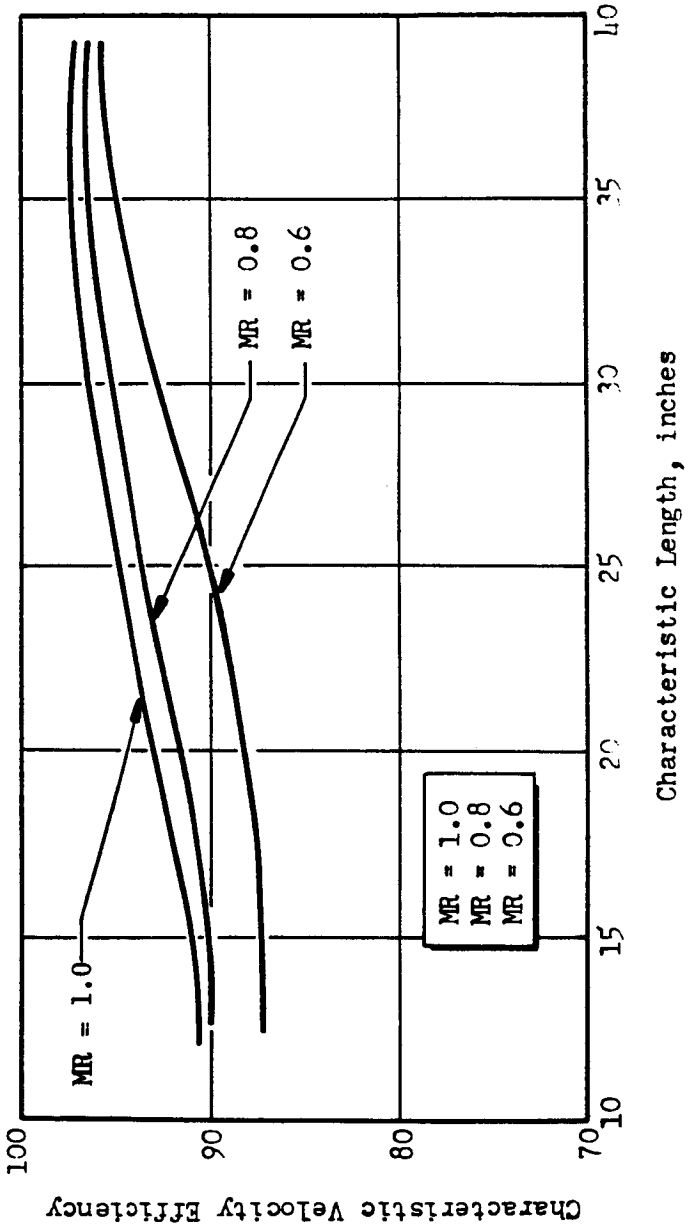

Figure 58. Experimental Results for 150-Lb Catalytic Thrustor Operating on 500° R Propellants (O_2/H_2). Characteristic Length is Defined in Terms of Combustion Volume Downstream of Catalytic Bed.

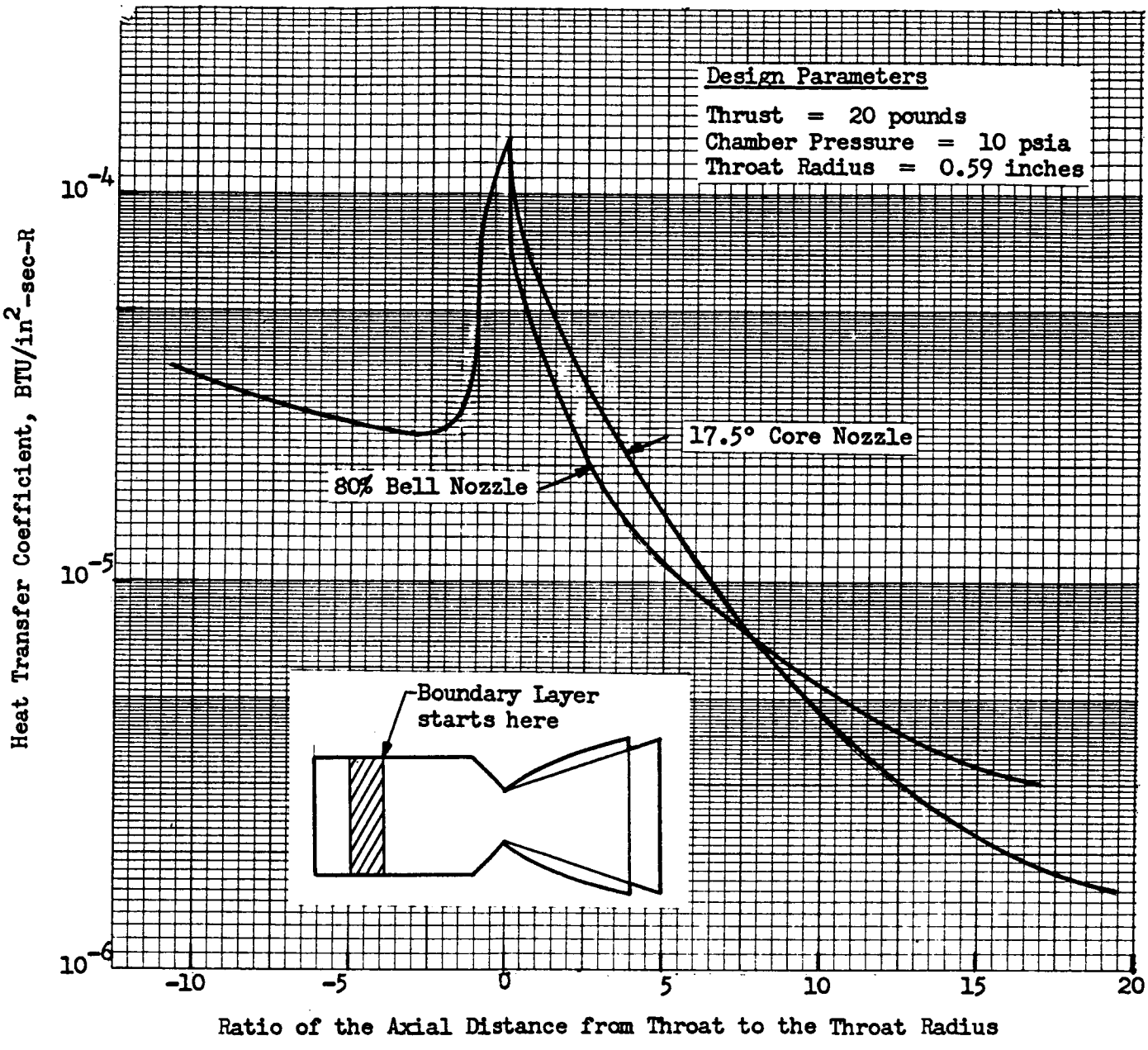

Figure 59. Predicted Heat Transfer Coefficients for a 20 Pound-Thrust Hydrogen-Oxygen Engine with Two Nozzle Designs, an 80% Bell Nozzle and a 17.5° Core Nozzle - 10 psia Chamber Pressure

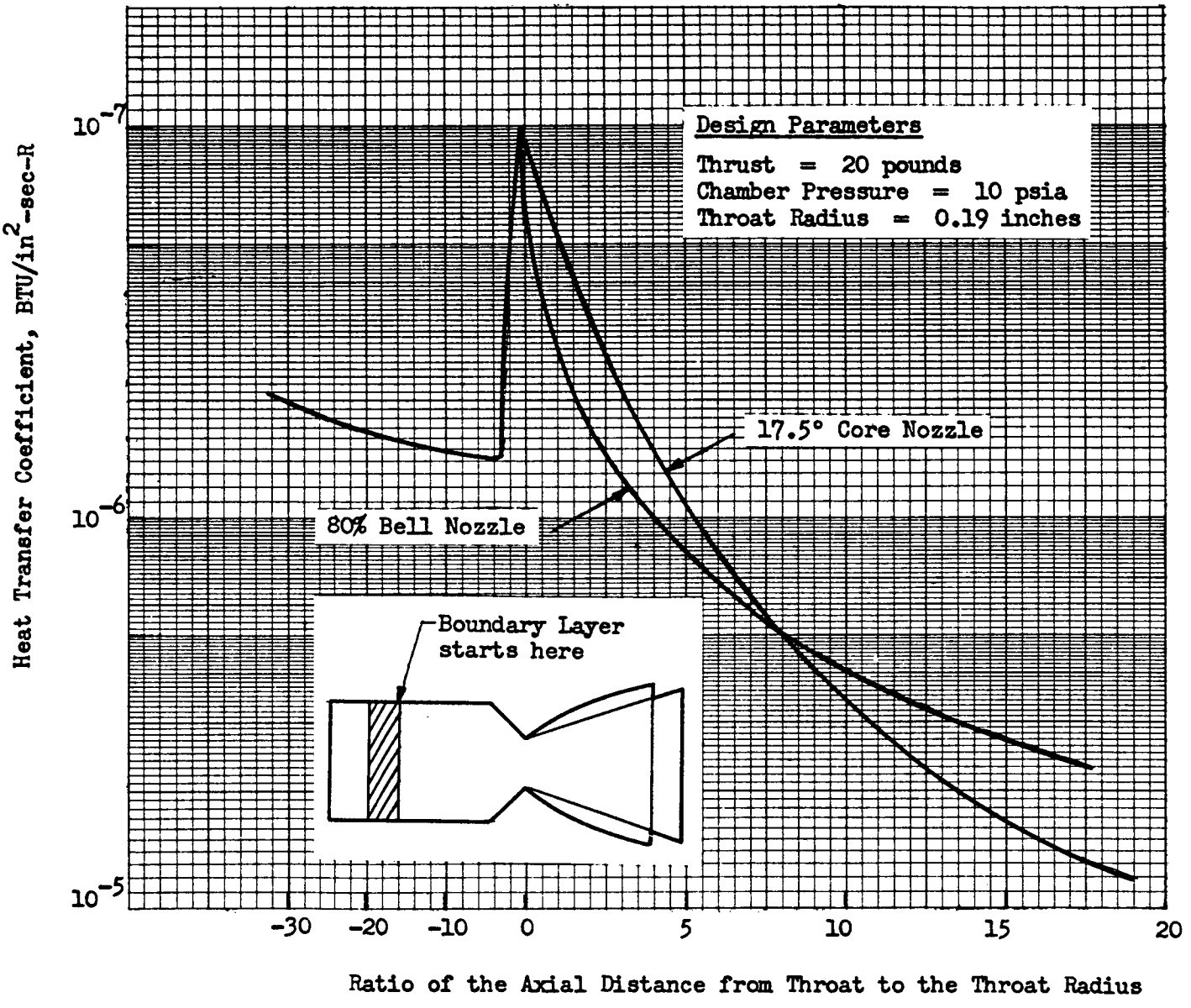

Figure 60. Predicted Heat Transfer Coefficients for a 20 Pound-Thrust Hydrogen-Oxygen Engine with Two Nozzle Designs, an 80% Bell Nozzle and a 17.5° Core Nozzle - 100 psia Chamber Pressure

COMPONENT ANALYSIS--CONDITIONER

INTRODUCTION

For reliable operation of the cryogenic RCS thrustors, the temperature of the incoming propellants must be raised above a minimum value to insure reliable catalytic reaction and the thermodynamic state (pressure, quality and temperature) sufficiently controlled to allow reliable control of the flow to the thrustors. The conditioner subsystem is included in the cryogenic RCS to accomplish these tasks.

Several conditioning concepts were formulated and evaluated. These are described below. The general conditioner design and effect on performance is also discussed. This establishes a basis for analytical evaluation and selection of a single concept for experimental evaluation.

The conditioner concepts were to be compatible with two distinct types of reaction control systems; a high pressure system (at $\sim$ 100 psia) representative of a separate pressure-fed system and a low pressure system (at $\sim$10 psia) representative of a system fed from the main tankage of a vehicle with a pump-fed main propulsion system.

The propellant supply restraints placed on the conditioner subsystem were established at the initiation of this program:

Hydrogen Thermodynamic State - 37R liquid to 500R gas, in single or mixed phases

Oxygen Thermodynamic State - 163R liquid to 500R gas, in single or mixed phases

Propellant Composition	-	propellants contain 0 to 50 percent helium pressurant at the low chamber pressure level, undiluted propellant at the high chamber pressure level.
Supply Pressures	-	20 ± 5 psia for 10 psia chamber pressure, 175 ± 5 psia for 100 psia chamber pressure

General System Design Considerations

A general RCS design requires a conditioning subsystem which would be utilized to increase the temperature and regulate the thermodynamic state of the propellants. The conditioning would serve the following two purposes, respectively:

1. Raising the temperature to a value which would guarantee reliable catalytic ignition, and

2. Regulating the physical state of the propellants to a degree which would insure positive flow control.

Schematically, the RCS might be represented as below:

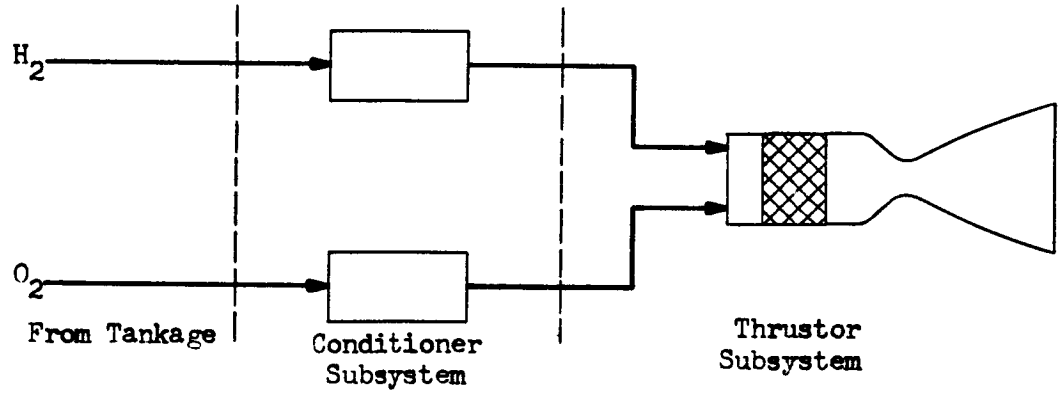

The propellant flows from the main tankage to a conditioner and then to the RCS thrustors.

The system, as schematically shown, is separated into two distinct subsystems. Implied in this separation is a corresponding separation of control systems; the thrustor control system is distinct from that of the conditioner.

Integrated Subsystems. The two subsystems could be integral instead as shown in the above schematic. However, in such a case, the heat and momentum (pressure loss) exchange processes in the conditioner would be closely coupled with the thrustor itself which could make the thrustor operation extremely sensitive to upstream variations. Further, a varying thermodynamic state of the inlet propellant would have a closely coupled effect on the thrustor dynamics and operating levels.

Two solutions are thought to exist for the problems associated with such an integral system:

1. Provide a fast response automatic control function within the integral system which can cope with transient behavior typical of the start and shutdown phases of operation, and of varying inlet propellant temperatures and densities.
2. Deliberately insure an overdamped system--one not designed for fast response but with a sufficiently slow response to insure operability utilizing a more normal control concept.

The second alternative ignores one of the prime objectives of the program, that of providing for a moderately fast response thrust system and so was not considered in detail for this program. However, such a thrust system would appear highly feasible for such slow response applications as propellant settling.

The first alternative is thought quite difficult from both an evaluation and a design standpoint. The close pneumatic coupling of the two

subsystems leads to a feedback of the dynamic characteristics of the thrustor into the conditioner. Thus, the conditioner and thrustor functions would necessarily be linked by a fast response control concept. The incorporation of a provision for handling a wide variety of propellant inlet conditions would add complexity. In any case, the design and operability of such a system would depend in large part on the dynamic and steady-state characteristics of the thrustor, and on the details of the control systems and devices.

Separate Subsystem Approach. The distinct subsystem approach was selected for this program for three primary reasons; (1) an uncertainty in the thrustor and conditioner dynamic characteristics, (2) a lack in availability of applicable control devices, and (3) a program goal more general than a specific device approach. The dynamic characteristics observed in this program can then serve as a basis for the design of close-coupled systems.

The conditioning subsystem can accomplish a second task in addition to supplying enthalpy to the propellants, one of smoothing propellant temperature and density fluctuations to aid in system control. The conditioner and thrustor functions in the general RCS concepts examined were separated by a surge volume (accumulator) included in the conditioner subsystem. This provides a smoothing of variations in thermodynamic state as well as a station for measuring temperature and pressure. The accumulator serves to pneumatically decouple the conditioning and thrust functions as well as provide a source of conditioned propellant upon demand. The former serves to separate the thrustor response from the conditioner.

Thermal Requirements

Conditioner Energy Source Considerations. The task of raising the propellant temperature to given level to assure reliable catalytic action is one of supplying energy. A minimum temperature has not been defined; however, experience has shown LOX at 163R and GH_2 at 210R will give reliable ignition. Conversely, hydrogen at 40R leads to a freezing of the oxygen and erratic catalytic reaction. A temperature of 200R was chosen as representative of the minimum for catalyst reaction purposes. A temperature of 500R was specified as a maximum for consideration.

The conditioning energy could be obtained from external electrical power sources, radioisotope sources, thermal energy transfer from the vehicle, or O_2-H_2 chemical reaction energy. Figure 61 shows the power requirements for conditioning from the propellant normal boiling point to 200R and 500R. Electrical power sources were rejected in order to minimize system interface power requirements.

Isotopic energy sources were considered and a summary is shown in Table 9. Assuming a 100 percent conversion efficiency relatively heavy power source weights are necessary for applications involving isotope shielding. Isotope costs are high and the least expensive isotope shown in Table 9 has nearly the highest weight. For applications without shielding requirements and where half lives of less than six months are acceptable, C_m-242 and P_c-210 may be used as cost is not a major factor. These two isotopes could also be extremely attractive for the small make up heat sources (less than five watts) that might be required.

Thermal energy transfer from the vehicle was not considered for the bulk of the energy supply since it is extremely dependent upon vehicle

design. Also, it is doubtful that sufficient energy would be available under high usage conditions.

The remaining energy source, hydrogen-oxygen combustion, was deemed most appropriate for the subject program. This concept can provide energy over a wide range of power levels and thus meet the rather wide range of operating specifications on the system. Such an energy supply concept utilizes propellant non-propulsively, which causes a reduced specific impulse. However, this can be a relatively small reduction with the proper system design.

Evaluation of H_2-O_2 Combustion Energy for Conditioning. Propellant conditioning was examined from the viewpoint of the energy required to increase the temperature of the feed propellants. Two combinations of propellant thermodynamic states were assumed; one of liquids at the normal boiling points (37 and 163R for LH_2 and LO_2 respectively), and the second of gases at somewhat higher temperatures (60 and 190R) reflecting a moderate thermal energy input.

Propellant conditioning to thrustor inlet temperatures varying from 200 to 500R were considered to provide a realistic temperature excursion. Because the energy requirements of the conditioning system are highly dependent on engine mixture ratio, a range from 1.0 to 5.0 was evaluated. To determine a minimum propellant consumption necessary to supply the required energy, stoichiometric burning of the oxygen and hydrogen was assumed. Two final conditions of the water were assumed after energy exchange with the thrustor propellants; (1) a final temperature of 500R with sufficiently low partial pressure to prevent condensation or solidification, and (2) complete ice formation at a final temperature equal to that of the thrustor propellant. Figures

62 and 63 present the water formation requirements for the two conditions. These requirements are based on overall system enthalpy balances and do not explicitly consider any particular method of energy exchange.

An alternative conditioner concept, which has received attention, utilizes a pressure augmentation device for the low pressure RCS application. There is, of course, a tradeoff between weight, volume, and complexity added by such a device and the benefits of reduced component size and pneumatic response due to higher pressures. Such a device also increases the pressure available for propellant mixing at the injector-mixer in the thrustor. Reacted H_2-O_2 mixtures were the only power supplies considered as a driver for such a device.

Thermal Energy Transfer Concepts for Conditioning. Many different conditioning systems which utilize transfer of the O_2-H_2 combustion energy can be envisioned. One is direct heating of the propellants by cross bleeding small amounts of propellants and accomplishing the reaction via a catalytic bed. In this case the chemical reaction energy is released directly into each propellant stream. However, in this case the conditioned temperatures must be raised to about 500 R to insure against ice formation in the bed.

Another thermal concept is heat exchange of the propellants with hot combustion (H_2-O_2) gases produced by a catalytic gas generator. The thermally depleted gases are then vented overboard. Two variations of this method were investigated; one where the heat exchanger is kept at operational temperature at all times, and a second where the heat exchanger is allowed to cool between energy transfer demands. The latter will necessarily have a slower response.

CONCEPTUAL DESIGNS

Subsystem Concepts

The four subsystems considered in the initial comparison, the direct heating and the three heat exchanger concepts, are shown schematically in Figs. 64 through 67. It is emphasized that these concepts are directed for utilization in a general type of application. Use of a cryogenic RCS in certain specific applications, such as a stage settling engine system running only under steady-state conditions, should not require such a general approach. Under such conditions, where response is not critical, a more integrated conditioner-thrustor will be more optimum.

Direct Heating Concept. A schematic representation of the direct heating subsystem is shown in Fig. 64. This conceptual subsystem is operated as follows: When the accumulator pressure transducer senses a low pressure in the accumulator, the main propellant valves are opened, allowing the propellants to flow through the catalyst beds into the accumulators. The cross-feed solenoid valves are actuated permitting oxygen to flow into the hydrogen catalyst bed (or hydrogen into the oxygen bed), react with the hydrogen, and increase the hydrogen temperature to 500R. A feedback of the hydrogen temperature can be utilized to control the quantity of oxygen cross-fed to the catalyst bed, thus providing a measure of control on this temperature. A similar control would be utilized on the oxidizer side.

The propellant feedback must be accomplished from a lower total pressure condition to a greater one. This could be accomplished with the use of a venturi-type device to lower the static pressure of the main propellant

stream. Thus, on the hydrogen side of the conditioner, the hydrogen would be fed through a venturi and oxygen bled in the venturi throat. It is noted that the operation of such a system is quite difficult from a control dynamics standpoint.

Conventional Heat Exchanger Concept. The conventional (steady-state) heat exchanger subsystem is shown schematically in Fig. 65. Operation of this subsystem begins when the accumulator pressure transducer senses a low pressure. When the accumulator pressure is too low, the main propellant valve and the cross-feed valves are activated, adding additional conditioned propellant to the accumulator. If the pressure is too high, the relief valve opens, decreasing the accumulator pressure. The gas generator feeds are obtained from the accumulators to ensure positive control of the mixture ratio and, therefore, the generator gas temperature. Thermostats are provided to sense the tube temperature and prevent tube burnout during the system start-up prior to the point where fully conditioned propellants exist in the accumulators.

Preliminary estimates of the response times prevailing in the heat exchanger system show that the thermal response of the exchanger wall is controlling and is on the order of 1 second for 0.020-inch stainless steel walls. Since the system sizing is a function of response time, methods of decreasing the response times were investigated.

The thermal response time of the conventional heat exchanger system can be approximated as

$$\frac{C_p \rho_m t}{h_g} \left[\frac{T_{rec} - T_{init}}{T_{rec} - T_{final}} \right] \qquad (22)$$

Several methods of decreasing the system response time are available.

1. The use of different tube materials--however, substitution of beryllium or copper for stainless steel will increase the response time approximately 18% and 7%, respectively.
2. The tube thickness can be halved to 0.010 inches, halving the response time.
3. The hot gas film coefficient can be increased by increasing the allowable pressure drop.
4. Both the hot gas film coefficient and the propellant side film coefficient (the temperature term is a function of both film coefficients) can be increased by increasing the allowable pressure drop. The strong dependance of response time on pressure drop is shown in Fig. 68, which also illustrates the desirability of investigating a pressure augmented system.
5. The thermal response term can be eliminated entirely by keeping the heat exchanger tubes at operational temperatures at all times.

Methods 1 and 2 do not reduce the response time to a sufficient degree to result in what can be considered a fast response system. Therefore, concepts embodying the remaining methods were investigated.

Pressure-Augmented Heat Exchanger Concept. A schematic representation of a pressure-augmented heat exchanger system is shown in Fig. 66 along with a nominal pressure profile. This system utilizes a pressure augmenting device to increase the system response times, thereby reducing the accumulator weights and volumes. Additionally, the component weights decrease due to the larger available pressure drop. Both of the propellant pumps can operate off a single prime mover. The pump power

requirements are presented in Fig. 69 as a function of pressure ratio and pump efficiency. Operation of this system is identical to the conventional heat exchanger system, with the exception of an additional control loop to operate the pumps and prime mover.

Hot-Tube Heat Exchanger Concept. Figure 67 is a schematic representation of a hot-tube heat exchanger. During both pulse mode and steady-state operation this systems' operational characteristic is identical to that of the conventional heat exchanger previously described. During any inactive period, however, an additional control loop senses the tube temperature and activates the catalytic gas generators when the tube temperature drops below a predetermined minimum. A check valve and solenoid vent valve are provided to vent the propellant to space prior to activation of control loop. This venting subsystem prevents overheating of the propellant stored in the exchanger during the conditioners inactive period and may not be required if recirculation effects are kept to a minimum.

The advantage of rapid response for the hot-tube heat exchanger over the conventional exchanger concept is only gained at the expense of a propellant comsumption necessary to supply the enthalpy to balance heat losses. To find the resulting missions, an optimization of shell and tube exchangers was accomplished and propellant consumption calculated for various insulation thicknesses.

The results for a 220 day mission are presented in Fig. 70 and show that the propellant consumption can be reduced to a 20 to 30 pound level. The resulting tube wall temperatures were reduced to the 1000 to 1200R level

from approximately 1800R for an increase in exchange area of 40 to 60 percent. The temperature optimization curves shown in Fig. 71 indicate the sensitivity of the heat loss to both insulation thickness and maximum tube temperature. The high temperature, high vacuum insulation used in the analysis, Min K 2000, is a bonded material reinforced with fibrous media ($k = \sim 0.02$ BTU/hr-ft-R) and is commerically available.

Subsystem Design

Subsystem Design Assumptions. A number of assumptions are necessary in sizing the subject subsystems due to the general nature of the operating modes. All oxygen side components were sized based on the worst possible helium dilution case (50 weight percent in each propellant) while the hydrogen side components were sized for pure hydrogen. This is the worst condition experienced by each of the components.

The accumulator tanks were sized to provide propellant flow to operate the thrustor subsystem for a time period five times larger than the response time of the conditioner. Such an initial sizing was assumed to insure against pneumatic coupling of the two subsystems as well as to separate the thrustor response from that of the conditioner. Hence, the accumulator size is directly proportional to the response of each conditioner subsystem.

The individual components are based on state-of-the-art design as nearly as possible. It is noted that the low-pressure components do represent a fairly large departure in terms of volumetric requirements. In this case the resultant sizes and weights represent a best extrapolation of Rocketdyne experience to the subject requirements.

Use of a single, catalytically ignited gas generator to operate both heat exchangers is not considered feasible because of the need for

high-temperature solenoid valves downstream of the gas generator. Similarly, the use of a single heat exchanger divided into two parts (one for each propellant) operating with one gas generator would present a complex controls problem and will prevent independent operation of each propellant loop. The feasibility of using conditioned hydrogen to condition the oxygen was also investigated. This concept, if feasible, would eliminate the need for the oxygen side catalytic gas generator and the attendant valves. Low log mean temperature differences and low pressure drop requirements when operating with main tank propellants dictate an exchanger area requirement of approximately 5 ft^2 (MR=2.5). The relatively large area requirement coupled with pressure starvation considerations eliminate this conditioning method from further consideration.

The effects of thermal energy transfer from the gas generators, heat exchangers, and accumulators were ignored during the preliminary evaluations. Possible transfer rates and their effect on design and operation were deemed of secondary importance in this phase and relegated to a follow-up effort after the subsystem evaluation had been essentially completed.

Use of Pressure Regulators. The conceptual designs prepared for the initial concept comparisons do not include pressure regulators. Instead, on-off control with a pressure relief valve to prevent accumulator overpressure was utilized. The exclusion of regulators was made because they are relatively heavy and have a relatively low reliability as compared with the other system components. Weight penalties associated with the use of regulators are shown in Table 10.

The on-off control system design utilizes a pressure switch to energize and de-energize the main propellant valve in the conditioner, thus maintaining a relatively constant thrustor inlet pressure. The relief valve functions should any excessive pressure occur.

A more definitive analysis of the necessary between control system requirements was made following this initial comparison and is described below. The results do not change the relative comparison between the conditioner concepts, since all of the system concepts are affected in the same manner.

Subsystem Simplification. As discussed above, the propellant conditioning subsystem has two major objectives; (1) specification of the propellant thermodynamic state as fed to the thrustor for flowrate control, and (2) maintenance of a hydrogen temperature which is above the minimum compatible with the thrustor catalytic bed. The latter requires only the hydrogen be conditioned, which results in a considerably less complex conditioner. However, such a subsystem is not applicable if the thermodynamic state of the oxygen fed to the RCS is allowed to vary.

It is noted that in many applications where low-pressure boiloff might be utilized in the subject propulsion system, the oxygen boiloff rates are substantially below those of the hydrogen. In these cases it may be feasible to utilize the positive expulsion device in the oxygen tank to ensure a liquid feed and to simplify the conditioner subsystem by utilizing only the single hydrogen conditioner. It is realized that such a simplification is entirely dependent on the mission and vehicle design.

SYSTEM PERFORMANCE

The details of component design and system performance analysis are dependent on material and energy relationships within the system. Material and energy balances were made to establish a basis for these tasks. These were accomplished for the hot-tube heat exchanger system. As discussed below, this conditioning concept was selected for experimental evaluation and demonstration. Further, the performance for the direct heating concept can be calculated independently without detailed material and energy balances.

Material and Energy Balances for Hot-Tube Heat Exchanger Concept

The hot-tube heat exchanger concept utilizes hydrogen-oxygen combustion to supply thermal energy for increasing the temperature of the feed propellants. To accomplish this, a portion of the propellant flow to the thrustor must be diverted to the conditioning system for combustion and indirect heat transfer with the inlet propellants. The exact amount diverted can only be determined after the thrustor mixture ratio and thrust are fixed, and such conditioner parameters as the gas generator mixture ratio, heat exchanger hot-gas outlet temperature, and propellant inlet quality are fixed. Six sets of important parameters were investigated and the results are summarized in Tables 11 through 13 .

The initial set of nominal parameters and calculated heat and material flows are presented as Case I in Table 11 . The important parameters for this case are:

1. Saturated liquid propellant at the conditioner inlet, thus giving the maximum heat and flow loads
2. Theoretical optimum thrustor mixture ratio of 2.5 and 20 pounds of thrust

3. Gas generator mixture ratio set at 1.32 with injection of O_2 downstream of the catalyst bed to produce a 2500 R combustion temperature
4. Propellant conditioning to 200 R

Under these conditions, 9.0 percent of the total flow was diverted to the conditioner system where the calculated heat load for the O_2 and H_2 systems is 3.85 and 10.1 Btu/sec, respectively.

An alternative set of operating conditions was also used for analysis. The gas generator mixture ratio was reduced to 1.0 which allows an in-line bed design without downstream injection of additional oxygen. Also, the possibility of a heat exchanger tube burnout is reduced, thus improving system reliability. Comparison of this second set of conditions (Case II) with Case I reveals the design change causes the percent diverted flow and the H_2 heat exchanger heat load to increase only slightly, thus negligibly affecting the heat exchanger and gas generator designs.

Case III illustrates steady-state conditions for saturated vapor inlet propellants. Under these conditions, the O_2 heat load is reduced to approximately 7 percent of the maximum heat load while that for H_2 is 65 percent. The net effect is to half the percent of diverted flow.

Material and energy balances were also prepared for conditioning to higher temperatures, 500 and 400 R (Cases IV, V, and VI in Table 11). Such a change in operating conditions causes a very large increase in the percentage of flow diverted to the gas generators and on the heat load on the hydrogen heat exchanger.

The effect of conditioned temperature level on percent of flow diverted is illustrated in Fig. 72 . The lower line represents the theoretical minimum required flow when the gas generators are operated at stoichiometric conditions. The large difference in these two curves is caused by the extra fuel flowrate required to cool the indirect combustion products to 2000 F (a safe-operating temperature for stainless steel) and to the large increase in the heat load for the H_2 heat exchanger with conditioned temperature.

Conditioner Performance. A detailed analysis of those cases presented in the previous section was made from a systems performance viewpoint. This procedure is illustrated by the example shown in Table 14 for the original nominal design, Case II. First, the theoretical thrust specific impulse was determined as a function of the conditioner outlet temperature. The most efficient system is a conditioner concept which mixes the combustion products directly with the propellants to be conditioned with no removal of the water formed.

The next most efficient system is a stoichiometric or direct-mixing system having a water removal mechanism. The conditioner percent of total flow vs conditioner outlet temperature is presented in Fig. 73 . When the theoretical thrustor specific impulse for 200 R propellants is multiplied by percent of flow to the thrustor, the theoretical system efficiency is obtained. The net loss of 9 seconds specific impulse can be attributed to removing the water.

In the case of a single-stage combustion conditioner system, the system specific impulse is further reduced by 30 seconds because of the additional amount of hydrogen required to cool the combustion temperature to 2000 F (Fig. 73).

The system specific impulse is further reduced by thrustor inefficiencies to approximately 367 seconds from the original 440 seconds. Thus, the total loss can be broken down into a 9-second H_2O removal loss, a 30-second single-stage combustion loss, and other uncontrollable losses of 34 seconds.

A plot of theoretical and actual system performance for various conditioner outlet temperatures is presented in Fig. 73 . As the conditioner outlet temperature is increased to give reliable catalytic ignition, the specific impulse loss attributed to single-stage combustion increases markedly.

Two methods for efficiency improvement are: (1) more efficient combustion, and/or (2) injection of the conditioner hot-gas stream into the thrustor chamber. The latter was deemed unsatisfactory for pulse-mode operation.

The former method of increasing the combustion efficiency was analytically investigated. This method utilizes a series of indirect heat-exchange stages at an overall stoichiometric ratio although the individual stages are operated near a mixture ratio of 0.5 to 1.0. Thus, the efficiency of the indirect system can be made to approach the direct system without the inherent water removal problems associated with the direct system. Such a multistaged reactor has already been reported (Ref. 18), and could result in a saving of 8 to 75 lbm of H_2 per hour for steady-state operation and an increase in specific impulse of from 30 to 83 seconds.

The overall system specific impulse can also be improved markedly for several applications by incorporating design changes specific to each application. For example, an attitude control system with a propulsion requirement of small impulse bits spread regularly over a long time period might utilize other energy sources in conjunction with energy storage in

the heat exchanger. A low-power source such as solar radiation might be feasible for such an application. Also, the design for a steady-state settling engine usage might include the regenerative heating of the propellant in the thrustor, thus reducing or eliminating the conditioner hot-gas flow requirements.

COMPONENT DESIGN

The component designs for the hot-tube heat exchanger subsystem were considered in detail, particularly the heat exchanger. This was because as discussed below, the hot-tube heat exchanger concept was selected for experimental evaluation. Conversely, the component designs associated with the other subsystem concepts were only considered in a fairly general manner.

Combined Heat Exchanger and Gas Generator

A flight-type conceptual design for a combined heat exchanger and gas generator is shown in Fig. 74 . In this design, an annular heat exchanger encloses the gas generator unit. A helical coil of tubing for the hot gas is positioned in the annular space. The cold fluid is to flow in the annulus. The design was selected for the advantages in packaging, and simplicity of fabrication. Also, the nature of the flow path for the cold fluid as a series of restrictions was thought to aid in damping flowing instabilities due to boiling.

Heat Exchanger Design

The basic equation used to size the heat exchangers was:

$$q = U A \Delta T_m \qquad (23)$$

SYSTEM CONTROL CONSIDERATIONS

The thrustor catalyst bed temperature is sensitive to upstream conditions, particularly the difference between the upstream pressures in the accumulators. The analysis of this sensitivity is described in the Systems Analysis and Simulation section. To assure reliability and controlled operation, pressure and temperature control and/or equalizing devices must be included in the conditioner subsystem.

Pressure Regulation and Equalization

Control of upstream pressure, particularly of the difference between accumulator pressures, is a key factor in system operation. Pressure regulators were initially considered and discarded in favor of a lighter, more reliable pressure relief valve and an on-off controlled main valve. However, as a result of theoretical analyses of control limits, pressure regulators were considered as a method of eliminating catalyst bed temperature fluctuations. The basic components common to each scheme includes a heat exchanger, hot-gas generator, an accumulator, and the main valve for the thrustor.

In addition to the use of pressure regulating and following devices for maintaining pressure control, bellows and bladders were also evaluated on a preliminary basis for use in equalizing pressure between accumulators.

Method A: No Pressure Equalizing System. This represents the initial control scheme proposed. The system concept was based on dividing the conditioner system into individual components and maximizing the performance of each component. A schematic of the system is shown in Fig. 67. The principal control loops are as follows.

1. Hot-tube temperature control in the heat exchanger--This loop controls both the hydrogen and oxygen flow to the gas generator during the coast modes of the vehicle. The tubes are kept hot to circumvent the relatively long time (~ 2 to 5 seconds) needed to heat the tubes to steady-state conditions. An automatic reset capability of the reference temperature is included to allow for variations in the quality of the propellants delivered from the main tanks. The reference point is determined prior to closing the main thrustor valve and is maintained through the coast period.

2. Accumulator temperature control--When the hot-tube temperature control is nullified (during thrustor operation) the accumulator temperature controls the flow of hydrogen and oxygen to the gas generator.

3. Accumulator pressure control--The accumulator pressure control causes the tank valve to open at a specified low pressure and close at the nominal accumulator pressure. If the accumulator pressure exceeds the nominal value, the pressure relief valve will open to relieve the overpressure.

Four valves and three principal control loops are used. A conceivable problem exists in the pressure controlling device for the accumulator. An oscillation could be established between the pressure relief valve and the tank valve although, if significant, an increase in accumulator volume will eliminate the oscillation. This oscillation could develop during the conditioning cycle, from pressure perturbations caused by liquid slugging in the heat exchanger. In addition, the pressure in the fuel accumulator may cycle out of phase with the oxidizer accumulator pressure. Another problem is in sizing an effective orifice for

where

$$\frac{1}{u} = \frac{1}{h_g} + \frac{1}{h} \tag{24}$$

The hot gas heat transfer coefficients were calculated using the following correlation obtained from Ref. 19 :

$$Nu = 0.023\ Re^{0.8}\ Pr^{0.33} \tag{25}$$

where fluid properties are evaluated at the film condition.

The heat transfer coefficients on the propellant side were calculated using a more complicated procedure. For boiling hydrogen, the previous equation (Eq. 25) was used to calculate a theoretical Nusselt Number, which was then modified using the Martinelli procedure (Ref. 20 and 21):

$$\frac{(Nu)_t}{(Nu)_e} = 0.611 + 1.93X_{tt} \tag{26-a}$$

where the Martinelli parameter is defined as:

$$X_{tt} = \left[\frac{W}{W_g}\right]^{0.9} \left[\frac{\mu_\ell}{\mu_g}\right]^{0.1} \left[\frac{\rho_g}{\rho_\ell}\right]^{0.5} \tag{26-b}$$

and $(Nu)_t$ and $(Nu)_e$ are the theoretical single phase and experimental two phase heat transfer coefficients, respectively. The Reynolds Number as applied in Eq. 25 for two phase flow is defined as:

$$Re = \frac{vD}{\left(\frac{x}{\rho_{gf}}\right)\mu_{gf} + \left(\frac{1-x}{\rho_{\ell f}}\right)\mu_{\ell f}} \qquad \text{for } 0.05 \leq x \leq 0.95 \tag{27}$$

The heat transfer coefficients for superheated hydrogen flowing over tubes was calculated with the following equation:

$$Nu = b\ Pr^{1/3} \left[\frac{D_o\ G_{max}}{f}\right]^n \qquad (28)$$

The constants b and n were determined from the data of Grimson (Ref. 22) as 0.348 and 0.592, respectively. These values were selected as theoretically maximizing the heat flux per unit axial length and are compatible with a longitudinal pitch of 1.25.

The heat transfer coefficients for the oxygen propellant were calculated using the procedure outlined above.

The pressure drop on the shell side tube was obtained from Eq. 29-a which linearly sums the friction losses and acceleration losses:

$$P = \frac{G_{max}^2}{g}\left[v_2 - v_1 + \frac{v_m}{2} f \frac{A_{ht}}{A_{min}}\right] \qquad (29\text{-}a)$$

The friction factor for flow inside helical tubes was corrected using Eq. 29-b:

$$f^* = \left[1 + 3.5 \frac{D_{tube}}{D_{helix}}\right] f \qquad (29\text{-}b)$$

The pressure-drop values obtained from Eq. 29-a were increased by adding the exit and entrance losses. The results revealed a predicted propellant pressure drop of 1 psi and a hot-gas pressure drop of 8 psi. Both of these estimated pressure drops were consistent with the conditioner system pressure profiles detailed in Fig. 67 .

the gaseous propellant tank valve. The specific volume of the propellant can vary considerably because of all-liquid to all-gas transitions as well as possible helium content in the propellant. Consequently, the flowrate of propellant delivered to the heat exchanger could vary over a large range for a fixed valve orifice area.

Method B: Pressure Regulator. A possible way to circumvent the problems that would be incurred with Method A is to use a pressure regulator in place of the main valve.

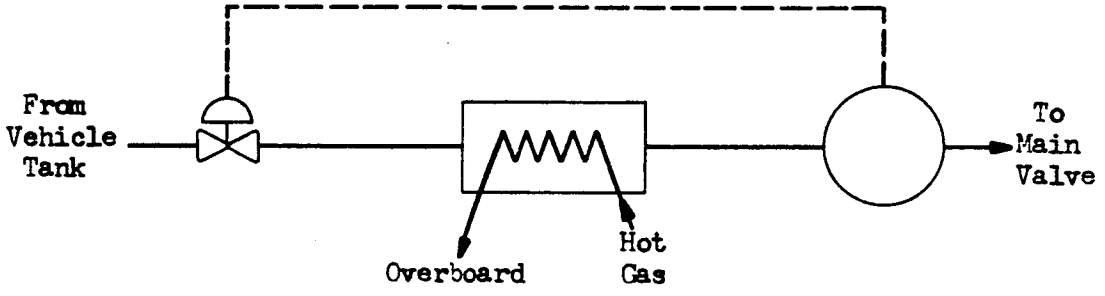

The regulator would take its reference point from the accumulator which contains propellant entirely in a gaseous state. The need for a pressure relief valve would be eliminated for control purposes, although a relief valve could be employed as a safety device. The accumulator is conservatively sized such that the regulator does not have to function for every short (~ 50 millisecond) pulse of the thrustor. The fuel-side regulator deadband would be matched with the oxidizer regulator such that the pressure differential between the accumulators would at no time exceed a set value. Based on control analyses discussed in another section, 1 psi appears to be a reasonable deadband.

A difficulty could arise during the coast mode. Even though the regulator is closed and the accumulator topped off, the gas remaining in the

heat exchanger is continuously being heated by the hot tubes. This gas will affect the accumulator state by either conductive heat transfer or pressure gradient mass flow. An estimate will be made of the gas temperature and pressure increase in the accumulator. The relative sizes of the heat exchanger and the accumulator are again important. The larger the accumulator the smaller the pressure flow effects during the coast mode. Likewise, the longer the conduction path, the smaller the conductive heat transfer effects will be. An attenuating effect evolves from keeping the heat exchanger tubes and the gas generator at an elevated temperature. This requires an intermittent flow of conditioned propellant from the accumulator even during the coast mode.

Another possible problem arises from the two-phase flow conditions in the heat exchanger which can lead to pressure drop and flowrate fluctuations through the heat exchanger. The accumulator will be sized to successfully damp the pressure fluctuations that might be encountered.

The accumulators need to be sufficiently large to provide time for the regulator to respond from a fully closed (locked up) position to an open position. This problem might be eliminated by not having the regulators lock up. During the coast mode, the conditioned propellant would flow back toward the main vehicle tanks. However, the line volume between the main tanks and the regulators should be large enough to account for the increased propellant temperature from the heat exchanger.

Method C: Pressure Regulator Between the Heat Exchanger and Accumulator.

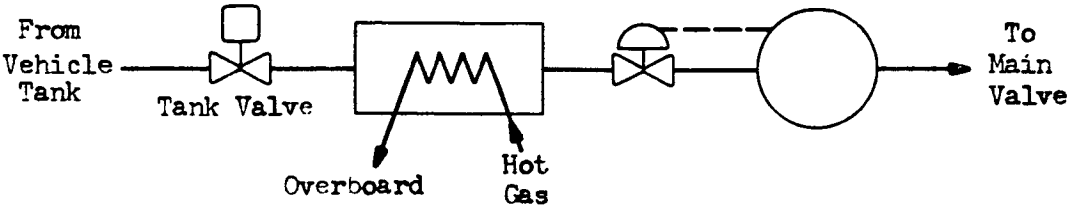

If the pressure regulator never locks up the response of the system is increased and the need for an accumulator might be eliminated. In practice, however, a small accumulator will be necessary. Placing the regulator downstream of the heat exchanger might require either a tank valve or a check valve to prevent back flow from the heat exchanger during the coast mode. If the tank valve is necessary, a danger exists in overpressurizing the gas in the heat exchanger during the coast mode. However, a demand will be placed on the accumulator during the coast period (to maintain heat exchanger tube temperature), thus attenuating the overpressure condition.

Method D: Pressure Regulator Plus Follower.

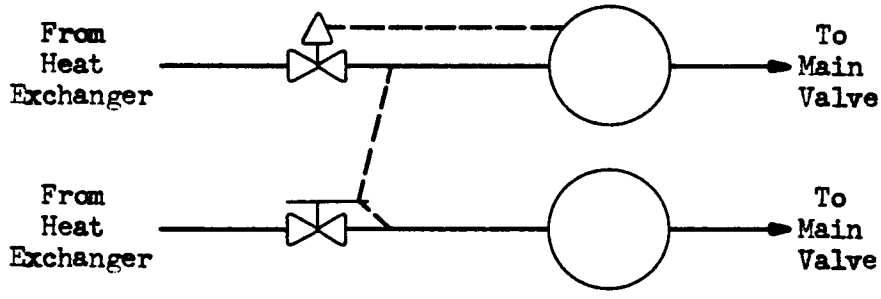

Instead of using a pressure regulator for each side, a follower valve can be placed on one side. This would tend to equalize the pressures to a greater extent, since the possible error would be reduced to a single tolerance as opposed to a two regulator system where it is the sum of the tolerances. In addition, the weight of the system would be decreased since the follower is not as elaborate a device as a regulator. The position of the follower in the system is a function of the same criteria that applies to the regulators.

Preliminary Evaluation of Bellows and Bladders for Pressure Equalization. The need for reducing or controlling the pressure difference between the two accumulators led to a feasibility study of separating the containers with a diaphragm or bellows. A cursory literature survey revealed two investigations of the use of expulsion bladders for cryogenic fluids (Ref. 23 and 24). Since any one of three listed limitations, incompatibility with LOX, low cycle life, and permeability, could have catastrophic results, bladders at that time were not considered feasible.

The feasibility of integrating a bellows O_2 accumulator into the larger H_2 accumulator was evaluated as follows:

1. The bellows would have to be 7.5 inches long with a 6.5 inch ID and would have to be capable of expanding 6.6 inches and contracting 1.1 inches at a frequency of 10 to 15 cps. A spring constant of 2.5 lbf/in. or less would be desirable. A cursory mathematical description of the bellows dynamics action was programmed on the digital computer using the Midas technique, Ref. 25 and 26. It appears that the mass and spring constants necessary to give a rapid response are compatible with present day manufacture.

2. A local representative of a company with considerable experience in designing bellows-type expulsion bladders was given the preliminary sizing requirements and reported that a bellows with the following parameters could be built:

   OD = 9 inches; ID = 7.2 inches; spring constant (K) = 5 lbf/in.

Free length - 6 inches; L Maximum contraction - 4.17 inches; L Maximum extension = 9.25 inches; volume displace compression = 215 cu. in.; volume displaced, expansion = 219 cu. in.

P_{max} = 3 psi; mean effective area - 51.5 sq. in.

347 stainless steel; weight = 3.25 pounds; operating temperature = 200R; cycle life = 30,000

Generally, it was concluded that cycle-life failure would be the chief shortcoming although the reported 30,000 cycle life is much greater than that which might be expected from past experience (Ref. 27 and 28). However, the cycle life is sufficiently long so that serious consideration should be given to the device.

Temperature Control Considerations

In addition to a pressure control system, a temperature control system is also needed. The determination of the type of temperature control system can be divided into three separate questions: (1) what type of temperature sensor to use, (2) where to place it, and (3) what should it control.

The temperature sensing devices should give a relatively large current or electromotive force (emf) delta output for a small change in temperature in the cryogenic range. A thermister appears to meet these qualifications. The placement of the sensor should be upstream of the main thrustor valve since an erroneous temperature would be after the fact. The sensor, however, should probably not be placed either in or immediately downstream of the heat exchanger due to the possibility of local temperature and pressure fluctuations which may drive the control system unstable.

The temperature control will open or close the gas generator valves that provide reactants for forming the hot fluid. No provision is made for cooling the gas in the accumulator other than radiation losses. It is expected that the control loop will sense a slug of overheated gas entering the accumulator and shut off the gas generator valves fast enough for the accumulator volume to assimilate the slug without exceeding the mean temperature deadband. The ideal situation is to use a bipropellant valve for the gas generator so that both propellants enter the mixing volume simultaneously. The volumes should be sized such that the gas generator will not go oxidizer rich during either the start or stop transients.

SUMMARY OF CONDITIONER SUBSYSTEM ANALYSIS

A general RCS design for cryogenic O_2-H_2 propellants requires a conditioner subsystem which is utilized to raise the temperature of the propellants fed to a thrustor to a minimum acceptable value and to regulate the thermodynamic state of propellants such that flow control is maintained. A distinct subsystem approach to such an RCS design was selected because the overall program goals were general in nature and therefore the requirements on system operation were quite general. Accordingly, the accompanying "applications" were only loosely defined. In addition, the dynamic characteristics of actual system components were unknown and control component availability unknown. However, results obtained with such a general system could be applied to specific designs when given applications are clearly defined.

The general requirements on system operation specified at the initiation of the program included a mission time of from one hour to 220

days. The former requires a high conditioning power requirement (13 to 30 kilowatts), the latter an efficient energy transfer. Hence, an energy supply method that could meet the high power requirement at a reasonable efficiency was selected. Hence, energy supply methods that could meet the high power requirement at a reasonable efficiency were considered and conceptual designs prepared. The evaluation of system dynamics and response was another prime goal, and therefore conditioner subsystem was designed to provide conditioned propellant to the thrustor upon demand and to decouple the conditioner response from that of the thrustor. This was accomplished by providing a surge volume (accumulator) between the heat exchanger and the thrustor subsystem.

Energy and material balances accomplished on the conditioner subsystem showed a sizeable percentage (5 to 30 percent) of the total propellant flow must be diverted to the gas generators for conditioning purposes. This diversion of propellant could result in specific impulse losses of up to 140 seconds if the propellants were conditioned to a temperature of 500 R. However, the cited specific impulse losses refer only to the system designed for demonstration purposes in the present program. Several design changes are possible which could result in large efficiency gains. These include the use of auxiliary energy sources and integrated reaction control system designs for specific applications, the use of improved catalysts, and/or catalyst bed heater devices to circumvent the low temperature ignition difficulties.

System control considerations show pressure control to be most significant, particularly control of the difference between accumulator pressures. Three types of pressure control were evaluated; (1) a pressure sensor operating an on-off valve, (2) a regulating device, and (3) a bellows-bladder device connecting the two propellant flow systems for pressure equilization. The bellows concept was not considered further in this program because of an uncertainty as to cycle-life under the conditions

of interest. The other two concepts were to remain under consideration pending analytical and experimental evaluations of specific devices. Since suitable off-the-shelf components were not available for this program, modified components were to be considered satisfactory for this program.

TABLE 9

COMPARISON OF ISOTOPE POWER SOURCES

FOR A 12.8 KILOWATT REQUIREMENT

Isotope	Half-Life years	Specific Thermal Power Watts/gm	Total Weight of Isotope lbs.	Wt. of Shielding for Minimum Radiation Hazard lbs.	Weight of Isotope Plus Shielding lbs.	Present Cost of Isotope $
Po - 210	.38	134	.21	26	26.2	$2 \times (10)^6$
Cm - 242	.44	98	.288	40	40.3	$2 \times (10)^6$
Pu - 238	90	.39	73.2	2.5	75.7	$(10)^7$
Tm - 170	.35	1.75	16.1	80	96.1	500,000
Pm - 147	2.6	.27	104	1.8	105.8	$6 \times (10)^6$
Cm - 244	18	2.3	12.25	120	132.3	$5 \times (10)^6$
Cc - 144	.78	3.8	7.41	305	312.4	63,000
Sr - 90	28	.20	141.0	208	349	$9 \times (10)^5$
Cs - 137	27	.07	402	170	472	$(10)^6$

TABLE 10

ESTIMATED WEIGHTS OF PRESSURE REGULATORS[1.2.]

Temperature	500°R		400°R		300°F		200°R	
Mixture Ratio	O_2	H_2	O_2	H_2	O_2	H_2	O_2	H_2
0.5	13	20	13	19	12	19	11	18
1.0	14	18	13	17	13	17	12	16
2.0	15	16	14	15	13	15	12	14
4.0	16	14	15	13	14	13	13	12
6.0	16	12	15	11	14	11	13	10

1. Weights in pounds
2. Regulator pressure drop of 2 psi

TABLE 11

OVERALL MATERIAL BALANCE FOR STEADY-STATE OPERATION OF PROPOSED CONDITIONER

Conditions	Case No.	Propellant at Conditioner Inlet or Propellant Tanks				Propellant at Gas Generators			Percent of Total Flow to Gas Generator	Propellant at Thrustor		Combined Temperature, F
		Oxygen State	$\dot{w}_o$, lb/sec	Hydrogen State	$\dot{w}_f$, lb/sec	MR, o/f	$\dot{w}_o$, lb/sec	$\dot{w}_f$, lb/sec		$\dot{w}_o$, lb/sec	$\dot{w}_f$, lb/sec	
200 R Conditioned Propellants and 20-pound Thrust	I	O_2 Liquid	0.03852	Liquid H_2 with 5-percent He	0.01642	1.32	0.002822	0.002121	9.0	0.0357	0.0143	3570
	II	O_2 Liquid	0.0388	H_2 Liquid	0.0174	1.00	0.00309	0.00309	11.0	0.0357	0.0143	3570
	III	O_2 Vapor	0.03722	H_2 Vapor	0.01582	1.00	0.00152	0.00152	5.73	0.0357	0.0143	3570
500 R Conditioned Propellants and 20-pound Thrust	IV	O_2 Liquid	0.04518	H_2 Liquid	0.02457	0.85	0.00948	0.01117	29.2	0.0357	0.0143	3750
500 R Conditioned Propellants and 10-pound Thrust	V	O_2 Liquid	0.01918	H_2 Liquid	0.01119	0.85	0.00406	0.0049	29.2	0.01572	0.00629	3750
400 R Conditioned Propellants and 10-pound Thrust	VI	O_2 Liquid	0.01901	H_2 Liquid	0.00992	0.88	0.00313	0.00357	23.1	0.01588	0.00635	3690

TABLE 12

DETAILS FOR STEADY-STATE OPERATION OF PROPOSED DESIGN OF OXYGEN HEAT EXCHANGER

Hot Side

Case No.*	Propellant Flowrate $\dot{w}_o$, lb/sec	Propellant Flowrate $\dot{w}_f$, lb/sec	MR	T_c, R	T_{outlet} R	ID, inch	ΔP psi	h_g, Btu/hr-ft^2-F	Area in.^{2}	L, inches
I	0.000778	0.000585	1.33	2500	672	0.335	8.0	59.2	124	105
II	0.00080	0.00080	1.00	2000	672	0.354	8.0	59.2	144	122.2
III	0.0000596	0.0000596	1.00	2000	672	--	--	--	--	--
IV	0.00132	0.00156	0.85	2000	672	--	--	--	145.44	--
V	0.00055	0.00066	0.85	2000	672	--	--	--	61.8 (6.35 coils)	--
VI	0.00049	0.00056	0.88	2000	672	--	--	--	43.3 (5.5 coils)	--

Cold Side

Case No.*	$\dot{w}_o$, lb/sec	T_i, R	T_o, R	q, Btu/second	ΔP psi	h_ℓ, Btu/hr-ft^2-F	h_g, Btu/hr-ft^2-F	U_ℓ	U_g
I	0.03852	163	200	3.85	1.0	18.1	72.7	13.1	32.6
II	0.03879	163	200	3.86	1.0	18.1	72.7	13.9	32.6
III	0.03722	163	500	0.2905	--	--	--	--	--
IV	0.04518	163	500	7.48	--	--	--	25.0	--
V	0.01918	163	500	3.17	--	--	--	25.0	--
VI	0.01901	163	400	2.73	--	--	--	25.0	--

$\dot{w}_o$ = oxidizer weight flowrate
$\dot{w}_f$ = fuel weight flowrate
MR = mixture ratio
T_c = combustion temperature
T_{outlet} = temperature at heat exchanger outlet
ID = inside diameter
ΔP = differential pressure
h_g = heat transfer coefficient (gas)
h_e = heat transfer coefficient (liquid)
L = length
T_i = inlet oxidizer temperature
T_o = heat exchanger outlet oxidizer temperature
q = heat exchanger heat load
U_ℓ = overall heat transfer coefficient (liquid)
U_g = overall heat transfer coefficient (gas)

* Refer to Table 11 for definition of cases

TABLE 13

PROPOSED STEADY-STATE DESIGN OF HYDROGEN HEAT EXCHANGER

Hot Side

Case No.*	Propellant Flowrate $\dot{w}_o$, lb/sec	Propellant Flowrate $\dot{w}_f$, lb/sec	MR	T_c, R	T_{outlet}, R	ID, inch	ΔP, psi	h_g, Btu/hr-ft^2-F	Area	L, inches
I	0.002044	0.001536	1.33	2500	672	0.46	8.0	71.4	110.0 sq in.	70.0
II	0.00229	0.00229	1.0	2000	672	0.50	8.0	71.4	136.0 sq in.	86.6
III	0.00146	0.00146	1.0	2000	672	-	-	-	-	-
IV	0.00816	0.00961	0.85	2000	672	-	-	-	2.25 sq ft	-
V	0.00351	0.00424	0.85	2000	672	-	-	-	0.989 sq ft	-
VI	0.00264	0.00301	0.88	2000	672	-	-	-	0.71 (7.5 coils)	-

Cold Side

Case No.*	$\dot{w}_f$, lb/sec	T_i, R	T_o, R	q, Btu/seconds	ΔP, psi	h_ℓ, Btu/hr-ft^2-F	h_g, Btu/hr-ft^2-F	U_ℓ	U_g
I	0.01642	37	200	10.13	1	39.2	275	25.4	56.7
II	0.01739	37	200	11.2	1	39.2	275	25.4	56.7
III	0.01582	37	200	7.12	-	-	-	-	-
IV	0.02517	37	500	46.1	-	-	-	70.0 Overall Assumed	-
V	0.01119	37	500	20.3	-	-	-	70.0 Overall Assumed	-
VI	0.00992	37	400	14.55	-	-	-	70.0 Overall Assumed	-

* See Table

TABLE 24

SAMPLE SPECIFIC IMPULSE ANALYSIS AND COMPARISON
FOR DIRECT AND INDIRECT CONDITIONERS
(CASE II)

Theoretical Thrustor Specific Impulse, ϵ = 50, Full Frozen			
Specific Impulse Saturated Liquid Propellants, seconds			440
Specific Impulse, 200 R Gaseous Propellants, seconds			450
Theoretical Thrustor + Conditioner System Specific Impulse			
Direct Conditioner With no H_2O Removal Starting With Saturated Liquid Propellants, seconds			440
200 R Conditioner, Stoichiometric or Direct With H_2O Removal, seconds	450 (1.00 - 0.044)	=	431
Specific Impulse Loss Due to H_2O Removal, seconds			9
Single-Stage, 200 R Conditioner Specific Impulse, seconds	450 (1.00 - 0.11)	=	401
Specific Impulse Loss Due to Single-Stage Combustion, seconds	431 - 401	=	30
Actual Conditioner + Thrustor Specific Impulse (Fig. 60, Page 130, Ref.)			
ηSpecific Impulse (Thrustor), percent	92		
ηc^* (Gas Generator), percent	98		
Specific Impulse Direct, seconds	0.920 (440)	=	405
Specific Impulse Direct (With Water Separation), seconds	450 (1 - 0.044) 0.92	=	396
Specific Impulse Loss Due to H_2O Removal, seconds			9
Specific Impulse Indirect, seconds	450 (0.920)(1.00 - 0.11/0.98)	=	367
Specific Impulse Due to Single-Stage Combustion, seconds	396 - 367	=	29

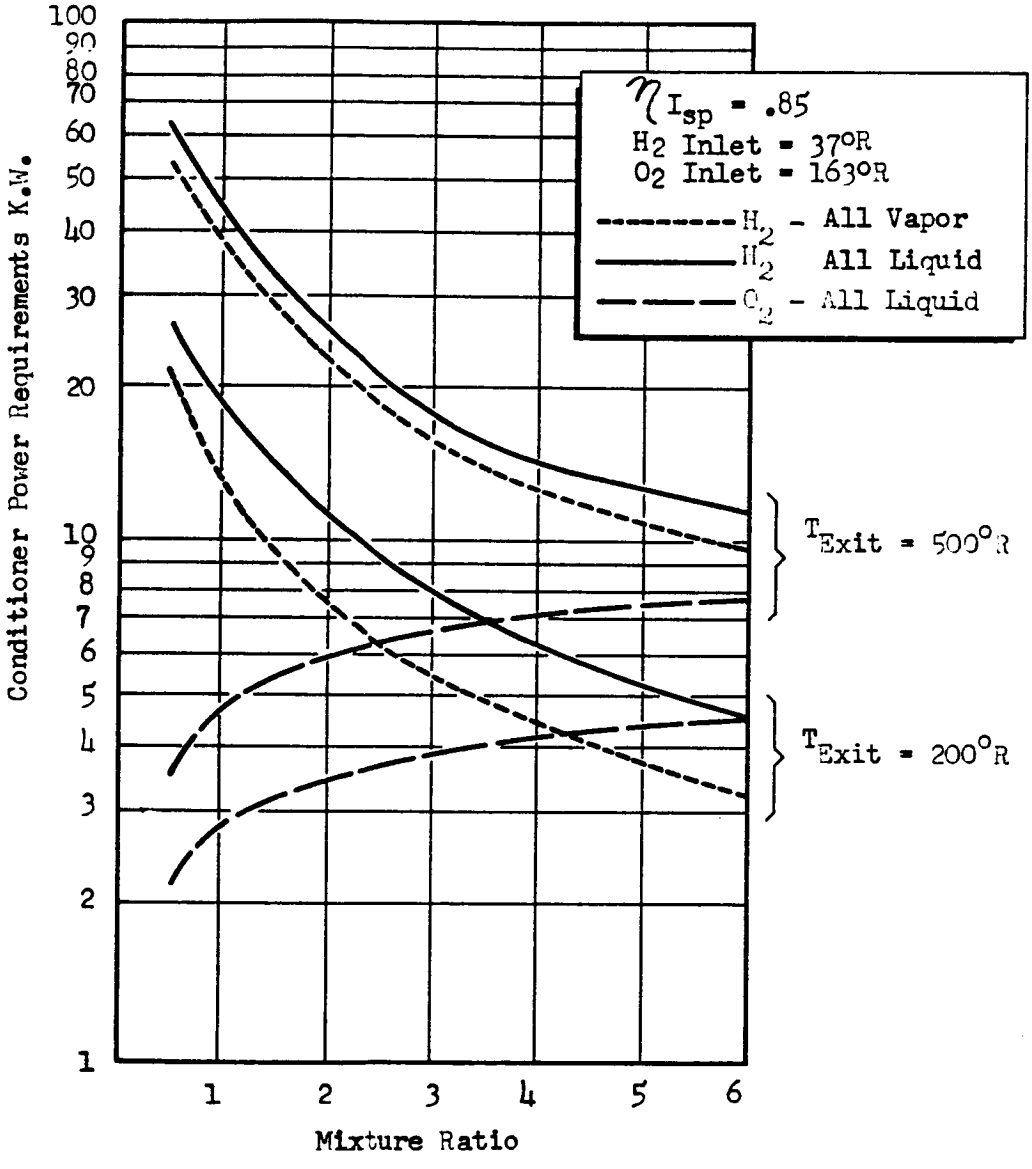

Figure 61. Conditioner Power Requirements for Steady Propellant Flow

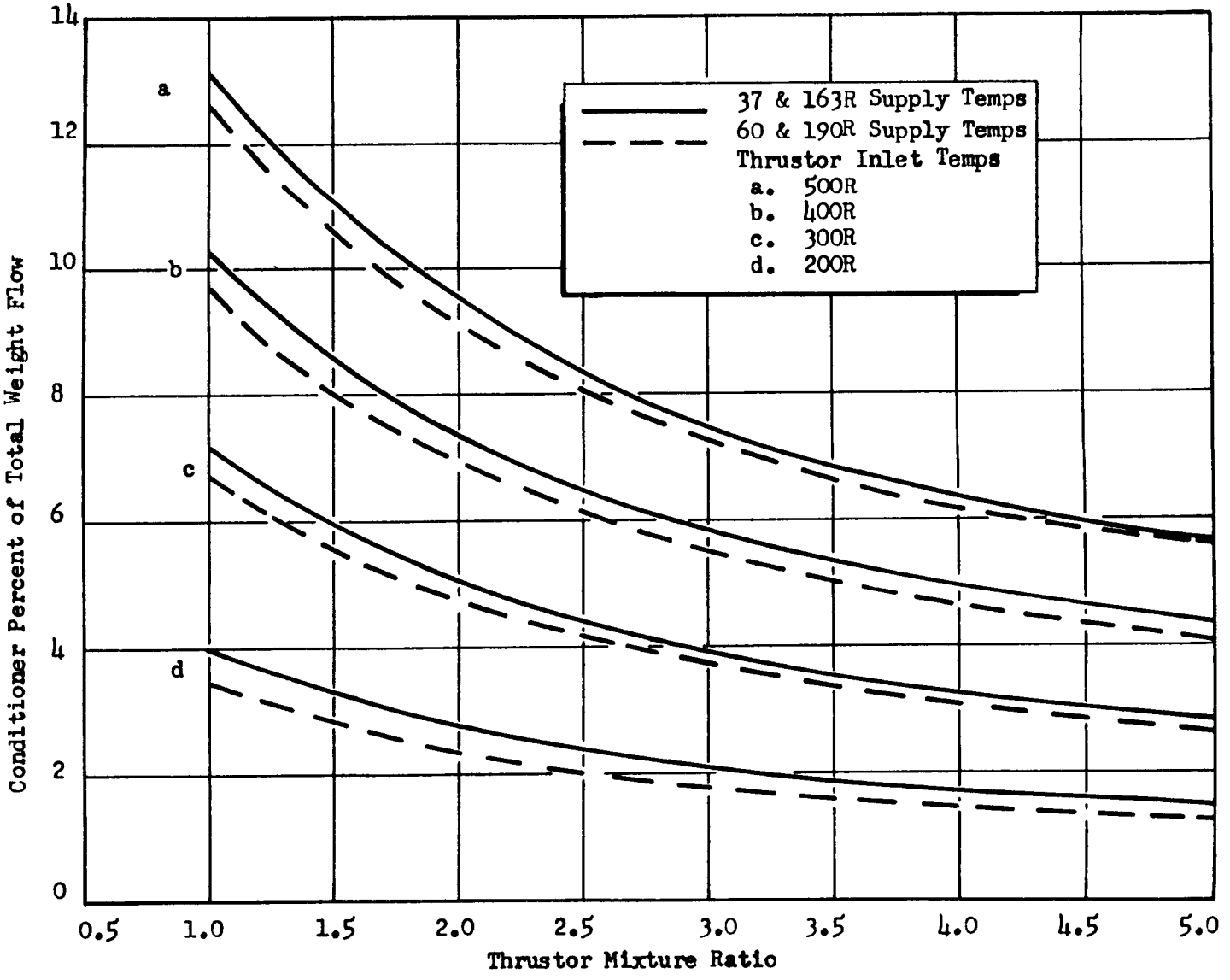

Figure 62. Conditioner Requirements With No Phase Change

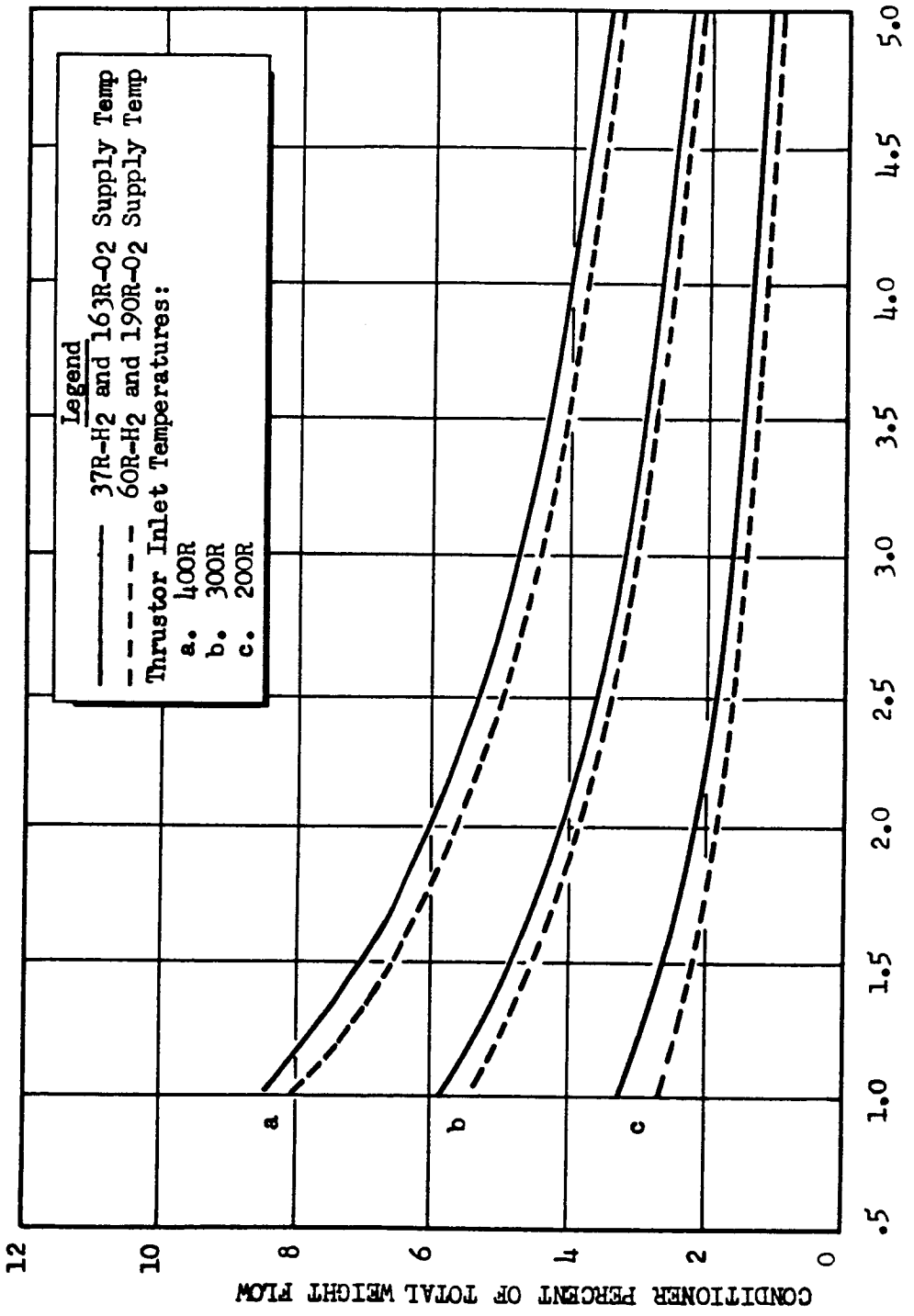

Figure 63. Conditioner Requirements with Phase Change

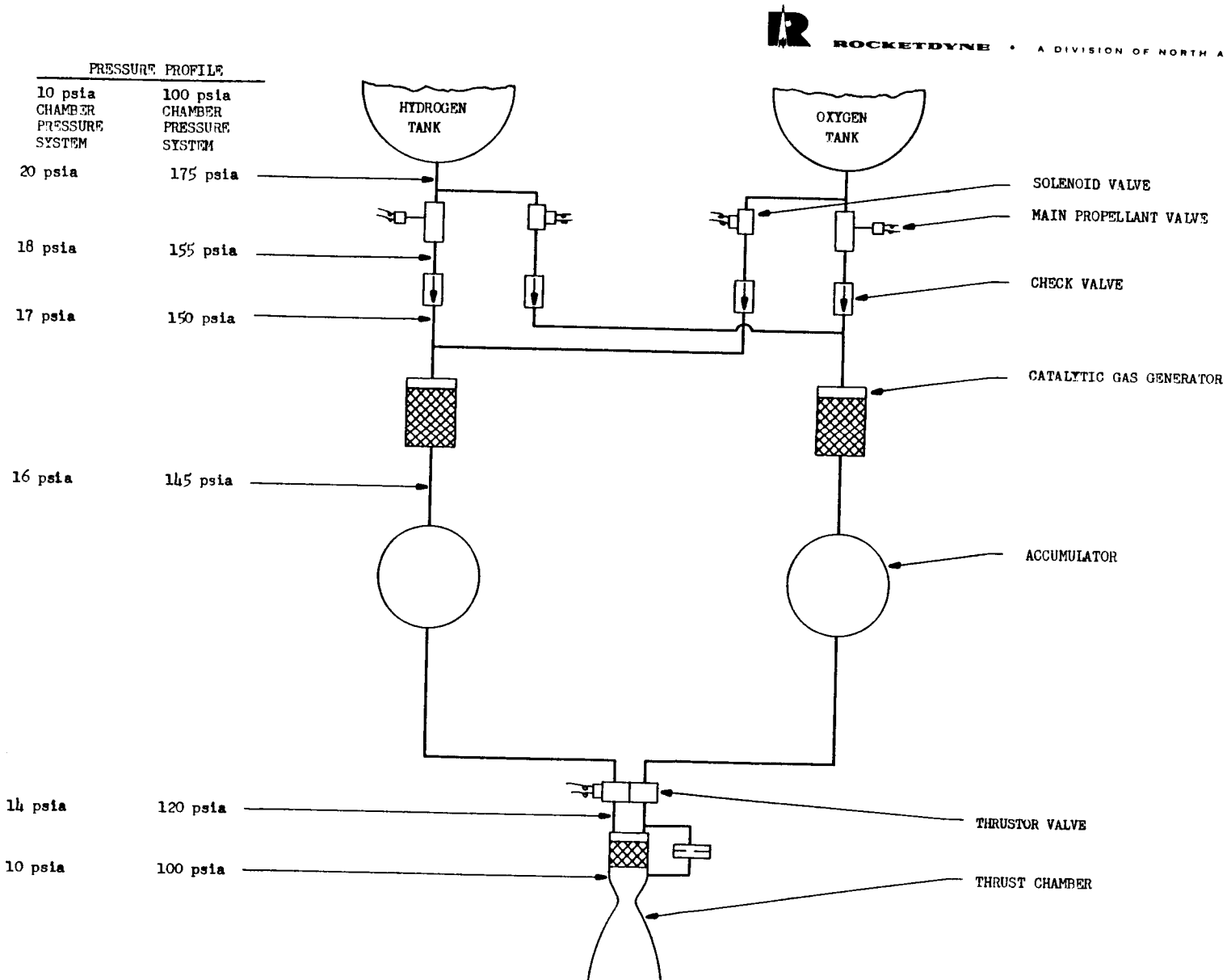

FIGURE 64. SCHEMATIC REPRESENTATION OF DIRECT HEATING (CHEMICAL) PROPELLANT CONDITIONER UNIT

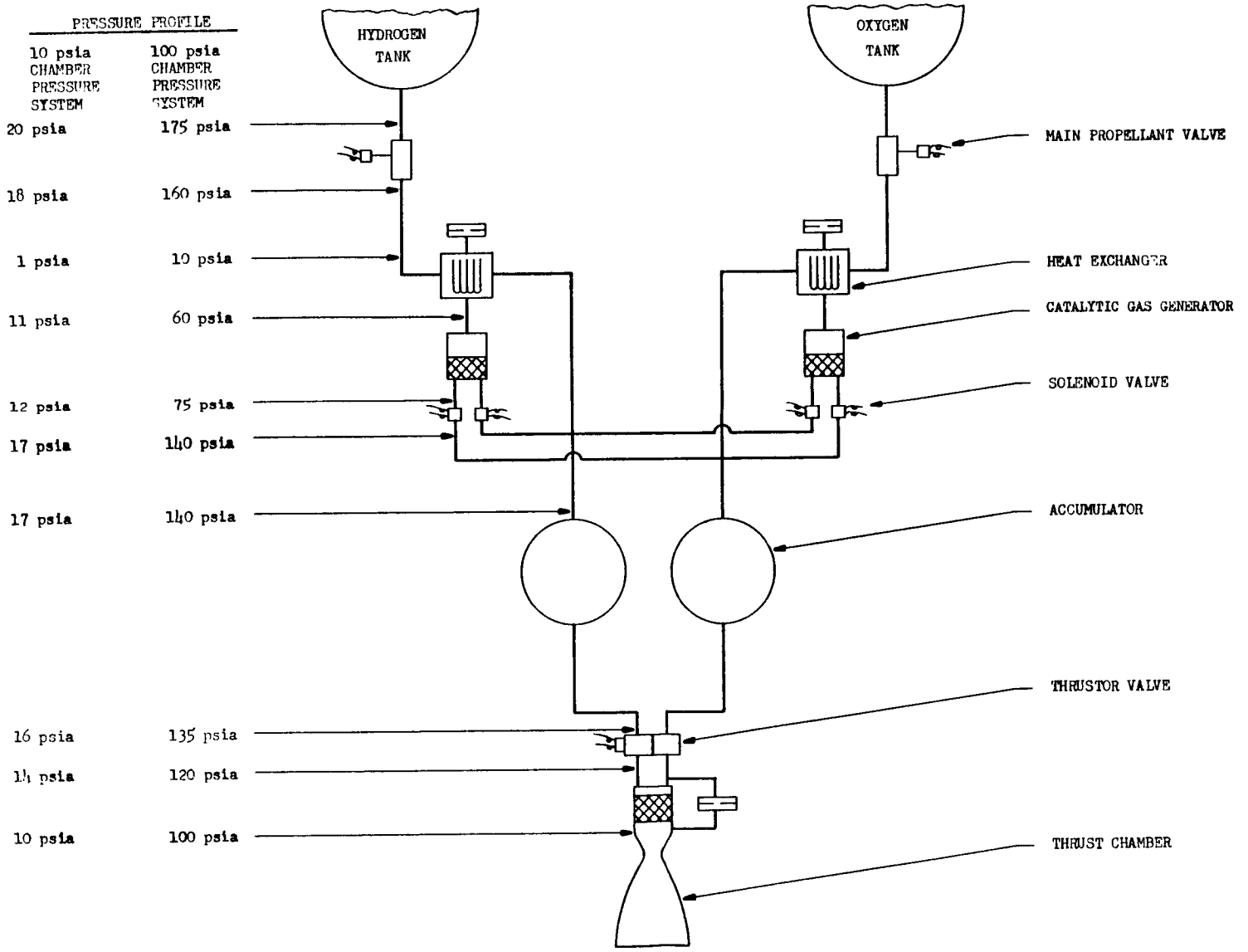

FIGURE 65. SCHEMATIC REPRESENTATION OF A HEAT EXCHANGER PROPELLANT CONDITIONER UNIT

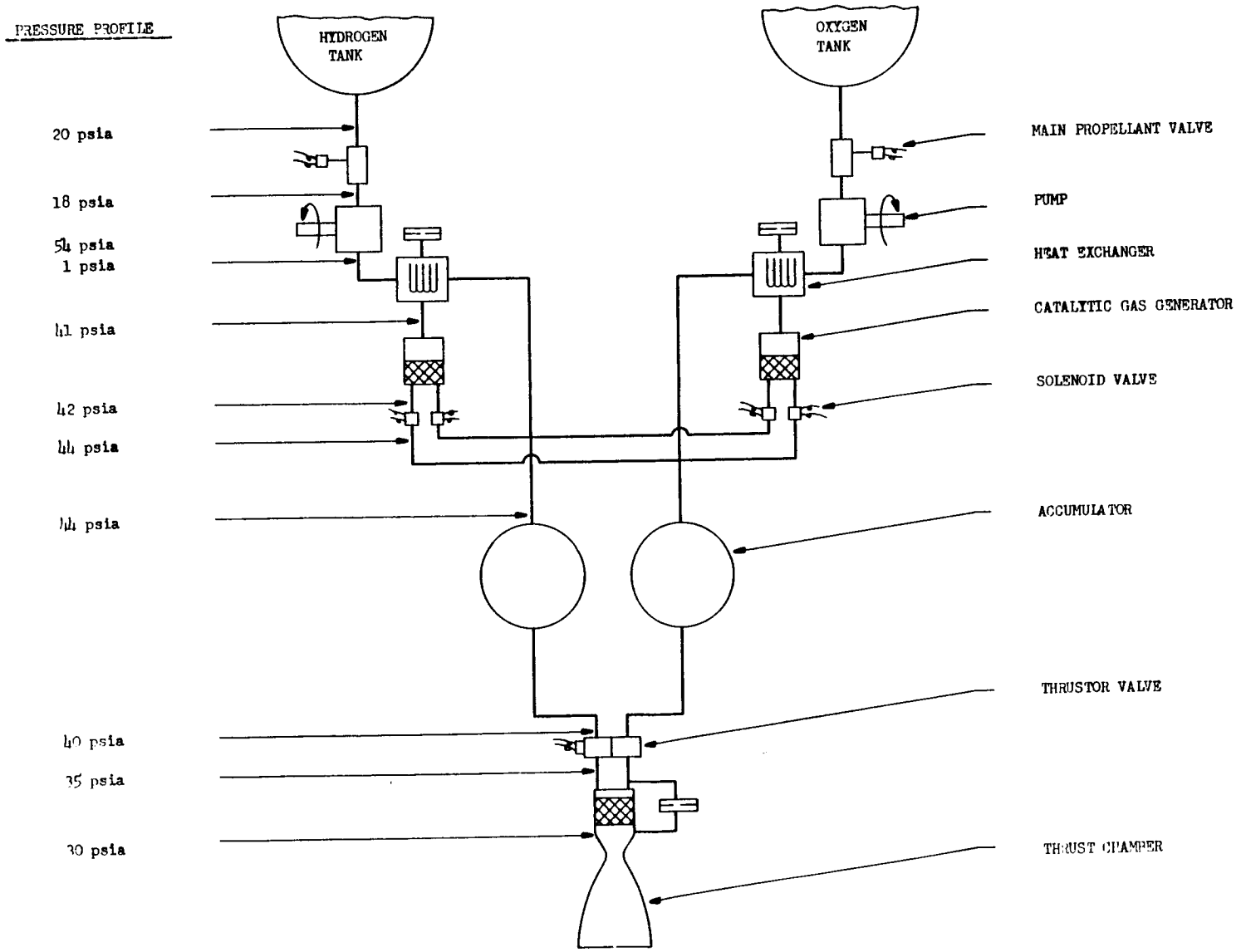

FIGURE 66. SCHEMATIC REPRESENTATION OF A PUMP FED HEAT EXCHANGER PROPELLANT CONDITIONER UNIT

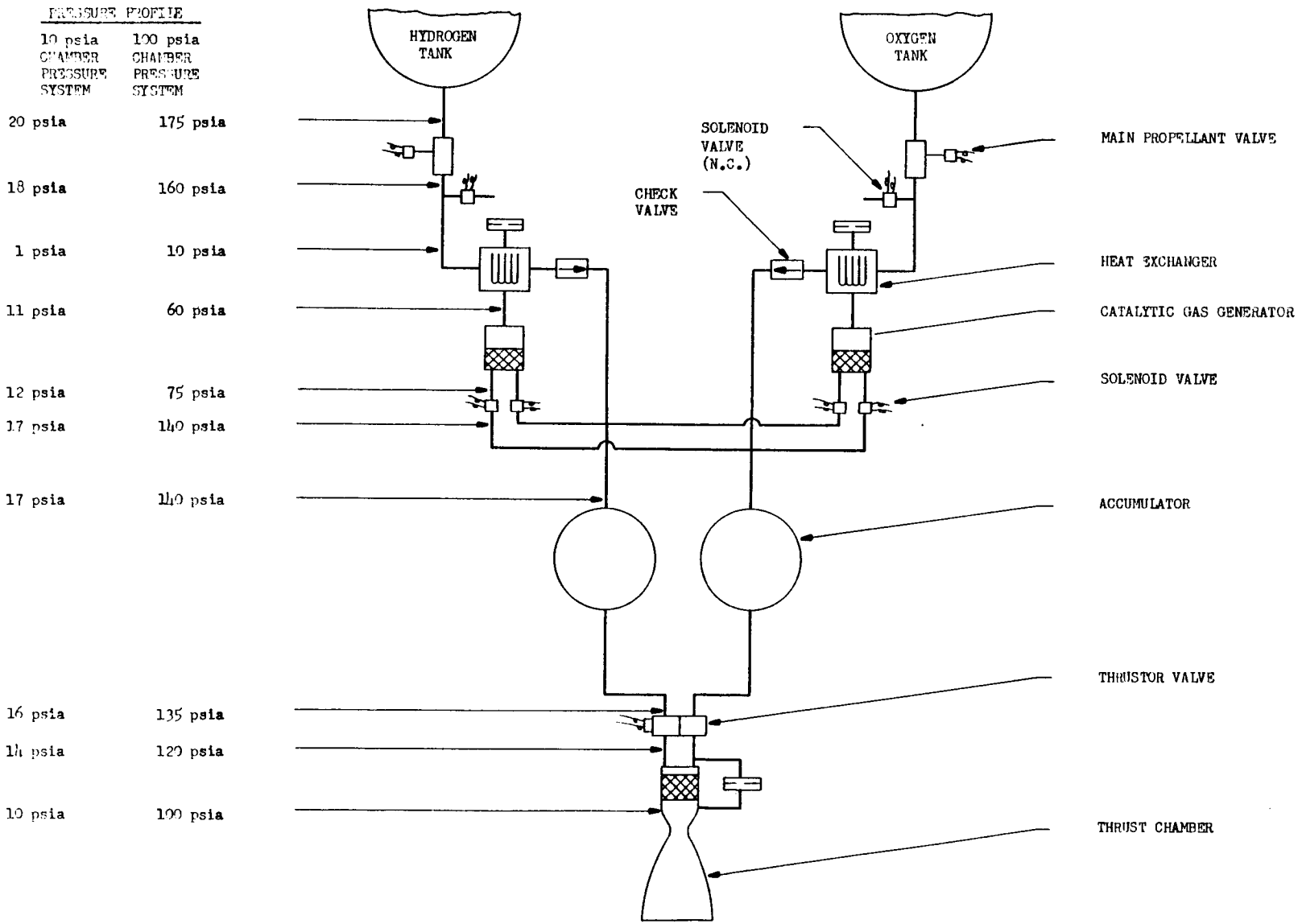

Figure 67. Schematic Representation of a Hot Tube Heat Exchanger Propellant Conditioner Unit

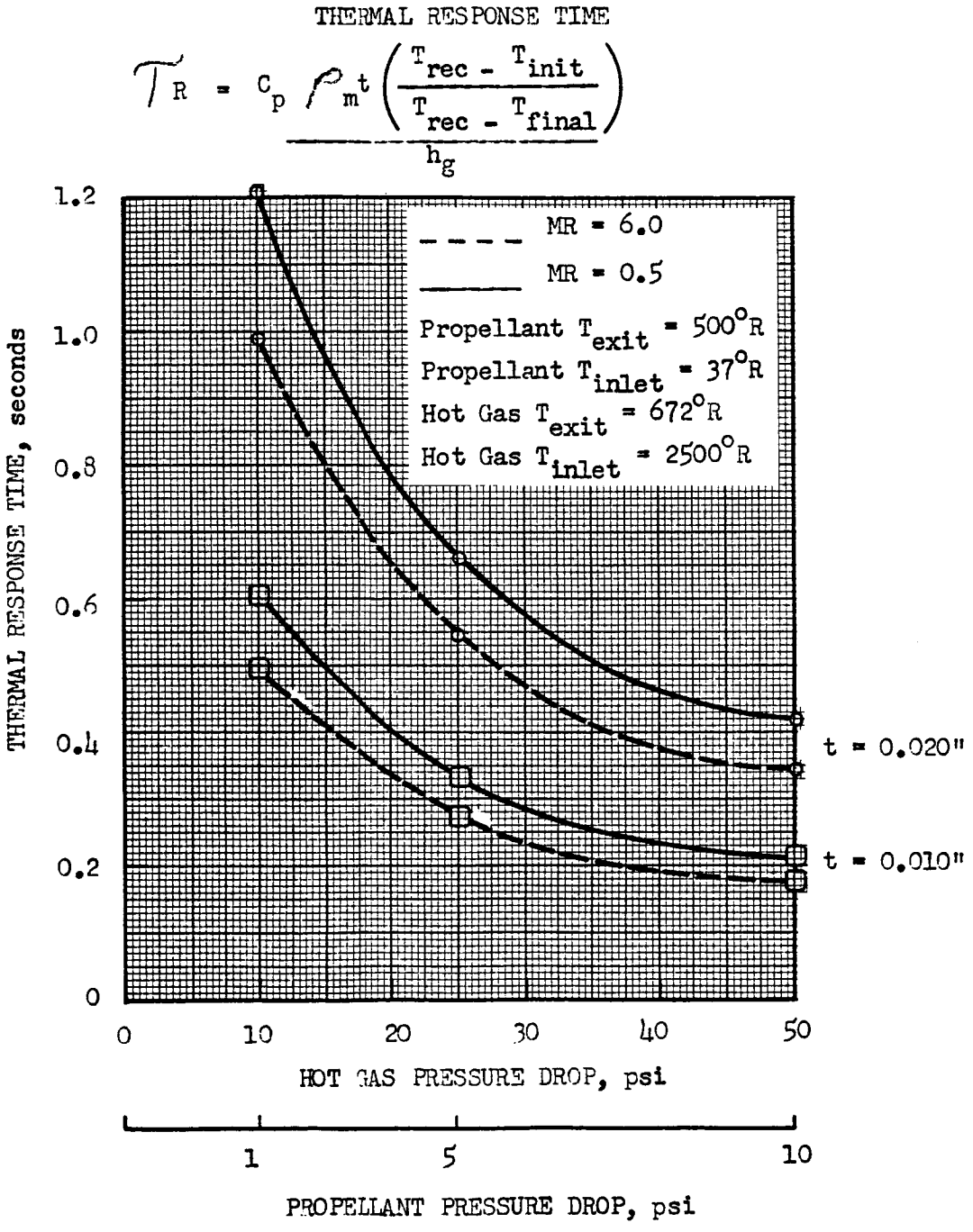

Figure 68. Heat Exchanger Thermal Response Time as a Function of Hot Gas Pressure Drop

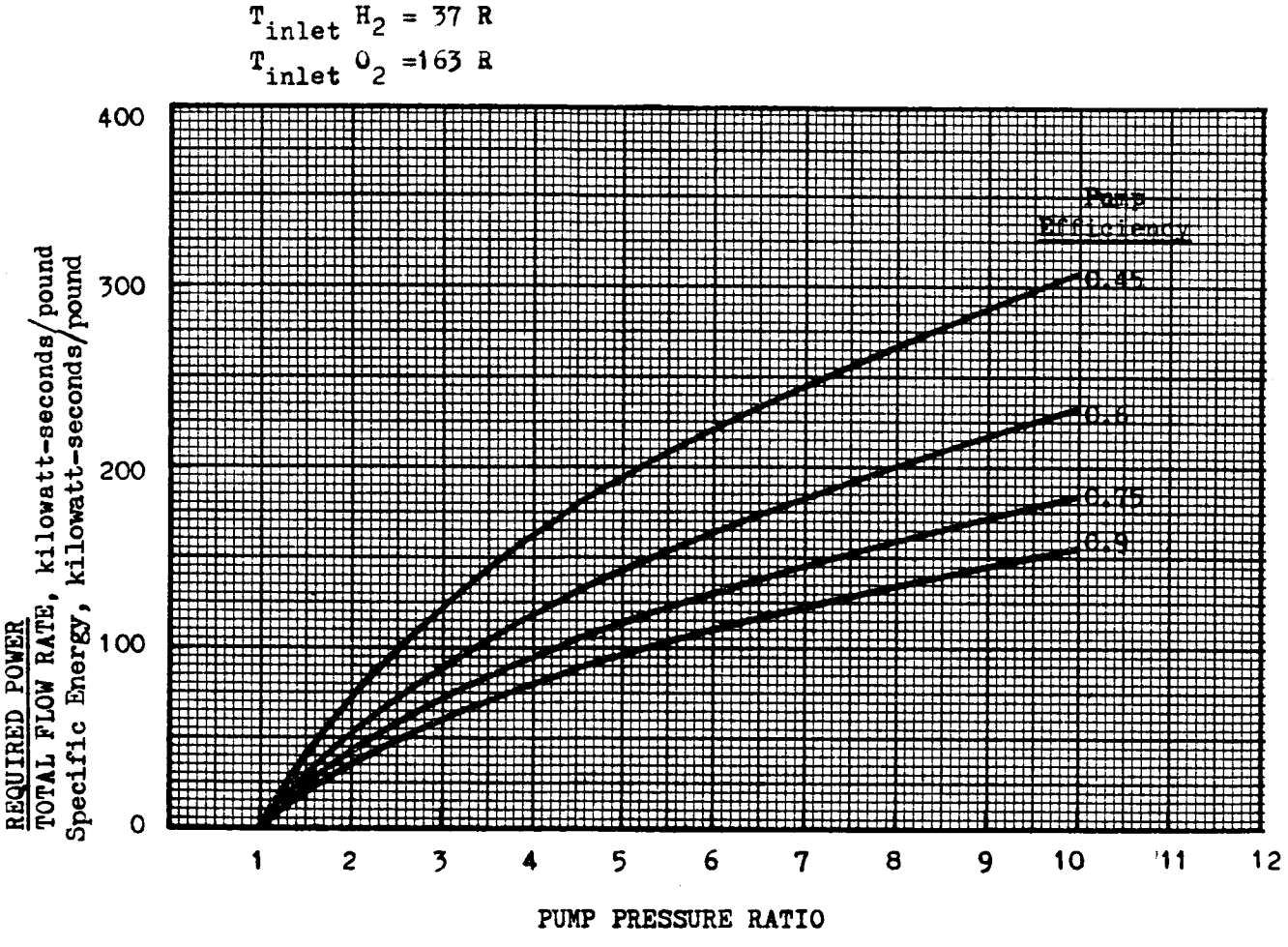

Figure 69. Specific Energy Requirements for a Pump-Heat Exchanger Propellant Conditioning System

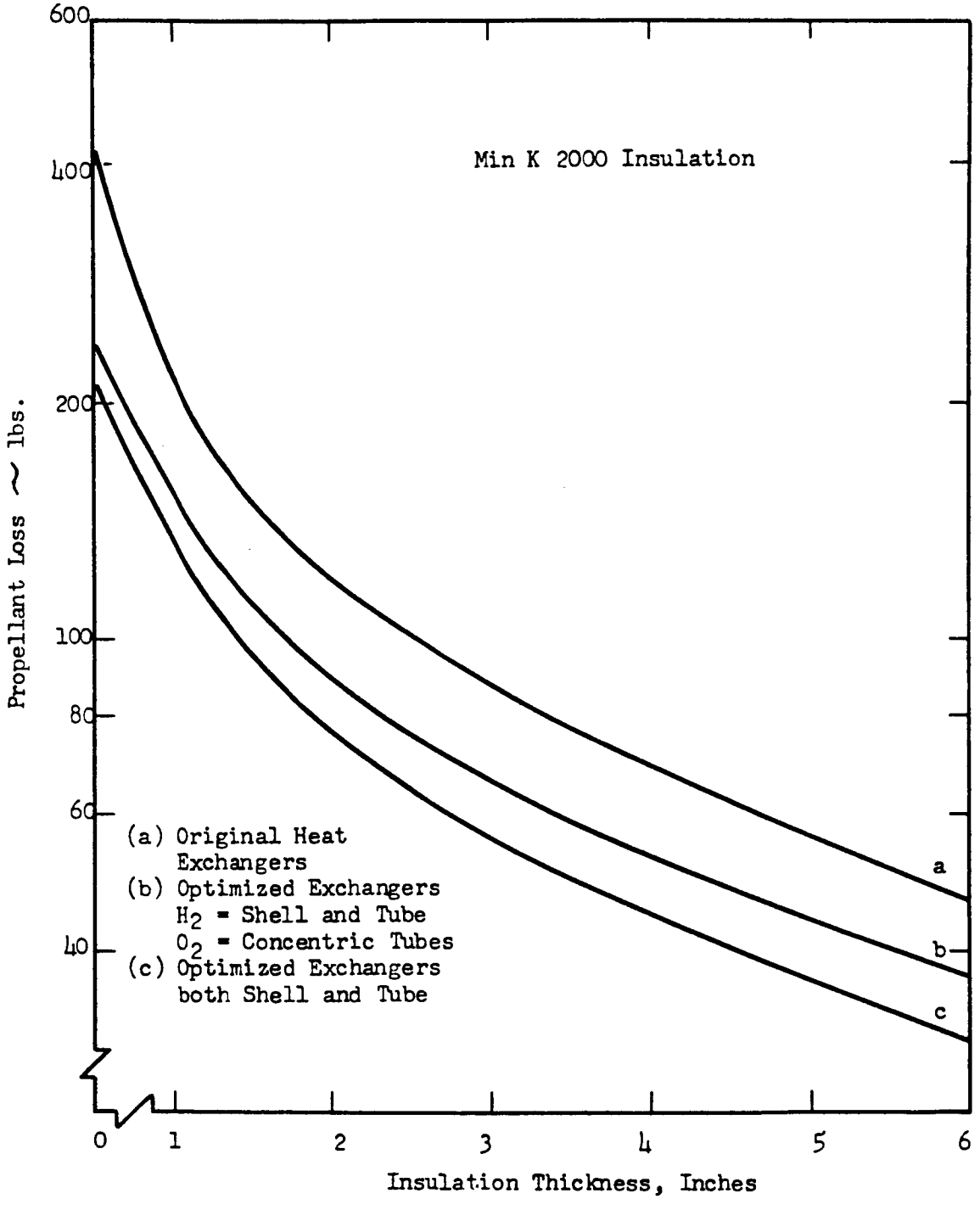

Figure 70. The Effect of Insulation Thickness on Propellant Consumption Required to Make-up Heat Leak to Vacuum for a 220-day Mission

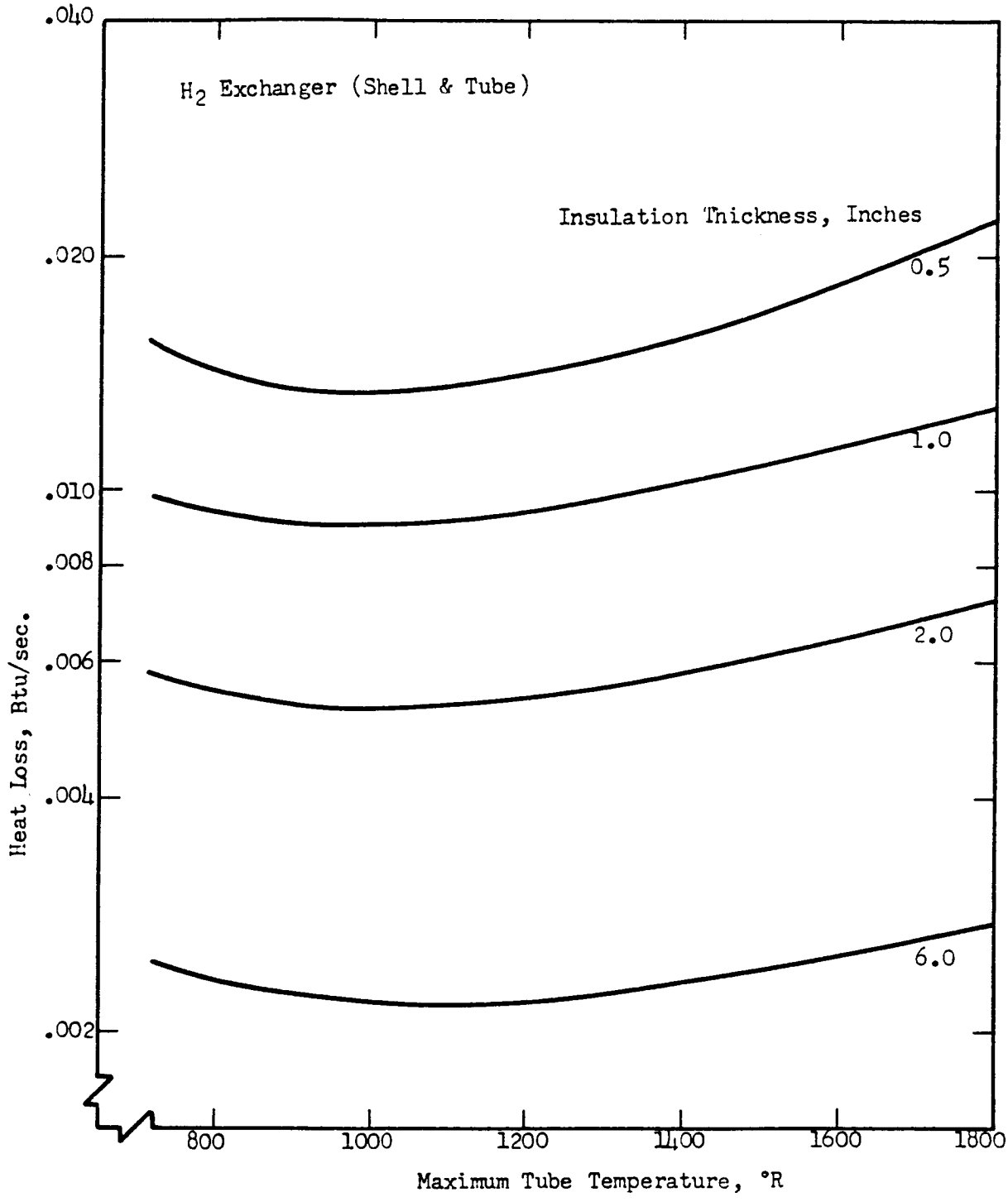

Figure 71. The Effect of Maximum Heat Exchanger Tube Wall Temperature on Heat Loss to Vacuum for a 220-day Mission Showing the Effect of Changes in Heat Exchanger Size

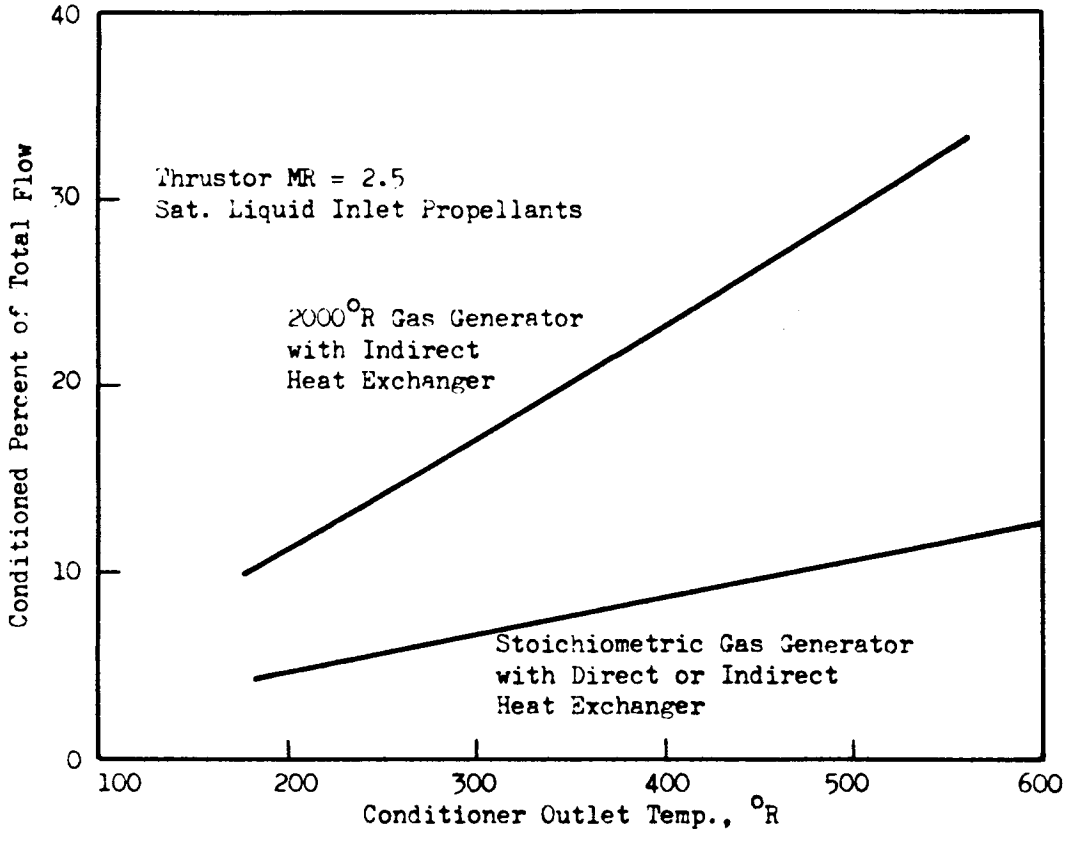

Figure 72. The Effect of Conditioner Outlet Temperature on Propellant Requirements for Conditioning

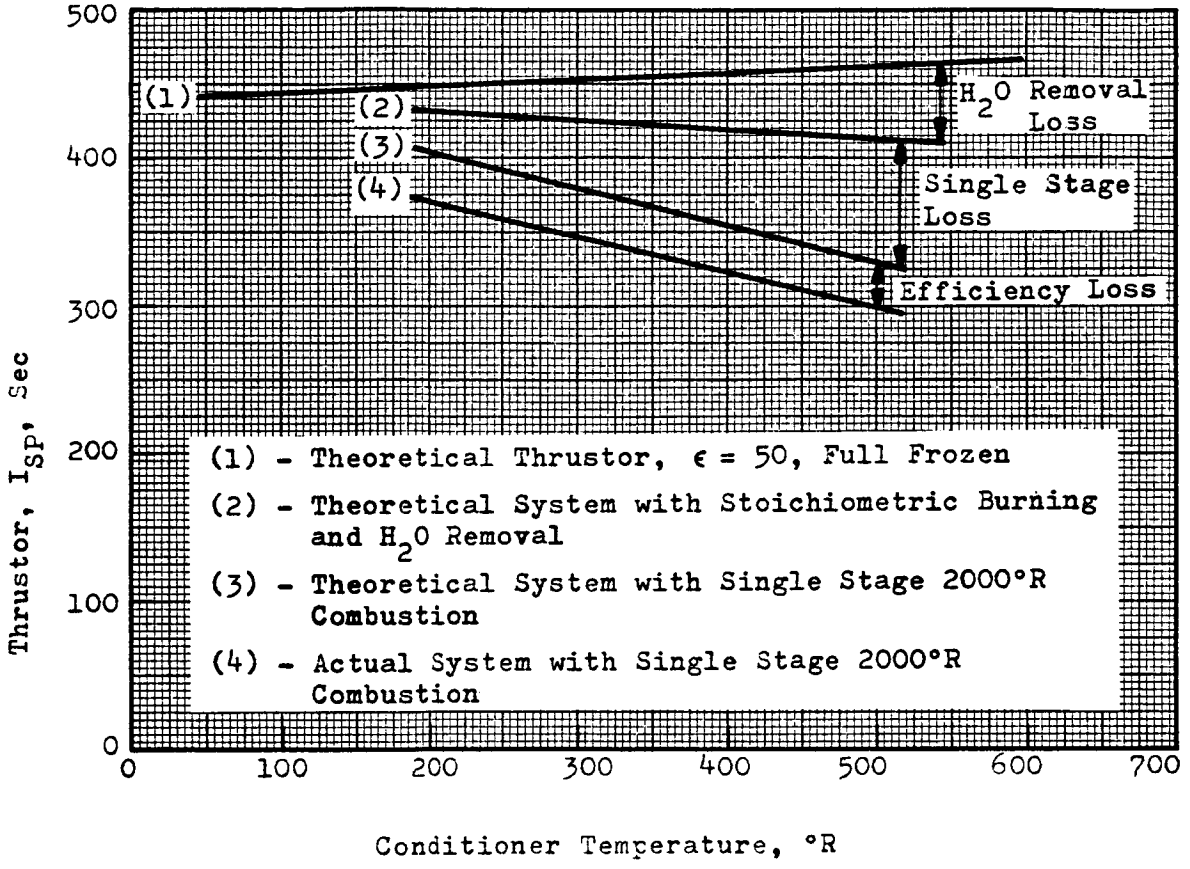

Figure 73. Thrustor I_{SP} Versus Conditioner Temperature, °R

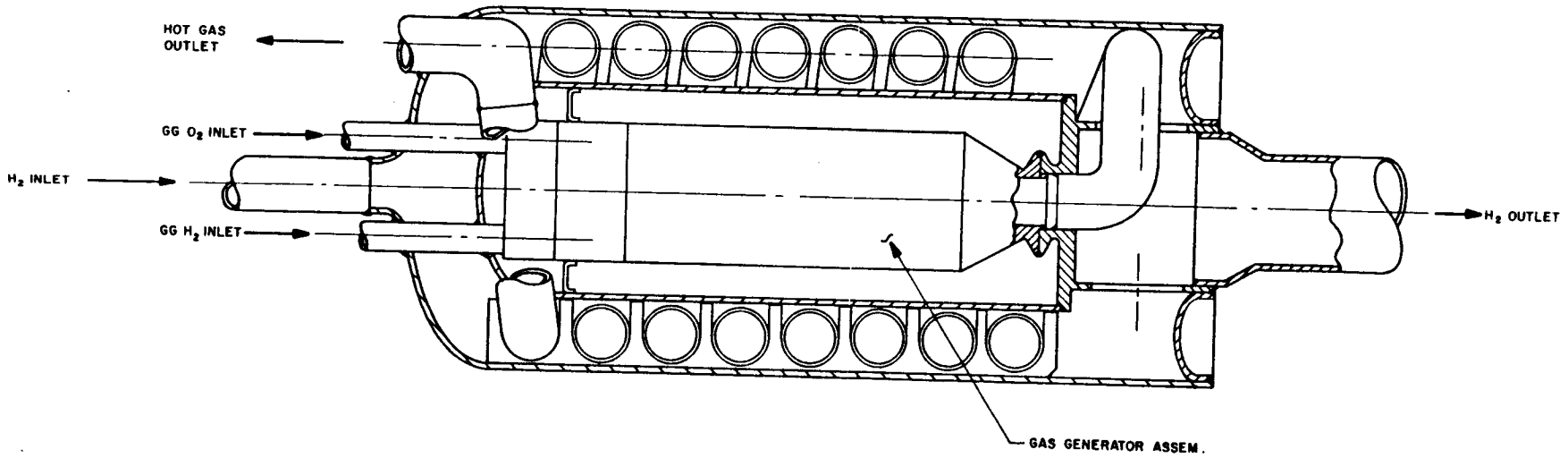

BASIC SPIRAL TUBE DESIGN

Figure 74. Conceptual Flight Design of the Gas Generator and Heat Exchanger for the Hydrogen Conditioner

OVERALL SYSTEM CHARACTERISTICS AND COMPARISONS

Cryogenic reaction control systems based on the conditioning concepts presented in the previous section were compared with the objective of selecting a system concept for experimental evaluation and demonstration. The basic comparison was accomplished at the 10 psia pressure level for a single thrustor-conditioner pair, and included the factors of:

a) system weight and volume (dry weight)
b) operability
c) reliability
d) maximum power requirements
e) anticipated development problems

The weight savings for multiple thrustors per conditioner were calculated. The lowest weight systems were also compared at 100 psia and their characteristics noted. The resulting information was used in the selection of a system for further effort. Finally, a first-order comparison of the system with a present day storable system was made to outline the total impulse requirements where the use of a cryogenic RCS would be advantageous.

LOW PRESSURE CONCEPT COMPARISONS

Concept Comparisons of Weight and Volume

Sizing of each of the representative conditioning systems was accomplished for comparison purposes. The pressure profiles shown in Figs. 64 through 67 were used as the basis for sizing each of the components.

Although the pressure profiles so utilized are not optimum in terms of minimum total weight, or volume or of maximum reliability, it was defined with consideration of these factors.

Weight Comparison. Figure 75 presents the weights of the conventional heat exchanger system as a function of mixture ratio and propellant exit temperature for the low chamber pressure operation. The system weights

are presented for a propellant exit temperature range between 200 R and 500 R. 200 R was chosen as the nominal minimum operating temperature for this type of conditioner based on thrustor inlet temperature considerations. Figure 75 illustrates the desirability of operating at the lowest possible thrustor inlet temperature.

A weight comparison of the four candidate systems is presented in Fig. 76 as a function of the operating mixture ratio, for the lowest operational temperature of each system. The direct heating system operating temperature was set at 500 R because of ice formation at lower temperatures. The remaining systems are limited only by thrustor operating limits and/or controllability considerations.

The hot-tube heat exchanger conditioner has the lowest weight and is from 10 to 20% lighter than the direct heating system, the next lightest system (Fig. 76). The gross weight differences between the conventional and hot-tube heat exchanger systems is primarily due to the large differences in accumulator sizes, which are directly proportional to the system response time. The response time of the conventional heat exchanger system is very long due to the necessity of heating the exchanger tubes during the initial transient. The hot-tube concept is not limited by such considerations.

The direct heating system suffers a higher operating temperature limitation which increases the size and weight of the accumulator. The weights of the hot tube heat exchanger include the propellant venting subsystems for clearing the heat exchanger of hot gas. If these subsystems are not necessary, approximately 1.5 lbs may be deducted from the values presented in Fig. 76. The use of a pump provides no significant weight advantage over the conventional heat exchanger system and, at the lower mixture ratios, is even slightly heavier than the conventional heat exchanger system.

The heat exchanger system curves presented in Fig. 76 are based on a hot gas temperature of 2500 R at the inlet to the heat exchanger. A change in this parameter from the nominal value of 2500 R changes the required hot gas flowrate which manifests itself in different gas

generator, heat exchanger, and gas generator solenoid valve sizes. Further, changes in the hot gas flowrate requires an adjustment in the heat exchanger minimum area, which for the same hot gas side pressure drop changes the hot gas film coefficient and the heat exchanger response times. The variation of system weights with hot gas inlet temperature for a constant hot gas exit temperature of 672F are shown in Fig. 77. Weight (and volume) penalties result from large decreases in inlet temperature. Weight saving of about 7% and volume savings of about 11% could be attained by raising the hot gas inlet temperature from 2500R to 3000R. These result from a decrease in the percentage of propellant fed back to the heat exchanger as hot gas.

Volume Comparison. Figure 78 presents a volume comparison between the four candidate systems. Again, the hot-tube heat exchanger appears as the most attractive system, followed closely in order by the pump heat exchanger system and the direct heating system. The net result of using a pressure augmenting device is a large decrease in conditioner volume requirements accompanied by an increase in system complexity (and attendant decrease in reliability). The volume requirements of the direct heating system are approximately double those of the hot tube heat exchanger system. The volume requirements of the conventional heat exchanger are over one order of magnitude greater than the most attractive system.

Concept Operability

The candidate conditioning systems differ somewhat in operation and start-up characteristics. To aid in a qualitative comparison between the subsystem concepts, a preliminary description of control circuits and system operation is given below.

Direct Heating Concept. A schematic of this subsystem concept is shown in Fig. 64. Initially, the main propellant valves, the cross-feed solenoid valves, and the thrustor valves are closed. A temperature control loop controlling the gas generator catalyst bed temperature has provided sufficient energy to the bed to ensure a bed temperature above the minimum limit. This control loop is also required to control the mixture ratio entering the gas generator catalyst bed to prevent overheating of the catalyst.

To start the conditioner the main propellant valves are opened allowing propellant to flow through the catalyst bed and into the accumulators. A temperature sensor measures the accumulator temperature and if the temperature is too low, the cross-feed solenoid valve is actuated, permitting oxygen (or hydrogen) to flow into the catalyst bed, ignite with the hydrogen (or oxygen), and increase the propellant temperature. A safety device is provided by only allowing activation of the cross-feed solenoid valve when the main propellant valve is open.

If the pressure transducer sensing accumulator pressure measures a pressure that is too low, the main propellant valve and subsequently the cross-feed solenoid valve are actuated, providing additional mass to the accumulator tanks.

Heat Exchanger Concept (Conventional). A schematic of the conventional heat exchanger concept is shown in Fig. 65. To start the conditioner, the main propellant valves are opened, permitting the propellant to flow through the heat exchanger and into the accumulator. If the accumulator temperature control loop senses the propellant temperature is too low, the gas generator solenoid valves are activated permitting propellant to flow into the gas generator, react, and heat the heat exchanger.

A control loop monitoring the catalyst bed temperature has the following functions: (1) ensure the gas generator catalyst bed is above 163 R, and (2) control the mixture ratio in the catalyst bed to be above 163 R, and (3) control the mixture ratio in the catalyst bed to prevent overheating. A secondary control loop may also be required to control the hot-gas inlet temperature due to the presence of helium in the propellants.

Operation of the control loop controlling the accumulator pressure is identical to its operation in the direct heating system.

If startup problems occur due to the initial lack of conditioned propellants in the accumulators, the system can be preloaded with preconditioned propellants prior to launch.

Pressure-Augmented Heat Exchanger Concept. Operation of the pump heat exchanger conditioning system is identical to the operation of the conventional heat exchanger with the exception of a turbine control loop. The turbine and pump rotors would be kept at operational speed at all times, independent of load, by varying the turbine inlet gas flowrate. When the main propellant valves are opened, the turbine inlet gas flowrate would be increased.

Hot-Tube Heat Exchanger Concept. Operation of the hot-tube heat exchanger is also identical to the conventional heat exchanger with the exception of an additional control loop which senses the tube temperature. If the main propellant valves are shut and the tube temperature falls below a determined level, the solenoid valves are

activated, permitting propellants to enter the catalytic gas generator, ignite, and raise the tube temperature. This effectively eliminates the thermal response time term and the response time of this system is approximately equal to the main propellant valve opening time.

Conditioner Subsystem Reliability

A comparison of the conceptual systems was made to determine their relative reliability. The components of each system were compared on a relative basis, considering both the number used in each system and the relative failure probability of each component. The analysis did not consider the components downstream of the accumulator tanks, since these components are common to all of the conditioning system concepts and will not affect the relative reliability among the concepts. The comparison is presented in Table 15. Two values are presented for the hot tube heat exchanger. The first is predicated on the schematic diagram shown in Fig. 67, and the second is predicated on the elimination of the propellant venting subsystem since the necessity of venting has not been definitely established.

Table 15 shows that the direct heating system has the highest reliability followed by the conventional heat exchanger and hot tube heat exchanger. The pump heat exchanger conditioning system has the highest probability of failure due primarily to the presence of the pumps. For very high reliabilities the reliability can be estimated as:

$$R = 1 - \sum_{x=1}^{x=n} \frac{P_x N_x}{(10)^5}$$

- = 0.988 for the direct heating system
- = 0.983 for the conventional heat exchanger system and hot tube heat exchanger system (without venting subsystem)

= 0.978 for hot tube heat exchanger system (with venting subsystem)
= 0.963 for the pump-heat exchanger system

assuming the system mean time between failures is much larger than the total projected mission fixing time.

Table 16 lists the major failure modes expected in each system along with the relative percentage which each failure mode contributes to the overall unreliability of the listed component.

Maximum System Power Requirements

The maximum power requirements for each of the candidate systems were obtained by linearly summing the valve power requirements, the catalyst bed power requirements, and the accumulator tank power requirements. The power requirements for the two solenoid vent valves used in the hot-tube heat exchanger system were not considered since they are only operative when the conditioning system is inoperative.

The results presented in Table 17 show the hot-tube heat exchanger and pump heat exchanger systems have the lowest maximum power requirements followed by the conventional heat exchanger system and the direct heating system, respectively. The total variation in maximum power requirements is very small, being 14 watts or approximately 10%. Exact power consumption comparisons cannot be made unless both the ACS firing duration and operational mode have been prescribed.

System Development Problems

Each conditioning system has several potential problem areas associated with its development for use on flight vehicles. Knowledge of these anticipated problem areas is mandatory if a comparative system analysis is to be made.

One of the major problem areas associated with the development of a direct heating propellant conditioning system is due to the presence of liquid water in the propellants which may

(1) reduce the activity of the thrustor and conditioner catalyst beds
(2) freeze in the thrustor catalyst bed impairing or destroying catalytic activity
(3) increase the uncertainty of reliable catalyst activity in the conditioner catalyst bed
(4) cause slugging in the thrustor feed lines due to two-phase flow.

The effect of the water on the catalyst activity is not known at present, but at temperatures of approximately 500R, activity degradation is not expected to be a problem. Freezing of water at temperatures below 472 could be more of a problem. One solution would be to utilize an electrical heater in the thrustor catalyst pack to maintain a 500R temperature. This would require relatively little power, approximately 5 watts.

Another method of preventing ice formation in the main catalyst bed as well as preventing slugging is to separate the water and the propellant. Several methods of accomplishing the separation were considered. The most promising would appear to be chemical in nature, such as the use of silica gel

and molecular sieve materials to absorb or adsorb the water. Such methods will pose development problems. Weight penalties are not expected to be unduly severe, $\sim$ 10-20 lbs per conditioner system. However, these methods will require two parallel systems so that regeneration can be included in the cycle and regeneration times are not definitely known, so that some uncertainty exists with respect to these weights.

A second anticipated major problem associated with the development of the direct heating conditioning system is the presence of low temperature hydrogen ($\ll$163R) entering the catalyst bed and freezing the incoming oxygen on the catalyst pellets degrading their activity. This problem may be partially circumvented by using conditioned hydrogen to feed the oxygen catalyst bed. The use of conditioned oxygen to feed the hydrogen catalyst bed is precluded, however, due to the low heat capacity of the oxygen and the relatively low mixture ratio ($\ll$1).

This problem may be eliminated by a "boot strap" arrangement whereby a small amount of the hydrogen flow is heated by some energy source (such as electrical or isotopic heaters) above 163R and allowed to ignite with some oxygen. This combusted propellant is then used as a pilot igniter for the balance of the propellants.

The third major problem area with the direct heating system is concerned with the propellant feedback and the use of an accelerating device, such as a venturi, to accomplish this feedback against a total pressure gradient. The possible changes in the state of the entering propellants make an adjustable venturi area necessary. Such a device would require additional development effort.

The chief problem area with the heat exchanger concept is associated with the cold side heat transfer in the exchangers. With liquid or two phase propellant entering the exchangers, slugging may occur.

The heat exchanger systems also have the problem of low temperature hydrogen entering the catalytic gas generators. However, only conditioned propellants can be used to feed the gas generators (after startup) as shown in the system schematic diagram. The weight penalty associated with the additional heat exchanger flowrates is approximately one lb. For system startup a "boot strap" described previously may be utilized.

Integrated Conditioner--Thrustor (Steady-State) Comparisons

An integrated conditioner-thrustor system is possible for certain applications, principally a steady-state propellant settling engine which is started and then runs for extended periods of time. The absence of an intermittent propellant flow demand and of a need for fast response would allow the removal of the components associated with such provisions. Figure 79 presents a system weight comparison for two candidate systems. The heat exchanger system is lighter than the direct heating system throughout the entire mixture ratio spectrum considered. Two different heat exchanger curves are presented in order to illustrate the small system weight penalty associated with using conditioned propellants to feed the catalytic gas generators. Figure 80 shows that additional weight savings for the heat exchanger configuration are possible utilizing 3000R hot gas instead of 2500R hot gas. System weight penalties of approximately 3% and 8% are associated with operation using hot gas inlet temperature of 2000R and 1500R, respectively.

A volume comparison of the candidate system is presented in Fig. 81. The effect of using conditioned propellants to feed the gas generators is again shown. The volume required by the direct heating system is less than that required by the hot tube heat exchanger, even though the latter system is lighter, due to the relatively large void volumes of the heat exchanger and gas generators.

The relative reliability and controllability of the integrated conditioner-thrustor system would be approximately the same, as discussed previously, for the pulse mode conditioning system.

Use of Regenerative Cooling

The desirability of using hydrogen to regeneratively cool the thrustor suggests the feasibility of a combined conditioning system; one which uses thrustor regenerative cooling as a means of supplying a portion of the conditioner power requirements.

If turbulent flow exists in the thrustor, approximately 6.5 BTU/sec (MR = 2.5) can be transferred to the hydrogen from the thrustor. This is sufficient to heat the propellant to 200R if the conditioner can supply sufficient energy to the hydrogen to raise it to 163R. Since the hydrogen flow into the catalytic gas generators comes directly from the accumulator tank, it is necessary to condition the hydrogen to at least 163R to prevent the oxygen from freezing on the gas generator catalyst bed which may manifest itself in catalyst degradation. This temperature (163R) represents the limiting case (maximum weight savings).

Figure 82 presents the weight savings resulting from the combined regenerative-hot tube heat exchanger conditioning concept and Fig. 83

represents the volume savings resulting from use of this concept. A system weight savings on the order of 5% and a system volume saving on the order of 15% are shown. The volume savings is primarily due to the smaller hydrogen accumulator tank.

Number of Thrustors per Conditioner Subsystem

Low Pressure System. To determine the feasibility of utilizing one propellant conditioner for more than one thrustor, all of the components were sized for multiple flowrates. Sizing of the system components (excluding the heat exchangers and accumulators) resulted in a nonlinear weight increase as shown in Fig. 84. The heat exchanger system component weights increase at a slower rate than the direct-heating system components. This is primarily due to different weight rate increases of solenoid valves and check valves. The direct-heating-system solenoid valve equivalent orifice diameters are initially on the very steep portion of the propellant valve weight curve.

The accumulators were sized according to the following equations:

$$V = \frac{5 \tau_T \dot{W}_2}{\rho_g} = \frac{4}{3} \pi r^3 \tag{30}$$

$$M = 4 \pi t \rho_m \left[\frac{15 \tau_T}{4 \tau \rho_g} \right]^{2/3} \tag{31}$$

subject to the restriction that

$$t = \frac{P_t r}{225} \geq 0.020 \text{ inches} \tag{32}$$

The response times of the heat exchanger systems remained constant, because the values were related to the thermal response times of the heat exchangers. The response time of the direct heating system equals the response time of the slowest valve (main propellant inlet valve). This was approximated as the sum of the solenoid (pilot) actuation time, the

fill time, and the poppet opening time. The solenoid actuation time was obtained from the Gemini 100-pound-thrust engine as 0.020 seconds. The fill time was calculated as:

$$\theta_F = \frac{V_F}{A_o \alpha} \sqrt{\frac{2\alpha}{(\alpha-1)(RT_e)g}} \tag{33}$$

The time required for the poppet to open was calculated as:

$$\theta_p = \sqrt{\frac{2 S A_p L_p \rho_m}{\Delta P A_F g}} \tag{34}$$

The valve times were conservatively estimated by assuming the valve centerbody cross-section area is proportional to the orifice area:

$$A_c \propto A_o \tag{35}$$

Then the fill volume is approximated as:

$$V_F \cong D_c gL = gL \sqrt{4\pi A_c} \tag{36}$$

where the length (L) is considered constant, and the gap thickness (g) increases by 10 percent when the flowrate is doubled. Using these criteria, the accumulators were sized. Minimum thicknesses can be utilized virtually throughout the entire range of the numbers of thrustors considered.

The results of the multiple thrustor analysis are presented in Fig. 85 which shows both the hot tube heat exchanger and direct heating system become increasingly attractive as the number of thrustors is increased. For a module of 4 thrustors (only 3 can operate at a given time) the conditioner weight increases by approximately 2.1 times for the hot tube heat exchanger and 2.3 times for the direct heating system. A single conditioner may also be used for 2 modules (6 operative thrustors) dependent on the vehicle geometry and mission duration which will affect piping and insulation weights. The relative volume comparison can also be inferred to follow that of the weight comparison of Fig. 85. The inference is possible because the accumulators comprise a significant portion of the total system weight and over 90 percent of the total volume.

PRESSURE LEVEL COMPARISONS

Effect of Pressure on Component Weights

Significant component weight savings can be achieved with separate RCS tankage operating at 175 psia (with a 100 psia chamber pressure) due to smaller volumetric flow requirements and a larger available pressure drop. Fig. 86 shows the effect of increased pressure on conditioner system weight. At a tank pressure of 175 psia and a chamber pressure of 100 psia both the hot tube heat exchanger system and direct heating system have virtually the same weight. The weight of the conventional heat exchanger system decreases more rapidly than the other systems since the accumular size decreases from both a pressure increase and a decrease in thermal response time. The decrease in system dry weight for the lowest weight system (hot-tube heat exchanger concept) of from $\sim$25 to $\sim$8 pounds is quite significant. It is noted, however, that propellant usage charges may differ between the two pressure levels. Pressurant and propellants which might be normally "boiled off" might under some circumstances be considered free for the low pressure system. Moreover, tankage and pressurization system dry weight charges may differ between the two pressure levels.

Using the sizing criteria discussed previously, multiple thrustor sizing of the two most promising systems was made for operating conditions of P_T = 175 psia and P_c = 100 psia. The results are presented in Fig. 87 along with the weights of the low pressure systems. Little weight difference is noted between the two systems operating at 100 psia. Again, the advantages of using a single conditioner per module is apparent since the conditioner weight of a 4 thrustor module (1 redundant) exceeds by about 1.6 times the weight for a single thrustor module.

Effect of Pressure Level on System Characteristics.

To evaluate the effect of pressure level on the characteristics of the overall system, two configurations were compared;

1. Attitude control systems consist of: 4 modules, each module is composed of 4 thrustors, 1 propellant conditioner, and two tanks storing propellants at 175 psia.

2. Attitude control system consists of 16 thrustors in groups of 4, and 4 conditioners, with propellants supplied from the two main tanks storing propellants at 20 psia.

The comparisons were made on the basis of weight, volume, reliability, and controllability. The two pressure levels were compared with respect to the weights and volumes of the dry system, necessary propellant charge, pressurization components, and pressurant. Two alternative assumptions were made with respect to the propellant charge for the low pressure system, no propellant charge and 100 percent charge. In neither case were main tankage pressurization charges applied. Several alternatives were used with the high pressure system; (1) propellant charge only, (2) propellant charge only, but with 50 percent hydrogen boiloff, (3) propellant and pressurization charges, and (4) propellant and pressurization charges, but with 50 percent hydrogen boiloff. The 50 percent hydrogen boiloff case was selected arbitrarily. Detailed boiloff and energy transfer studies were not accomplished, and weight and volume charges for the necessary insulation are not included in the reported values.

Weight Comparison. Fig. 88 presents the weight comparisons between the systems with the various cases described above. The break point between the two systems lies in the range above 6400 lb-sec per module of four thrustors (three active and one redundant).

Volume Comparison. The volume of the high pressure system is considerably smaller than the low pressure system volume due to both an increase in accumulator pressure and a decrease in conditioner response time. The ratio of accumulator volumes, which comprises a very significant portion of the module volume, can be approximated as:

$$\frac{V_L}{V_H} = \frac{P_H \tau_L}{P_L \tau_H} \simeq 22 \qquad (37)$$

Therefore, the volume of the high pressure system is approximately 22 times smaller than the volume of the low pressure system. Additionally, the increase in module volume is directly proportioned to the module's total impulse requirements. Figure 89 presents a low pressure-high pressure module volume comparison which shows the high pressure system requires lower volumes below 5250 lb-secs and 7000 lb-secs dependent on the low pressure thrustor configurations. If the design is predicated on 50% boiloff, the total impulses at which the low pressure system volumes become smaller are 3700 lb-secs and 4900 lb-secs.

The volume comparisons shown in Fig. 89 represent a limiting case in that thrustor volumes were included. If the thrustors are mounted external to the vehicle and volume charges are not assessed for the thrustors the break points are lowered. In the case of no hydrogen boiloff, the two systems have equal volume requirements at approximately 4100 lb-sec total impulse, a decrease of approximately 700 lb-sec and 2600 for the truncated spike and bell low pressure thrustors, respectively.

Reliability Considerations. A reliability analysis of the two proposed configurations was made to determine which configuration would yield a greater probability of safe return to earth. A study of the two configurations shows that the component parts are identical except for the propellant tanks. Assuming that the interactive effects between the

two tank configurations and the remainder of the system are similar, a comparison of Configurations I and II can be achieved by comparing the tanks only. This comparison is presented in Table 18 and shows the modularized (high pressure) system has a slightly higher reliability. Failure rate estimates are based upon data from generic systems.

Controllability and Operability. Systems operating at the two specified pressure levels have associated characteristics resulting from the method of propellant supply. The low pressure system characteristically has a large relative uncertainty in the propellant supply pressure which depends on the opposing effects of pressure generation (heat leakage rates) and propellant usage. The net result will be dependent on the mission and vehicle under consideration.

Likewise, there is a probable uncertainty in thermodynamic state and composition of the propellants delivered to the RCS. In a spacecraft designed for long duration missions, the hydrogen will probably be near a temperature of 40R, but in a mixed phase condition; and small amounts of helium will probably be present. The oxygen state is likely to be similar but with the possibility of a greater fraction of helium present. Conversely, other vehicles designed for short duration missions, such as upper stages or orbital tankers, may use heat exchange methods or appreciable quantities of helium as an ullage gas supply in which case the state of the propellant would be specific to a given vehicle.

The low pressure system also presents the difficulty of a minimum pressure inventory under the ground rules of nominal supply and chamber pressures of 20 and 10 psia, respectively. It was noted in the applications survey effort that in many cases the oxygen main-tank storage

pressures are nominally 30 instead of 20 psia. This indicates the 20 psia level to be on the conservative side. It is expected that the final storage pressures and the chamber pressure would result from a vehicle trade-off involving tankage weight, RCS controllability, RCS component weights and volumes, and the thrustor size and operating characteristics. However, for the purposes of evaluating system concepts and demonstrating the feasibility of such a system, this conservative ground rule was maintained.

The higher pressure system utilizing separate propellant tankage does not have the same pressure inventory problem, thus making the system more controllable. Also, the higher gas pressures and greater allowable pressure drops lead to significantly smaller equipment which are closer in design to the present state-of-the-art. Although heat leakage to the RCS storage tanks could be of major importance in causing excessive boiloff, this might be circumvented by thermally tieing the RCS tasks to the main propellant storage tanks.

SELECTION OF SYSTEM CONCEPT AND PRESSURE LEVEL

Concept Selection

Relative Comparisons of Subsystem Concepts. Each of the candidate conditioning systems was evaluated with respect to a number of considerations including weight, volume, and reliability. To accomplish this rating, a numberical rating system was devised in which the optimum system receives a rating of 10 and the other systems receive lesser

ratings dependent on their relative standing, with a minimum rating of unity being imposed. Each of these rating factors must then be weighted with respect to the type of mission and engine application. The relative rating system was based on the following criteria:

1. Weight
2. Volume
3. Reliability
4. Control level
5. Development problem areas
6. System integration (feed system and power requirements)
7. Prior experience
8. Duty cycle (system specific impulse)
9. Temperature effects (material requirements and insulation requirements)
10. Manufacturability
11. Growth potential (to 500-pound thrust)

Weighting factors were also developed for both manned vehicles and unmanned vehicle application. Since there are 11 categories to be evaluated, the most significant parameter was given a weighting factor of 11 followed by a 10 for the next most significant parameter, etc. The weighting factor was then multiplied by the rating factor and the results summed to achieve a final rating. The results of this comparison are presented in Table 19 for both manned and unmanned vehicle applications. The results show the direct heating system and hot-tube heat exchanger system are vastly superior to the other candidate systems. It is noted that small changes in the weighting factor and/or rating factor will not change the relative standings of the candidate systems.

The major advantage of the direct heating and hot-tube heat exchanger concepts over the conventional heat exchanger concept is one of system

response. The pressure-augmented heat exchanger concept represents an attempt to increase the response by increasing the pressure driving potential for heat transfer. However, this requires additional weight.

Selection of Conditioner Concept. The hot-tube heat exchanger concept is thought to be subject to less technical uncertainty than the direct heating concept. In the latter, the interaction effects of the presence of water on the low temperature reaction and the water contamination effects on flow control are unresolved. The heat exchanger operation is more straightforward technically. The chief uncertainty lies in the possibility of liquid slugging in the heat exchangers because of boiling induced instabilities. This is of major concern on the oxygen side. Although the calculated heat transfer coefficients are not considered exact, errors in their estimation should only influence the size and weight of the system to a minor extent. This is because the heat exchanger does not represent the major component in either a weight or volume sense.

Based on the results presented above the hot-tube exchanger concept would seem to present the optimum combination of technical knowledge and system design characteristics such as weight, volume, reliability, etc. Therefore, this concept was chosen for further study.

Selection of Pressure Level

The preliminary concept comparisons show the low pressure (10 psia) system to represent a smaller weight and volume penalty for high total impulse requirements. The actual value of the crossover point between the two systems must result from a detailed tradeoff between hydrogen boiloff and insulation for the separate tankage system and consideration of propellant and pressurization charges for the low pressure system. Control aspects of the separate tankage system should be

more amenable to solution because of the greater pressure potential available. However, control of the low pressure system does seem feasible.

The low pressure system utilizing main tank propellants has several advantages not quantitatively evaluated in the foregoing discussion. The system would be capable of utilizing boiloff propellants which would normally be vented overboard in controlling the main tankage pressures. This could result in a considerable propellant weight saving over a long duration mission.

Further, the total availability of propellant from a single source eliminates the complexity of maintaining separate, well-insulated propellant systems for each RCS module. However, such a system would necessarily require placement of the RCS modules in close proximity to the main tankage. In this case the separate tankage system is seen as the more versatile.

Two other factors must be considered. There is almost no technical background for the low pressure system. Second, data obtained for both the thrustor and conditioner subsystems at the 10 psia chamber pressure level can be extrapolated to higher pressure in conjunction with existing data with a substantial degree of confidence. This would not be true for the extrapolation to lower pressure.

The pressure level selected for further effort in the present program was the 10 psia chamber pressure. The selection was based on favorable system volume and weight for high total impulse missions (> 700 lb-sec) and on the lack of existing technology at this low chamber pressure.

CRYOGENIC AND STORABLE PROPELLANT REACTION CONTROL SYSTEM COMPARISONS

This section presents comparisons between storable and cryogenic reaction control system with the purpose of outlining the areas of total impulse for which the cryogenic RCS is most attractive.

Although the comparisons presented herein are based on system weight and total impulse, other factors must also be considered. Such factors as temperature compatibility with the vehicle, power and electrical energy requirements, reliability, simplicity, etc., must also be considered. Final comparisons must be made in terms of a vehicle tradeoff. However, the simple comparison presented herein can serve as a guideline in illustrating the general attractiveness of the cryogenic (O_2-H_2) reaction control systems.

Three reaction control systems are compared; (1) storable bipropellant (NTO/MMH), (2) 100-psia chamber pressure cryogenic, and (3) 10-psia chamber pressure cryogenic. Systems (2) and (3) were considered in the present contract; system (3) represents the system experimentally evaluated. The comparison is based on a module of four thrustors with a single set of tankage.

System Definitions and Assumptions

Storable Bipropellant System. An NTO/MMH system was selected as the base system for comparison. A delivered specific impulse of 300 lbf-sec/lbm was assumed for calculational purposes. Although the storable RCS is compared directly with the cryogenic systems and application to cryogenic vehicles is assumed, no weight charges for insulation or auxiliary heating is assumed. These are a function of the mission and vehicle particulars, and cannot be determined a priori. Hence, the resulting storable system weights are considered conservative for comparison purposes.

The storable system weights are in general based on state-of-the-art components but without the redundancies associated with man-rated systems. The storable system includes the pressurizing system and pressurant, the propellant tankage and propellant, and four thrustors.

Low-Pressure Cryogenic System. The low-pressure cryogenic system design is based on withdrawing propellant from the main vehicle tankage associated with a pump-fed main propulsion system. A nominal chamber pressure of 10 psia and tankage pressures of 20 psia are assumed. This is somewhat conservative because the pressures in such tankage are usually at higher levels. Catalytic reactor ignition is assumed in the thrustor and gas generator designs.

The comparisons are based on liquid propellants (at the normal boiling point) delivered from the main tankage to the module and on a conditioned propellant temperature of 200 R. Assuming a liquid propellant feed is conservative in the sence that specific impulse will increase if propellants of higher enthalpy are fed to the system. Also, the necessary conditioning weight will decrease if this condition can be guaranteed. A 200 R value for the temperature of the propellant feed to the thrustors is used, based on the possibility that improved catalyst, slight relaxation in the pressure, or maintenance of warm catalyst beds will alleviate the cryogenic ignition difficulty.

A heat exchanger conditioning system similar to the one experimentally evaluated is assumed. Insulation weight for reducing the heat leakage from the heat exchanger is included. No insulation is included for the purpose of isolating the system from the surrounding environment.

The hot gas used for conditioning purposes is dumped overboard, resulting in a specific impulse degradation. However, such a system design would not be optimum for a slow response application such as a settling engine. In such a case the conditioner could be combined with the thrustor in a manner similar to regenerative cooling. A specific impulse gain because of increased propulsive mass flow would result.

Component weights are estimated, based on the present state-of-the-art. This represents considerable extrapolation in some cases because the low pressure, low-pressure drop, moderate volumetric flowrate application is somewhat unique.

The optimum control system for the low-pressure cryogenic system has not been determined and may differ, according to the applications. One strong possibility involves the use of pressure regulators. Estimates of the weight for such devices result in values that are a sizable fraction of the total system weight because of the requirement for large, equivalent-orifice diameters. Because of the possibility that major advances can be made in the design of such devices, that inlet pressures might be raised, thus decreasing the equivalent orifice diameter, or that alternative control systems might be used, the system weights were determined both with and without regulators. When sizing without regulators, sufficient valves were included to allow on-off control.

High-Pressure Cryogenic System. The high-pressure cryogenic system design is based on separate propellant storage for each module of four thrustors, complete with a pressurization system for the oxygen. Pressurization was assumed as unnecessary for the hydrogen. Nominal tankage pressures of 175 psia and a chamber pressure of 100 psia were used for sizing purposes. Again, a heat exchanger maintained at operating

temperature was assumed as the basic conditioning device. Insulation (min K 2000) for the exchangers and gas generators were included in the system weight; insulation for the remainder of the system was not considered.

A 200 R temperature was used as the thrustor feed temperature. Previous studies (Ref. 2 and 3) have indicated reliable ignition at this temperature and the pressure of interest.

Pressure regulator weights were again found to be a significant, although smaller, fraction of the overall system weight. Therefore, the weights of two systems, with and without regulators, were determined.

System Comparisons

Storable With Low-Pressure RCS. The comparison of the low-pressure cryogenic RCS with a storable RCS is presented in Fig. 90 and 91 for conditioned propellant temperatures of 200 and 400 R, respectively. Two low-pressure system dry weights are indicated, both with and without regulators for system pressure control (regulator weights are discussed earlier). Two propellant charge lines are also indicated in Fig. 90, corresponding to a charge for only the oxygen and for both propellants. The weight crossover point is in the range of ~50,000 lb-sec total impulse for the 200 R conditioned propellant temperature. For oxygen charges only, and no propellant charges, the crossover point drops considerably. It is also emphasized that insulation weights are not included. When this is included, the storable values will be increased and the crossover point will be moved to lower values of total impulse.

The effect of conditioning the propellant to a higher temperature is seen to move the crossover points to a higher total impulse value (Fig. 91) for both the dry weight and oxygen charge cases. The

delivered specific impulse for total propellant charges is depressed to the point where the weight curve almost parallels the storable system. This shows the undesirability of conditioning the propellant to such a high temperature. It is reiterated that ignition with ~200 R propellants and ambient catalyst bed temperature have been reliably achieved. Thus, 400 R propellant conditioning is not presently envisioned as a requirement, if the catalyst bed temperature is suitably controlled.

The comparisons suggest a low-pressure cryogenic system, which utilizes main tankage propellant, is more attractive than a storage system from a total system weight standpoint at high values of total impulse (50,000 lb-sec and above) irrespective of other advantages such as thermal compatibility. At higher total impulse values (Fig. 92), the weight differences became substantial.

Cryogenic System With Separate RCS Propellant Tankage. A comparison of the higher-pressure (100-psia chamber pressure) cryogenic system which is representative of separate storage of the RCS propellants is shown in Fig. 93. The dry weight of the system is smaller than with the low-pressure system, but the slope is slightly larger because of a charge for oxidizer pressurant. The crossover point for the higher pressure cryogenic system with the storable system lies at about the same total impulse as the storable system crossover point with the low-pressure system. The low-pressure system is seen to result in lower system weights than the 100 psia system for high total impulse requirements.

SUMMARY OF SYSTEM SELECTION

A comparison of cryogenic reaction control systems utilizing the conditioning concepts described in the previous section showed the hot-tube heat exchanger concept to be most attractive from minimum weight and

volume, technical state-of-the-art, and operability and controllability standpoints. This concept was selected for experimental evaluation and demonstration purposes.

A choice of the low pressure level RCS system (10 psia for thrustor chamber pressure) over the higher pressure system (100 psia) was made. The selection was chiefly based on a favorable weight comparison for high total impulse system (~7000 - 10,000 lb-sec) and the lack of existing technology at this pressure level for both the conditioner and thrustor. Interpolation of the results experimentally obtained in this program and those previously obtained at higher pressures (100 to 200 psia) can be used to cover all pressure ranges of future interest. Further, the low-pressure system imposes the more difficult control problem because of a lower acceptable pressure drop and the large size required for the components. Thus, it was felt that effort on the low pressure system would provide the technology required to distinguish between the alternatives in future efforts and to define the technical problems associated with each.

A first-order system comparison of the cryogenic systems with a present-day storable bipropellant RCS showed the attractiveness of the cryogenic RCS concept. This is especially true in the case of large total impulse requirements (~50,000 lb-sec) with a low-pressure cryogenic system drawing propellant from the main propulsion system tankage. The attractiveness is more pronounced in the case of boiloff propellant usage.

The high-pressure system was also indicated to be more attractive than the storable system at total impulses above 40,000 lb-sec. However, the weight of such a system was found to increase faster than the low-pressure system (Fig. 93). This resulted from oxygen pressurization requirements.

The aforementioned conclusions are subject to consideration of other significant factors such as temperature compatibility, reliability, simplicity, etc. Final comparisons must be accomplished in terms of vehicle tradeoffs. However, the weight comparisons do indicate an attractive potential for the cryogenic RCS concept.

TABLE 15

RELIABILITY OF CONDITIONER SUBSYSTEM CONCEPTS

Component	System Relative Failure Probability--P_x	Direct Heating System		Conventional Heating Exchanger		Pressure Augmented Heat Exchanger		Hot-Tube Heat Exchanger			
								With Vent Subsystem		Without Vent Subsystem	
		N_d	$P_x N_d$	N_e	$P_x N_e$	N_f	$P_x N_f$	N_g	$P_x N_g$	N_h	$P_x N_h$
Valves											
Solenoid	250	2	500	4	1000	4	1000	6	1500	4	1000
Main Propellant	250	2	500	2	500	2	500	2	500	2	500
Check	15	4	60		-		-	3	80		-
Catalyst Pack	40	2	80		-		-		-		-
Heating Element	5	4	20	4	20	4	20	4	20	4	20
Accumulator Tasks	4	2	8	2	8	2	8	2	8	2	8
Heat Exchanger	40		-	2	80	2	80	2	80	2	80
Gas Generator	40		-	2	60	2	80	2	80	2	80
Pump	1000		-		-	2	2000		-		-
Turbine	40		-		-	1	40		-		-
TOTAL Unreliability $\sum_i P_x N_i$			1168		1688		3728		2218		1688
TOTAL Reliability $1 - P_x N_i/(10)^5$			0.988		0.983		0.963		0.978		0.983

TABLE 16

COMPARISON OF MAJOR FAILURE MODES

Failure Mode	Failure Mode Distribution, percent		
	Direct-Heating Systems	Heat Exchanger Systems	Pump Heat Exchanger
Solenoid Valve			
Internal Leakage	75	75	75
Fail to Open	12.5	12.5	12.5
Fail to Close	12.5	12.5	12.5
Main Propellant Valve			
Internal Leakage	75	75	75
Fail to Open	12.5	12.5	12.5
Fail to Close	12.5	12.5	12.5
Check Valve			
Reverse Leakage	100	100	
Catalyst Pack			
Catalyst Degradation	Not Available	--	--
External Leakage			
Internal Leakage			
Heating Element			
Open Circuit	100	100	100
Accumulator Tank			
External Leak	100	100	100
Gas Generator (Catalytically Ignited)			
Catalyst Degradation	--	Not Available	Not Available
External Leakage			
Internal Leakage			
Heat Exchanger			
Internal Leakage	--	Not Available	Not Available
Pump			
Piston Galling			
Valve and/or Piston Leakage	--	--	Not Available
Bearing Failure			

TABLE 17

SYSTEM MAXIMUM POWER REQUIREMENTS

System	Maximum Power Requirement, watts
Direct Heating	161
Conventional Heat Exchanger	153
Hot-Tube Heat Exchanger	147
Pump Heat Exchanger	147

$$\text{Maximum Power Requirement} = P_{\text{accumulator}} + P_{\text{valves}} + P_{\text{heaters}}$$

TABLE 18

RELIABILITY COMPARISON

	Modularized Configuration I	Non-Modularized Configuration II
Number of Tanks	8	2
Estimated Probability of Total Propellant Loss in one Tank (q)	$q_1 = .00032$	$q_1 = .00064$ Tank Failure $q_2 = .00063$ Main Engine Valve Stuck Open
Reliability (R_1) of each Tank	$R_1 = (1 - q_1) = .99968$	$R_1 = (1-q_1)\ (1-q_1) = .99873$
Probability of no propellant loss from any tank (P (o))	$P(o) = R^8 = .99744$	$P(o) = R^2 = .99746$
Probability of no propellant loss from at least 7 of 8 tanks (P(7 or 8))	$P(7 \text{ or } 8) = (8R_1^7(1-R_1)+R_1^8 = .999994$	- - - - - - - - - -

TABLE 19

SUMMARY OF THE CONCEPT COMPARISONS FOR SYSTEMS WITH PULSE-MODE CAPABILITY

	Conditioner Concepts				Manned Vehicles					Unmanned Vehicles				
	Direct Heating	Convection Heat Exchanger	Hot-Tube Heat Exchanger	Pumpheat Exchanger	Weighing Factor	Direct Heating	Convection Heat Exchanger	Hot-Tube Heat Exchanger	Pumpheat Exchanger	Weighing Factor	Direct Heating	Convection Heat Exchanger	Hot-Tube Heat Exchanger	Pumpheat Exchanger
Weight	8	3	10	3	8	64	24	80	24	11	88	33	110	33
Volume	8	1	10	9	10	80	10	100	90	9	72	9	90	81
Reliability	10	7	6	3	11	110	17	66	33	10	100	70	60	30
Prior Experience	10	8	8	5	4	40	32	32	20	6	60	48	48	30
Control Level	10	7	7	3	9	90	63	63	27	7	70	49	49	21
System Integration	6	8	10	10	7	42	56	70	70	4	24	32	40	40
Duty Cycles	9	10	5	3	5	45	50	25	15	5	45	50	25	15
Temperature Effects	9	10	2	4	1	9	10	2	4	1	9	10	2	4
Problem Areas	2	10	8	4	6	12	60	48	24	8	16	80	64	32
Manufacturability	10	6	5	3	3	30	18	15	6	3	30	18	15	9
Growth Potential	8	4	10	8	2	16	8	20	16	2	16	8	20	16
Total						538	408	521	332		530	407	523	311

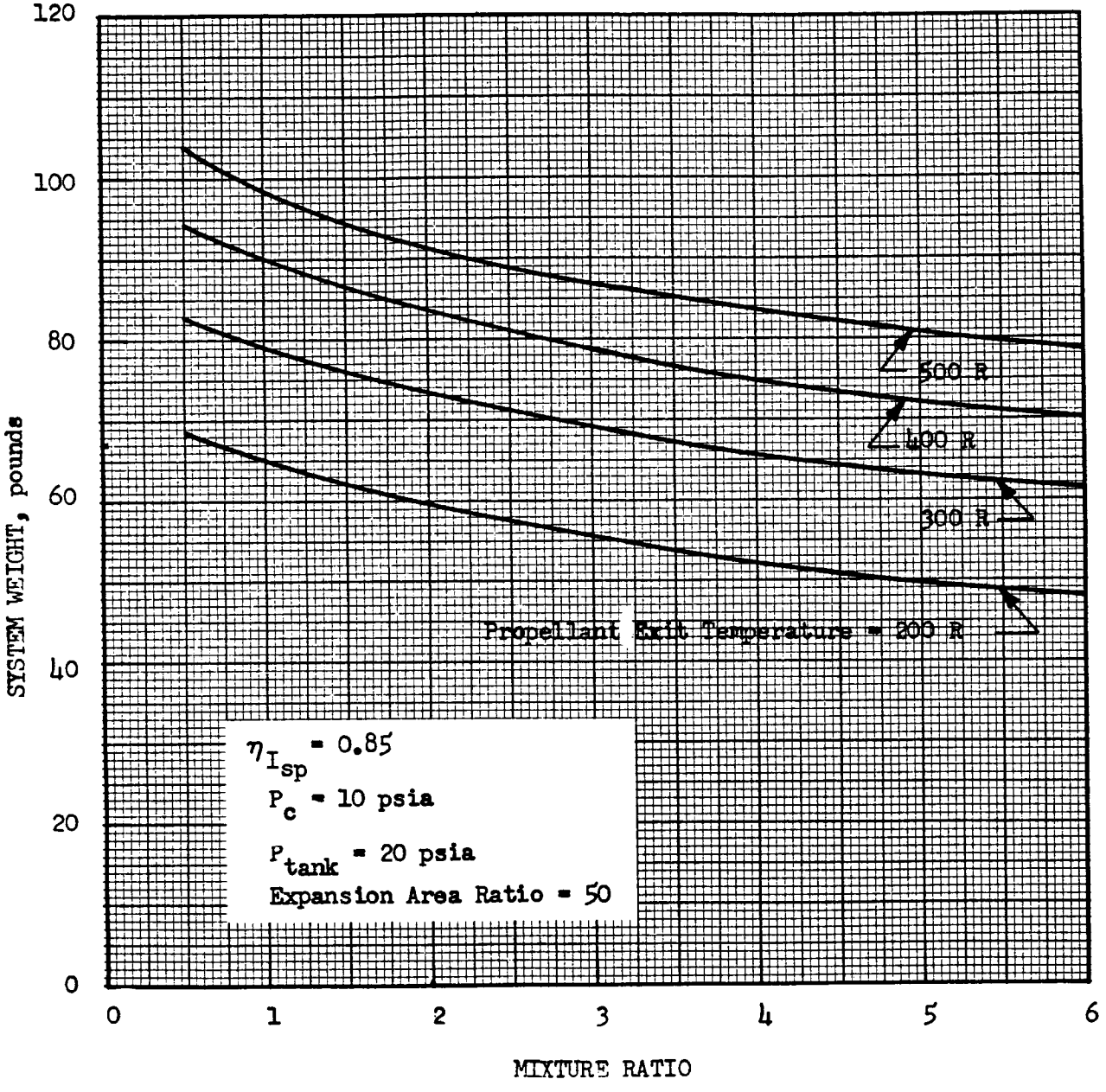

Figure 75. System Weight Characteristics Illustrating the Effect of Propellant Temperature at the Conditioner Exit

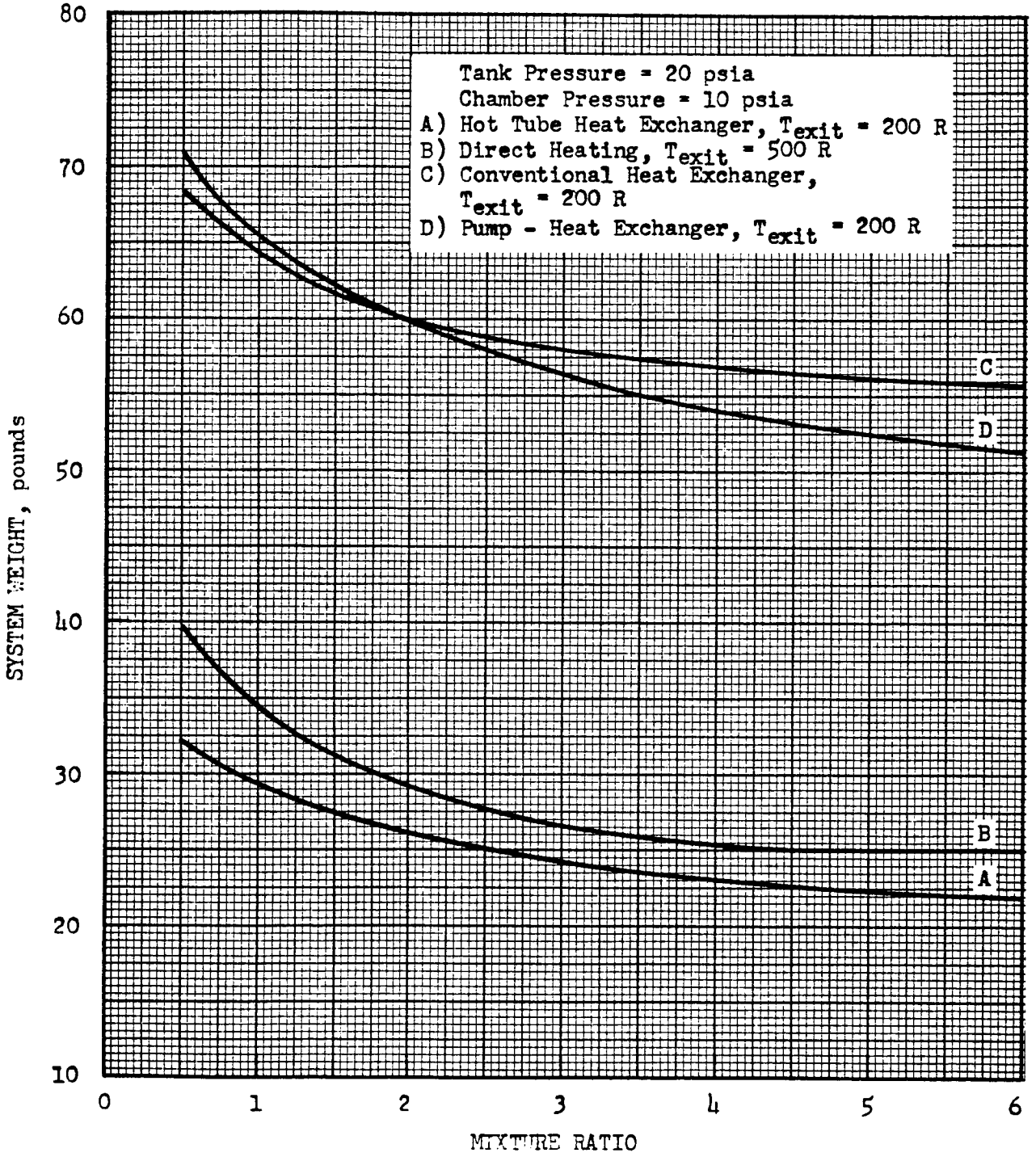

Figure 76. Comparison of System Weights for Four Conditioner System Concepts

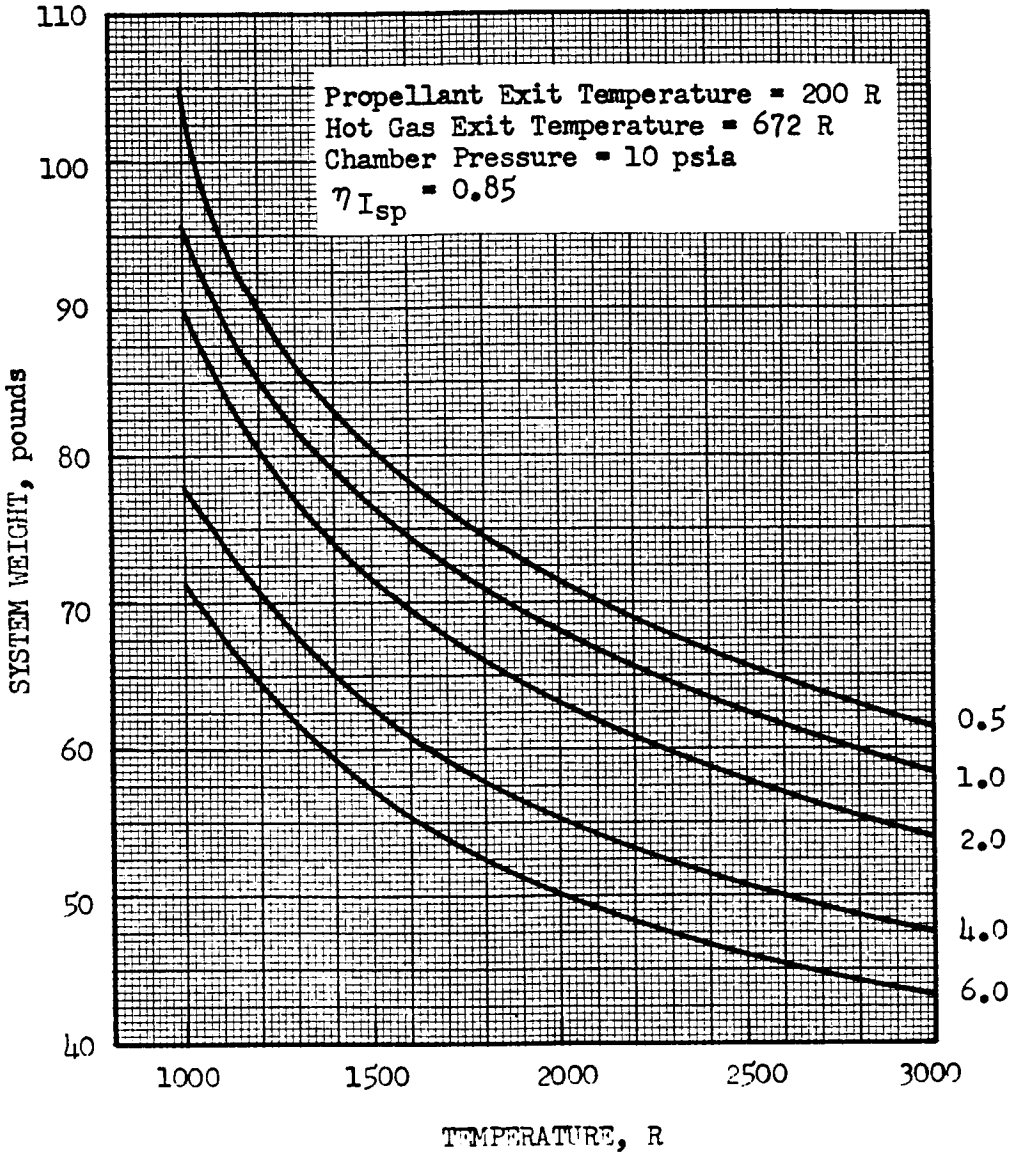

Figure 77. Variation of Heat Exchanger Conditioner Weight with Hot Gas Temperature at Heat Exchanger Inlet (System with Accumulators)

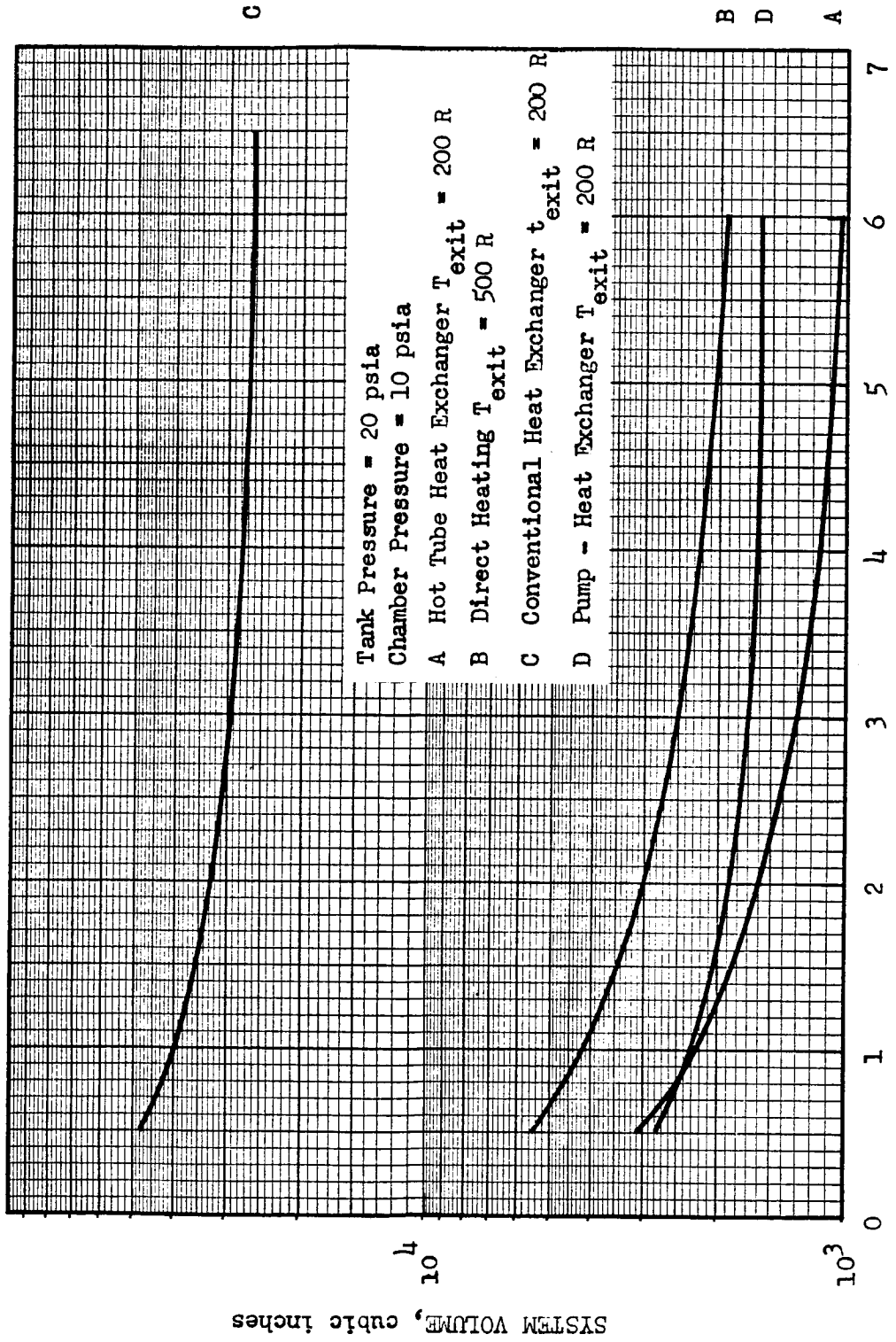

Figure 78. Comparison of System Volume for Four Conditioner Concepts

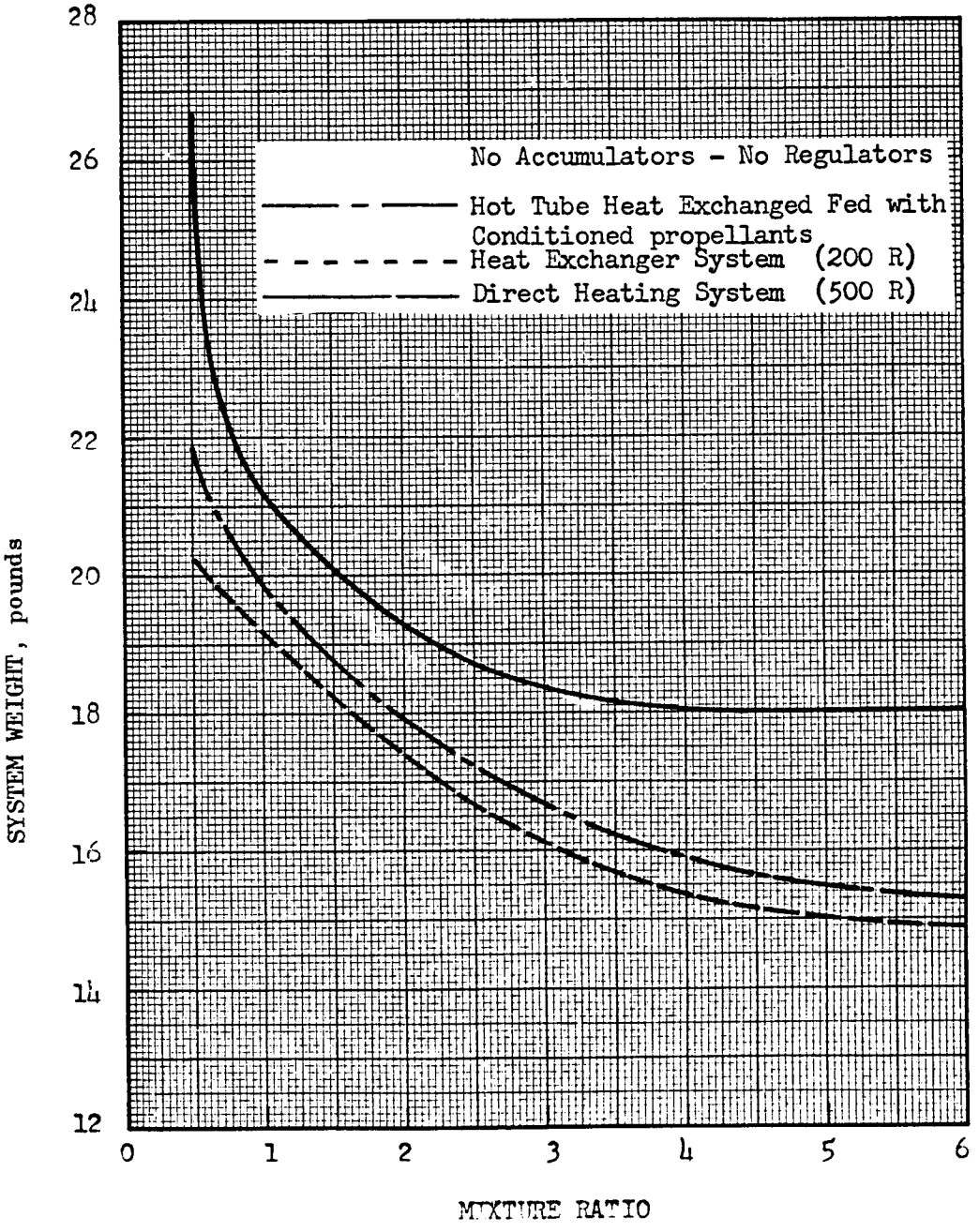

Figure 79. System Weight Comparison for a Steady State Propellant Conditioner

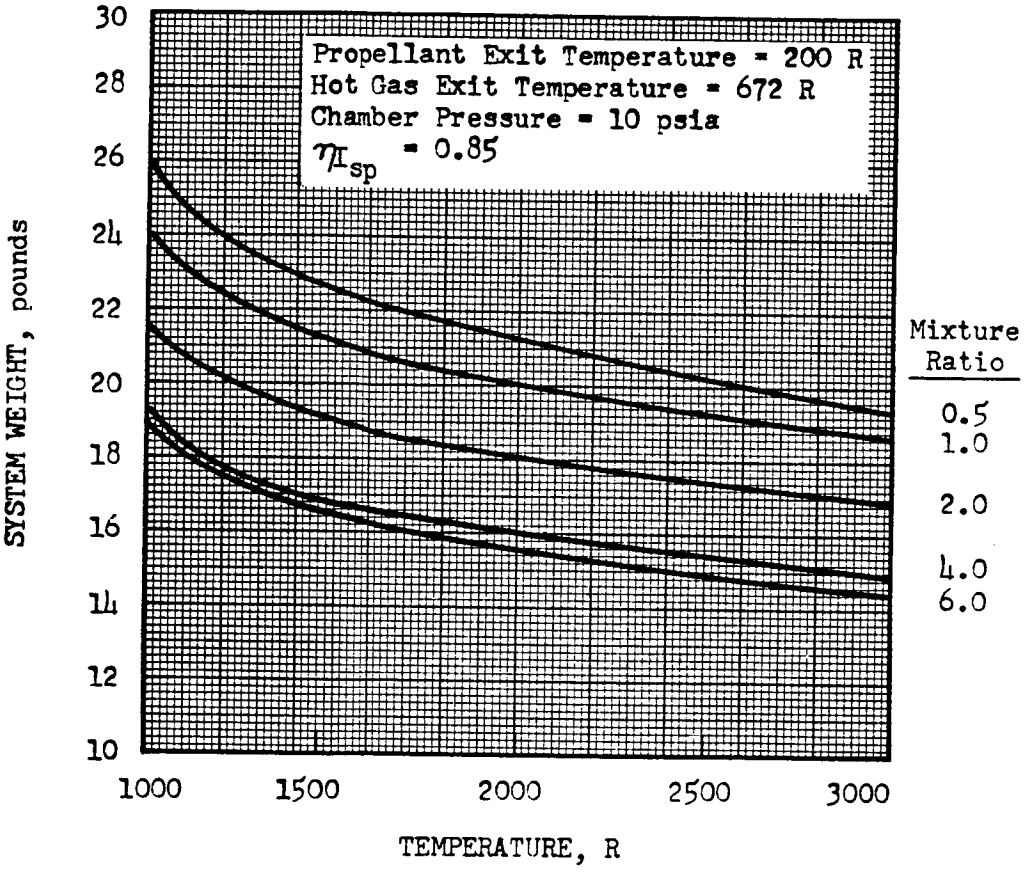

Figure 80. Variation of Heat Exchanger Conditioner Weight with Hot Gas Inlet Temperature (System without Accumulators)

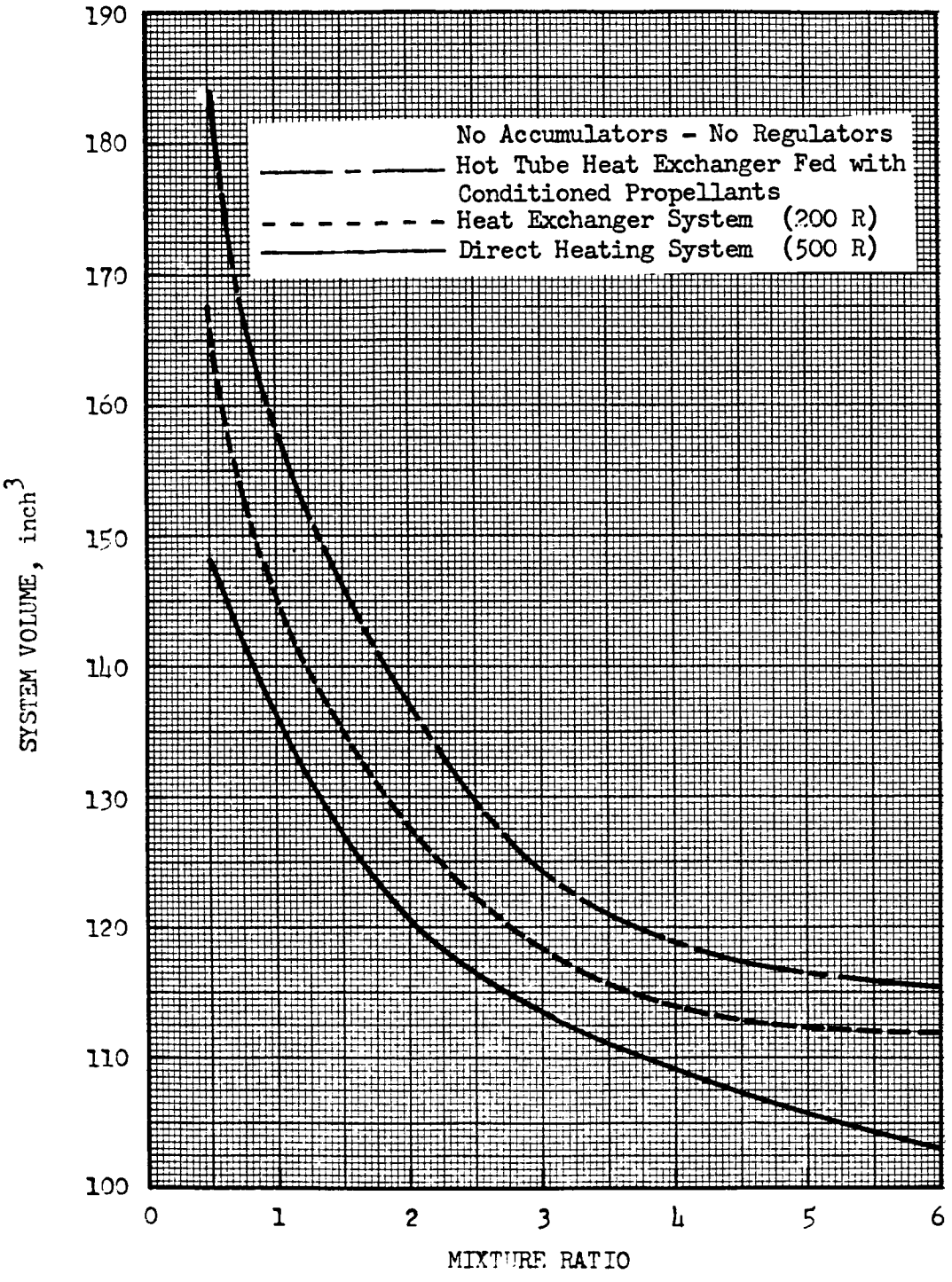

Figure 81. System Volume Comparison for a Steady State Propellant Conditioner

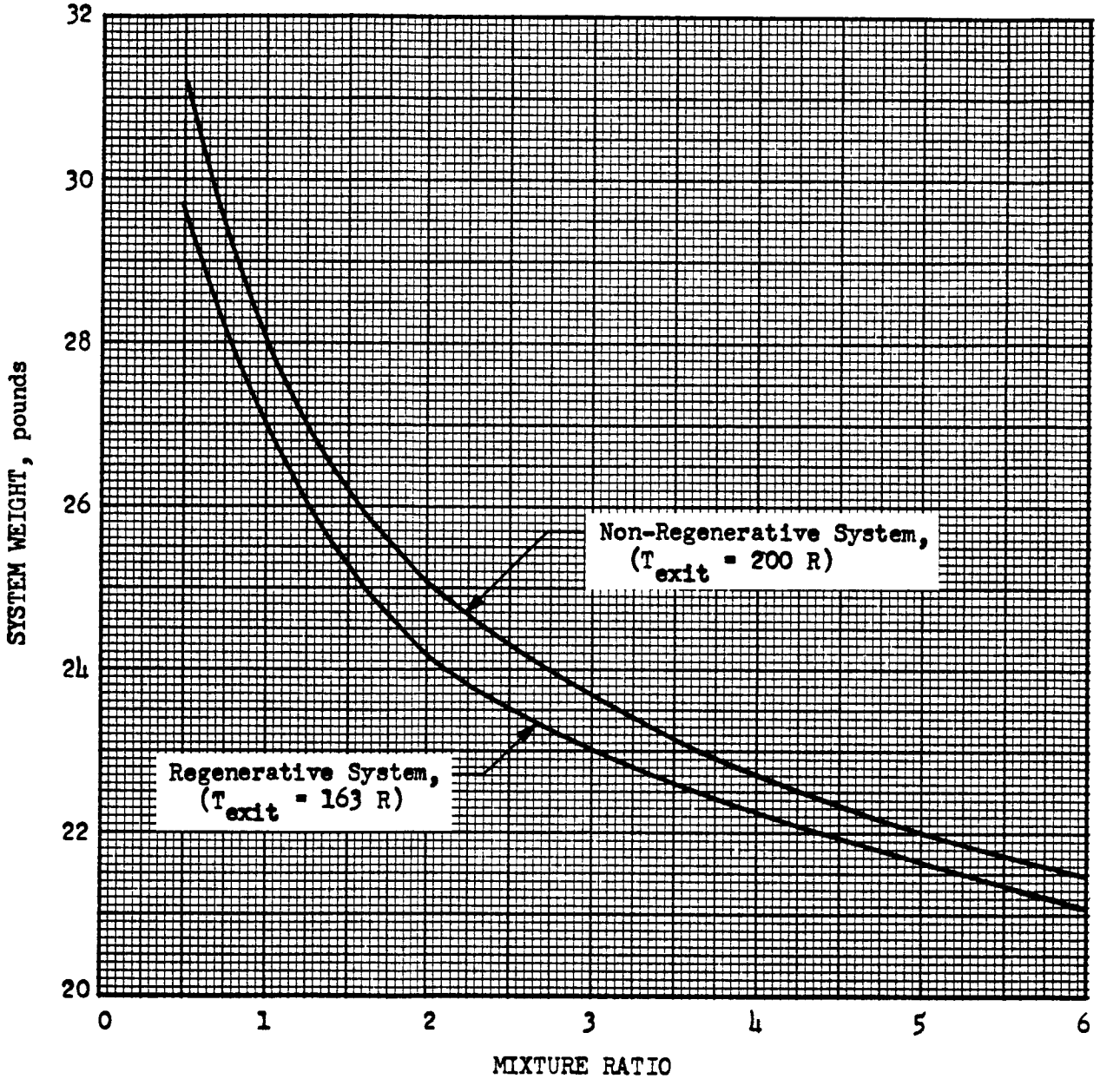

Figure 32. Weight Savings Resulting from a Combined Regenerative-Hot Tube Heat Exchanger Conditioning System

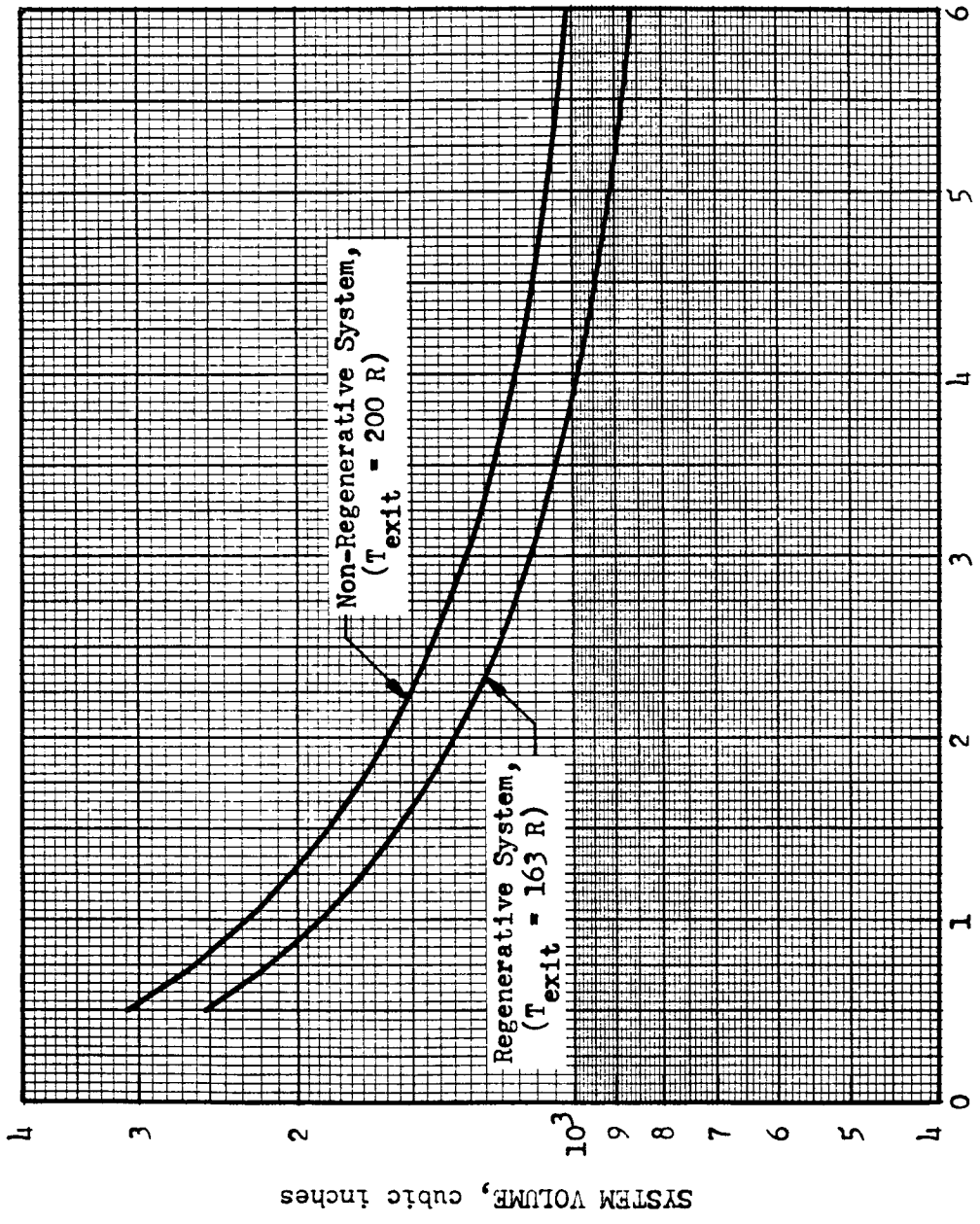

Figure 83. Volume Savings Resulting from a Combined Regenerative-Hot Tube Heat Exchanger Conditioning System

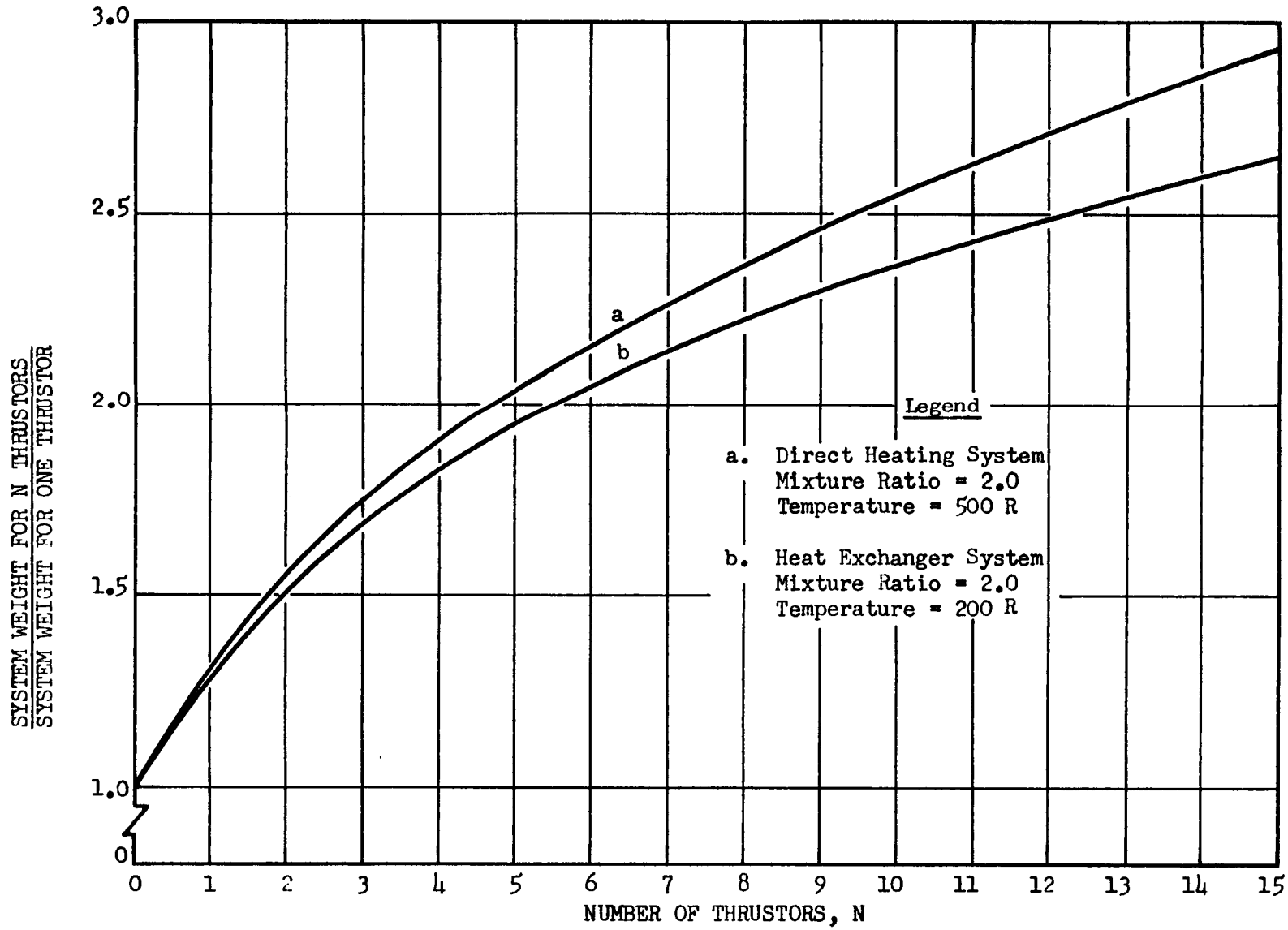

Figure 84. Weight Ratio of Valves and Catalyst Packs for Systems with Multiple Thrustors

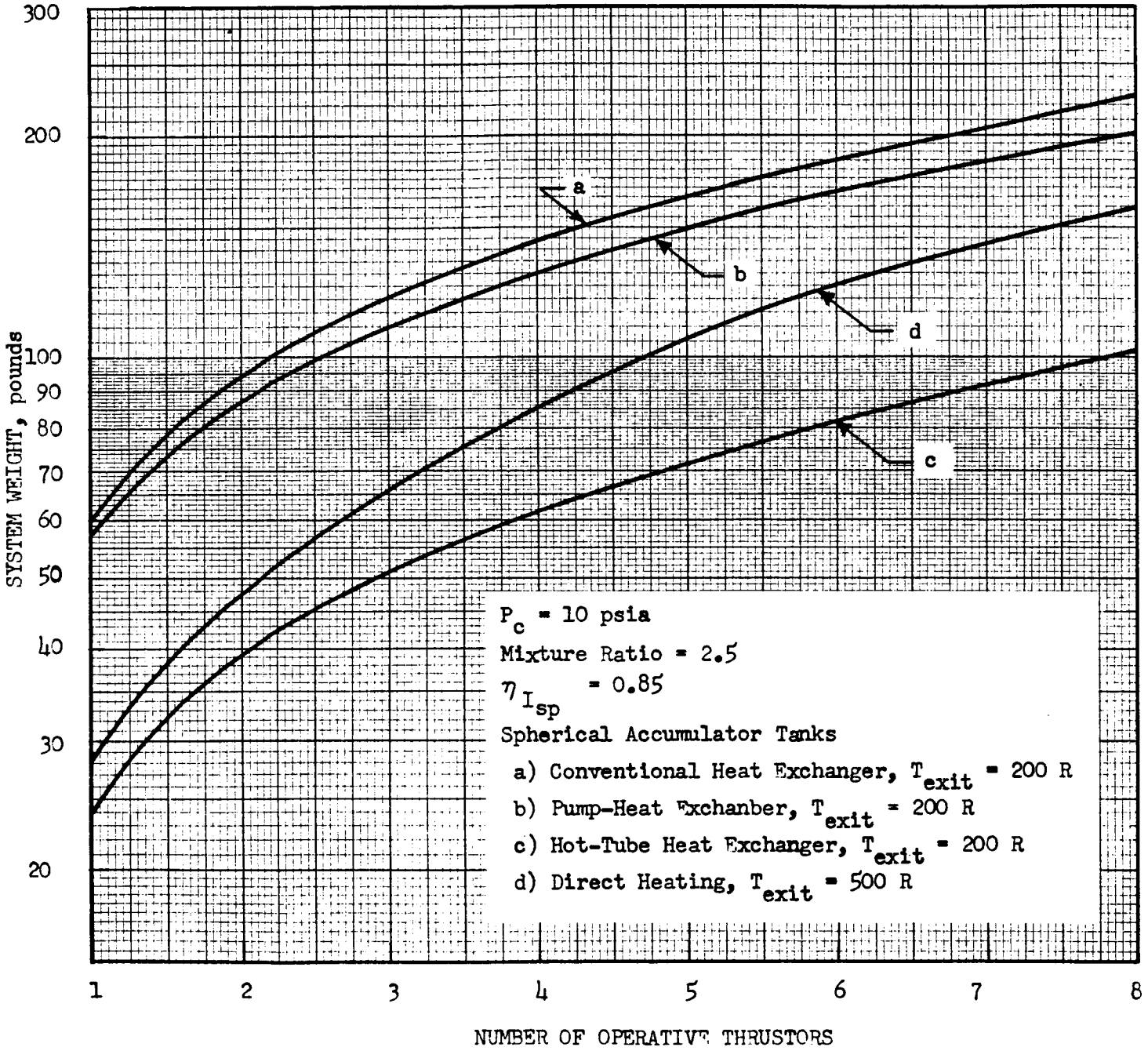

Figure 85. The Effect of the Number of Thrustors Per Module on System Weight

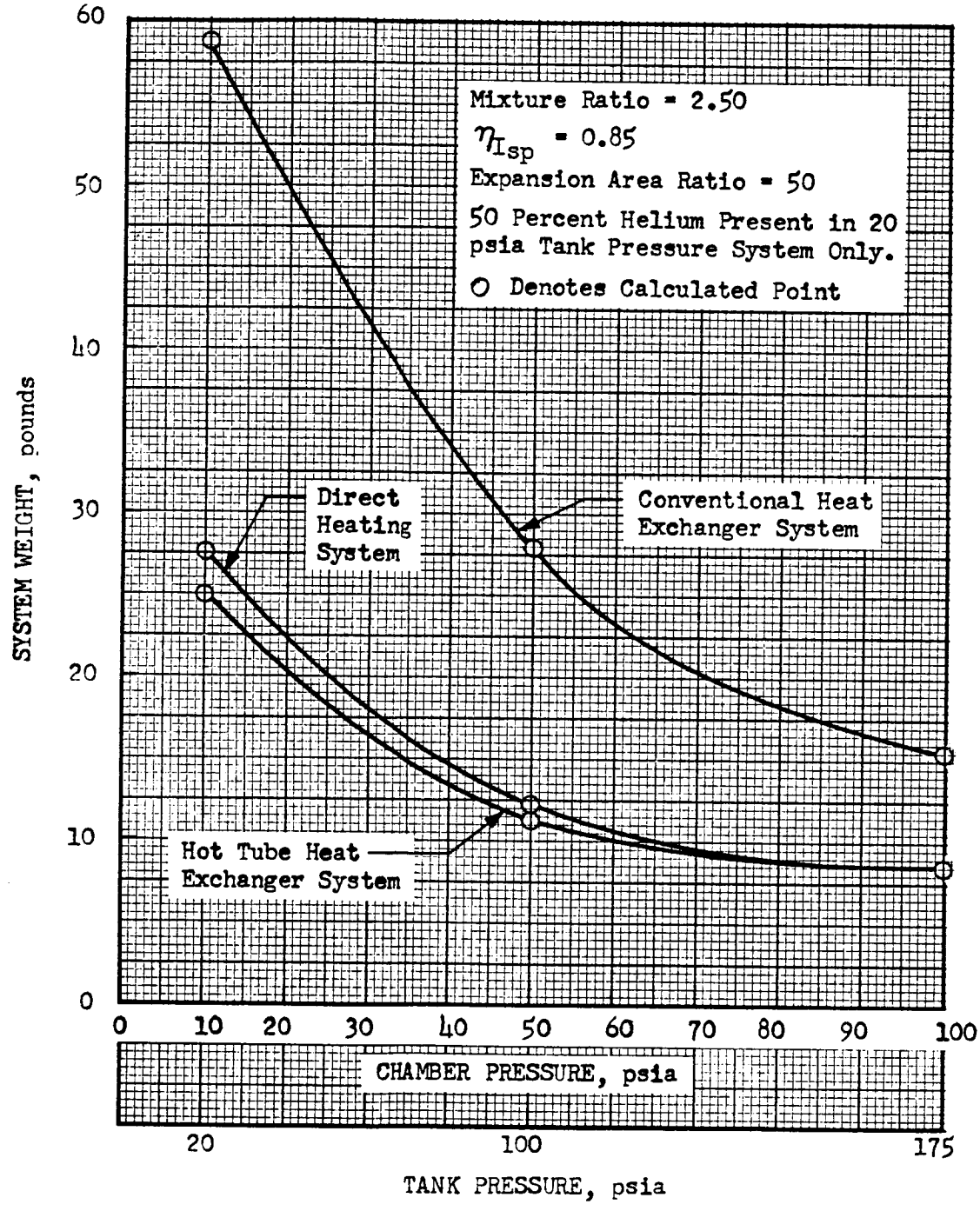

Figure 86. Effect of Pressure on Propellant Conditioner System Weight

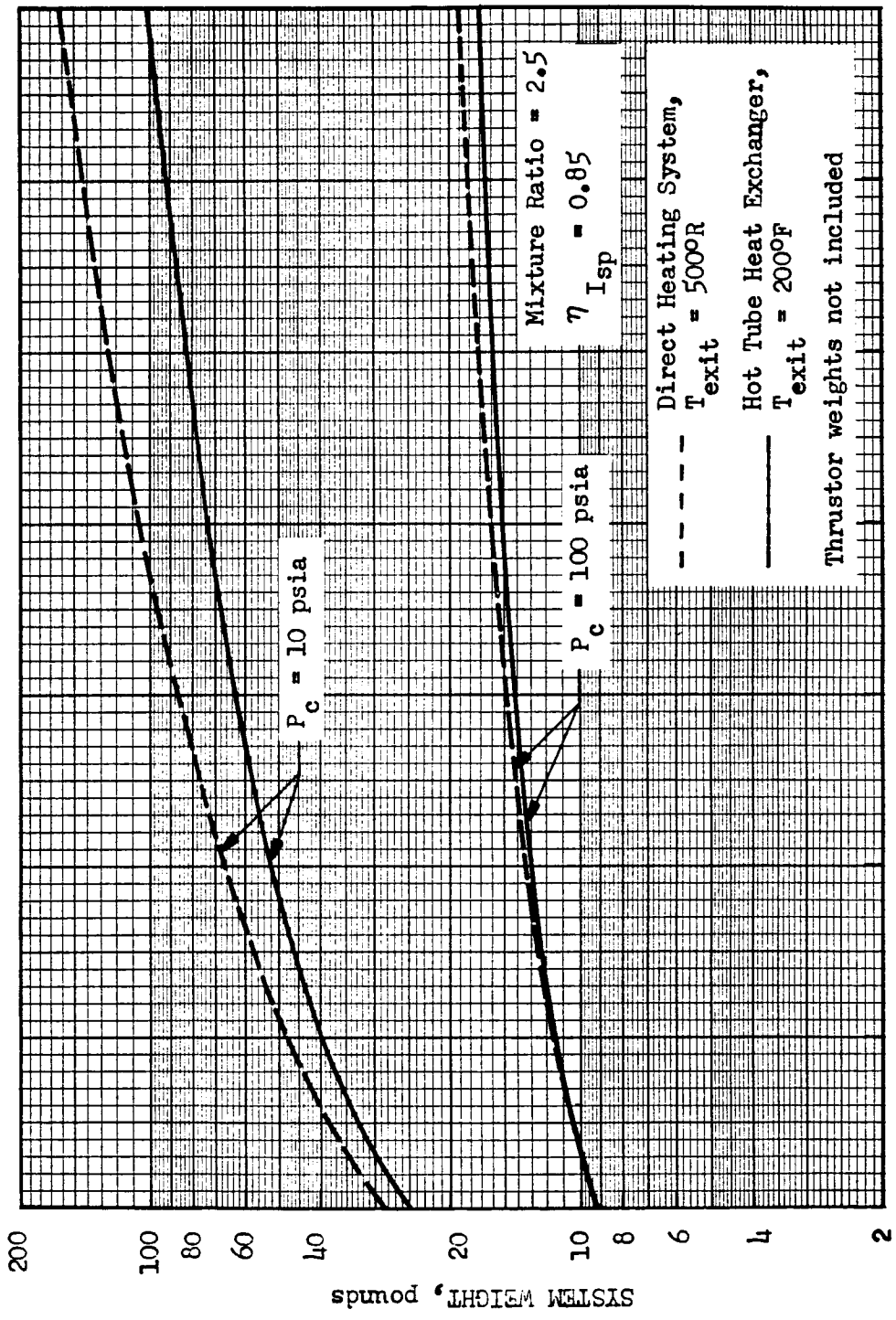

Figure 87. The Effect of the Number of Thrustors per Conditioner on System Weight for Two Conditioner Concepts and Two Pressure Levels (10 and 100 psia)

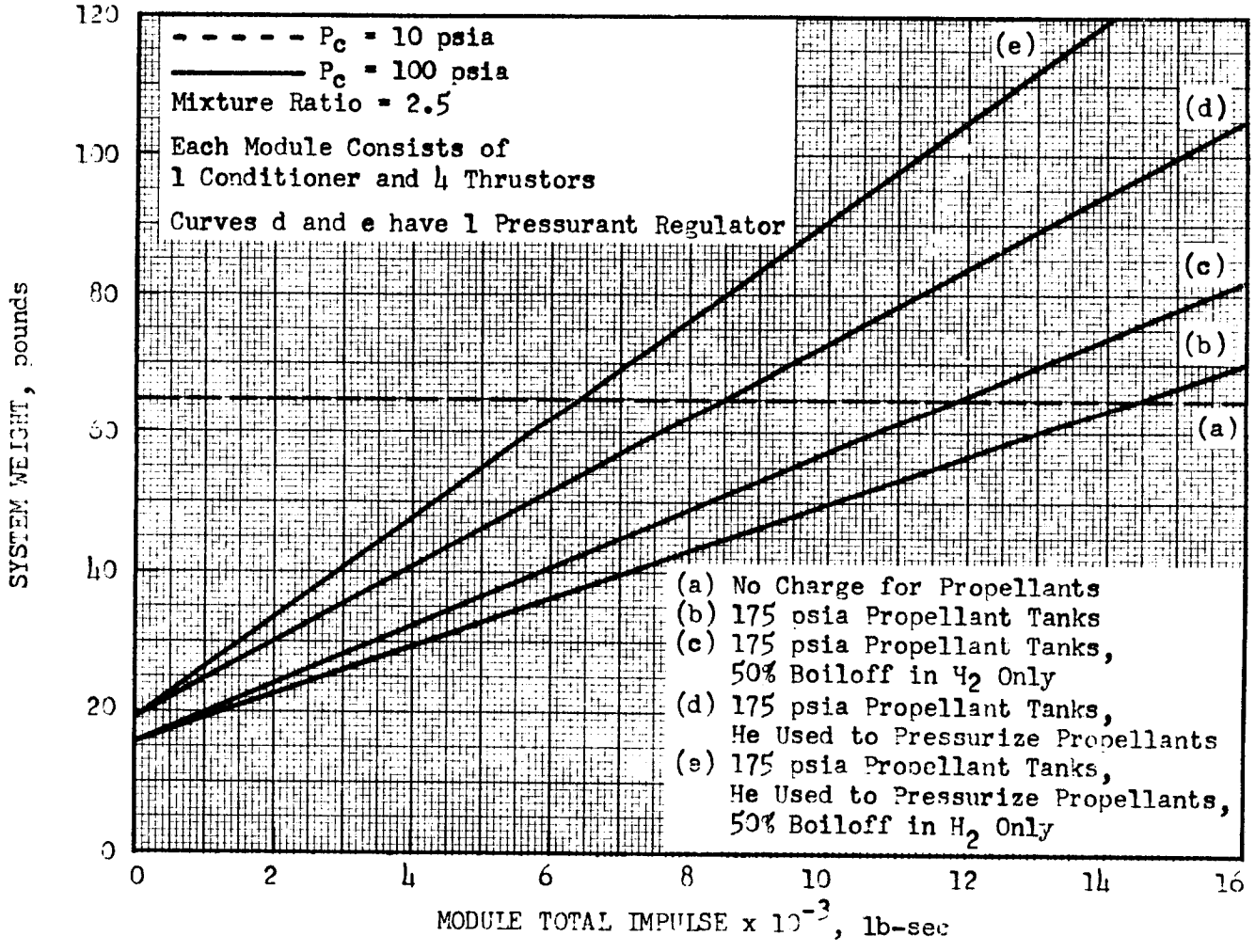

Figure 88. Low Pressure and High Pressure Module Weight Comparison for a Hot Tube Heat Exchanger Concept

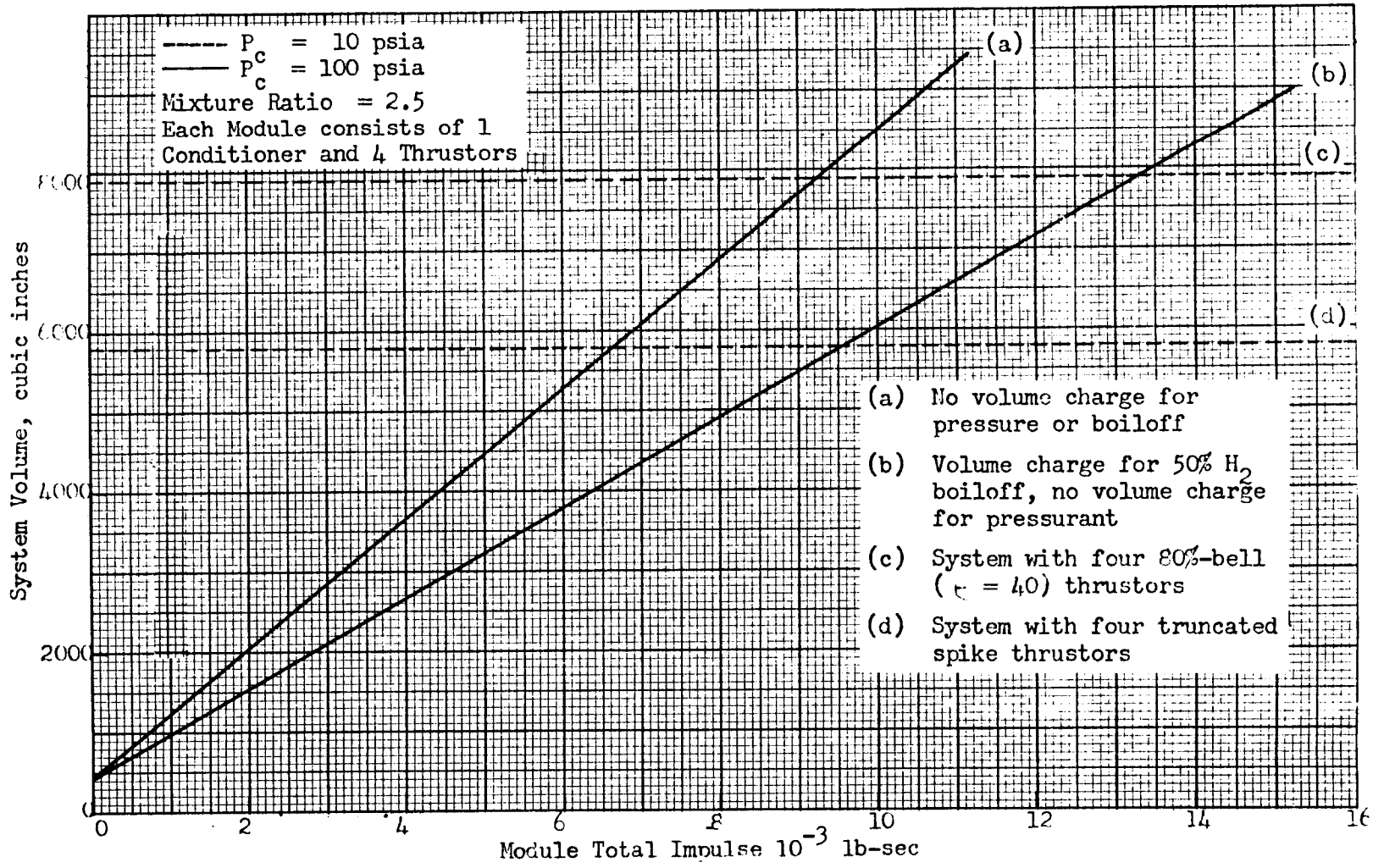

Figure 89. Low Pressure and High Pressure Module Volume Comparison for a Hot Tube Heat Exchanger Concept

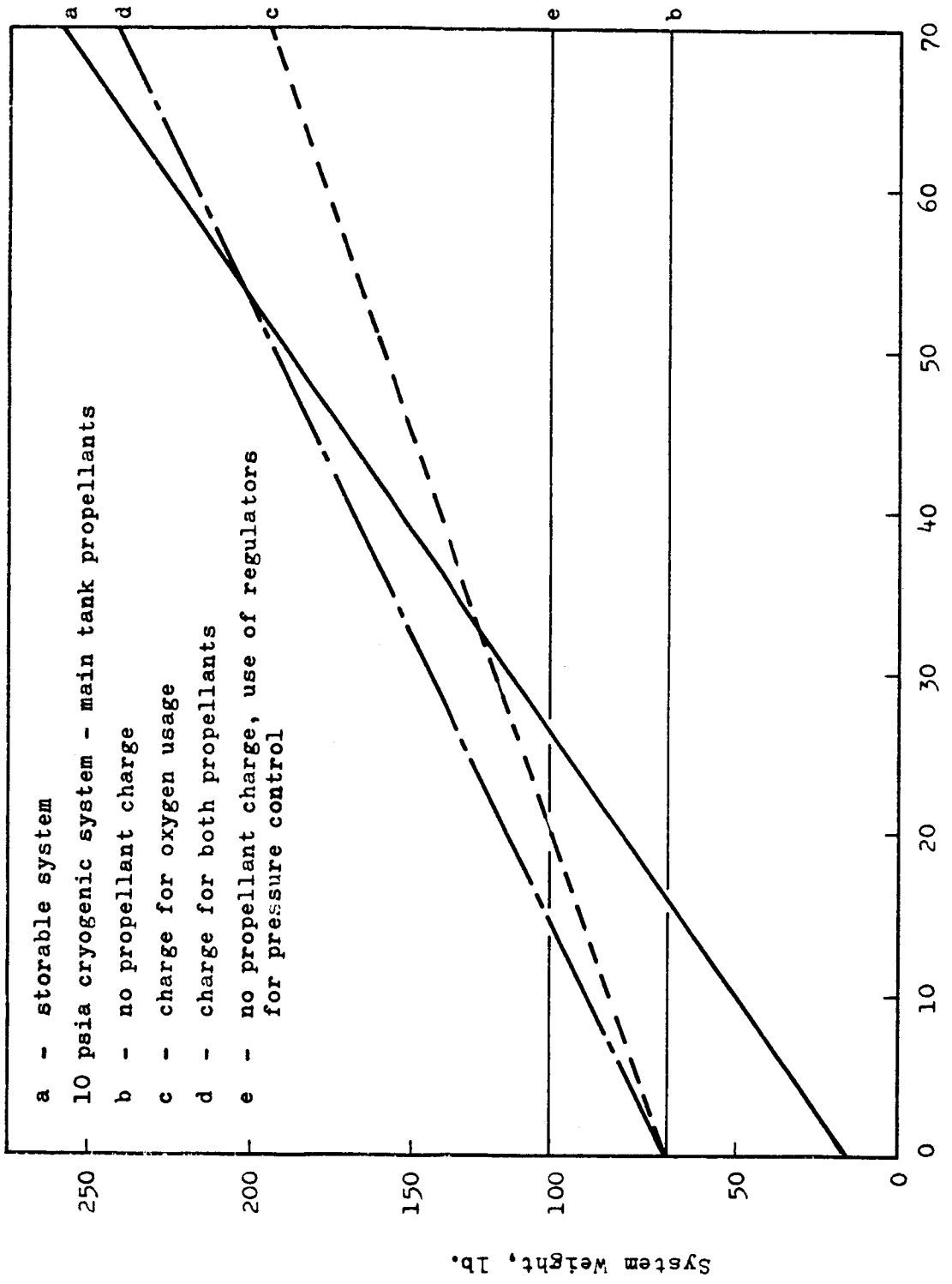

Figure 90. Comparison of System Weight (Module for 4 Thrustors) for a Storable (NTO-MMH) RCS With a Low Pressure Cryogenic (O_2-H_2) RCS Utilizing Main Tank Propellants (Conditioned Propellant Temperature of 200 R)

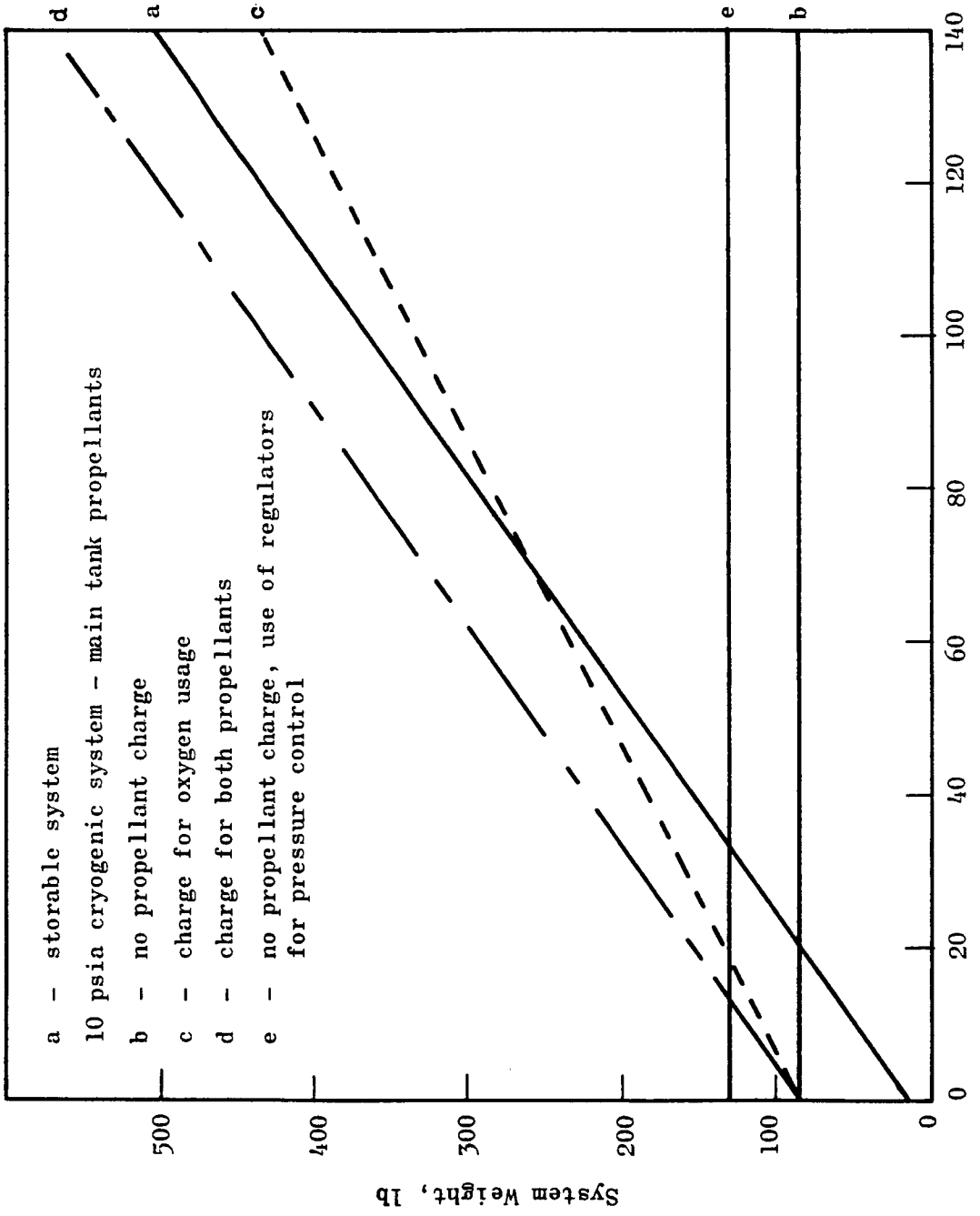

Figure 91. Comparison of System Weight (Module for 4 Thrustors) for a Storable (NTO-MMH) RCS With a Low Pressure Cryogenic (O_2-H_2) RCS Utilizing Main Tank Propellants (Conditioned Propellant Temperature of 400 R)

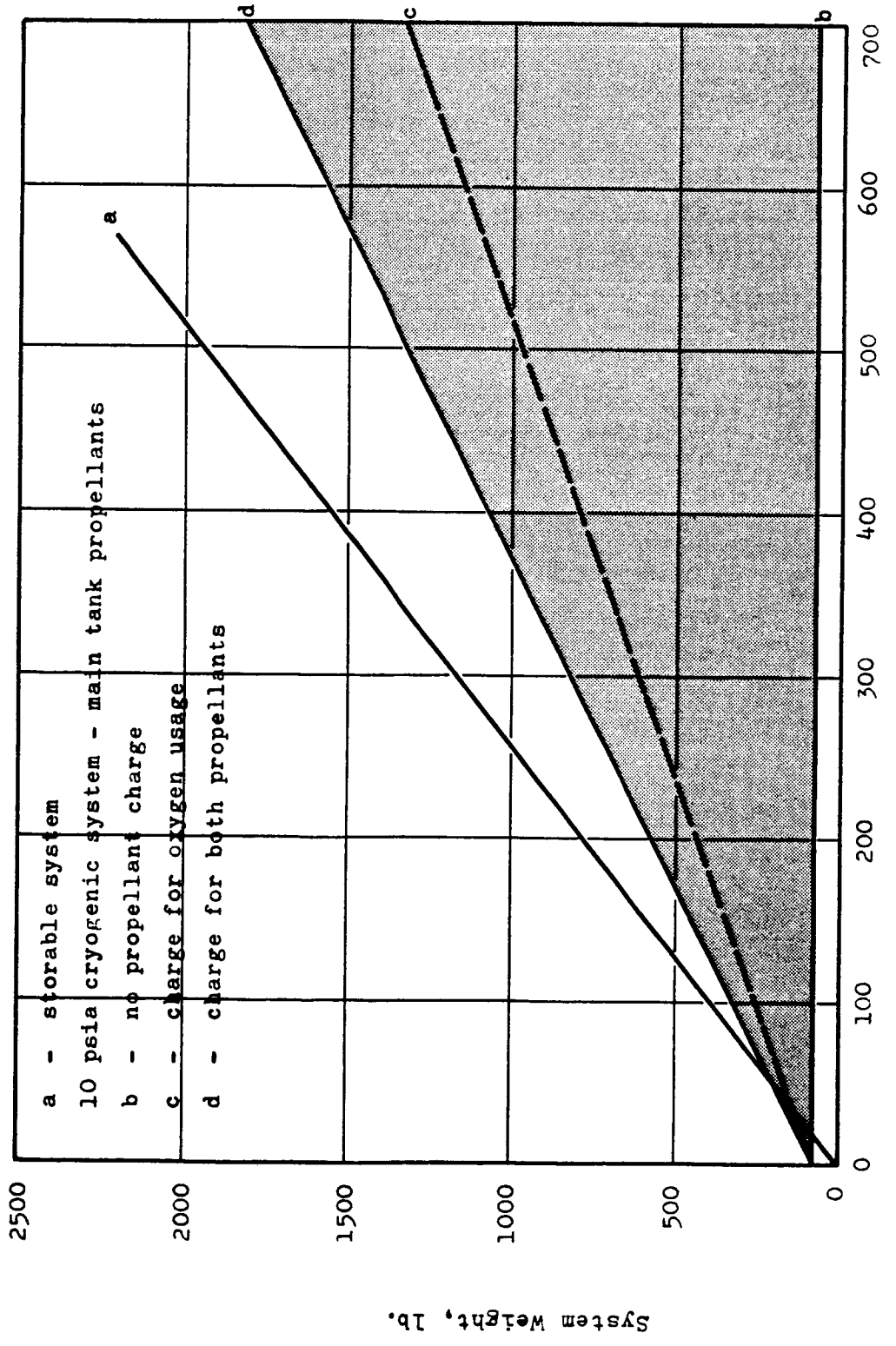

Figure 92. Comparison of System Weight (Module of 4 Thrustors) at Large Total Impulses for a Storable (NTO-MMH) RCS With a Low Pressure Cryogenic (O_2-H_2) RCS Utilizing Main Tank Propellants (Conditioned Propellant Temperature of 200 R)

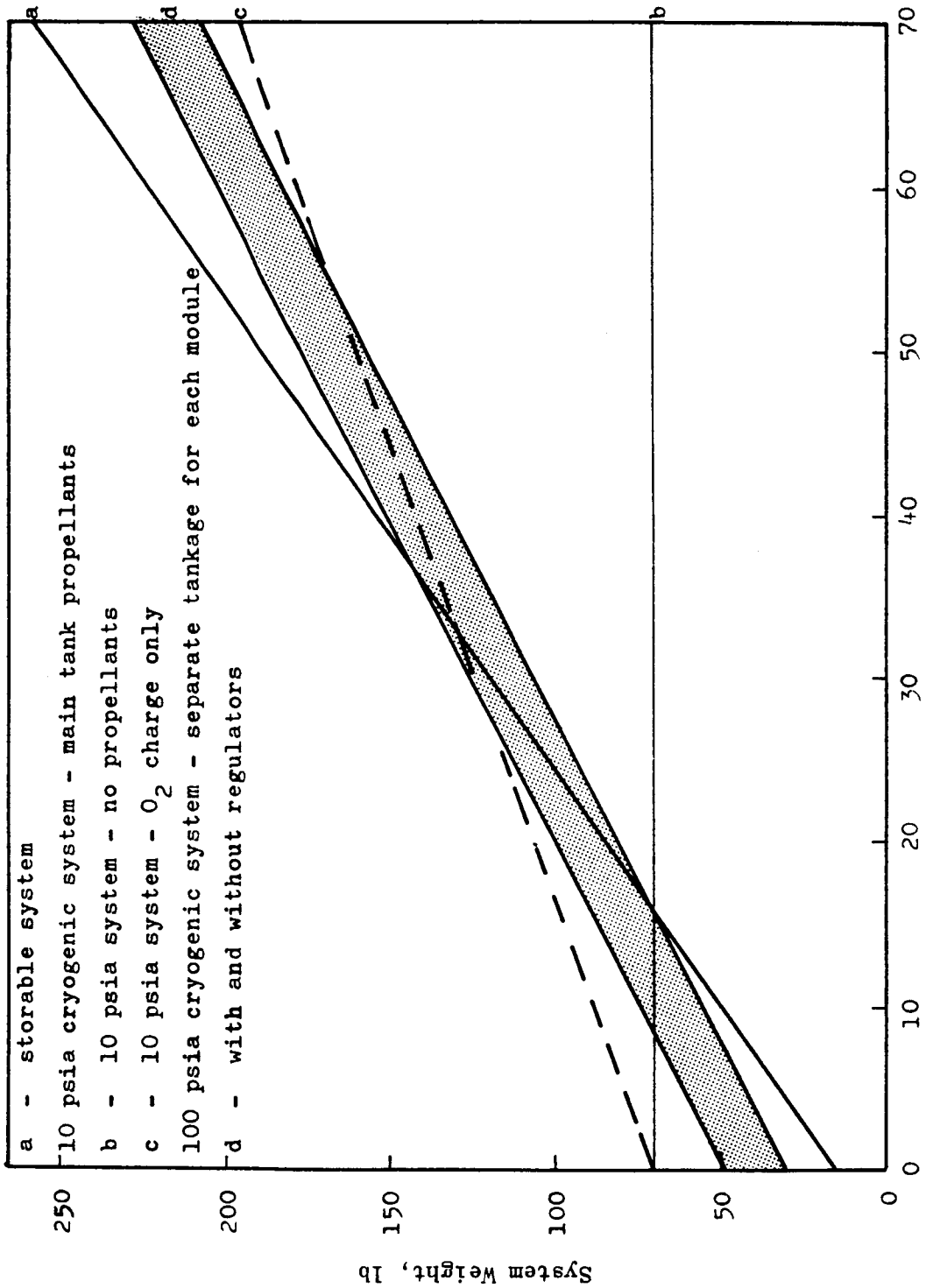

Figure 92. Comparison of System Weight (Module of 4 Thrustors) for a Storable RCS with Two Cryogenic Systems (Conditioned Propellant Temperature of 200 R)

SYSTEM ANALYSIS AND SIMULATION

The program objectives of maximum response and repeatability, as well as the unknown nature of the possible problem areas associated with the system, made necessary more detailed analyses of the individual components and component interactions. This was accomplished prior to the experimental work and was utilized in final component design and in the selection of control devices.

The analysis effort was complicated by the complexity of the dynamic interaction between components and, at least initially, by unknowns in the component operational characteristics. The approach was to model each component in terms of mass and material balances and transfer processes, to translate this model into a computer subprogram, and then to combine subprograms as necessary to simulate subsystem or system operation.

The overall system simulation was used to predict the operating characteristics of the system and the degree of component interaction. In addition, the adequacy of the control system was evaluated. The component subprograms were used to determine the effects of design parameters and system operating parameters (temperature and pressure) on operating characteristics. The thrustor model was also used to predict transient and pulse-mode operating characteristics.

THRUSTOR SIMULATION

A mathematical model of the catalytic thrustor was formulated and programmed for computer simulation. Primarily, the computer model was used to demonstrate the system operating characteristics including both transient and steady-state operation. Cause and effect relation-

ships were determined by varying the design parameters and observing changes in system operation. The effects of changes at the interface with the conditioner (propellant temperature and pressure) were also evaluated.

Description of the Thrustor Model

The computer model is made up of fluid resistive elements to simulate pressure drop, fluid capacitive elements to simulate the storage of mass, and thermal capacitive elements to simulate the storage of heat energy. These elements are linked together in a network of equations with appropriate control elements and program logic to form a model of the above system. Function generators have been added to simulate the variation of accumulator pressures and to simulate the thrustor duty cycle. One assumption implicit in the model is that chemical reaction does not control the response and/or the steady-state operation of the thrustor. This assumption was extrapolated from the higher pressure results from Ref. 2.

The model is non-linear and uses lumped parameters. The catalyst bed model is multi-nodal and describes variable reaction, temperature, and pressure along the bed length.

A typical thrustor is illustrated in Fig. 94. A corresponding computer model schematic is shown in Fig. 95. Note that there is an optional bypass upstream of the injector for both oxygen and hydrogen. The oxygen bypass represent downstream injection whereas the hydrogen bypass can be used to simulate the flow for regenerative or film cooling of the chamber. In some cases, it is of interest to have no propellant bypass.

The computer model is a mathematical description of mass and energy flow and storage as well as the combustion process in the thrustor system coupled with computer logic to simulate its operation. The model is capable of depicting the effects of varying system parameters such as: the inlet pressures and temperatures, steady-state pressure drops throughout the system, volumes, valve opening times, valve sequencing, catalyst bed heat capacity and initial temperature, steady-state catalyst bed temperature distribution, steady-state propellant flowrates, and thrustor duty cycle. The computer program sizes the system on the basis of given steady-state operating parameters and then determines the system pressures, temperatures, and flowrates as functions of time for a specified duty cycle. Both a graphical and numerical output are produced.

The equations used to formulate the model are presented on the following pages.

Inlet Pressure Function Generators. The oxidizer inlet pressure is described by:

$$P_o' = P_o + B_o \sin\{2\pi f_o (t - t_o)\} \tag{38-a}$$

or

$$P_o' = P_o\left(1 - \exp\{-t/a_o\}\right) \tag{38-b}$$

The fuel inlet pressure is similarly described:

$$P_h' = P_h + B_h \sin\{2\pi f_h (t - t_h)\} \tag{39-a}$$

or

$$P_h' = P_h\left(1 - \exp\{-t/a_h\}\right) \tag{39-b}$$

By setting the amplitude of the a.c. component of the sinusoidal function to zero, a constant inlet pressure is obtained.

Valve Flow Rate Descriptions. The oxidizer flow through the propellant valve is determined by:

$$\dot{W}_o = C_o A_o Y_o \left\{2g\rho_{oi}(P_{oi} - P_{ol})\right\}^{1/2} \tag{40}$$

This equation is modified such that:

$$P_{ol} \geq (r_c) P_{oi} \tag{41}$$

so that the sonic flowrate cannot be exceeded. Any pressure drop due to line friction is considered lumped with the valve.

The hydrogen flow through the propellant valve is similarly:

$$\dot{W}_h = C_h A_h Y_h \left\{2g\rho_{hi}(P_{hi} - P_{hl})\right\}^{1/2} \tag{42}$$

Line Pressure Description. The pressure in the oxygen line is:

$$P_{o\ell} = (R_o T_o / V_{o\ell}) \int (\dot{W}_o - \dot{W}_{o1} - \dot{W}_{o2})\, dt \qquad (43)$$

The pressure in the hydrogen line is similarly:

$$P_{h\ell} = (R_h T_h / V_{h\ell}) \int (\dot{W}_h - \dot{W}_{h1} - \dot{W}_{h2})\, dt \qquad (44)$$

Line Flow Rate Description. The oxygen flow to the injector is:

$$\dot{W}_{o1} = C_{o1} A_{o1} Y_{o1} \left\{ 2 g \rho_{o1} (P_{o1} - P_c) \right\}^{1/2} \qquad (45)$$

The hydrogen flow to the injector is similarly:

$$\dot{W}_{h1} = C_{h1} A_{h1} Y_{h1} \left\{ 2 g \rho_{h1} (P_{h1} - P_c) \right\}^{1/2} \qquad (46)$$

Injector Storage and Mixing Description. The weight of propellant in the injector is:

$$W_i = \int \left\{ \left(\dot{W}_{o1} - \frac{MR_i}{1+MR_i} \dot{W}_m \right) + \left(\dot{W}_{h1} - \frac{\dot{W}_m}{1+MR_i} \right) \right\} dt \qquad (47)$$

The temperature of the propellant mixture in the pre-mix volume is:

$$T_i = \left\{ \int \left(\dot{W}_{o1} c_{p_{o1}} T_{o1} + \dot{W}_{h1} c_{p_{h1}} T_{h1} - \dot{W}_m c_{p_i} T_i \right) dt \right\} / W_i c_{p_i} \qquad (48)$$

Catalyst Bed and Mixer Parameter Descriptions. The pressure in the mixer volume is:

$$P_i = W_i R_i T_i / V_i \qquad (49)$$

The flow to the mixer is:

$$\dot{W}_m = C_m A_m Y_m \left\{ 2 g \rho_i (P_i - P_m) \right\}^{1/2} \quad (50)$$

The pressure in the mixer section is:

$$P_m = (R T_c / V_m) \quad (51)$$

The flow through the catalyst bed is based on an average density through the bed:

$$\dot{W}_b = C_b A_b \left\{ 2 g \rho_b (P_m - P_c) \right\}^{1/2} \quad (52)$$

The temperature and pressure distribution through the bed is prescribed.

Chamber Parameter Description. The chamber pressure is obtained from:

$$P_c = \int (R T_c / V_c)(\dot{W}_L + \dot{W}_{o_2} + \dot{W}_{h_2} - \dot{W}_n)\, dt \quad (53)$$

The combustion temperature is computed as a function of chamber mixture ratio and then adjusted for the heat lost to the catalyst bed.

$$T_c = f(MR) - Q_b / (c_{p_L} \dot{W}_L + c_{p_2} \dot{W}_{o_2} + c_{p_h} \dot{W}_h) \quad (54)$$

The oxygen bypass flow is:

$$\dot{W}_{o_2} = C_{o_2} A_{o_2} Y_{o_2} \left\{ 2 g (P_{o_1} - P_c) \right\}^{1/2} \quad (55)$$

and the hydrogen bypass flow is:

$$\dot{W}_{h_2} = C_{h_2} A_{h_2} Y_{h_2} \left\{ 2 g (P_{h_1} - P_c) \right\}^{1/2} \quad (56)$$

The flow out of the combustion chamber is assumed sonic at all times and is described by:

$$\dot{W}_n = \frac{P_c A_t g}{\sqrt{K_c g R_c T_c}} \sqrt{\left(\frac{2}{K+1}\right)^{\frac{K+1}{K-1}}} \qquad (57)$$

Thrust is obtained by:

$$F = P_c A_t (C_f) \qquad (57\text{-a})$$

where

$$C_f = f(MR) \qquad (57\text{-b})$$

Sequence of Computer Logic

The computer program can be broken down into a number of sub-sections: input, computation of system constants, setting of initial conditions, main program computation and logic time sequencing, and output. Feeding the main program computation section are various subroutines which represent system components. The input and output parameters are presented in Table 20.

The system constants are based on the input data relating to steady state information. The most significant of these are the various component flow areas and the percent reaction at each node through the catalyst bed. Except for the initial mixer and propellant bed temperatures, all initial conditions are set to zero.

The main program computation and logic is briefly described by the chart in Figure 96. A time sequencing section merely increments time

at each pass through through the computation. In addition, printing and plotting indicator variables are sequenced. The output section stores the results in computer memory and at the proper time, as noted by the indicator variables, prints and plots the data.

Effect of Feed Perturbations on
Thrustor Operation

The thrustor performance variation (ΔF) and the fluctuation in catalyst bed temperature are a function of changes in propellant inlet pressure and temperature from nominal design. Variations in the propellant inlet condition are governed by pressure and temperature design tolerances of the conditioning system.

Operation of the selected conditioner concept calls for on-off operation controlled by sensing the accumulator pressure; on at 16.0 psia, off at 17.5 psia. For a subsystem with an accumulator volume of 1200 cubic inches, a steady-state thrustor demand should impose a conditioner operating cycle at a frequency of approximately 10 to 20 cps. It is necessary to determine the effect of a worst case perturbation on thrustor performance characteristics. A worst case condition results when the highest O_2 density couples with the lowest H_2 density or vice versa. More specifically, the worst case is defined as one propellant inlet pressure at 17.5 psia (the accumulator relief pressure), and the other inlet pressure at the given minimum pressure. Similarly, the inlet temperatures are such that the lower temperature propellant is that at the higher pressure. For example, if the minimum pressure is 15 psia at the oxygen inlet and the temperature band is $\pm$ 20 R, the inlet conditions would be 15 psia and 220 R at the oxidizer inlet and 17.5 psia and 180 R at the hydrogen inlet.

These steady-state pressure and temperature perturbations were fed into the thrustor computer model and the changes in catalyst bed temperature and thrust were determined.

Two nominal inlet pressures; 17 and 20 psia, and an overshoot of 0.5 psia were considered. Thus, maximum pressures of 17.5 and 20.5 psia were selected. The effects of deviations in the other inlet pressures for both oxidizer- and fuel-rich conditions were determined. Also, by changing injector pressure drops, several values of catalyst bed pressure drops were considered. An adverse temperature deviation of ±20 R on each propellant was also imposed such that the density deviations were amplified.

The change in catalyst bed temperature from the nominal design of 2000 R for a thrustor with downstream injection of oxygen is shown in Fig. 97 as a function of the deviation in inlet pressure. To illustrate, the parameters for the two upper middle curves are:

1. $\Delta P_{cat} = 2.0$
2. O_2 inlet pressure = 17.5 psia for solid and 20.5 for dashed lines
3. O_2 inlet temperature = 180 R
4. H_2 inlet temperature = 220 R

As the H_2 inlet pressure is reduced from nominal, the H_2 flow decreases causing the mixture ratio and consequently the bed temperature to increase. The extreme lefthand point considered the worst oxidizer-

rich case since the highest O_2 pressure and lowest O_2 temperature are coupled with the lowest H_2 pressure and highest H_2 temperature, thus giving the highest MR change.

For the bottom set of curves, the temperature deadband has been reversed and the H_2 inlet pressure has been set at 17.5 psia while the O_2 pressure has been varied, thus illustrating the fuel-rich case.

It can be concluded from Fig. 97 that catalyst bed pressure drop has a most pronounced effect on catalyst bed combustion temperature. As the nominal design pressure drop across the catalyst bed is increased, the allowable nominal pressure drop across the injector face decreases. For example, when the ΔP_{cat} is 4.0, the nominal pressure drop across the injector face is 3.0 psi. When the hydrogen inlet pressure is decreased to 15.0 psia, the hydrogen ΔP across the injector face is decreased to about 1 psi or by a factor of 3. Thus, the net effect of a large ΔP_{cat} is to choke off the flow of the lowest pressure propellant and thus cause large variations in the catalyst bed combustion temperature.

The net effect of increasing the nominal pressure to 20 psia is to attenuate the shift in combustion temperature with ΔP_{cat}.

Hand calculations were made for the case of $\Delta P_{cat} = 0$ for a nominal pressure of 17.0. The computer curves seem to approach this limit as ΔP_{cat} is lowered, thus the results are deemed in agreement.

The effect of temperature deadband of ± 20 can be isolated from inlet pressure variations by noting the righthand point where propellant pressures are equal. It can be concluded that shifts in propellant inlet temperatures are less important than shifts in propellant inlet pressure.

Figure 98 shows how the thrust varies as a function of the same inlet perturbation and parameters as used in the previous example. In this case the O_2 bypass valve was programmed to close when the catalyst bed temperature decreased 500 R from nominal. This causes the discontinuity in the lower fuel-rich thrust curves of Figure 98.

The thrust variation curves for the oxidizer-rich case (upper curves) appear to be relatively insensitive to hydrogen inlet pressure. These curves are displaced a horizontal distance of about 0.05 which indicated that the temperature deadband of ± 20 R is the controlling factor. The reverse is true for the lower curves.

Changes in catalyst bed temperature for full flow (nominal bed temperature 4000 R) as a function of inlet propellant perturbations (Fig. 99) have not been fully investigated. But, the results are similar to those shown in Figure 99 for the downstream injection case with the exception that the swings in temperature for a given perturbation are larger for full flow. The relationship for a perturbed mixture ratio (for no catalyst bed pressure drop)

$$MR = \frac{P_{O_2 \text{ inlet}}}{P_{H_2 \text{ inlet}}} \sqrt{\frac{T \text{ inlet } H_2}{T \text{ inlet } O_2}} \quad \text{(MR nominal)} \qquad (58)$$

shows that a given inlet perturbation is multiplied by the original mixture ratio. Thus, the larger the nominal mixture ratio, the larger the swings in catalyst bed temperature.

Also, the thrust variation should be the same for downstream injection and full flow for the special case of $\Delta P_{cat} = 0$. This results from the fact that the change in the combustion chamber mixture ratio for both cases is identical.

Worst Case Definition. It was noted that the previous definition of the worst case situation assumed the highest O_2 pressure (17.5 psia) and the lowest O_2 temperature (180R) are coupled with the lowest H_2 pressure (15.0 psia) and the highest H_2 temperature (270R). This may be unduly restrictive, since the accumulator pressure cycles within a deadband with a frequency near that of the pulse frequency and is not constant as previously assumed. A dynamic accumulator perturbation was studied using the most recent version of the computer thrustor model which has a sinusoidal accumulator pressure generator ($Po + \frac{\Delta P}{2} \sin 2 \pi ft$) and provisions for inserting any desired temperature gradient (or gradient in fraction of reacted propellant) across the bed. The particular input data as noted in Fig. 97 through 99 was the same as for the previous worst oxidizer-rich case so that a direct comparison could be made with the original results to check the original definition.

Fig. 100 through 102 show the pneumatic, thermal, and weight flowrates for a typical experimental thrustor being pulsed for 150 milliseconds near operating temperature. The inlet pressure frequencies are typical for accumulator designs presently being considered.

Simultaneous inspection of the three plots reveals that:

1. The pressure in the mixing zone and, less strongly, chamber pressure and thrust follow the cyclic H_2 pressure. The effect on chamber pressure and thrust results from the fact that the molal (or volumetric) flowrate ratio of hydrogen to oxygen at design conditions is 6.4. Thus, a 10- to 20-percent variation in O_2 flowrate has an insignificant effect on total molal flow.

2. When the propellant pressures are 180 degrees out-of-phase with P_{H_2} being a maximum, the P_{O_2} injector will be at a minimum of about 0.2 psia. Consequently, the O_2 flowrate cycles through a wide amplitude as shown in Fig. 101. The instantaneous combustion temperature (T_o) in Fig.102 also cycles through wide extremes.

3. The maximum increase in catalyst bed node temperatures are approximately 400R or about one-third of the increase in combustion temperature. The increase in temperature of each node is dependent upon the assumed nominal temperature, e.g., fraction reaction and the mass represented by the node. It appears that the gradient of propellant reacted through the bed is beneficial in damping out temperature swings or spreading out the increase in combustion enthalpy release.

4. The frequency of the throat flowrate corresponds to the frequency of the O_2 weight flowrate because there is nominally 2.5 times more O_2 flowing than H_2 by weight.

When these results are compared to the original results, the swings in catalyst bed temperature are shown to be significantly less than previously expected. This improvement is attributed to a better description of the system, so that the previously defined pressure band limit can be considered as quite conservative.

Simulation of Thrustor Dynamic Operation

Thrustor operation was simulated with the computer subprogram to gain insight into thrustor response characteristics (pneumatic, thermal, and thrust response) and to evaluate transient mixture ratio variations during start-up and shut-down operation.

Thrustor Response. Typical start-up pneumatic and thermal responses for a 0.525" catalyst bed are presented in Figures 103, 104, and 105. Figure 103 shows the response of the chamber, mixer section, and inlet pressures and thrust to valve actuation. The latter is indicated by changes in valve orifice area.

The inlet temperatures to the catalyst bed, T_o, and the temperatures of the five segments of the bed are depicted in Fig. 104. Each bed segment corresponds to a given length increment. For example, the first curve represents a bed of about a 2 pellet thickness, the second of 4 pellets thickness, etc. For the case of full flow, the last segment also represents the combustion chamber temperature. Instantaneous flow rates and chamber mixture ratio as functions of time are shown in the bottom chart.

To clearly understand how the thrustor performs one must interpret all three charts simultaneously rather than individually. Looking first at the left-hand side of the charts, one sees that it takes approximately 75 milliseconds for the temperature of the last node to start to rise. During this time period, the instantaneous chamber pressure, thrust, I_{sp}, and flow rates reach steady-state values indicative of cold flow.

Then as the temperature of the last node of the catalyst bed increases, chamber pressure, thrust, and I_{sp} exponentially approach their steady-state values. Since the throat will allow a higher flow rate at low temperature, or high density, than at operating temperature, the flow rates decrease to their steady-state values.

Transient M.R. Variations. Figure 105 illustrates the fuel-rich M.R. variation which occur on start up. Although not shown, the reverse is true on shut-down. The cause of this undesirable M.R. variation is the difference in the rate of filling of the O_2 and H_2 pre-injector volumes. For the filling and emptying times to be identical, the ratio of injector volumes must be the same as the ratio of the molal flow rate of propellants ($V_{H_2}/V_{O_2} = \left(\frac{1}{M.R.}\right)\left(\frac{MW_{O_2}}{MW_{H_2}}\right) = 6.4$). The example shown is for the geometry (volume ratio of 1.26) of the initial experimental thrustor. The hydrogen chamber fills and empties much more rapidly on start-up and shut-down than the oxygen chamber, thus causing the M.R. to be fuel rich on start-up and oxidizer rich on shut-down.

Two solutions to this problem were investigated. One involved valve sequencing. Even with a 100 millisecond O_2 closure lead, it was concluded that the M.R. would still go oxidizer rich on shut-down. It was further concluded that valve sequencing would not be satisfactory for pulse-mode operation.

The only feasible solution to this problem is to readjust the pre-injector volume ratio to that of the nolal flow rate ratio. This correction in the design of future thrustors is necessary for safe operation in a pulse-mode fashion.

Another undesirable feature of excess pre-injector volume is that the residual propellants must pass through the thrustor after shut-down, consequently putting a "tail" on the thrust curves. Thus, there is a great deal of incentive to keep the pre-injector volumes small as well as in the correct volume ratios.

CONDITIONER SIMULATION

The design of a system such as the conditioner subsystem requires knowledge of the dynamics of each component and the interaction between components. Also, the imposition of control on the system results in additional interaction during operation. To develop the necessary design parameters and to predict operational characteristics, a systems analysis and component modeling task was accomplished. This resulted in a computer program which could simulate the complete system or specific components.

The program consists of simultaneous equations linked by program logic to describe the processes in the conditioner as a function of time. Therefore, use of the simulation program could provide information on the system transient and steady-state operating characteristics and could relate these characteristics to specific changes or perturbations in the system. In essence, a tool was provided for demonstrating cause and effect relationships within the system.

More specifically, the program was used to accomplish the following:

1. Determine the basic operating characteristics of the system
2. Determine the appropriate type on control system:
   a. Define the controlled variables
   b. Determine parameters to be monitored
   c. Determine where and how control is to be exercised
   d. Determine control limits
   e. Determine compensating requirements and methods
3. Determine the effects on system operation caused by perturbations in tank pressure and thrustor duty cycle
4. Define the minimum accumulator volume
5. Determine specific problem areas
6. Simulate planned tests
7. Indicate the instrumentation response requirements

Details of the Conditioner Model

The computer model is a lumped, nonlinear representation system. At present, the temperature and pressure of a given component are considered as a single node with the exception of the heat exchanger, which is represented by two nodes. In a schematic of the computer model (Fig.106) the solid lines indicate fluid flow paths whereas the dotted lines indicate control pats. Each component is described by a separate subroutine and is linked by program logic. Function generators are placed at each of the system interfaces to simulate variations in interface conditions with time. A detailed description of the mathematical model is presented in the following paragraphs.

Basic Equations. The basic equations used in describing the system components are described below. These equations are then suitably combined as described later.

The low of liquid in a line is described by:

$$\Delta P = R\dot{W}^2 + L(d\dot{W}/dt) \tag{59}$$

where R is the effective resistance and L is the line inertance. The effective resistance is the ratio of the nominal resistance to the square of the nominal flowrate:

$$R = \Delta Pn/\dot{W}n^2. \tag{60}$$

The line inertance is the ratio of line length to the product of equivalent line cross-sectional area and gravitational constant:

$$L = l/gA. \tag{61}$$

The flow of liquid through a valve or orifice is described by Eq. 59 with the second term on the right hand side deleted. The flowrate is then described as:

$$\dot{W} = C_D A \left\{ 2g \rho (\Delta P) \right\}^{\frac{1}{2}} \tag{62}$$

The flow of gas through a line or valve was described as in the thrustor modeling:

$$\dot{W} = CAY \left\{ 2g \rho (\Delta P) \right\}^{\frac{1}{2}} \tag{63}$$

and inertial effects were neglected.

The weight of propellant in a component at any time was calculated from the integrated difference in flowrate in and out:

$$W = \int_{o}^{t} (\dot{W}_{in} - \dot{W}_{out})dt + W_{initial} \qquad (64)$$

A thermal balance was used to calculate the temperature of gaseous propellant in a component. The balance included heat transfer to the component:

$$W\, c_v \frac{dT}{dt} + c_p \dot{W}_{out}\, T_{out} - c_p \dot{W}_{in}\, T_{in} - q = 0 \qquad (65$$

The heat transfer to the component from the propellant was described in terms of a driving force, effective heat transfer coefficient, and exchange area:

$$q = U\, A\, \Delta T \qquad (66)$$

The effective heat transfer coefficient was dependent on the propellant flowrate and temperature. In the heat exchanger, an effect of propellant quality was also included:

$$U = f(\dot{W},\ T,\ x) \qquad (67)$$

The rate of change in component temperature was determined as the ratio of heat input to thermal capacity:

$$dT_c/dt = q/Mc \qquad (68)$$

The vaporization rate for the liquid propellant at its boiling point was described as the ratio of the heat input to the heat of vaporization:

$$\dot{W}_v = q/\lambda \tag{69}$$

The P-V-T relationship for gaseous propellant was as defined for the thrustor modeling:

$$P = WRT/V \tag{70}$$

However, for the case of combustion gases in the gas generators, both the gas constant and temperature were made functions of mixture ratio:

$$R = f(MR) \tag{71-a}$$

$$T = f(MR) \tag{71-b}$$

The venting of gas to vacuum was described as a sonic flow:

$$\dot{W} = \frac{P\ A\ C_d\ g}{\sqrt{Kg\ RT}} \sqrt{\left(\frac{2}{k+1}\right)^{\frac{K+1}{K-1}}} \tag{72}$$

Use of Equations in Computer Model. The computer model was based on the schematic shown in Fig. 106. Each component was described using the equations presented above based on this schematic. The specific combinations of equations is discussed below.

The flow of propellant from the tankage to the heat exchanger includes flow through a line and a valve. For liquid propellant, the flowrate-pressure relationship was described by Eq. 59. For gaseous propellants, Eq. 63 was used to describe the flow into the heat exchanger. In this case, the line was considered to have an appreciable volume and the net storage of mass in this volume was included in the description. The properties of the gas stored in this line (pressure and temperature)

were described using Eq. 64, 65, and 69 with the heat transfer term in Eq. 65 set at zero. The flowrate of propellant into this volume was described using Eq. 63.

The heat exchanger consists of two sides; hot and cold, modeled separately. For liquid flow to the cold side of the heat exchanger from the tankage, the amount of liquid in the heat exchanger was described as a function of the flowrate in the rate of propellant vaporization as described by Eq. 59 and 68. The properties of the gas in the cold side of the heat exchanger were described by Eq. 63 through 67 and Eq. 69.

The flow of conditioned gaseous propellant into the accumulators was by Eq. 63. The properties of the gas stored in the accumulators were described by Eq. 64, 65 and 69. The flow out the accumulator relief valve was described using Eq. 72.

The flow of propellant to the gas generators from the accumulators was considered as flow through an orifice (valve) and described by Eq. 63. The gas properties in the mixer section of the gas generator were described by Eq. 64, 65, and 69. The catalyst combustion temperature was described by Eq. 71. The catalyst bed temperature is described by:

$$Tcat - To + \frac{1}{Wc} \int_{\circ}^{\star} (Tg - Tcat)\, \dot{w}_g\, dt \qquad (73)$$

The temperature in the combustion chamber was described in Eq. 72, and the other parameters were described by Eq. 64, 65, and 69.

The flow of hot gas into the hot side of the heat exchanger from the gas generator was described by Eq. 63. The properties of this hot gas within the heat exchanger were described by Eq. 64 through 67 and 69. The venting of gas from the heat exchanger was described by Eq. 72. The temperature of the heat exchanger tube is described by Eq. 66 and 67.

Conditioner Control System. The control system is comprised of a number of control loops. The primary control variables are the accumulator pressure and temperature. If the pressure is less than the nominal pressure minus a deadband, the main propellant valve will open after an energizing delay time. If the pressure exceeds the nominal pressure plus a deadband, the main propellant valve will close after a de-energizing delay time. The temperature control loop, which is active only when there is power to the main propellant valve, causes the gas generator control valves to open if the temperature is below the nominal value minus a deadband or to close if the temperature is above the nominal value plus a deadband. In each case, the valves actuate after an energizing or de-energizing delay.

In addition, the gas generator catalyst bed temperature, gas generator combustion chamber temperature, and heat exchanger tube wall temperature are controlled. If the combustion temperature in the catalyst bed exceeds a specified temperature band during gas generator operation, the oxidizer gas generator valve closes and remains closed until the temperature drops below a specified temperature band. A similar loop controls the gas generator combustion chamber temperature.

When there is no power to the main propellant valve, the heat exchanger tube wall temperature control loop is active. If the tube temperature drops below a specified temperature band, both gas generator control valves open and remain open until the temperature band is exceeded.

Computer Input. A typical example of computer input data is presented in Table 21 for the special case of saturated O_2 vapor propellant feed to the O_2 conditioner. Important input data from Table 21 are:

1. Control points and deadbands:

   a. The accumulator set point pressure is 17.0 ± 0.5 psi. This control circuit operates the main propellant valve.

   b. The accumulator set point temperature is 200 ± 5.0 R. This control circuit turns the gas generator on or off when the main propellant feed valve is open.

   c. The tube wall set point temperature is 400 ± 120 R. This control circuit operates only when the main prepellant valve is closed and is designed to keep the tube hot during the coast model.

2. Main propellant valve delay is 0.020 second.

3. Accumulator volume is 250 cu in.

4. Thrustor duty cycle delay, frequency, and duration are 0.60 second, 1 cps, and 100 percent, respectively.

5. Thermal resistance within the heat exchanger and the tube wall heat capacity as shown in Table 21.

Simulation of Conditioner Operation

Conditioner operation is shown for the case described in Table 21. The system parameters were arbitrarily selected but are representative of typical conditioning system design for the subject program.

The valve, temperature, pressure, and weight response for this case are illustrated in Fig.107 through 110. The sequence of operation is approximately:

1. Initial wall temperature is low, causing the gas generator to turn on (Fig. 107), thus causing the wall temperature to increase.

2. Low accumulator pressure signals main propellant valve to open (Fig.107), causing:

   a. Buildup of the heat exchanger inlet pressure (Fig.109)

   b. Flow to surge into the heat exchanger (Fig. 110)

   c. Accumulator temperature to drop (Fig.108) because of the low wall temperature

3. When the accumulator pressure reaches 17.5 psia, a signal is sent to the main propellant valve to close. A 20-millisecond delay causes the pressure to overshoot.

4. Excess pressure is vented by the relief valve

5. The process is essentially repreated when the thrustor valve reopens at 0.6 second.

The gas generator does not turn off when the main propellant valve closes. Inspection of the tube wall control loop set point and deadband reveals that the gas generator will not close until a wall temperature of 520 R is reached.

Another control loop, not previously discussed, causes the oxidizer flow to the gas generator to shut off (Fig. 107) when the catalyst temperature reaches 2000 R, as shown in Fig.108. This valve cycling causes pressure and temperature perturbations as shown in Fig.108 and 109.

Under normal operation with saturated vapor feed, the gas generator must cycle on and off because it has been sized to supply enough heat to vaporize liquid. However, during the startup period, the tube wall is absorbing enough heat to keep the gas generator on.

Computer runs similar to those presented in the preceding paragraphs for saturated O_2 vapor were made for: (1) saturated O_2 liquid, (2) saturated H_2 vapor, and (3) saturated H_2 liquid for both pulse and steady thrustor demand. The main differences and conclusions are:

1. A large amount of liquid O_2 surges into the heat exchanger when the main propellant valve is opened because the propellant valve must be sized for saturated O_2 vapor flow which has a density several hundred times less than that for saturated liquid. The net effect of this pehnomenon is to cause the main valve to cycle on and off, although there is a steady flow demand by the thrustor.

2. There is not a great difference between H_2 vapor and liquid flow into the heat exchanger because of the small density difference between H_2 vapor and liquid. This factor can probably be used to advantage in the control circuit. For example, the on-off pressure controller should possibly be put on the H_2 side and the variable orifice follower on the O_2 side.

3. In one case the $\dot{w}_{O_2}$ gas generator and $\dot{w}_{H_2}$ gas generator rose to only one-half of their nominal design values of 0.0020 lb/sec. The trouble was traced to the hot-gas dump pressure which was approximately twice its normal value. It was concluded that the hot-gas orifice had been sized wrong. In this particular situation, flashback to the injector face might have occurred.

Evaluation of an Alternative Control Concept-Follower Valve System

In addition to constructing a model of the conditioner subsystem with the initial control system logic, a mathematical model of a pressure-actuated follower valve was incorporated into the oxygen propellant conditioner computer model. A schematic of the valve with the indicated installation into the conditioner system is illustrated in Fig. 111. There are virtually no damping forces within the valve except for the restrictive orifices at the pressure ports, a_1 and a_2.

Included in the mathematical model is a description of the forces acting on the poppet and their effect on its motion. In addition, the flow into and from each pressure cavity, as well as the pressure in the cavity, are described.

Several computer runs were made to determine an orifice size which would permit good valve response and yet not oscillate excessively. An orifice diameter of 0.06 inch resulted in reasonable operation. Additional computer runs were made over a thrustor duty cycle having a frequency of 4 cps and a pulse duty cycle of 0.5. In one case, the hydrogen accumulator pressure was varied sinusoidally at 3 cps with an amplitude of 1 psi. For purposes of comparison with the second case, an additional run was made by substituting an on-off valve for the follower valve. The frequency of the hydrogen accumulator pressure oscillation and thrustor demand were chosen at different values to demonstrate the difference in the phase of accumulator pressures resulting in each system.

The volume of the oxygen accumulator used during this analysis was 250 cu in., and the response of the on-off valve (signal to open or close) was 30 milliseconds.

The results of the first run, shown in Fig.112 and 113, indicate that the oxygen accumulator pressure is maintained at almost a constant level throughout the thrustor duty cycle. When the hydrogen accumulator pressure oscillates, the oxygen accumulator pressure follows as shown in Fig.114 and 115. The amplitude of the variation of oxygen accumulator pressure is attenuated, but it oscillates at the same frequency and it lags in phase by less than 45 degrees. With the on-off valve in the system, as shown in Fig.116 and 117, the oscillating frequency of the oxygen accumulator is not the same as that of the hydrogen accumulator, and the phase relationship is continually varying.

With the on-off valve in the oxygen system, both accumulators would tend to oscillate at the same frequency because the forcing function, thrustor demand, is common to both systems. However, because of variations in inlet conditions such as quality and pressure, as well as differences in response from one system to the other, an out-of-phase condition could result.

The follower valve appears to be limited in following decreases in hydrogen accumulator pressure. This is caused by the closing of the follower valve when the hydrogen pressure falls below that of the oxygen. When this occurs, the oxygen accumulator pressure will drop only as permitted by gas generator and/or thrustor demand or by loss of heat. This might be circumvented by reducing the oxygen accumulator volume to the extent that its pressure will cycle at a much higher rate (will be more quickly depleted) than the hydrogen accumulator.

Analysis of Accumulator Sizing

The chief purpose of the accumulator is to decouple the thrustor from the conditioner system. To accomplish this, the accumulator must be sized to attenuate:

1. pressure perturbations caused by the main propellant valve delays (both electrical and mechanical valve delays)

2. pressure and temperature perturbations produced by the heat exchanger.

Of these, the former is the more easily analyzed.

Accumulator Pressure Decay Caused by Valve Delays. The pressure perturbations caused by the electrical and mechanical valve delays can be predicted through a material balance on the accumulator for the time period between initiation of flow from the accumulator and the mechanical opening of the inlet valve:

$$\text{input} - \text{output} = \text{accumulation} \tag{74}$$

or

$$0 - \dot{w}_T = \frac{V}{TR} \frac{dP_{acc}}{d\theta} \tag{75}$$

where

$$\dot{w}_T = \dot{w}_{T\ nom} \left[\frac{(2g\ \rho_T\ \Delta P_{inj})}{(2g\ \rho_{T\ nom}\ \Delta P_{nom})} \right]^{1/2} \simeq \dot{w}_{T\ nom} \sqrt{\frac{P_{Acc}}{P_{nom}}} \tag{76}$$

Integration gives:

$$-\left[\dot{w}_{T\ nom} \frac{TR}{V} \right] \theta = 2\sqrt{P_o} \left[P_f^{1/2} - P_o^{1/2} \right] \tag{77}$$

A plot of predicted accumulator pressure as a function of valve time delay with accumulator volume as a parameter is presented in Fig. 118 . Worst-case accumulator limits presented above revealed that it was desirable to hold the accumulator pressures to within approximately

±0.5 psi of each other. If this pressure drop is used with a main propellant valve delay of 0.050 second, accumulator volumes of 2720 and 424 sq in are obtained for H_2 and O_2 sides, respectively.

Perturbations Caused by Heat Exchanger Flow Instability. Little was known concerning heat exchanger flow instability (caused by boiling) which could conceivably result in large pressure and temperature perturbations in the inlet stream to an accumulator. The development of a mathematical description of system behavior to such a process was dependent on the system characteristics observed experimentally. Based on the observed behavior, a model of the heat exchanger-accumular system is developed in Volume II of this report.

a rough estimate of the thermal response to steady-state inlet temperature perturbations can be obtained by considering a heat balance around the accumulator.

$$\dot{w}\, C_p\, T_{in} - \dot{w}\, C_p\, T_{acc} = M\, C_p\, \frac{dT_{acc}}{d\theta} \tag{78}$$

or

$$\frac{\dot{w}}{M}\,\theta = \ln\left[\frac{T_{in} - T_{f\ acc}}{T_{in} - 200}\right] \tag{79}$$

The time for the accumulator temperature to reach 220 R for T_{in} of 1000 and 500 R was computed to be 41 and 94 milliseconds, respectively, for the volumes sized in the previous paragraphs. This illustrates the importance of selecting the correct hot-tube temperature set point.

A cursory heat transfer analysis of the temperature-equalizing advantage of placing the O_2 accumulator inside the H_2 accumulator was made assuming concentric cylindrical containers 2 feet in length. Under steady-state conditions, there was a negligible equalizing effect for a 40 R temperature difference. A convective analysis for static no-flow conditions indicated that the response was somewhat better, although still small. It was concluded that if a temperature-equalizing device was necessary, a low-pressure-drop combination accumulator-heat exchanger should be investigated.

SUMMARY OF SYSTEMS ANALYSIS

A systems analysis, modeling, and simulation effort was accomplished. This resulted in computer programs which will be used in simulating system or component operation. The details of the model development are discussed.

The thrustor model was used to determine thrustor sensitivity to perturbations in upstream operating conditions and to predict thrustor response and pulse-mode operating characteristics. Operating characteristics of the conditioner subsystem and the interaction between components were evaluated using the conditioner model. Also, the adequacy of control system alternatives was evaluated.

TABLE 20

COMPUTER MODEL INPUT AND OUTPUT

The following list indicates the information input to the model:

- Computing time increment
- Run duration
- Printing and plotting increment
- Thrustor duty cycle
- Inlet pressure function, frequency, amplitude, and phase
- Catalyst bed steady-state temperature gradient and initial temperature
- Initial mixer temperature
- Component volumes
- Valve opening and closing electrical energizing times and mechanical actuation times
- System steady-state pressure distribution
- Propellant steady-state flowrates and inlet temperatures
- Perturbed inlet pressures and temperatures
- Heat capacity of catalyst bed and mixer

The computer output presents the following parameters as functions of time:

- Oxidizer line pressure
- Hydrogen line pressure
- Mixer pressure
- Catalyst bed pressures (5)
- Chamber pressure
- Mixer temperature
- Catalyst bed temperatures (5)
- Catalyst bed reaction temperature
- Combustion chamber temperature
- Oxygen flowrate to the injector
- Hydrogen flowrate to the injector
- Oxygen bypass flowrate
- Hydrogen bypass flowrate
- Flowrate into the combustion chamber
- Flowrate through the nozzle
- Propellant valve areas
- Thrustor duty cycle

TABLE 21

Input Data and Format For Conditioner Modeling Computer Program

FORTRAN FIXED 10 DIGIT DECIMAL DATA

DECK NO. Compute PROGRAMMER Input for Figure DATE 7 - O_2 PAGE ____ OF ____ JOB NO. Conditioned

	NUMBER	DESCRIPTION
1	1	
13	0.0002	CALC. TIME INCRE.
25	50.0	PRINT EVERY 50TH PT.
37	2.0	RUN DURATION
49	1999	GG DEAD BAND
61	5.0	ACC. TEMP. D.B.
IDENTIFICATION 73	10	80
1	6	
13	0.50	ACC. PRESS. D.B.
25	120.0	WALL TEMP. D.B.
37	200.0	NOT USED
49	0.0	ACC. HEAT LEAK
61	0.0	HEATER ELEC.
IDENTIFICATION 73	20	80
1	11	
13	0.02	MAIN PROP. DELAY
25	0.007	GG VALVE DELAY
37	0.	A RAT Ø
49	10.0	LINE VOL.
61	4.0	GG INJ. VOL.
IDENTIFICATION 73	30	80
1	16	
13	8.0	GG CHAMBER VOL.
25	11.5	HOT SIDE VOL.
37	250.0	ACC. VOL.
49	0.0	AMPL. OF GG
61	1.0	FREQ.
IDENTIFICATION 73	40	80

FORM 609-W-23 NEW 1-65

	NUMBER	DESCRIPTION
1	21	
13	0.60	THR. FLOW DELAY
25	0.036	THR. O_2 FLOW
37	1.0	THR. FREQ.
49	1.0	THR. DUTY CYCLE
61	0.0	AMP LH_2 TANK PRES.
IDENTIFICATION 73	50	80
1	26	
13	1.0	FREQ. H_2 TANK PRES.
25	200	TW INIT.
37	2000.	GG TEMP.
49	2000.	CAT TEMP.
61	200.	ACC. TEMP.
IDENTIFICATION 73	60	80
1	31	
13	400	WALL TEMP.
25	200	NOT USED
37	226	THERMAL RES. O_2 L
49	241	THERMAL RES. O_2 g
61	180	THERMAL RES. HOT SIDE
IDENTIFICATION 73	70	80
1	36	
13	0.097	WALL HEAT CAPACITY
25	1.0	PLT FLOWS
37	0.0	GAS FEED - 0.
49		LIQUID FEED - 1.
61		
IDENTIFICATION 73	80	80

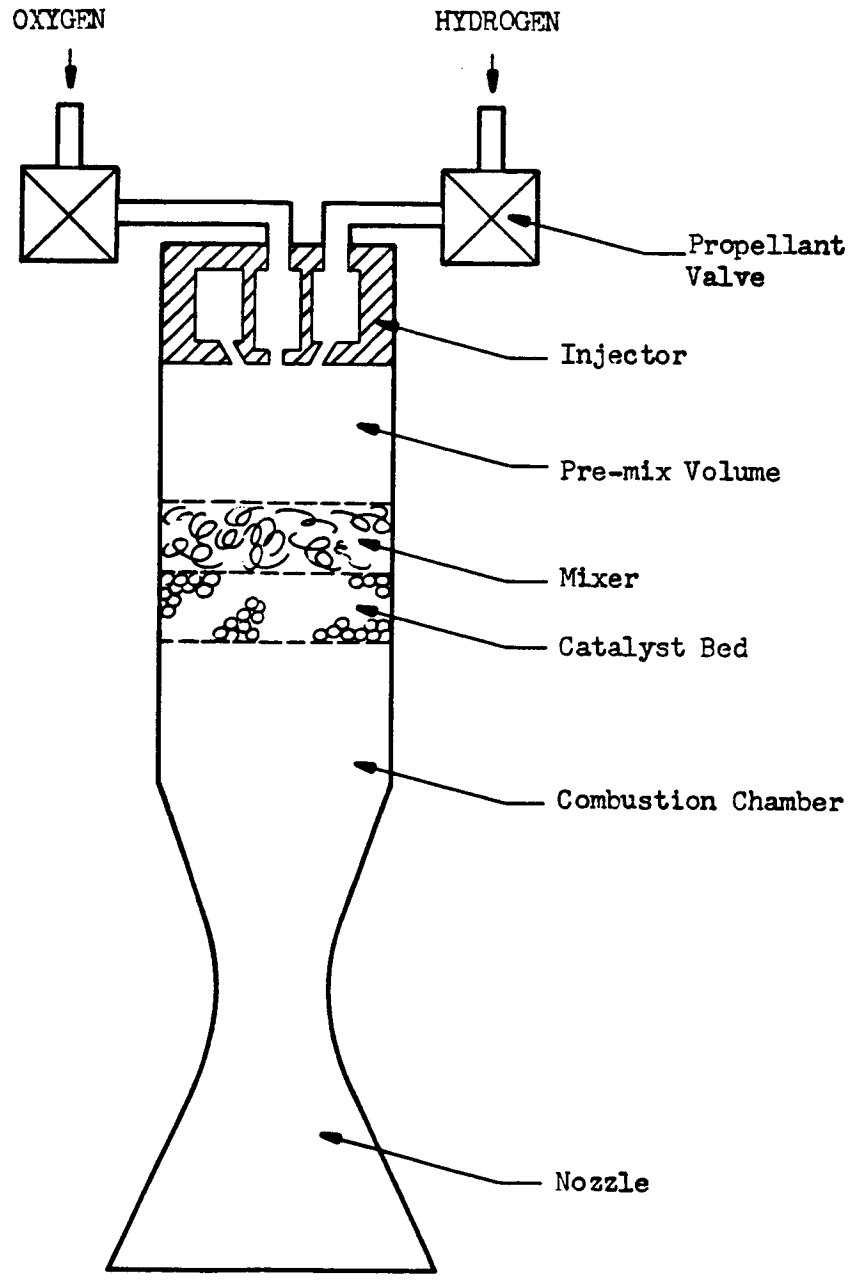

Figure 94. Schematic of Thrustor for Modeling Purposes

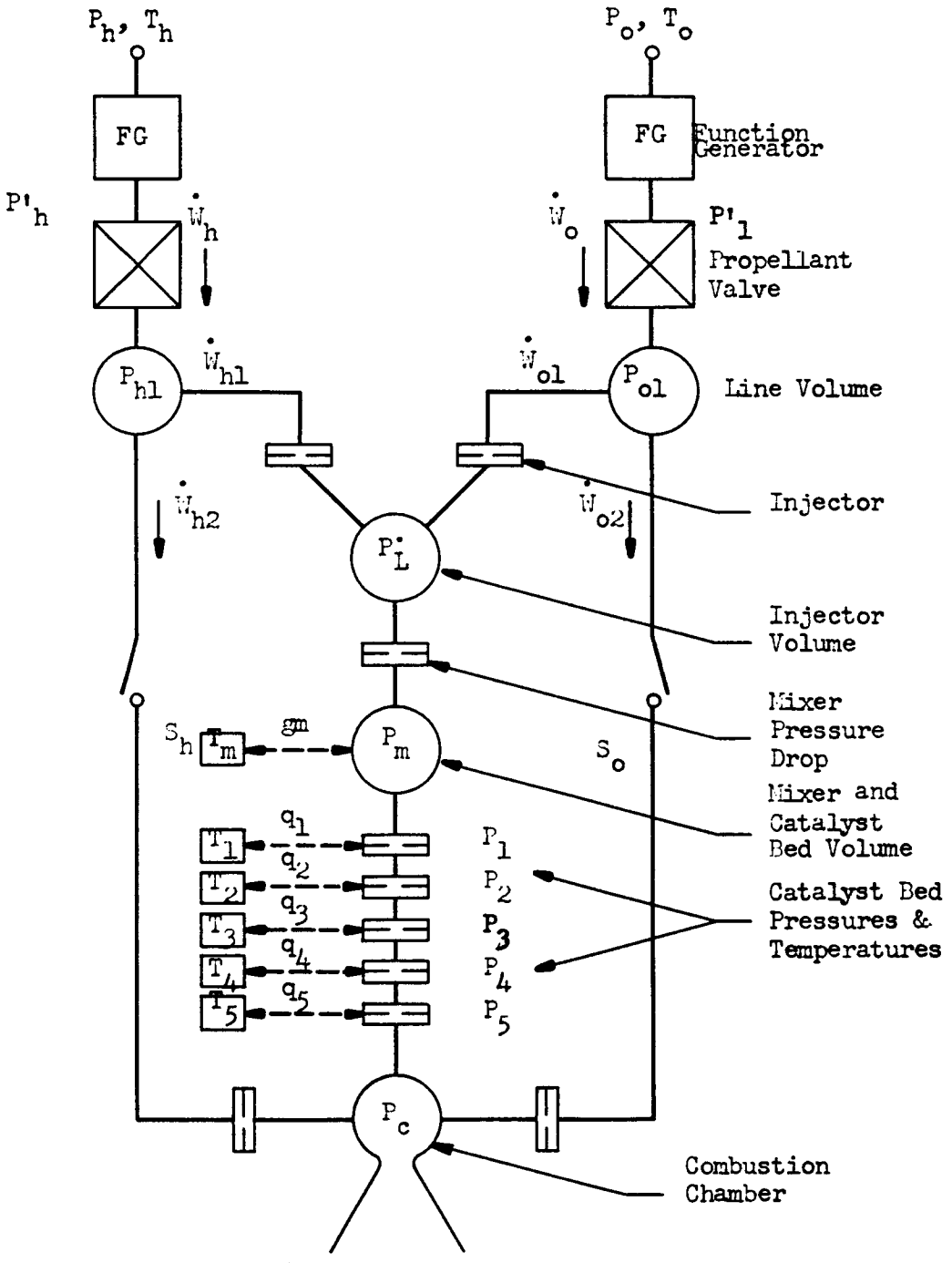

Figure 95. Computer Model Schematic of Thrustor

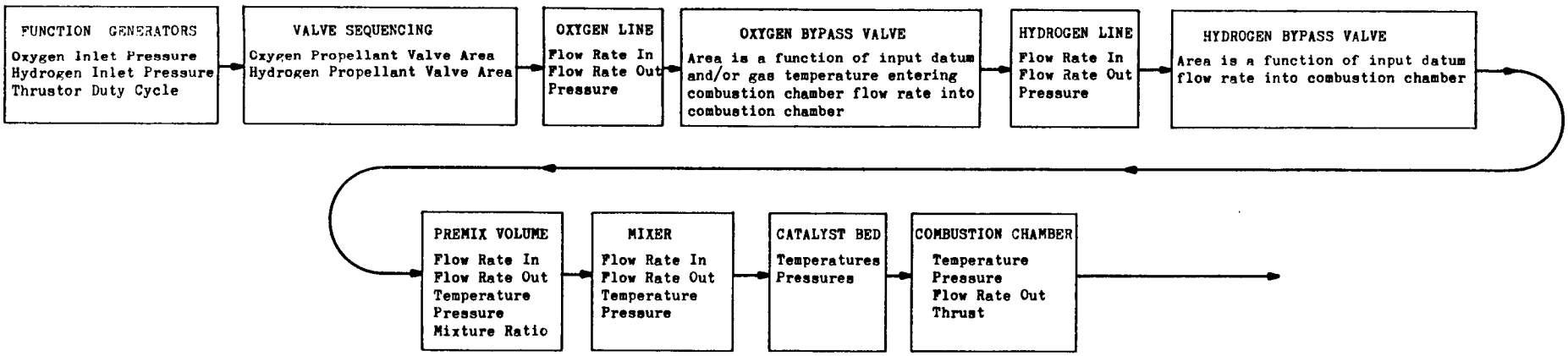

Figure 96. Outline of Main Program Computation Sequence

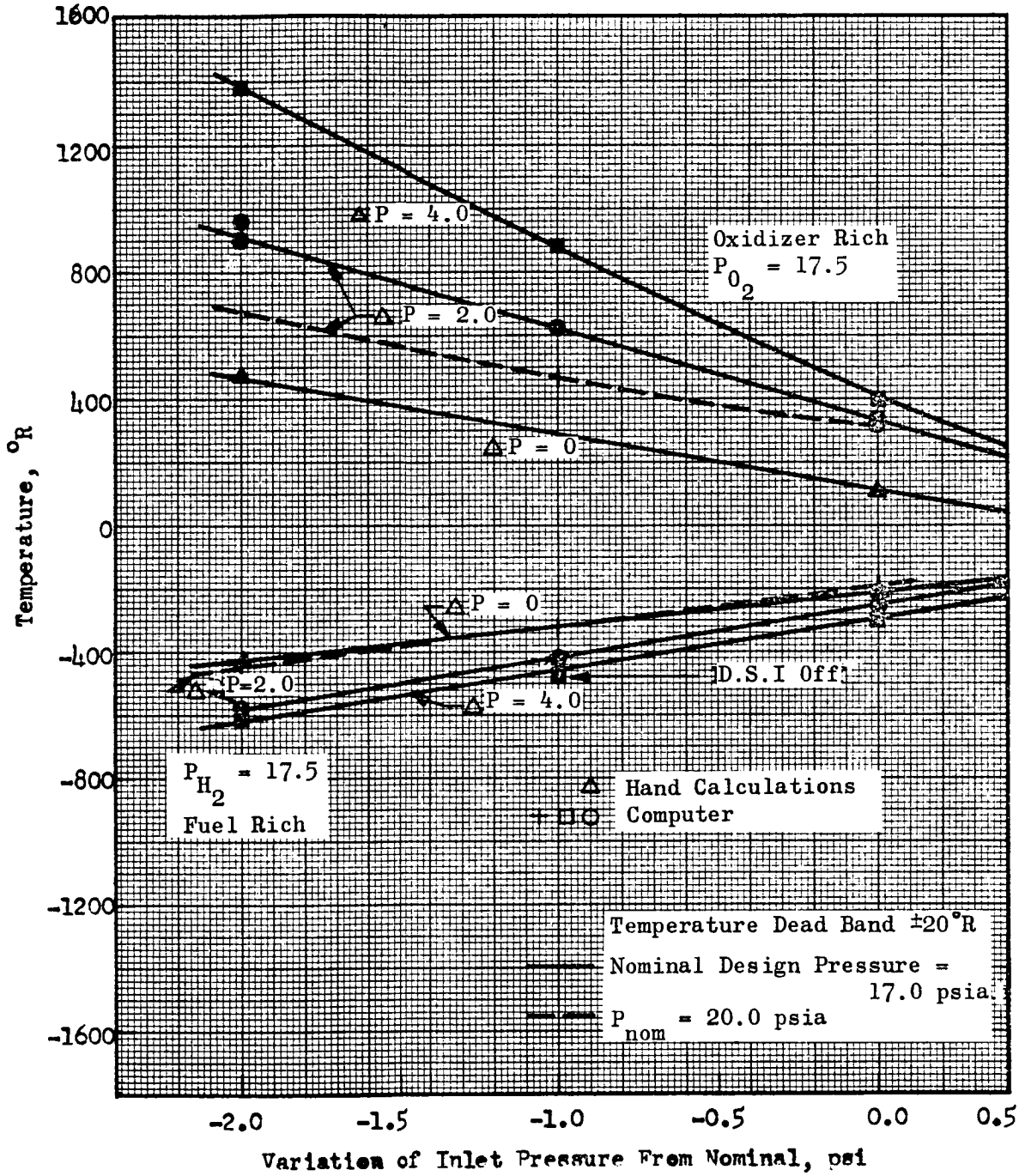

Figure 97. Change in Catalyst Bed Combustion Temperature as a Function of Inlet Pressure for D.S.I. With Catalyst Bed Pressure Drop and Nominal Pressure as Parameters

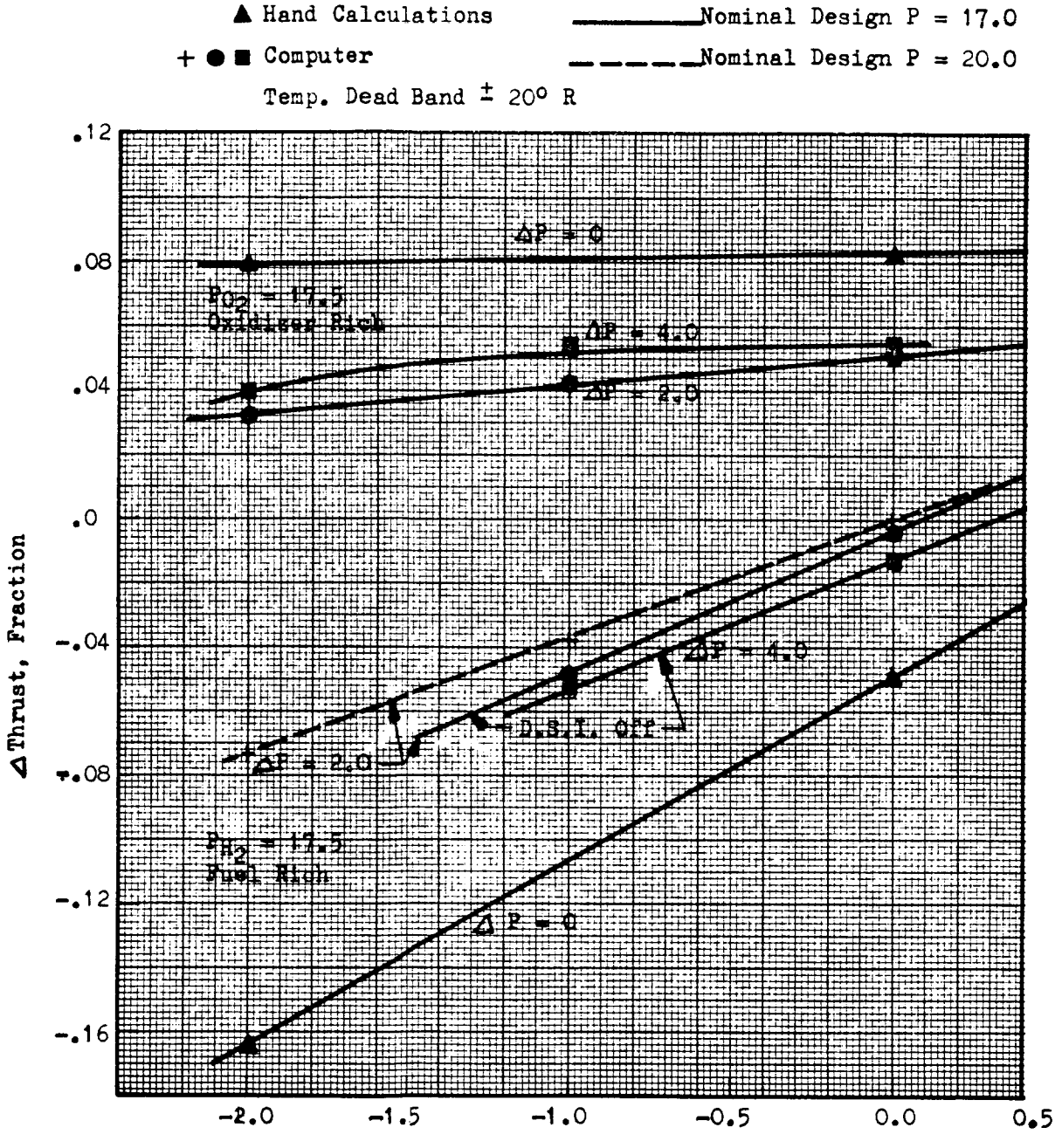

Figure 98. Change in Thrust as a Function of Inlet Pressure for D.S.I. With Nominal Pressure and Bed Pressure Drop as Parameters.

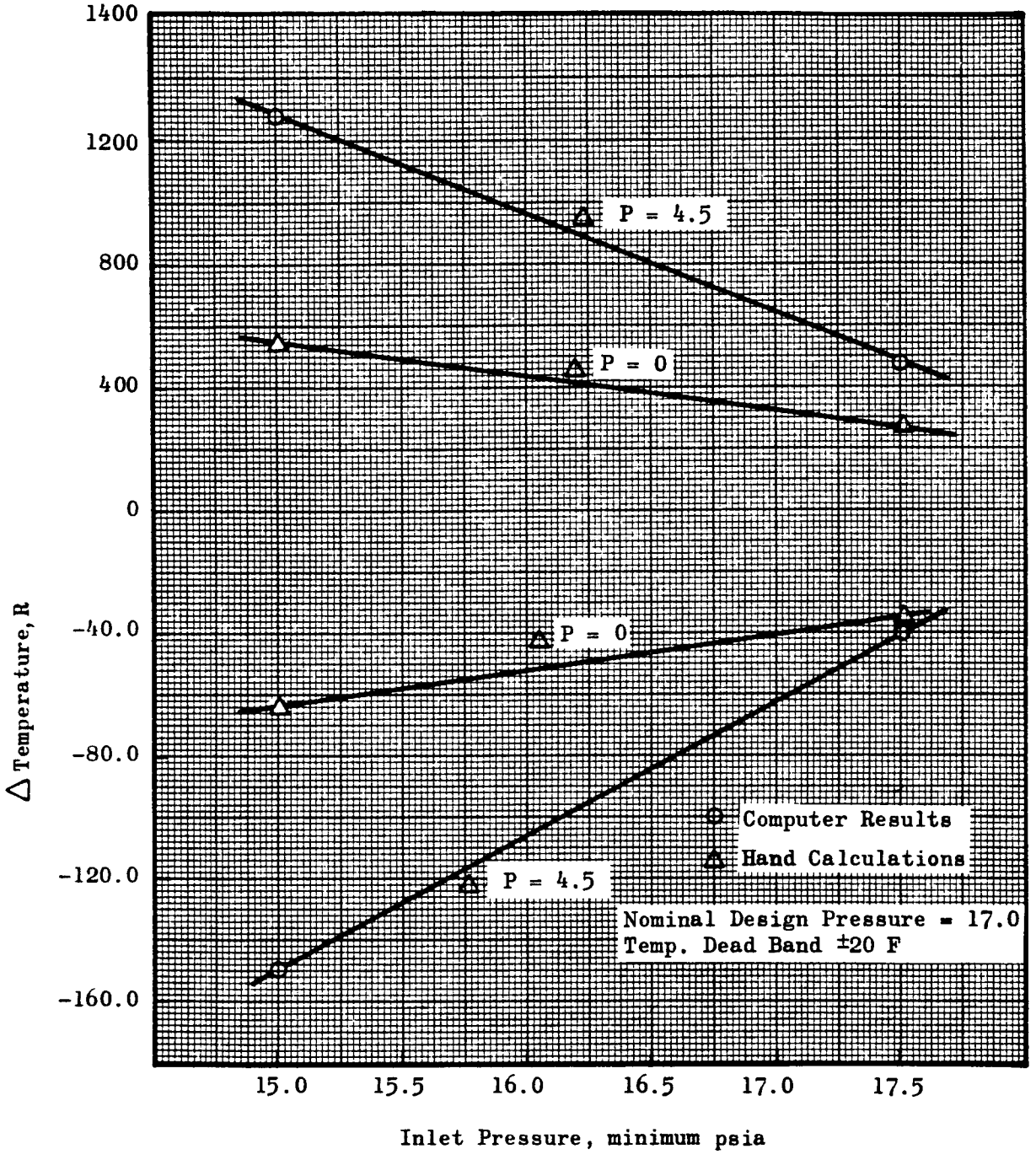

Figure 99. Changes in Catalyst Bed Combustion Temperature as a Function of Inlet Pressure for Full Flow With Catalyst Bed Pressure Drop as a Parameter

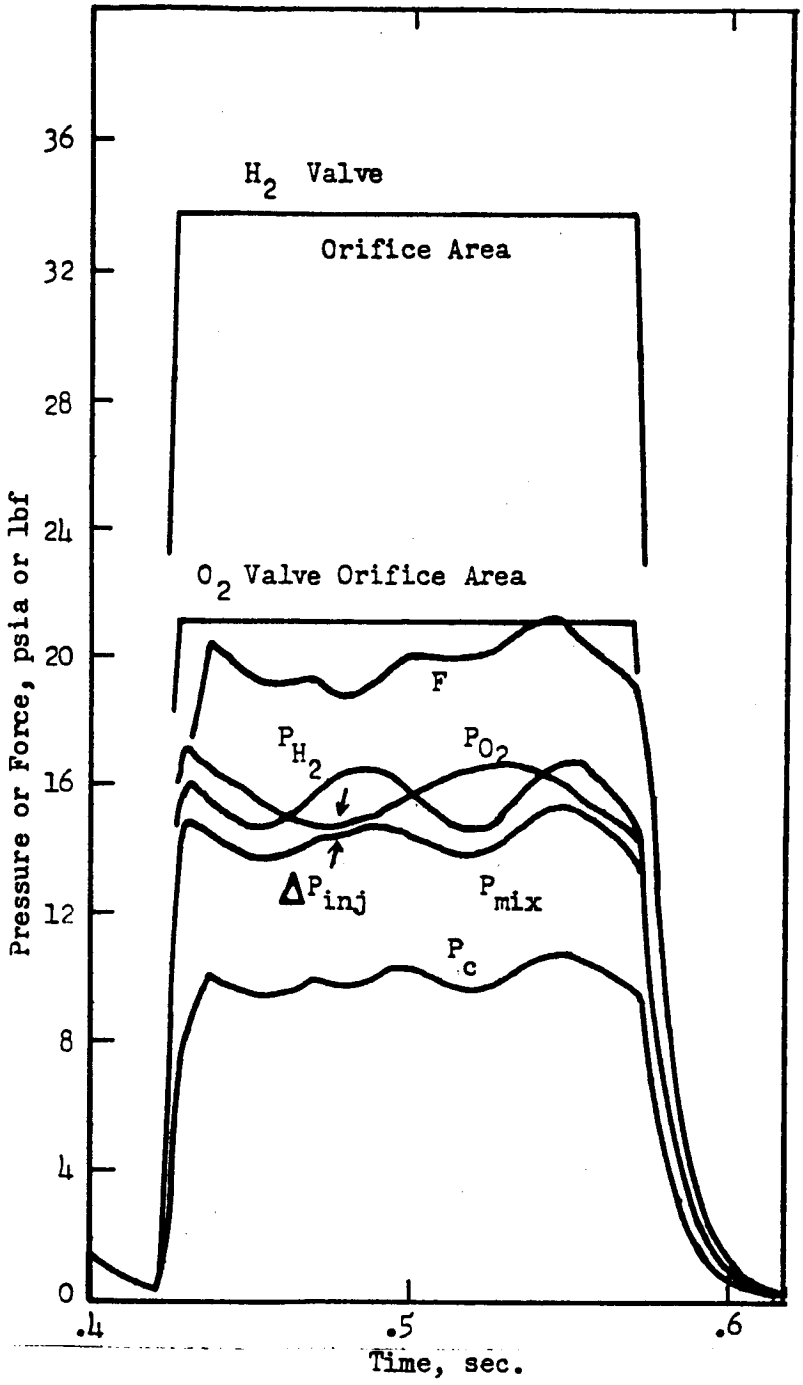

Fig. 100. Dynamic Analysis Evaluating Sensitivity of Thrustor Operation to Upstream Conditions--Pressure and Thrust Characteristics for Oxidizer-Rich Operation

Imposed Operating Conditions

A. Oxygen Side
Accum. Press. = 16.25 + 1.25 sin.Wt.
W = 10 cps
Temperature = 180 R

B. Hydrogen Side
Accum. Press. = 16.25 + 1.25 Wt.
W = 15 cps
Temperature = 220 R

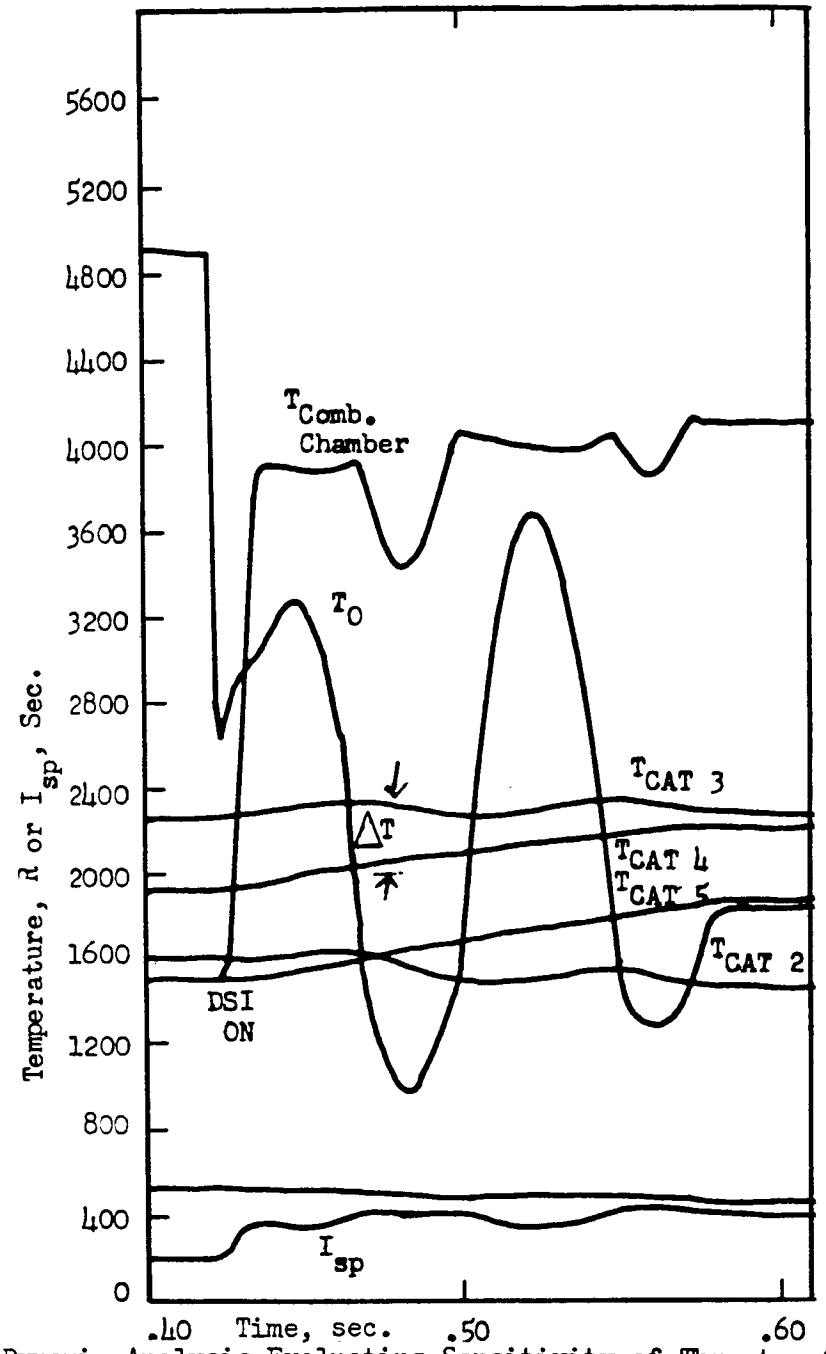

Fig. 101. Dynamic Analysis Evaluating Sensitivity of Thrustor Operation to Upstream Conditions--Temperature and Specific Impulse Characteristics for Oxidizer-Rich Operation

Imposed Operating Conditions

A. Oxygen Side
Accum.Press. = 16.25 + 1.25 sin.Wt.
W = 10 cps
Temperature = 180 R

B. Hydrogen Side
Accum.Press. = 16.25 + 1.25 Wt.
W = 15 cps
Temperature = 220 R

C. Nominal Temperature Conditions for 1-inch Catalyst Bed Divided into Five 0.20-inch Segments
T_{CAT_1} = 400R, T_{CAT_2} = 800R, T_{CAT_3} = 1200R, T_{CAT_4} = 2000R, T_{CAT_5} = 2000R

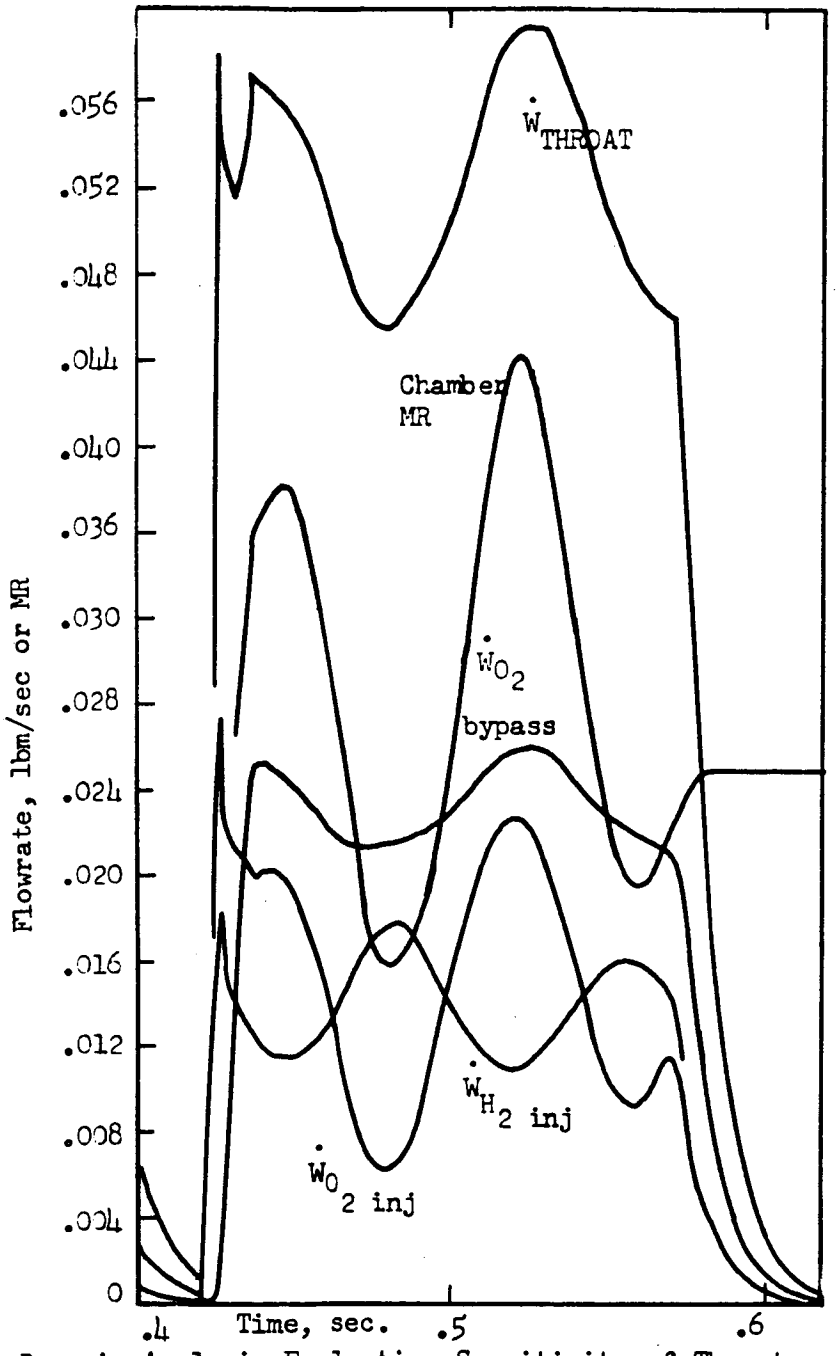

Fig. 102. Dynamic Analysis Evaluating Sensitivity of Thrustor Operation to Upstream Conditions—Flowrates and Mixture Ratio Characteristics for Oxidizer-Rich Operation

Imposed Operating Conditions

A. Oxygen Side
Accum.Press. = 16.25 + 1.25 sin.Wt.
W = 10 cps
Temperature = 180 R

B. Hydrogen side
Accum.Press.= 16.25 + 1.25 Wt.
W = 15 cps
Temperature = 220 R

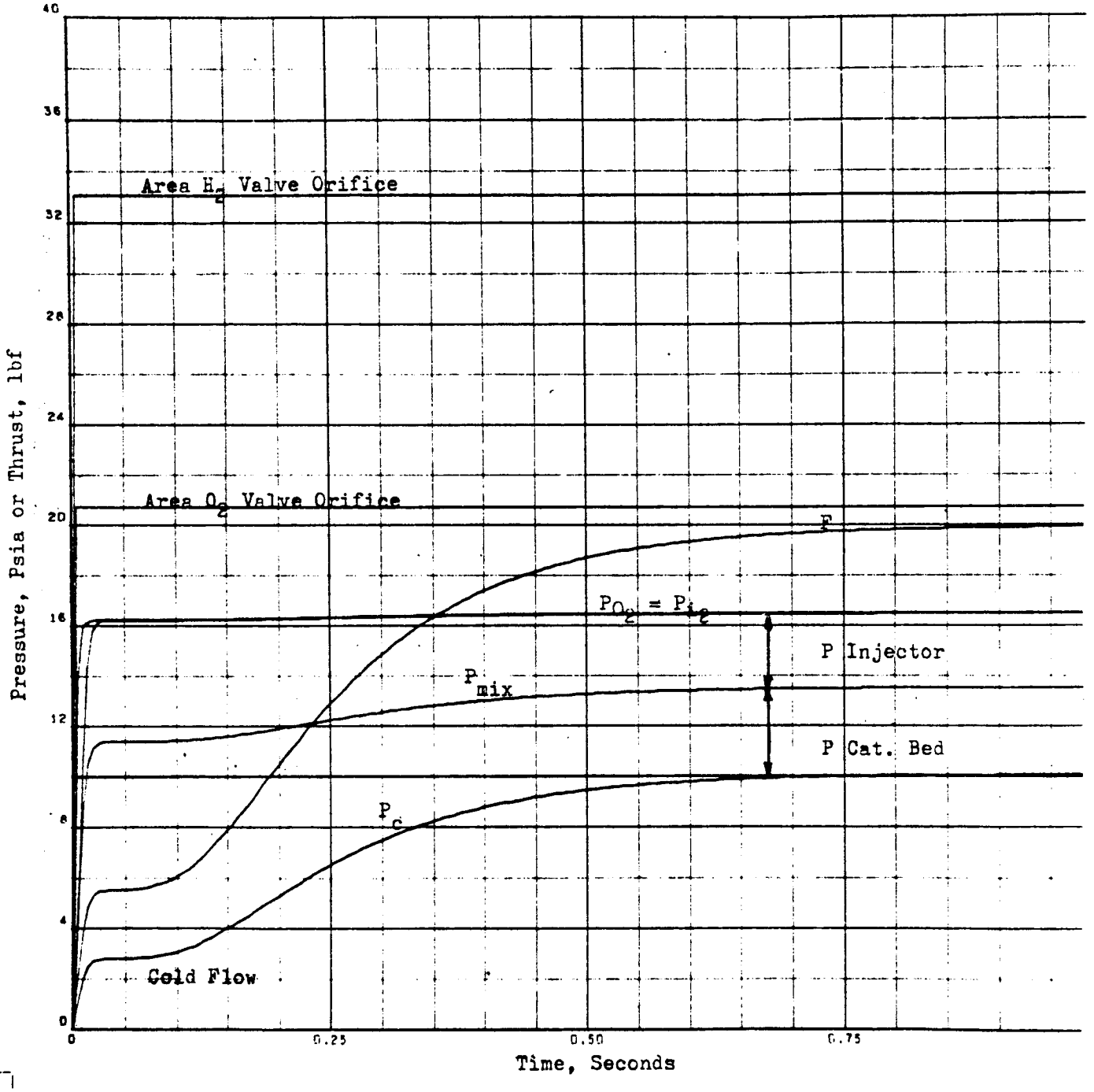

Fig. 103. Response Characteristics of a Full-Flow Thrustor with a 0.525-inch Catalyst Bed - Valve Operation and Pressure Response

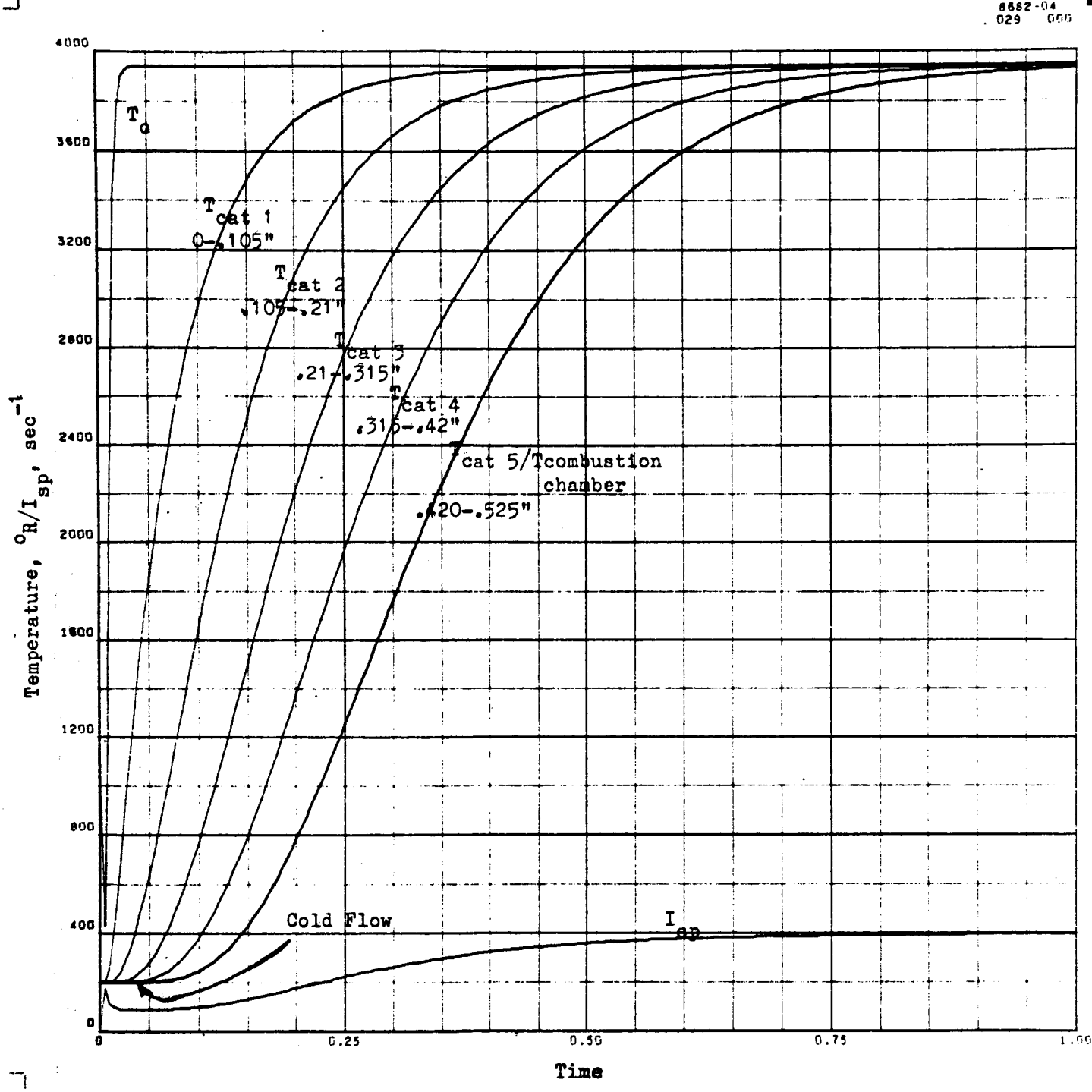

Fig. 104. Response Characteristics of a Full-Flow Thrustor with a 0.525-inch Catalyst Bed - Temperature Response

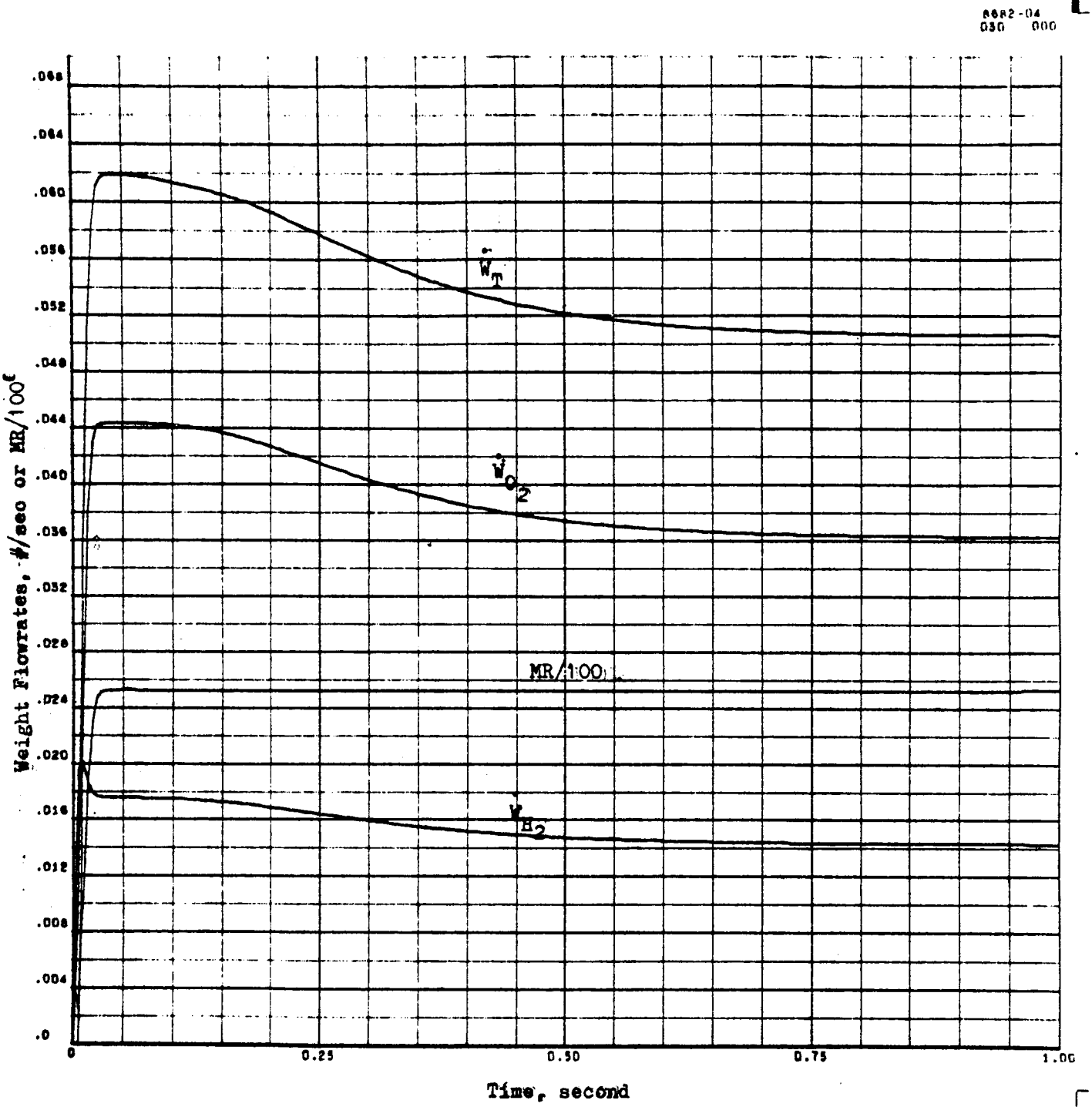

Fig. 105. Response Characteristics of a Full-Flow Thrustor with a 0.525-inch Catalyst Bed - Flowrate and Mixture Ratio Characteristics

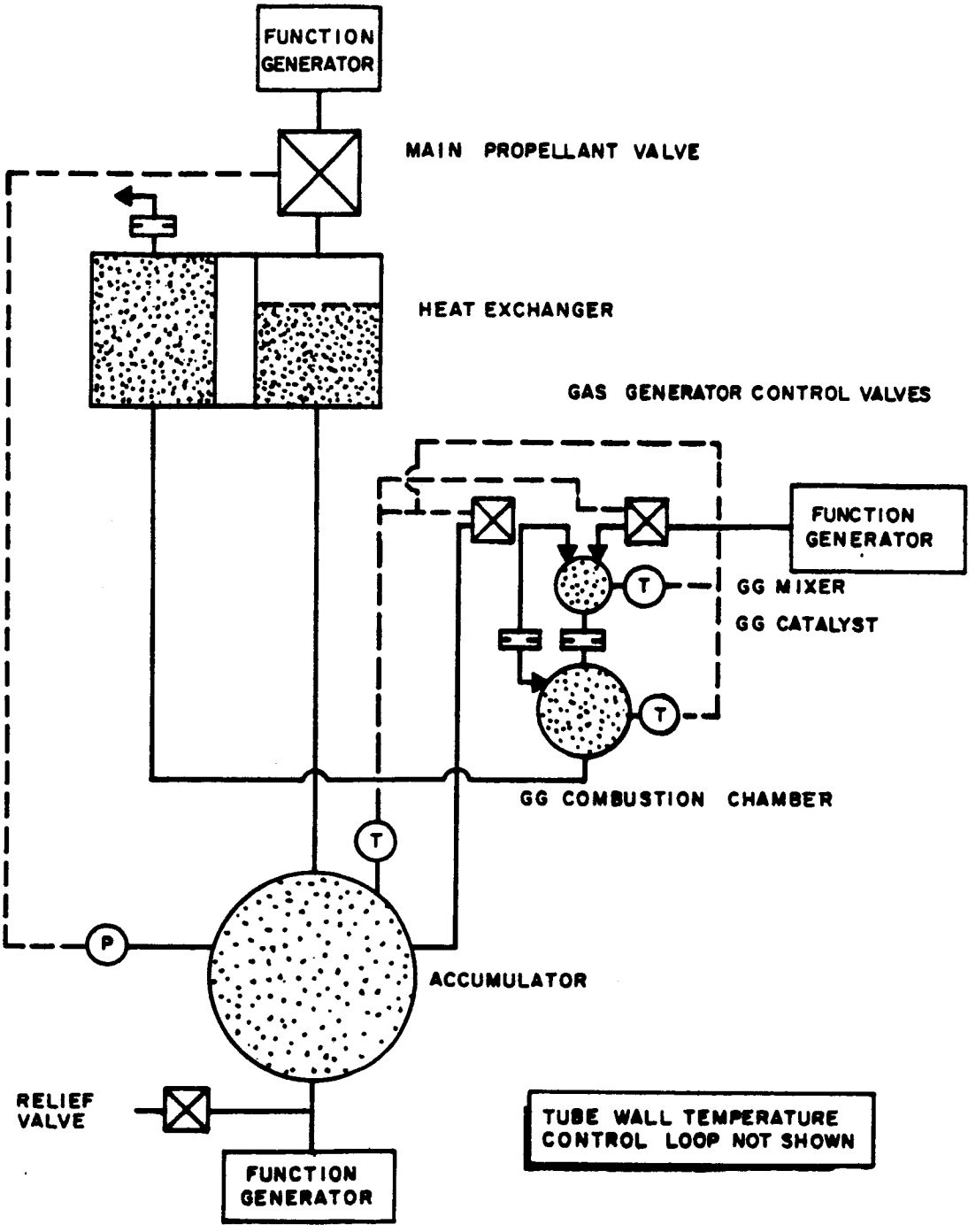

Figure 106. Conditioner Model Schematic

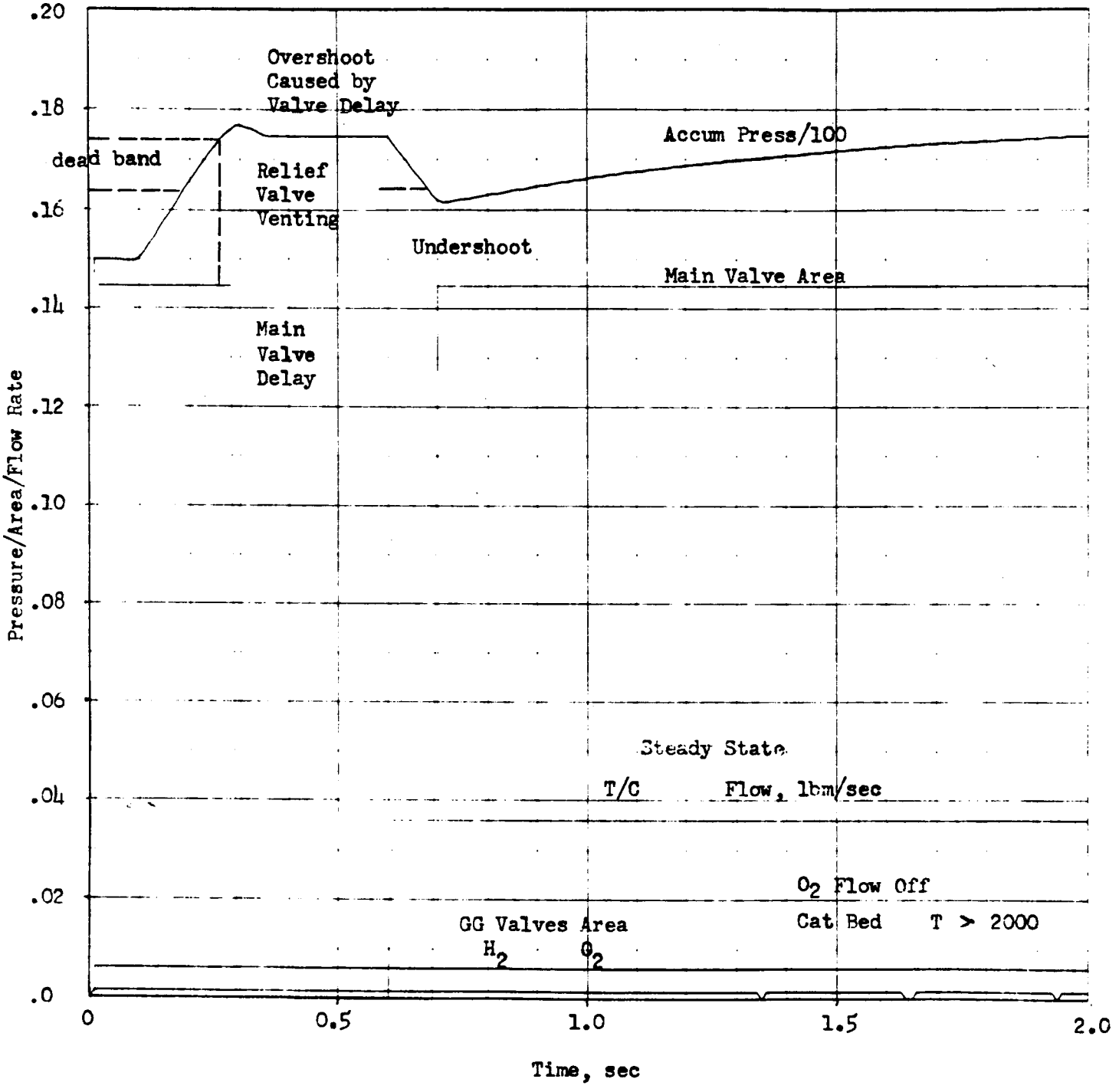

Figure 107. Conditioner System Dynamics for Saturated Vapor Propellant Delivered from the Propellant Tank and for a Steady Thrustor Demand - Valve Operation, Flowrate Dynamics, and Oxygen Accumulator Pressure Dynamics

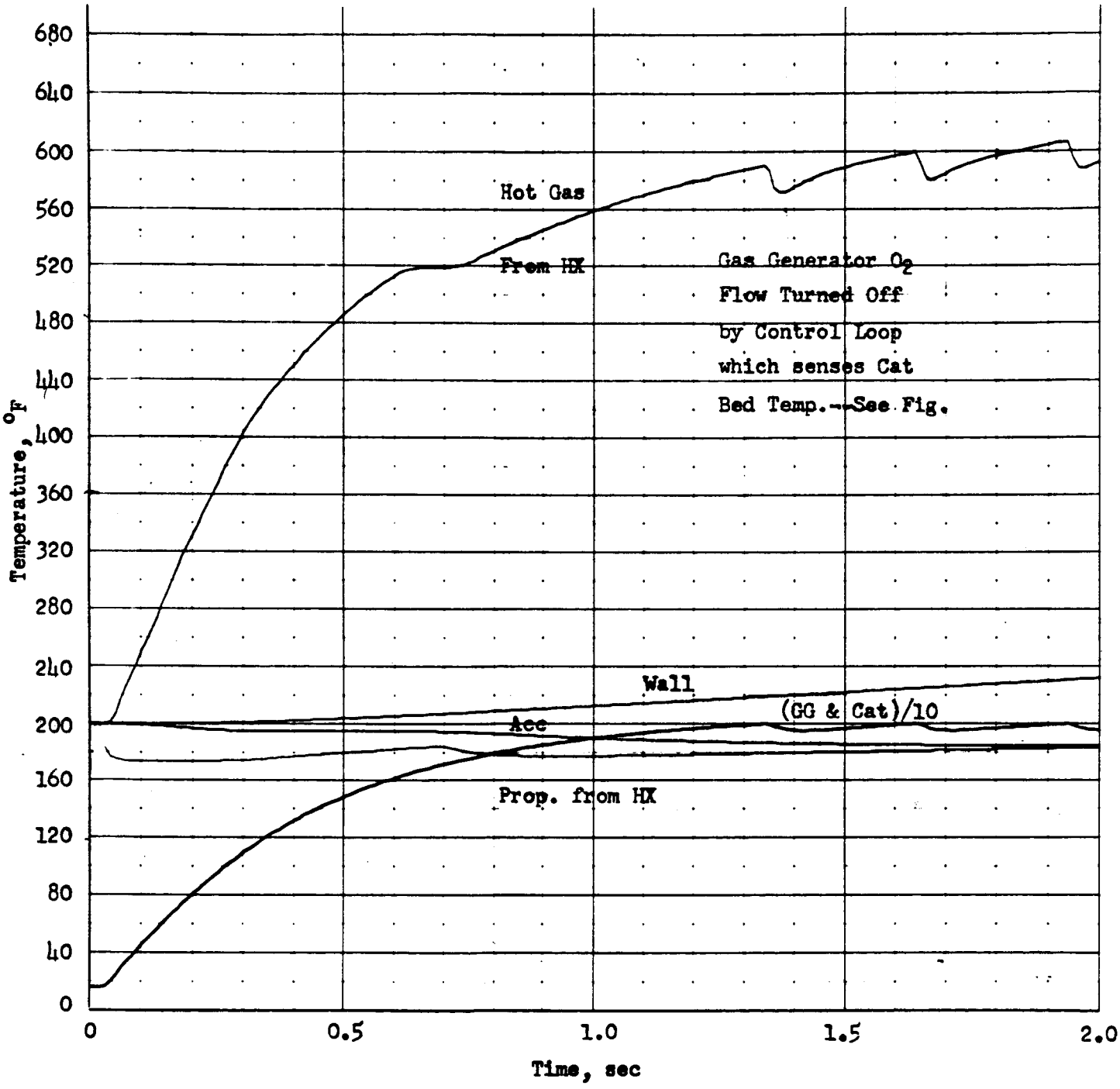

Figure 108. Conditioner System Dynamics for Saturated Vapor Propellant Delivered from the Propellant Tank and for a Steady Thrustor Demand - Thermal Response for the Oxygen Conditioning Subsystem

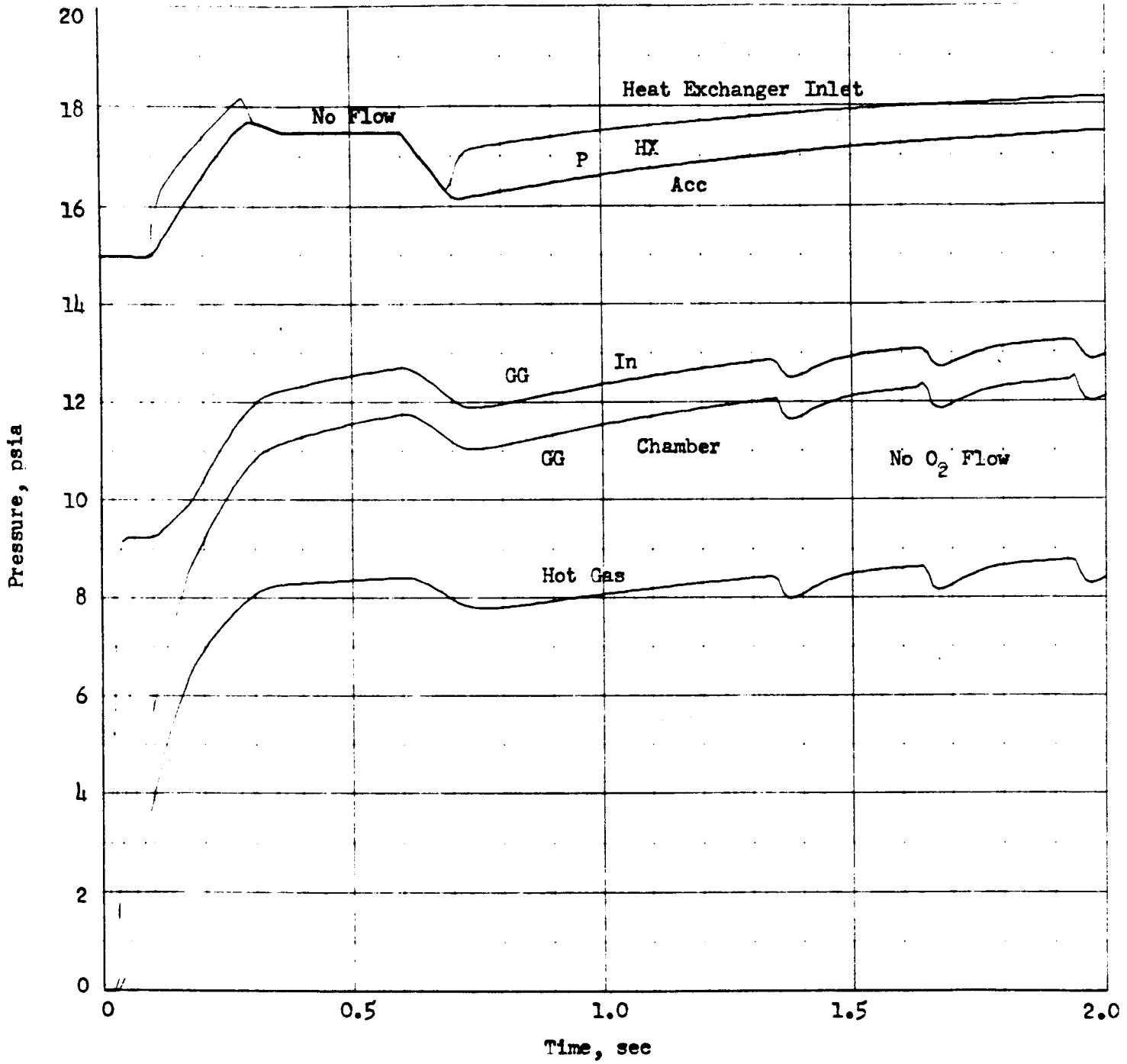

Figure 109. Conditioner System Dynamics for Saturated Vapor Propellant Delivered from the Propellant Tank and for a Steady Thrustor Demand - Pressure Response for the Oxygen Conditioning Subsystem

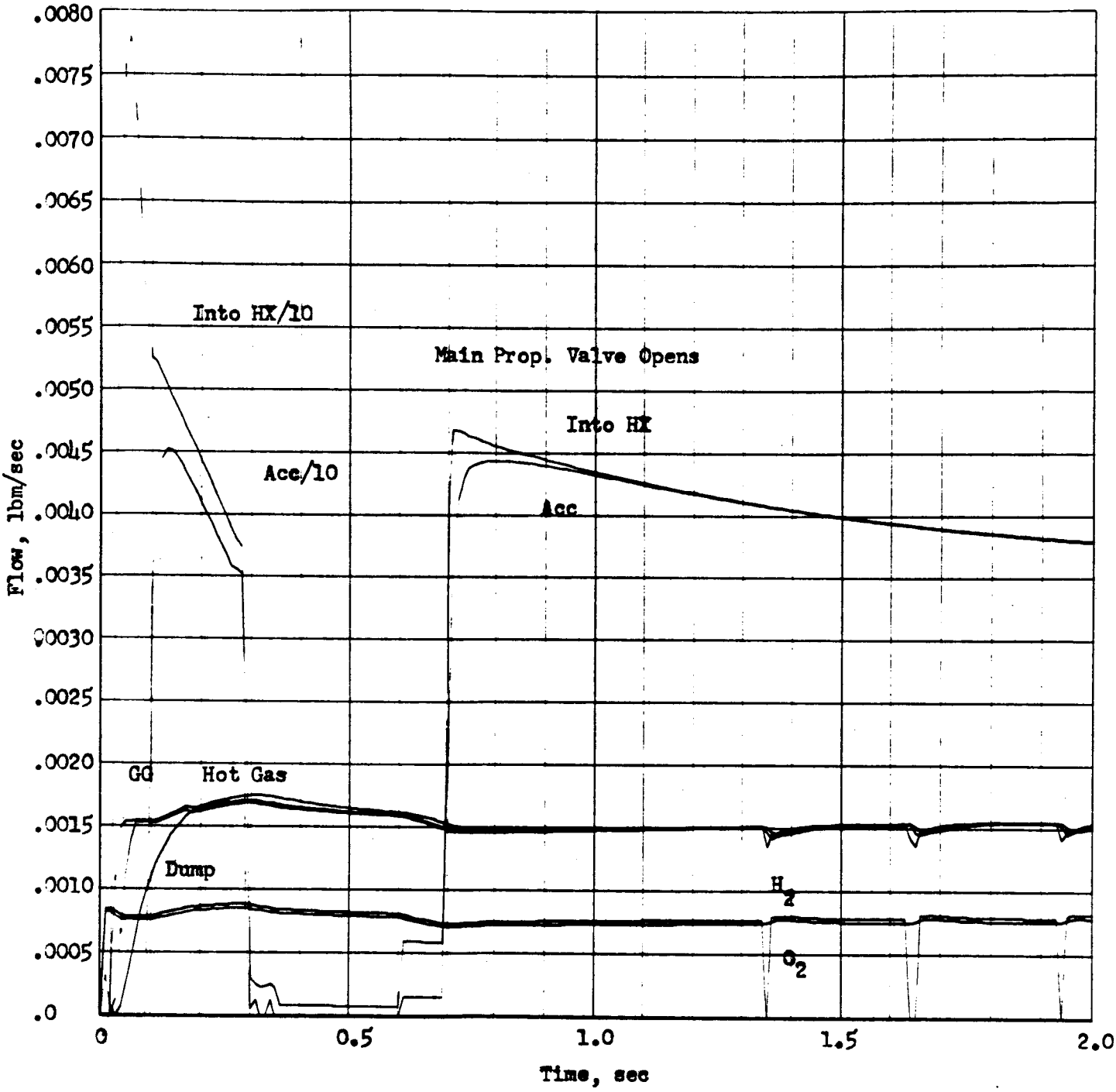

Figure 110. Conditioner System Dynamics for Saturated Vapor Propellant Delivered from the Propellant Tank and for a Steady Thrustor Demand - Flowrate Response for the Oxygen Conditioning Subsystem

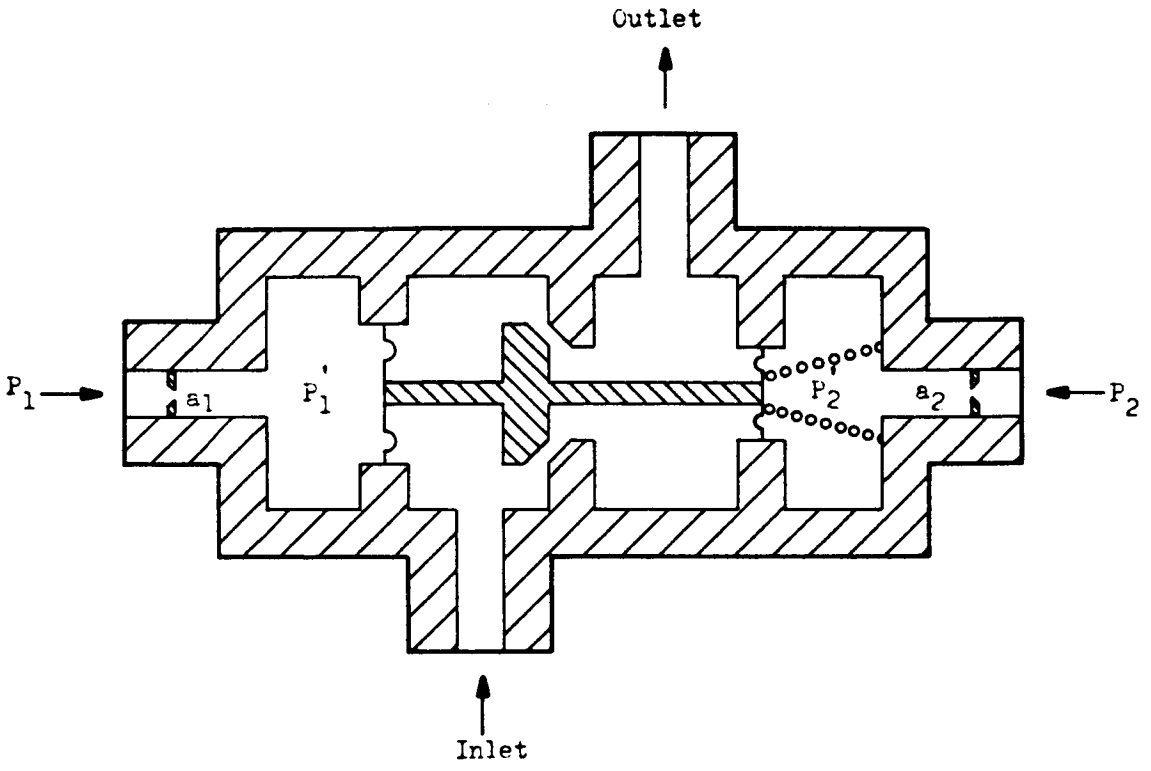

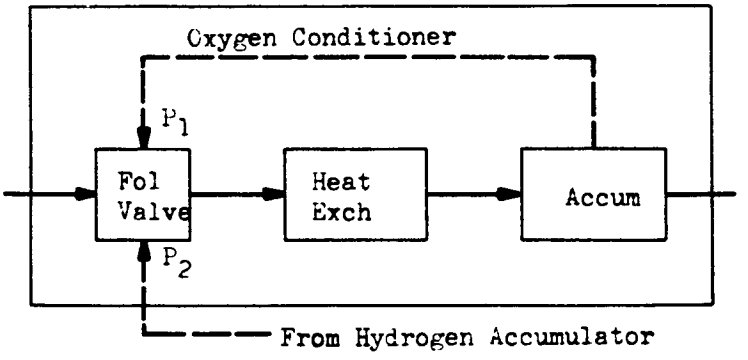

Figure 111. Follower Valve Schematic and Installation in Oxygen Side of Conditioner

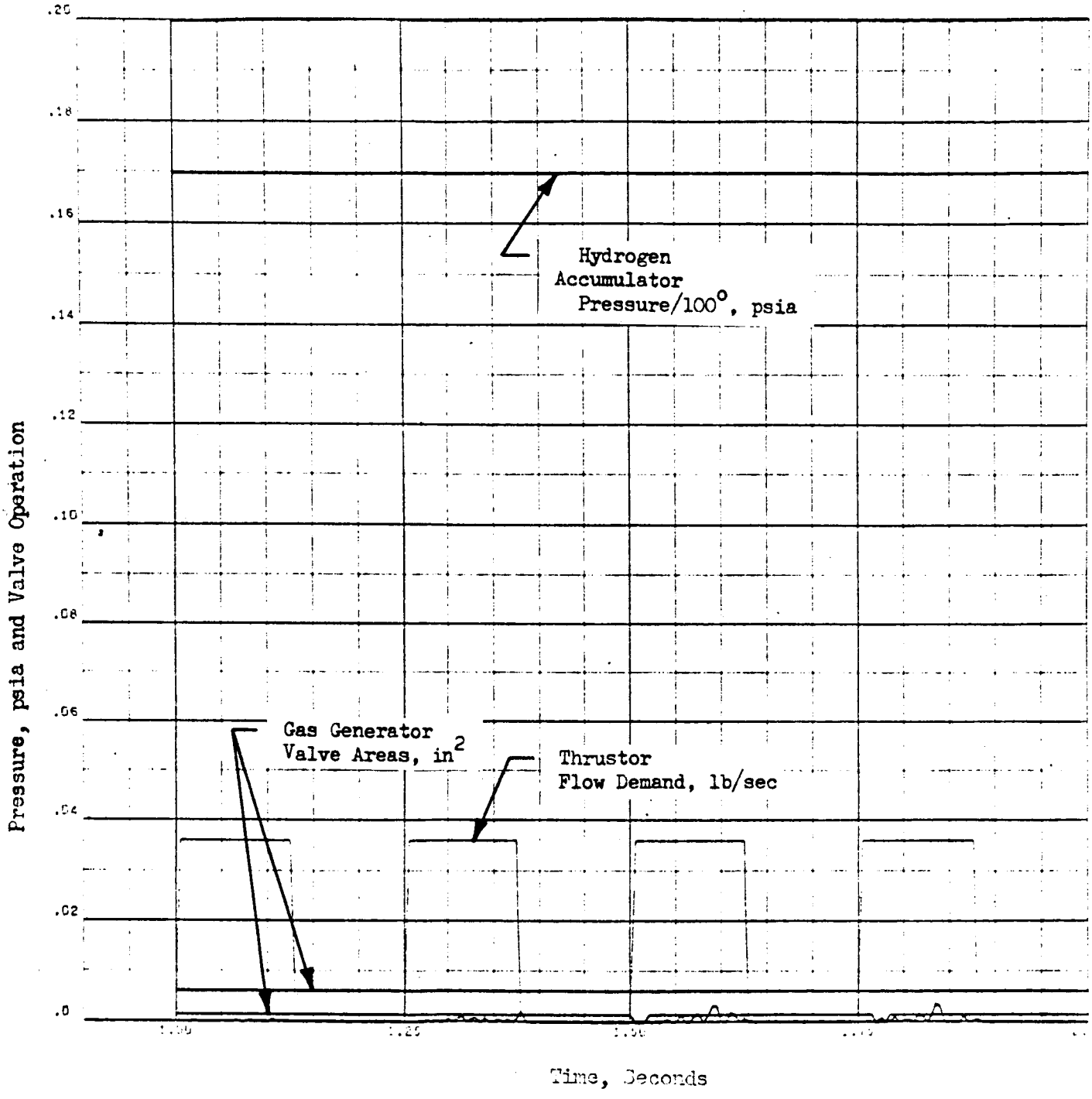

Figure 112. Results for Simulated Conditioner Operation with a Steady Hydrogen Accumulator Pressure - Valve Operation

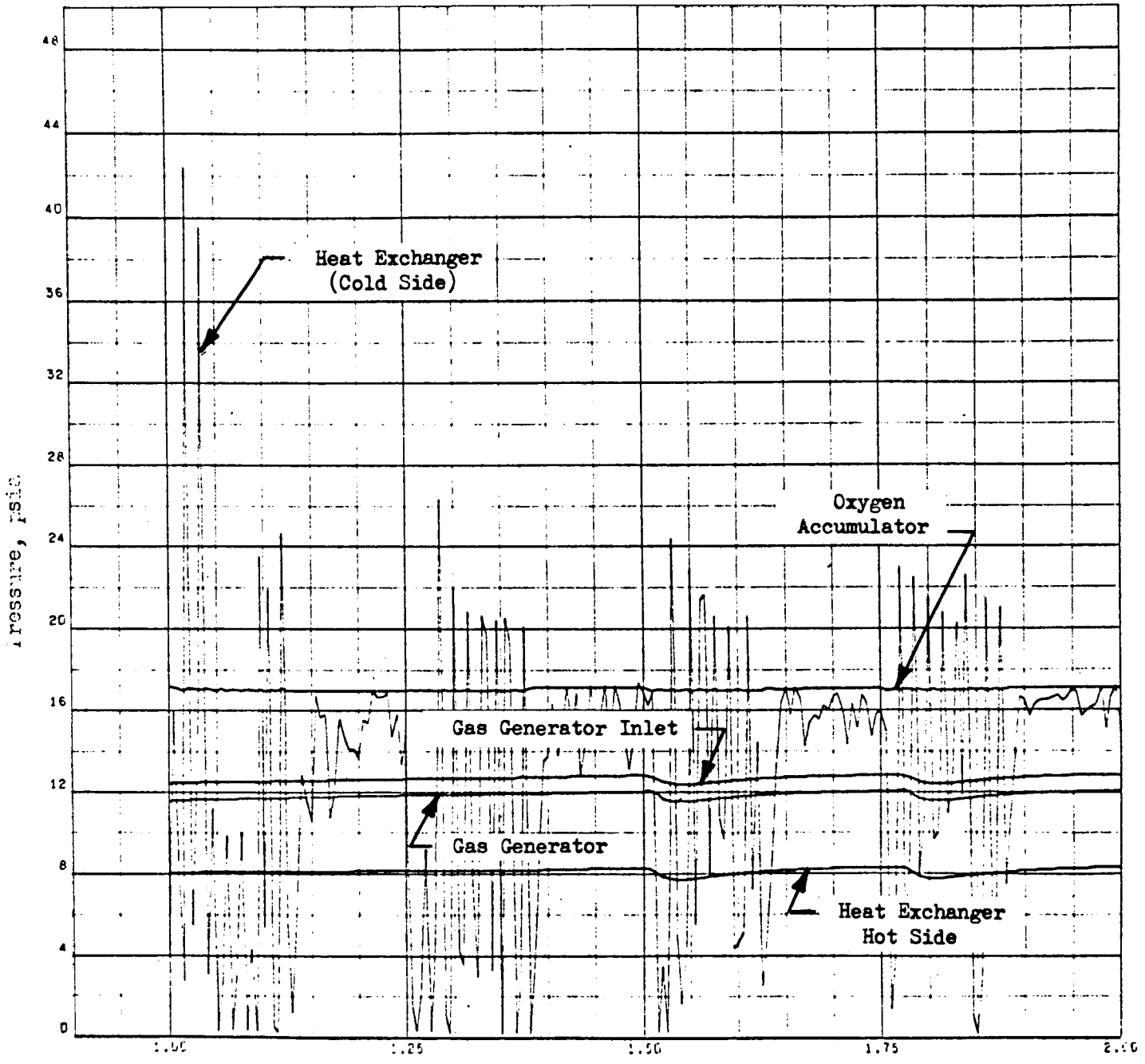

Figure 113. Results for Simulated Conditioner Operation with a Steady Hydrogen Accumulator Pressure - System Pressures

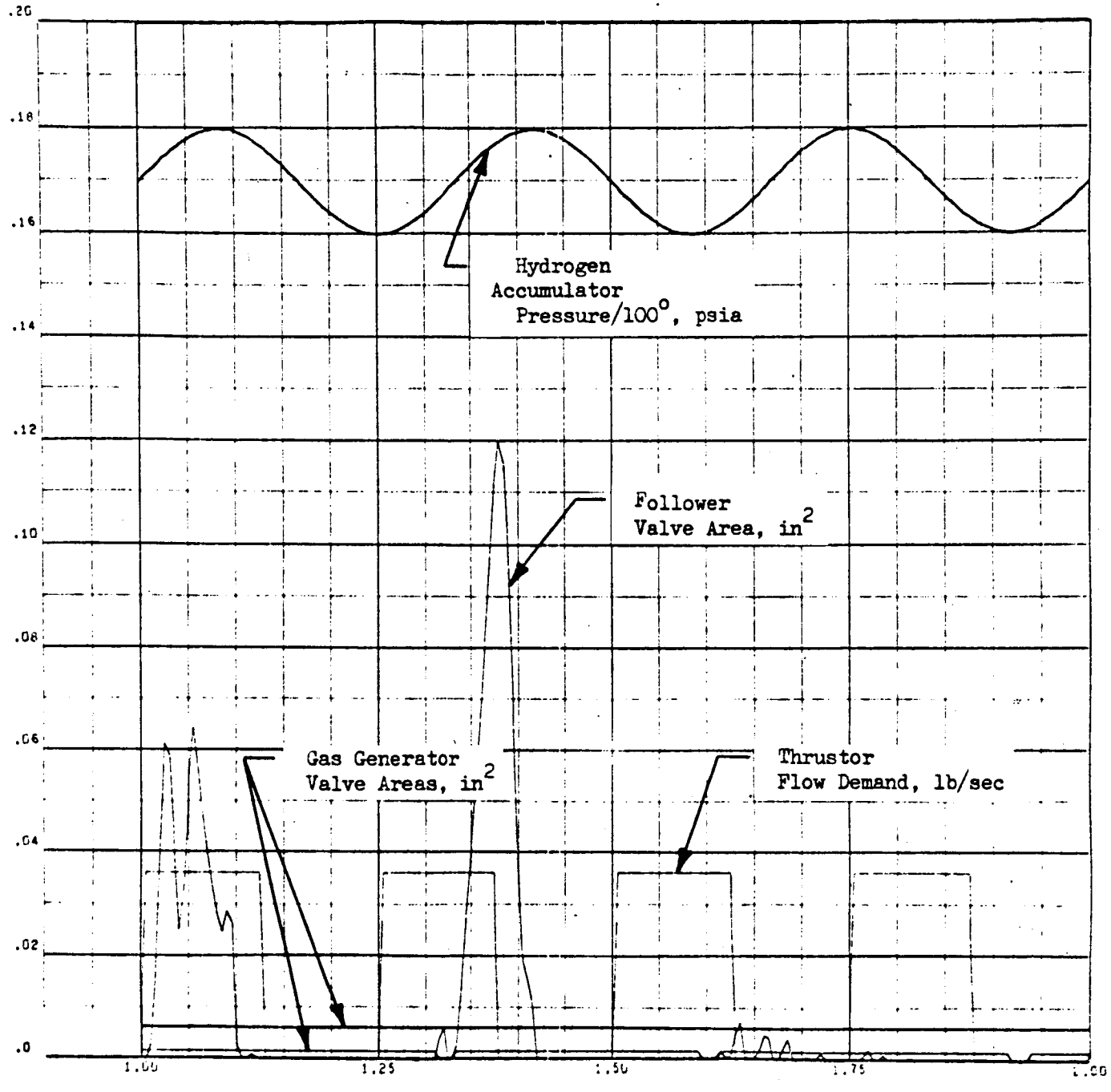

Figure 114. Results for Simulated Conditioner Operation with an Oscillating Hydrogen Accumulator Pressure and Follower Valve Control - Valve Operation

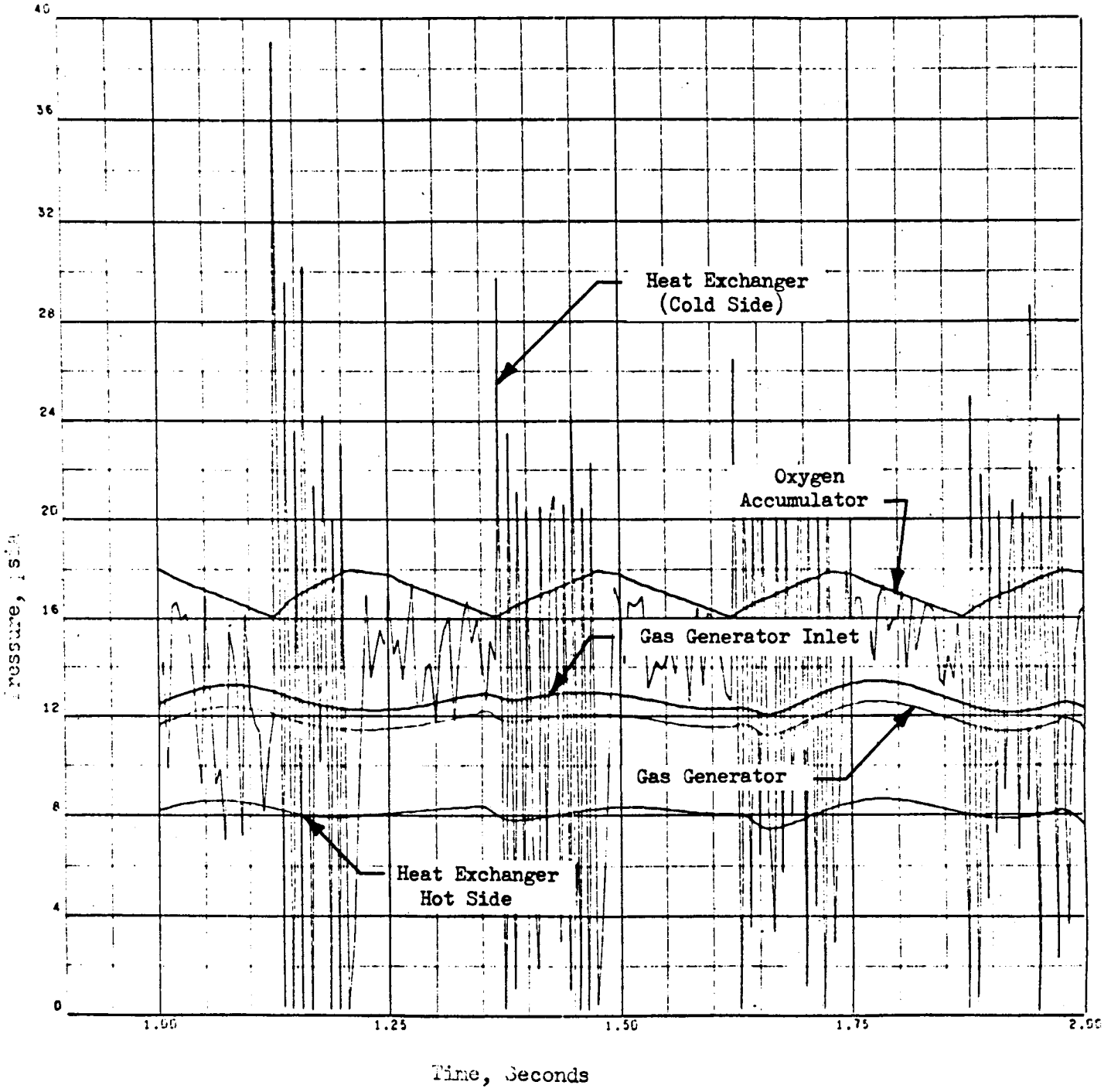

Figure 115. Results for Simulated Conditioner Operation with an Oscillating Hydrogen Accumulator Pressure and Follower Valve Control - System Pressures

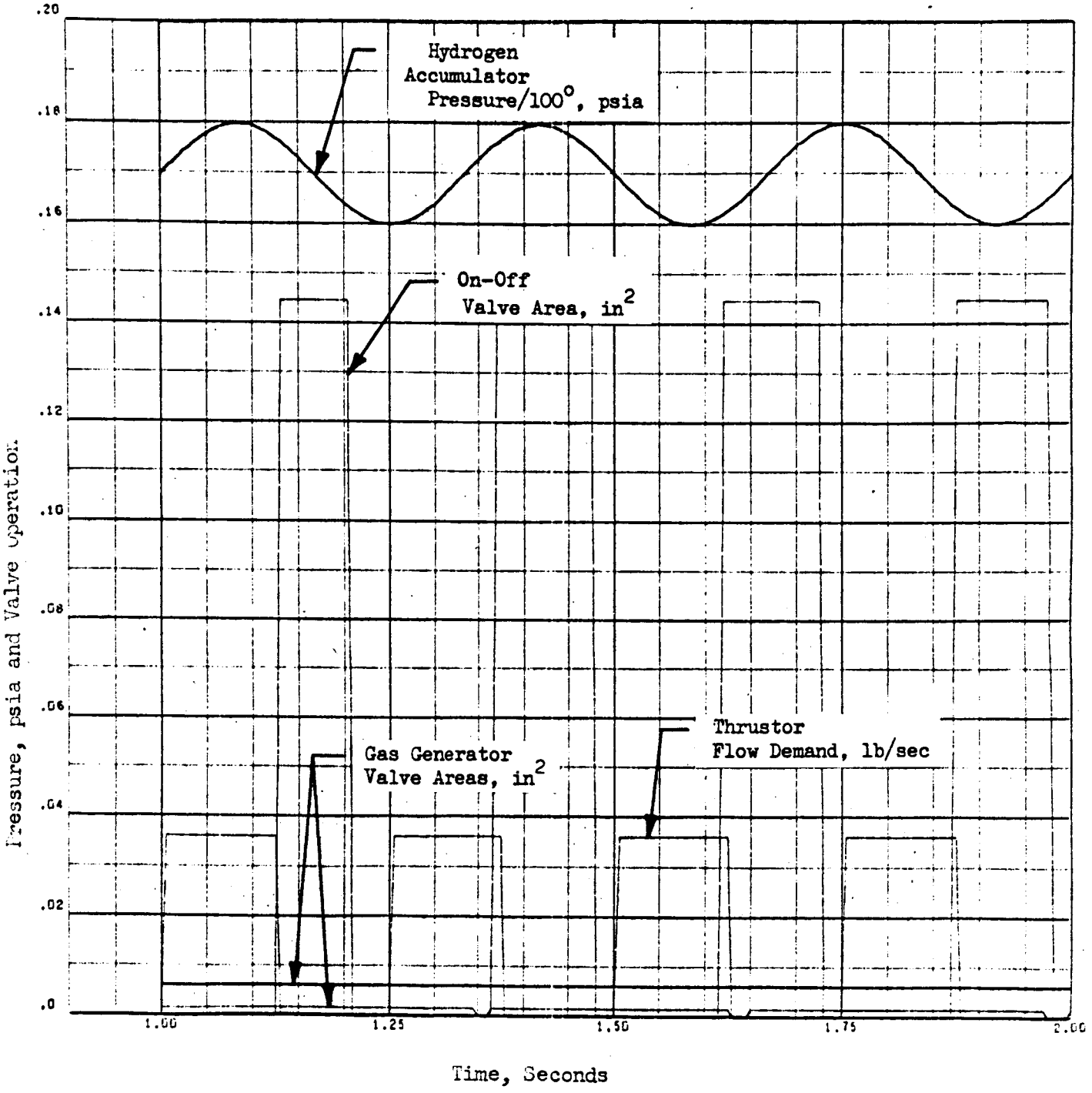

Figure 116. Results for Simulated Conditioner Operation with an Oscillating Hydrogen Accumulator Pressure and On-Off Valve Control - Valve Operation

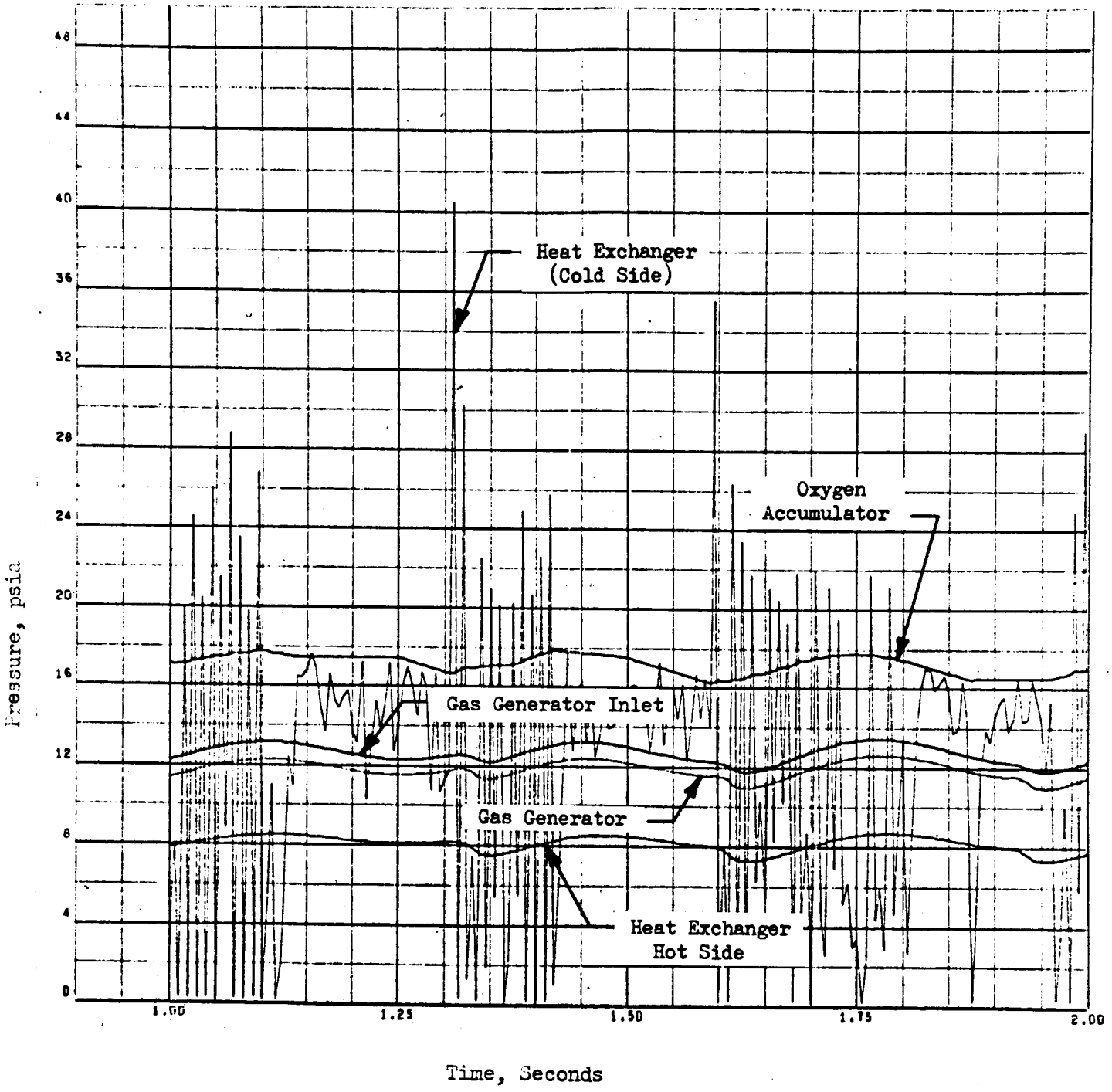

Figure 117. Results for Simulated Conditicner Operation with an Oscillating Hydrogen Accumulator Pressure and On-Off Valve Control - System Pressures

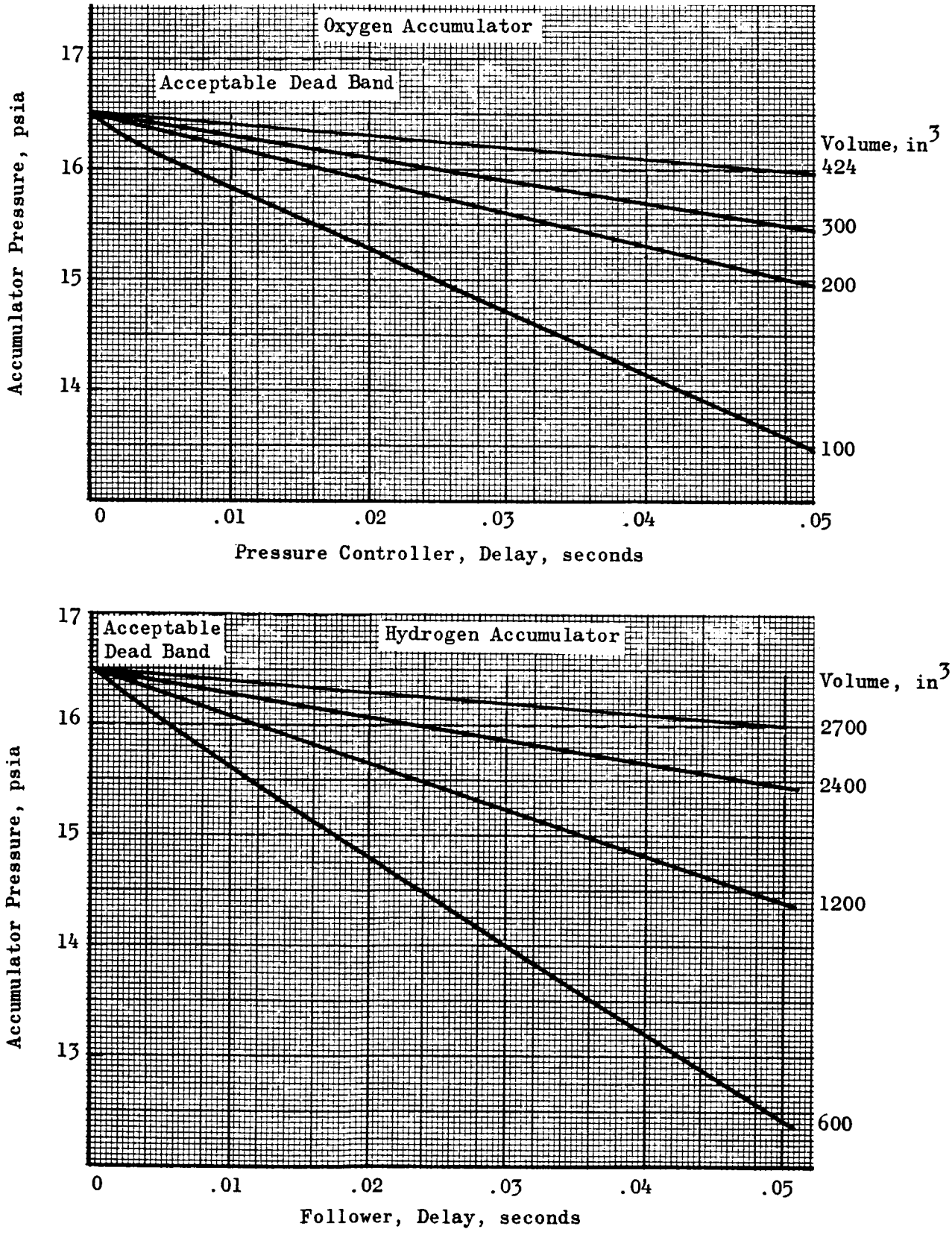

Figure118. Accumulator Sizing Chart Based on Valve Response

APPENDIX A

Computer Deck Listing of the Main Program for Thrustor Simulation

THE FOLLOWING IS A LISTING OF THE INPUT DECK DECK 1

```
C                  AL LIEBMAN  VN-2  X-6085      D2-H2 THRUSTER MODEL        00000100
      DIMENSION XT(250),XPCLD(250),XPCLH(250),XPCM(250),XPC(250),XTCM(250)00000200
     1D),XTCAT(250),XTC(250),XAVCD(250),XAVCH(250),XEUN(250),XXMR(250)     00000300
     2,XTCD(250),XE(250),XTI(250),XTMIX(250)                               00000400
     3,XTCAT1(250),XTCAT2(250),XTCAT3(250),XTCAT4(250),XTCAT5(250)         00000500
     4,XWDCD1(250),XWDCD2(250),XWDCH1(250),XWDCH2(250),XWDOT(250),XXISP(00000600
     5250),XPCAT1(250),XPCAT2(250),XPCAT3(250),XPCAT4(250),XPCAT5(250)     00000700
     6,XWDC(250)                                                           00000710
      COMMON TDEL,TMAX,PRT,FREQ,DC                                         00000800
     2,FREQD,AMPD,FREQH,AMPH,TSSG                                          00000802
     3,TSS1,TSS2,TSS3,TSS4,TSS5                                            00000804
     4,VCLD,VCLH,VCM,VMIX,VC                                               00000806
     5,TVDD,TVDH,TVCD,TVCH,TVDOT                                           00000808
      COMMON TVDH1,TVCDT,TVCH1,SWITCD,SWITCH                               00000810
     2,PAON,PAHN,PLON,PLHN,PIN                                             00000812
     3,PMN,PCN,WDOTN,WDD2N,WDH1N                                           00000814
     4,WDH2N,TAON,TAHN,PAD1,PAH1                                           00000816
     5,TAD,TAH,TCATD,TAUBV,TBV                                             00000818
      COMMON CC,TAUD,TAUH,TMIXD,CMIX                                       00000820
     1,EGD,EGH                                                             00000821
C                  EGD,EGH =1-SINE ,2-SQUARE,3-EXP                       00000822
C     WDT=.05,WDD1N=.0143,WDD2N=.0214,WDH1N=.0143,WDH2N=.00001             00000850
C     PAON=PAHN=17. ,TAD=TAH=200.                                          00000851
    5 CALL DRWR(TDEL,1)                                                    00001700
C                  CONSTANTS                                             00001800
      SIGD=-1.                                                             00002000
      SIGH=1.                                                              00002100
      NEGD=EGD+.1                                                          00002150
      NEGH=EGH+.1                                                          00002151
      ZD=.627                                                              00002200
      ZH=.95                                                               00002300
      RD=580.                                                              00002400
      RH=9200.                                                             00002500
      CPD=.24                                                              00002600
      CPH=.29                                                              00002610
      XMPI=WDD1N/WDH1N                                                     00002630
      XMW=(XMPI+1.)/(XMPI/32.+.5)                                          00002640
      RM=1545.*12./XMW                                                     00002649
```

THE FOLLOWING IS A LISTING OF THE INPUT DECK DECK 1

```
      TM=(WDO1N*CPO*TAON + WDH1N*CPH*TAHN)/(WDO1N*CPO+WDH1N*CPH)          00002650
      WDI=WDO1N+WDH1N                                                     00002660
      WDON=WDO1N+WDO2N                                                    00002670
      WDHN=WDH1N+WDH2N                                                    00002680
      WDT=WDON+WDHN                                                       00002690
      CALL AREA(PAON,PLON,TAON,RO,WDON,AVCOX)                             00003210
      CALL AREA(PAHN,PLHN,TAHN,RH,WDHN,AVCHX)                             00003220
      CALL AREA(PLON,PIN,TAON,RO,WDO1N,ACLO1)                             00003230
      CALL AREA(PLHN,PIN,TAHN,RH,WDH1N,ACLH1)                             00003240
      CALL AREA(PLON,PCN,TAON,RO,WDO2N,ACLO2X)                            00003250
      CALL AREA(PLHN,PCN,TAHN,RH,WDH2N,ACLH2)                             00003260
      CALL AREA(PIN,PMN,TM,RM,WDI,AMX)                                    00003270
      TSUM=TSS1+TSS2+TSS3+TSS4+TSS5                                       00004004
      PDCAT=PMN-PCN                                                       00004006
      DP1=TSS1*PDCAT/TSUM                                                 00004008
      DP2=TSS2*PDCAT/TSUM                                                 00004012
      DP3=TSS3*PDCAT/TSUM                                                 00004016
      DP4=TSS4*PDCAT/TSUM                                                 00004020
      DP5=TSS5*PDCAT/TSUM                                                 00004024
      PCT1=PMN                                                            00004028
      PCT2=PCT1-DP1                                                       00004032
      PCT3=PCT2-DP2                                                       00004036
      PCT4=PCT3-DP3                                                       00004040
      PCT5=PCT4-DP4                                                       00004044
      RHO=(PCT1/TSS1+PCT2/TSS1+PCT2/TSS2+PCT3/TSS2+PCT3/TSS3+PCT4/TSS3+P00004048
     1CT4/TSS4+PCT5/TSS4+PCT5/TSS5+10./TSS5)/(10.*RM)                     00004052
      AC=WDI/SQRTF(772.*RHO*PDCAT)                                        00004056
      XIM=WDON/WDHN                                                       00004060
      CALL RMIX(XIM,TCOMB)                                                00004064
      RCOMB=18540./(1.7)*XIM+2.3)                                         00004068
      AT=WDT*SQRTF(1.4*286.*RCOMB*TCOMB)/(PCN*286.*.8102)                 00004100
      WRITE OUTPUT TAPE 6,7,WDO1N,WDO2N,WDH1N,WDH2N,WDI,WDON,WDHN,WDT,XI00004150
     1M,TCOMB,RCOMB,PCN,AT                                                00004151
    7 FORMAT(6E17.8)                                                      00004152
      WRITE OUTPUT TAPE 6,7999                                            00004190
 7999 FORMAT(5X,2HAT,9X,2HAC,9X,3HAMX,8X,4HAVCO,7X,4HAVCH,7X,3HAIO,8X,3H00004191
     1AIF,8X,5HACLO2,6X,5HACLH2)                                          00004192
      WRITE OUTPUT TAPE 6,8000,AT,AC,AMX,AVCOX,AVCHX,ACLO1,ACLH1,ACLO2X,00004200
```

```
THE FOLLOWING IS A LISTING OF THE INPUT DECK                    DECK     1

      1ACLH2                                                                00004201
   8000 FORMAT(5E12.5)                                                      00004300
C                    INITIAL CONDITIONS                                    00004400
      WCLO=0.                                                               00004500
      WCLH=0.                                                               00004600
      WCO1=0.                                                               00004700
      WCH1=0.                                                               00004800
      WCM=0.                                                                00004850
      DAO=PAO1/(RO*TAO)                                                     00004900
      DAH=PAH1/(RH*TAH)                                                     00005000
      PCLO=0.                                                               00005100
      PCLH=0.                                                               00005200
      PCM=0.                                                                00005300
      PCAT1=0.                                                              00005350
      PC=0.                                                                 00005400
      F=0.                                                                  00005500
      AVCO=0.                                                               00005600
      AVCH=0.                                                               00005700
      T=0.                                                                  00005800
      TI=0.                                                                 00005900
      I=1                                                                   00006000
      IPRT=PRT+.1                                                           00006100
      IPR=IPRT-1                                                            00006200
      TCO=0.                                                                00006300
      TC=0.                                                                 00006400
      TMIX=TMIXO                                                            00006450
      TCAT1=TCATO                                                           00006500
      TCAT2=TCATO                                                           00006600
      TCAT3=TCATO                                                           00006700
      TCAT4=TCATO                                                           00006800
      TCAT5=TCATO                                                           00006900
      NO=0                                                                  00007000
      NH=0.                                                                 00007100
      NVO=0.                                                                00007200
      NVH=0.                                                                00007300
      TDOO=0.                                                               00007400
      TDCO=0.                                                               00007500
      TDOH=0.                                                               00007600
```

```
THE FOLLOWING IS A LISTING OF THE INPUT DECK                    DECK    1

      TDCH=0.                                                                  00007700
      WDC01=0.                                                                 00007800
      WDC02=0.                                                                 00007900
      WDCH1=0.                                                                 00008000
      WDCH2=0.                                                                 00008100
      XMR=0.                                                                   00008200
      TCATC=0.                                                                 00008300
      NBV=0                                                                    00008400
      ACL02=0.                                                                 00008500
      NCATR=0                                                                  00008600
      CALL QCAT(NCATR,TSSG,TSS1,TSS2,TSS3,TSS4,TSS5,1.,1.,1.,TDEL,1.,1.,00008700
     *1.,0.,0.,0.,0.,0.,0.)                                                    00008701
C                 COMPUTATION                                                 00008800
 8001 IF(T-TAUD)8002,8002,8002                                                00008900
 8002 TTD=T-TAUD                                                              00008910
      CALL FUNGEN(NEGD,AMPD,FREQD,PAD1,TTD,1.,PAD)                            00008920
      GO TO 104                                                               00008930
 8003 PAD=PAD1                                                                00008940
  104 IF(T-TAUH)106,105,105                                                   00008950
  105 TTH=T-TAUH                                                              00008960
      CALL FUNGEN(NEGH,AMPH,FREQH,PAH1,TTH,1.,PAH)                            00008970
      GO TO 8005                                                              00008980
  106 PAH=PAH1                                                                00008990
 8005 CONTINUE                                                                00009000
      CALL FUNGEN(2,-1.,FREQ,.5,T,DC,FP)                                      00009100
      IF(FP)110,110,120                                                       00009200
  110 TAUVD=TVDD                                                              00009300
      TAUVH=TVDH                                                              00009400
      GO TO 130                                                               00009500
  120 TAUVD=TVCD                                                              00009600
      TAUVH=TVCH                                                              00009700
  130 CALL DELAY(FP,ND,TDDD,TDCD,TAUVD,TDEL)                                  00009800
      CALL DELAY(FP,NH,TDDH,TDCH,TAUVH,TDEL)                                  00009900
      IF(ND)140,140,150                                                       00010000
  140 AVCD=AVCD-(TDEL/TVCD1)*AVCDX                                            00010100
      AVCD=MAXF(0.,AVCD)                                                      00010200
      GO TO 160                                                               00010300
  150 AVCD=AVCD+(TDEL/TVDD1)*AVCDX                                            00010400
```

```
      AVCO=MIN1F(AVCO,AVCOX)                                          00010500
      NVO=NVO+1                                                       00010600
  160 IF(NH)170,170,180                                               00010700
  170 AVCH=AVCH-(TDEL/TVCH1)*AVCHX                                    00010800
      AVCH=MAX1F(0.,AVCH)                                             00010900
      GO TO 190                                                       00011000
  180 AVCH=AVCH+(TDEL/TVCH1)*AVCHX                                    00011100
      AVCH=MIN1F(AVCH,AVCHX)                                          00011200
      NVH=NVH+1                                                       00011300
  190 IF(NVO)200,200,8007                                             00011400
 8007 IF(AVCO)8015,8015,8010                                          00011500
 8010 CALL FLOG(PAO,PCLO,AVCO,DAO,WDCLO)                              00011600
      GO TO 8017                                                      00011700
 8015 WDCLO=0.                                                        00011800
 8017 CALL ACCUM(SIGO,TDEL,WCLO,TAO,WDCLO,TAO,0.,0.,PCLO,VCLO,DCLO)   00011900
      CALL FLOG(PCLO,PCM,ACLO1,DCLO,WDCO1)                            00012000
      IF(NRV)8020,8020,8025                                           00012100
 8020 IF(SWITCO)8024,8024,8021                                        00012200
 8021 IF(TAURV)8023,8023,8022                                         00012300
 8022 IF(T-TAURV)8024,8025,8025                                       00012400
 8023 IF(TCATE-1500.)8024,8025,8025                                   00012500
 8024 WDCO2=0.                                                        00012600
      GO TO 300                                                       00012700
 8025 NRV=1                                                           00012800
      ACLO2=ACLO2+TDEL*ACLO2X/TRV                                     00012900
      ACLO2=MIN1F(ACLO2,ACLO2X)                                       00013000
      CALL FLOG(PCLO,PC,ACLO2,DCLO,WDCO2)                             00013100
  300 IF(NVH)320,320,8024                                             00013200
 8024 IF(AVCH)8040,8040,8030                                          00013300
 8030 CALL FLOG(PAH,PCLH,AVCH,DAH,WDCLH)                              00013400
      GO TO 8050                                                      00013500
 8040 WDCLH=0.                                                        00013600
 8050 CALL ACCUM(SIGH,TDEL,WCLH,TAH,WDCLH,TAH,0.,0.,PCLH,VCLH,DCLH)   00013700
      CALL FLOG(PCLH,PCM,ACLH1,DCLH,WDCH1)                            00013800
      IF(SWITCH)8060,8060,8070                                        00013900
 8060 WDCH2=0.                                                        00014000
      GO TO 320                                                       00014100
 8070 CALL FLOG(PCLH,PC,ACLH2,DCLH,WDCH2)                             00014200
```

```
THE FOLLOWING IS A LISTING OF THE INPUT DECK                    DECK    1

     220 IF(NVO+NVH)9000,9000,8080                                          00014300
    8080 CALL GMIX(TDEL,WCO1,WCH1,WDCO1,WDCH1,TAO,TAH,TCM,PCM,RCAT,VCM,DCM)00014400
         CALL FLOG(PCM,PCAT1,AMX,DCM,WDM)                                   00014500
         RCM=PCM/(DCM*TCM)                                                  00014504
         WCM=WCM+(WDM-WDC)*TDEL                                             00014507
         WCM=MAX1F(0.,WCM)                                                  00014508
         IF(WDM)8083,8083,8082                                              00014509
    8082 CPM=(RCAT*.24+2.9)/(RCAT+1.)                                       00014510
         TMIX=TMIX+(TCM-TMIX)/(1.+CMIX/(WDM*TDEL*CPM))                      00014511
         TCM1=TMIX                                                          00014512
         TCM1=MAX1F(0.,TCM1)                                                00014513
    8083 PCAT1=WCM*RCM*TCM1/VMIX                                            00014514
         IF(PC)8084,8084,8086                                               00014516
    8084 RHOC=.5*PCAT1/(RCM*TCM1)                                           00014520
    8086 DELP=PCAT1-PC                                                      00014524
         IF(RHOC)520,510,510                                                00014528
     510 IF(DELP)520,530,520                                                00014532
     520 WRITE OUTPUT TAPE 6,525,T,PCAT1,PC,RHOC                            00014536
     525 FORMAT(6F15.6)                                                     00014540
     530 RHOC=MAX1F(0.,RHOC)                                                00014544
         DELP=MAX1F(0.,DELP)                                                00014548
         WDC=AC*SQRTF(772.*RHOC*DELP)                                       00014552
         IF(WDC+PC)9000,9000,8095                                           00014600
    8095 CALL QCAT(NCATB,TCM1,TCAT1,TCAT2,TCAT3,TCAT4,TCAT5,TCATC,CC,WDC,TD00014900
        1EL,QCT,RCAT,PCAT1,PCAT2,PCAT3,PCAT4,PCAT5,PC,RHOC)                 00015000
         CALL COMB(TDEL,AT,VC,WDC,WDCO2,WDCH2,RCAT,TC,PC,XMR,QCT,WDOTN)     00015200
         TC=MAX1F(TC,TCAT5)                                                 00015300
         XXXMR=XMP                                                          00015400
         XMR=MAX1F(.2,XMR)                                                  00015500
         XMR=MIN1F(XMR,4.)                                                  00015600
         IF(XMR-1.)8100,8110,8110                                           00015700
    8100 CF=1.855-.105* XMR                                                 00015800
         GO TO 8140                                                         00015900
    8110 IF(XMR-1.5)8120,8120,8130                                          00016000
    8120 CF=1.75                                                            00016100
         GO TO 8140                                                         00016200
    8130 CF=1.68 + .047 * XMR                                               00016300
    8140 F=PC * AT * CF * .987                                              00016400
```

```
      XMR=XXXMR                                                    00016500
      TI=TI + F*TDEL                                               00016600
      WCLO=WCLO-(WDCO1+WDCO2)*TDEL                                 00016700
      WCLH=WCLH-(WDCH1+WDCH2)*TDEL                                 00016800
      WCO1=WCO1-(WDC*RCAT/(RCAT+1.))*TDEL                          00016900
      WCH1=WCH1-(WDC/(RCAT+1.))*TDEL                               00017000
C                  OUTPUT AND SEQUENCING                          00017100
 9000 IPR=IPR + 1                                                  00017200
      IF(IPR-IPRT)9040,9020,9020                                   00017300
 9020 XT(I)=T                                                      00017400
      XPCLO(I)=PCLO                                                00017500
      XPCLH(I)=PCLH                                                00017600
      XPCM(I)=PCM                                                  00017700
      XPC(I)=PC                                                    00017800
      XF(I)=F                                                      00017900
      XTI(I)=TI                                                    00018000
      XTMIX(I)=TMIX                                                00018020
      XTCAT1(I)=TCAT1                                              00018100
      XTCAT2(I)=TCAT2                                              00018200
      XTCAT3(I)=TCAT3                                              00018300
      XTCAT4(I)=TCAT4                                              00018400
      XTCAT5(I)=TCAT5                                              00018500
      XPCAT1(I)=PCAT1                                              00018504
      XPCAT2(I)=PCAT2                                              00018508
      XPCAT3(I)=PCAT3                                              00018512
      XPCAT4(I)=PCAT4                                              00018516
      XPCAT5(I)=PCAT5                                              00018520
      XTC(I)=TC                                                    00018600
      XTCO(I)=TCATC                                                00018700
      XAVCO(I)=AVCO*100.                                           00018800
      XAVCH(I)=AVCH*100.                                           00018900
      XFUN(I)=-10.*FR + 5.                                         00019000
      XXMR(I)=XMR/100.                                             00019100
      XWDC(I)=WDC                                                  00019110
      XWDCO1(I)=WDCO1                                              00019200
      XWDCO2(I)=WDCO2                                              00019300
      XWDCH1(I)=WDCH1                                              00019400
      XWDCH2(I)=WDCH2                                              00019500
```

```
      XWDOT(I)=WDOTN                                                    00019600
      IF(XWDOT(I))9024,9024,9026                                        00019700
 9024 XXISP(I)=0.                                                       00019800
      GO TO 9030                                                        00019900
 9026 XXISP(I)=F/XWDOT(I)                                               00020000
      XXISP(I)=MINF(420.,XXISP(I))                                      00020001
 9030 I=I+1                                                             00020100
      IPR=0                                                             00020200
 9040 T=T+TDEL                                                          00020300
      IF(I-202)9050,9060,9060                                           00020400
 9050 IF(T-TMAX)8001,8001,9060                                          00020500
 9060 NPT=I-1                                                           00020600
      WRITE OUTPUT TAPE 6,9080                                          00020650
 9080 FORMAT(1H1,3X,1HT,7X,4HPCLO,5X,4HPCLH,5X,3HPCM,6X,2HPC,7X,5HTCAT1,00020651
     14X,2HTC,7X,4HAVCO,5X,4HAVCH,5X,4HFGEN,5X,3HTCC,6X,1HF)            00020652
      WRITE OUTPUT TAPE 6,9061,(XT(I),XPCLO(I),XPCLH(I),XPCM(I),XPC(I),X00020700
     1TCAT1(I),XTC(I),XAVCO(I),XAVCH(I),XFUN(I),XTCO(I),XF(I),I=1,NPT)   00020800
 9061 FORMAT(12F9.3)                                                    00020900
      WRITE OUTPUT TAPE 6,9081                                          00020950
 9081 FORMAT(1H1,1X,4HTIME,4X,3HTOT,1X,3HIMP,3X,4HTIME,4X,3HTOT,1X,3HIMP00020951
     1,3X,4HTIME,4X,3HTOT,1X,3HIMP,3X,4HTIME,4X,3HTOT,1X,3HIMP,3X,4HTIME00020952
     2,4X,3HTOT,1X,3HIMP,3X,4HTIME,4X,3HTOT,1X,3HIMP)                   00020953
      WRITE OUTPUT TAPE 6,9062,(XT(I),XTI(I),I=1,NPT)                   00021000
 9062 FORMAT(6(F8.3,F10.1))                                             00021100
 9065 CALL SCPLTV(NPT,XT,1,48,IP,8,XPCLO,XPCLH,XPCM,XPC,XAVCO,XAVCH,XFUN00021200
     1,XF)                                                              00021200
      CALL LINPTV(NPT,XT,XPCLO,0,IR)                                    00021400
      CALL LINPTV(NPT,XT,XPCLH,0,IR)                                    00021500
      CALL LINPTV(NPT,XT,XPCM,0,IR)                                     00021600
      CALL LINPTV(NPT,XT,XPC,0,IR)                                      00021700
      CALL LINPTV(NPT,XT,XAVCO,0,IR)                                    00021800
      CALL LINPTV(NPT,XT,XAVCH,0,IR)                                    00021900
      CALL LINPTV(NPT,XT,XFUN,0,IR)                                     00022000
      CALL LINPTV(NPT,XT,XF,0,IR)                                       00022100
      CALL SCPLTV(NPT,XT,1,48,IP,9,XXISP,XTCAT1,XTCAT2,XTCAT3,XTCAT4,XTC00022200
     1AT5,XTC,XTCO,XTMIX)                                               00022300
      CALL LINPTV(NPT,XT,XXISP,0,IR)                                    00022400
      CALL LINPTV(NPT,XT,XTCAT1,0,IR)                                   00022500
```

```
      CALL LINPTV(NPT,XT,XTCAT2,0,IR)                                   00022600
      CALL LINPTV(NPT,XT,XTCAT3,0,IR)                                   00022700
      CALL LINPTV(NPT,XT,XTCAT4,0,IR)                                   00022800
      CALL LINPTV(NPT,XT,XTCAT5,0,IR)                                   00022900
      CALL LINPTV(NPT,XT,XTC,0,IR)                                      00023000
      CALL LINPTV(NPT,XT,XTCO,0,IR)                                     00023100
      CALL LINPTV(NPT,XT,XTMIX,0,IR)                                    00023110
      CALL SCPLTV(NPT,XT,1,48,IR,7,XWDCO1,XWDCO2,XWDCH1,XWDCH2,XWDOT,XXM00023200
     1R,XWDC)                                                           00023300
      CALL LINPTV(NPT,XT,XWDCO1,0,IR)                                   00023400
      CALL LINPTV(NPT,XT,XWDCO2,0,IR)                                   00023500
      CALL LINPTV(NPT,XT,XWDCH1,0,IR)                                   00023600
      CALL LINPTV(NPT,XT,XWDCH2,0,IR)                                   00023700
      CALL LINPTV(NPT,XT,XWDOT,0,IR)                                    00023800
      CALL LINPTV(NPT,XT,XXMR,0,IR)                                     00023900
      CALL LINPTV(NPT,XT,XWDC,0,IR)                                     00023910
      CALL SCPLTV(NPT,XT,1,48,IR,6,XPCAT1,XPCAT2,XPCAT3,XPCAT4,XPCAT5,XP00023950
     1C)                                                                00023951
      CALL LINPTV(NPT,XT,XPCAT1,0,IR)                                   00023955
      CALL LINPTV(NPT,XT,XPCAT2,0,IR)                                   00023956
      CALL LINPTV(NPT,XT,XPCAT3,0,IR)                                   00023957
      CALL LINPTV(NPT,XT,XPCAT4,0,IR)                                   00023958
      CALL LINPTV(NPT,XT,XPCAT5,0,IR)                                   00023959
      CALL LINPTV(NPT,XT,XPC,0,IR)                                      00023960
      WRITE OUTPUT TAPE 6,9082                                          00023980
 9082 FORMAT(1H1,3X,1HT,8X,5HWDCO1,5X,5HWDCO2,5X,5HWDCH1,5X,5HWDCH2,6X,200023981
     1HMR,7X,2HISP,5X,5HWDOTN,5X,5HWDOTC)                               00023982
      WRITE OUTPUT TAPE 6,9063,(XT(I),XWDCO1(I),XWDCO2(I),XWDCH1(I),XWDC00024000
     1H2(I),XXMR(I),XXISP(I),XWDOT(I),XWDC(I),I=1,NPT)                  00024100
 9063 FORMAT(9E10.4)                                                    00024200
      WRITE OUTPUT TAPE 6,9083                                          00024240
 9083 FORMAT(1H1,5X,1HT,6X,5HPCAT1,5X,5HPCAT2,5X,5HPCAT3,5X,5HPCAT4,5X,500024241
     1HPCAT5)                                                           00024242
      WRITE OUTPUT TAPE 6,9064,(XT(I),XPCAT1(I),XPCAT2(I),XPCAT3(I),XPCA00024250
     1T4(I),XPCAT5(I),I=1,NPT)                                          00024252
 9064 FORMAT(6E10.2)                                                    00024254
      IF(T-TMAX)9070,5,5                                                00024300
 9070 XT(1)=XT(201)                                                     00024400
```

```
      XPCLO(1)=XPCLO(201)                                          00024500
      XPCLH(1)=XPCLH(201)                                          00024600
      XPCM(1)=XPCM(201)                                            00024700
      XPC(1)=XPC(201)                                              00024800
      XTMIX(1)=XTMIX(201)                                          00024850
      XTCAT1(1)=XTCAT1(201)                                        00024900
      XTCAT2(1)=XTCAT2(201)                                        00025000
      XTCAT3(1)=XTCAT3(201)                                        00025100
      XTCAT4(1)=XTCAT4(201)                                        00025200
      XTCAT5(1)=XTCAT5(201)                                        00025300
      XPCAT1(1)=XPCAT1(201)                                        00025304
      XPCAT2(1)=XPCAT2(201)                                        00025308
      XPCAT3(1)=XPCAT3(201)                                        00025312
      XPCAT4(1)=XPCAT4(201)                                        00025316
      XPCAT5(1)=XPCAT5(201)                                        00025320
      XTC(1)=XTC(201)                                              00025400
      XTCO(1)=XTCO(201)                                            00025500
      XAVCO(1)=XAVCO(201)                                          00025600
      XAVCH(1)=XAVCH(201)                                          00025700
      XEUN(1)=XEUN(201)                                            00025800
      XE(1)=XE(201)                                                00025900
      XXMR(1)=XXMR(201)                                            00026000
      XTI(1)=XTI(201)                                              00026100
      XWDC(1)=XWDC(201)                                            00026110
      XWDCO1(1)=XWDCO1(201)                                        00026200
      XWDCO2(1)=XWDCO2(201)                                        00026300
      XWDCH1(1)=XWDCH1(201)                                        00026400
      XWDCH2(1)=XWDCH2(201)                                        00026500
      XWDOT(1)=XWDOT(201)                                          00026600
      XXISP(1)=XXISP(201)                                          00026700
      I=2                                                          00026800
      GO TO 8001                                                   00026900
      END                                                          00027000
```

APPENDIX B

Computer Deck Listing of Main Program for Conditioner Simulation

THE FOLLOWING IS A LISTING OF THE INPUT DECK DECK 1

```
C                AL LIEBMAN  VN-2  X-6095                                  C0000010
C             OX PROPELLANT CONDITIONER MODEL                               C0000020
      DIMENSION XT(250)     ,XTWC(250)  ,XTEXO(250),XTAC(250),XTGGO(250)   C0000030
     1,XTCATO(250),XTGEXO(250),XPEXC(250),XPAO(250),XPGO(250),XPGGO(250)C0000034
     2,XPGEXO(250),XAVO(250),XAGO(250),AGFX(250),XWDCO(250),XPTO(250),PEC0000038
     3XFX(250),XWDLO(250),XWDAO(250),XWDGC1(250),XWDGC2(250),WDGFX(250),C0000042
     4XWDGGC(250),XWDGXO(250),XWDXC(250)                                   C0000046
      COMMON TDEL,PRT,TMAX,DB1,DB3,                                        C0000100
     1DB3P,DB4,DB5,GL,QHX,                                                 C0000102
     2TDXVO,TDXGO,ARATC,VLOX,VGC,                                          C0000104
C                ARATO=AGO1/AGO2  WHEREAGO1 IS BYPASS,ZERO FOR NO BYPASSC0000105
     3VGGO,VGEXC,VAC,AGG,FREQGG,                                           C0000106
     4TAU,ATC,FREQTC,DCTC,ATO,                                             C0000108
     5FREQTC,TWC1,TC1,TC2,TO3,                                             C0000110
     6TO4,TO5,RLC,RGC1,RWO,                                                C0000112
     7CWO,PLT,XLIQ,VLIQ,FOLO                                               C0000114
     8,PARO,PACO                                                           C0000116
C          1-GG,2-CAT,3-ACC,4-HEX WALL,5-HEX OUTPUT                        C0000149
C                XLIQ=0.,GAS                                             C0000150
C                XLIQ=1.,LIQUID                                          C0000151
C                VLIQ=0.,MAIN PROP VALVE SIZED FOR GAS                   C0000152
C                VLIQ=1.AND XLIQ=1.,MAIN PROP VALVE SIZED FOR LIQUID     C0000153
C                PLT=0.,FLOWS NOT PRINTED PLT=1.,FLOWS PRINTED           C0000154
C                FOLO=0.,NO FOLLOWER VALVE                               C0000156
C                FOLO=1.,FOLLOWER VALVE                                  C0000158
C                FOLO=-2,NO FOL VALVE,NO PRESS CTL LOOP                  C0000160
    1 CALL DRWR(TDEL,1)                                                  C0000200
C                CONSTANTS                                               C0000300
      IPRT=PRT+.1                                                        C0000310
      PO3=17.                                                            C0000312
      NFOLO=FOLO+.1                                                      C0000314
      RHOLO=71.2/1728.                                                   C0000322
      DTO=.2837/1728.                                                    C0000324
      QVO=91.78                                                          C0000326
      CPO=.24                                                            C0000328
      RGF=9200.                                                          C0000330
      TLO=163.                                                           C0000332
      SIGO=-1.                                                           C0000334
```

THE FOLLOWING IS A LISTING OF THE INPUT DECK DECK 1

```
      RGO=588.                                                          CCOCC336
      ZO=.927                                                           CCOCC338
      IF(VLIQ+XLIQ-1.5)3,3,2                                            COOCC342
    2 AVOX=.C45/SQRTF(772.*RHOLC*2.)                                    CCOOC344
      GO TO 4                                                           CCOOC346
    3 CONTINUE                                                          CCOOC348
      CALL AREA(20.,19.,163.,578.,.C421,AVOX)                           COOOC350
    4 CONTINUE                                                          CCOCC351
      AEXO=AVOX                                                         CCOCC352
      CALL AREA(12.,11.,200.,3700.,.001363,AGGO)                        COOCC356
      CALL AREA(11.,6.,2500.,3700.,.001363,AGEXO)                       COOOC358
      CALL AREA(18.,17.,200.,578.,.C421,AAO)                            COOCO360
      CALL ASCN(1.4,3700.,600.,.0C1363,6.,AXO)                          COOOC362
      CALL ASCN(1.4,578.,200.,.C42),17.5,ARO)                           CCOCO364
      IF(ARATO)6,6,7                                                    COOCO368
    6 WDOGG=.CCC778                                                     COOCC369
      WDHGG=.CCC778                                                     COOCC370
      WDOHGG=WDOGG+WDHGG                                                COOOC371
      CALL AREA(12.,11.,200.,4914.,WDOHGG,AGGO)                         COOCO372
      CALL AREA(11.,6.,2000.,4914.,WDOHGG,AGEXO)                        CCOCC373
      CALL ASCN(1.4,4914.,600.,WDOHGG,6.,AXO)                           CCOCO374
      GO TO 8                                                           COOOC376
    7 WDOGG=.CCC778                                                     CCOCC378
      WDHGG=.CCC585                                                     COOOC38C
    8 CALL AREA(17.,12.,200.,578.,WDOGG,AGOX)                           COOCO382
      CALL AREA(17.,12.,200.,9200.,WDHGG,AGEXX)                         COOOO384
      XRO=1./((AVOX**2)*772.*RHOLC)                                     CCOCC430
      XLO=VLOX/((3.14**2)*386.)                                         COOOO432
      WLOX=RHOLC*VLOX                                                   CCOOC434
      WRITE OUTPUT TAPE 6,5,AVOX,AOOX,AGOX,AGGO,AGEXO,AAO,AXO,ARO,AGEXX CCOCC490
    5 FORMAT(9E10.6)                                                    00000491
C                   INITIAL CONDITIONS                                  COOCC500
      T=C.                                                              CCOOO505
      IPR=IPRT-1                                                        CCOCC5C6
      I=1                                                               CCOOC507
      WDTO=C.                                                           CCCCO5C9
      WDLO=C.                                                           COOCO510
      WDOO=C.                                                           COOOO515
```

```
      WDEXO=C.                                                    CCCCC520
      WDGO1=C.                                                    CCOC0525
      WDGO2=C.                                                    OOCCC530
      WDGF=0.                                                     COOCC535
      WDGGO=C.                                                    COCCC540
      WDGEXC=C.                                                   CCCOC545
      WDXO=C.                                                     COCCC550
      WDAO=C.                                                     COCCC555
      WORO=C.                                                     COOCC560
      WDCO=C.                                                     CCOOC565
      WLO=0.                                                      CCCCC600
      WLEXO=C.                                                    CCCCC603
      WEXO=PACC*29.0/(RGC*TWO1)                                   COOOC605
      WGF=0.                                                      COCCC610
      WGC2=C.                                                     CCCCC615
      WGGO=C.                                                     CCCCC620
      WGEXO=C.                                                    CCCCC625
      TEXO=TWC1                                                   COOCC655
      TEXC1=TEXC                                                  CCCCC656
      TEXF=TLO                                                    COOOC662
      TGC=TLO                                                     CCCCC665
      TAO=?CC.                                                    CCOCC670
      TTO=TLO                                                     CCCCC672
      TGGO=TLC                                                    COOOC680
      TCATC=TLC                                                   COOCC685
      TGEXO=TLO                                                   CCOCC687
      TWLO=TWO1                                                   COOOC689
      TWGO=TWO1                                                   CCCCC690
      TWO=TWO1                                                    COOCC691
      ER1=C.                                                      COCCC700
      ER2=C.                                                      COOCC705
      ER3=C.                                                      CCOOC710
      N1=0                                                        CCOCC715
      N2=C                                                        CCOCC720
      N3=0                                                        CCOCC725
      VEOL=C.                                                     CCCCC730
      PLO=C.                                                      COOCC740
      PEXO=15.                                                    COOCC750
```

THE FOLLOWING IS A LISTING OF THE INPUT DECK DECK 1

```
      PEXF=17.                                                          C0000755
      PGO=0.                                                            C0000760
      PGGO=C.                                                           C0000765
      PAO=PAOO                                                          C0000770
      DAO=PAO/(RGO*TAO)                                                 C0000771
      PGEXO=C.                                                          C0000772
      QH=0.                                                             C0000790
      TDO1=C.                                                           C0000800
      TDO2=C.                                                           C0000801
      TDO3=C.                                                           C0000802
      TDC1=C.                                                           C0000803
      TDC2=C.                                                           C0000804
      TDC3=0.                                                           C0000805
      AVO=0.                                                            C0000810
      AGO=0.                                                            C0000811
      AGF=C.                                                            C0000812
      XO=C.                                                             C0000816
      WAO=PAO*VAO/(RGO*TAO*ZO)                                          C0000820
      ISTART=C.                                                         C0000900
      NSTART=C.                                                         C0000901
      NPRIME=0                                                          C0000902
   10 CONTINUE                                                          C0001200
      CALL FUNGEN(1,ATC,FREQTC,20.,T,1.,PTC)                            C0001220
      IF(XLIQ-.5)11,11,500                                              C0001240
  500 IF(AVC)51C,51C,52C                                                C0001260
  51C WDLO=C.                                                           C0001280
      GO TO 55C                                                         C0001300
  52C NSTART=NSTART+1                                                   C0001320
      IF(PTO-PEXO)53C,53C,540                                           C0001340
  53C WDLO=C.                                                           C0001360
      GO TO 55C                                                         C0001380
  540 CALL FLOL(TDEL,XRC,XLO,PTC,PEXC,WDLC,WLC)                         C0001400
      IF(WLO-WLOX)55C,550,560                                           C0001410
  55C IF(NPRIME)12C,12C,580                                             C0001420
  56C NPRIME=NPRIME+1                                                   C0001430
  58C WDLO1=MAX1F(.C1,WDLO)                                             C0001434
      WDAO1=MAX1F(.C1,WDAC)                                             C0001438
      RWLO=RGO1 * ((.0391/WDLO1)**.8)/10.                               C0001442
```

```
 THE FOLLOWING IS A LISTING OF THE INPUT DECK                    DECK     1

      RWGO=RGO1 * ((200./TEXO)**.12) * ((.0391/WDAO))**.8)                  C0001446
      CALL FLEX(SIGO,TDEL,RWLO,RWGC,XC,XDELC,PEXC,TWLO,TWGO,TLC,TEXO,DEXC0001450
     1C,WLX,WEXC,VLCX,WLO,CWO,WLAC,WGAO)                                   C0001460
      TWO=XO*TWLC+(1.-XO)*TWGO                                              C0001465
      IF(WLAC)35,35,590                                                     C0001470
  590 TAO=(WAC*TAO+WLAC*(TLO-CVC/CPC)+WGAC*TEXC1)/(WAO+WLAC+WGAO)           C0001480
      TEXO1=TEXO                                                            C0001490
      WAC=WAO+WLAC+WGAC                                                     C0001500
      GO TO 35                                                              C0001510
   11 CONTINUE                                                              C0001600
      IF(AVO)12,12,20                                                       C0001610
   12 WDTO=0.                                                               C0001620
      GO TO 25                                                              C0001630
   20 NSTART=NSTART+1                                                       C0001705
      CALL FLOG(PTC,PLC,AVC,DTC,WDTC)                                       C0001710
   25 IF(NSTART)120,120,26                                                  C0001715
   26 CONTINUE                                                              C0001716
      CALL ACCUM(SIGO,TDEL,WLC,TLC,WDTC,TTO,0.,0.,PLO,VLCX,DLO)             C0001720
      CALL FLOG(PLO,PEXO,AEXC,DLC,WDLC)                                     C0001730
      WLO=WLO-WDLC*TDEL                                                     C0001732
      WLO=MAX1F(0.,WLO)                                                     C0001733
      WDLO1=MAX1F(.01,WDLC)                                                 C0001742
      RWGO=RGO1*((200./TEXO)**.12)*((.0391/WDLO1)**.8)                      C0001745
   34 CONTINUE                                                              C0001747
      CALL HEX(SIGO,TDEL,WDLO,RWGC,PEXO,TWO,TLO,TEXO,DEXC,WEXO,CWO)         C0001750
      TWGO=TWO                                                              C0001755
   35 CONTINUE                                                              C0001760
      IF(TAO-(TO3+DB3))50,50,80                                             C0001800
   50 IF(TAO-(TO3-DB3))100,120,120                                          C0001900
   80 ER2=1.                                                                C0002000
      ER3=1.                                                                C0002100
      GO TO 120                                                             C0002200
  100 ER2=-1.                                                               C0002300
      ER3=-1.                                                               C0002400
  120 IF(ISTART)240,240,125                                                 C0002450
  125 AGO2=AGO/(1.+ARATO)                                                   C0002495
      AGO1=AGO*ARATO/(1.+ARATO)                                             C0002496
  130 CALL FLOG(PAO,PGO,AGO2,DAO,WDGO2)                                     C0002520
```

```
      CALL FLOG(PAO,PGGC,AGO1,DAC,WDGC1)                                C0002525
      CALL FUNGEN(1,AGG,FREQGG,17.,T,1.,PEXF)                           CCOC2550
      TEXF=TAO                                                          C0002570
      DEXF=PEXF/(92CC.*TEXF)                                            CC002580
      CALL FLOG(PEXF,PGC,AGF,DEXF,WDGF)                                 C0002600
      CALL GMIX(TDEL,WGC2,WGF,WDGC2,WDGF,TAC,TEXF,TGO,PGC,XMRCAT,VGO,DG CCCC2700
     10)                                                                00002701
      CALL FLCG(PGO,PGGC,AGGO,DGC,WDGGC)                                CCOC2730
      CALL GGEN(WDGGO,WDGO1,XMRCAT,TDEL,TGGO,PGGO,VGGC,TCATO,WGGO,DGGO) 00002800
      CALL FLOG(PGGO,PGEXO,AGEXC,DGCC,WDEXO)                            C0C02900
      IF(TAC-(TC3+DB3))140,140,220                                      CCCC3000
  140 CONTINUE                                                          C0003100
      IF(TGGO-(TC1+DB1))150,150,180                                     00003300
  150 IF(TGGO-(TC1-DB1))160,190,190                                     CCOC3400
  160 ER2=-1.                                                           C0003500
      GO TO 200                                                         C0C03700
  180 ER2=1.                                                            C0C03800
      GO TO 200                                                         CC004000
  190 CONTINUE                                                          CCC04100
  200 IF(TCATO-TC2)220,22C,210                                          CCC04300
  210 ER2=1.                                                            C0004400
  220 CALL GGHEX(XC,TDEL,WGEXC,TGEXC,WDEXC,TGGO,TWLO,TWGO,RWO,CWO,VGEXO,CCCC4500
     1PGEXO)                                                            C0C04501
      TWO=XC*TWLC+(1.-XC)*TWGC                                          CC004510
  24C CONTINUE                                                          CCOC4690
      IF(AVO)25C,25C,276                                                C0004700
  250 IF(TWC-(TC4+DB4))260,260,274                                      CCCC4800
  260 IF(TWC-(TC4-DB4))270,276,276                                      CCCC4900
  27C ER2=-1.                                                           C0C05000
      ER3=-1.                                                           CC005100
      IF(TCATO-TO2)276,272,272                                          CC005120
  272 ER2=1.                                                            C0CC5130
      GO TO 276                                                         C0005200
  274 ER2=1.                                                            C0005300
      ER3=1.                                                            C0CC5310
  276 CALL DELAY(ER2,N2,TDC2,TDC2,TCXGC,TDEL)                           C0CC5320
      IF(N2)28C,28C,284                                                 CCOC5330
  280 AGO=C.                                                            C0C05340
```

```
      GO TO 288                                                          CC005350
  284 AGO=AGCX                                                           CC005360
      ISTART=ISTART+1                                                    C0005365
  288 CALL DELAY(ER3,N3,TD03,TDC3,TCXGC,TDEL)                            CCCC5370
      IF(N3)292,292,296                                                  C0005380
  292 AGF=C.                                                             CCC05390
      GO TO 300                                                          C0005400
  296 AGF=AGFXX                                                          CC005410
  300 CALL FLCSCN(SIGO,AXC,TGEXO,PGEXC,WDXC)                             C0CC5500
      IF(PEXO-PAO)305,305,310                                            CC005520
  305 WDAO=C.                                                            CCCC5530
      GO TO 315                                                          CCCC5540
  310 CALL FLOG(PEXC,PAC,AAO,DEXC,WCAC)                                  C0005550
      WEXO=WEXO-WDAC*TDEL                                                C0005555
      WEXO=MAXIF(C.,WEXO)                                                C0005556
  315 CALL ACCUM(SIGC,TDEL,WAC,TAC,WCAC,TEXO,QH,QL,PAC,VAC,DAC)          00CC5600
      IF(PAC-(PC3+DB3P))320,320,330                                      CCCC5700
  320 IF(PAC-(PC3-DB3P))350,360,360                                      CCCC5800
  330 ER1=1.                                                             CCCC5900
      IF(PAC-PARO)360,360,340                                            CC006000
  340 CALL FLCSCN(SIGO,ARC,TAC,PAC,WCRO)                                 CC006100
      GO TO 365                                                          C0006200
  350 ER1=-1.                                                            C0006300
  360 WDRO=C.                                                            CCCC6400
  365 IF(ER1)370,370,366                                                 CCCC6405
  366 IF(TAC-(TC3+DB3))380,370,370                                       C0006410
  370 QH=C.                                                              C00C6500
      GO TO 400                                                          CCCC6600
  380 IF(TAC-(TC3-DB3))390,400,400                                       CCCC6700
  390 QH=QHX                                                             CCCC6800
  400 IF(NFCLO)420,405,425                                               CCCC6850
  405 CALL DELAY(ER1,N1,TDC1,TDC1,TDXVO,TDEL)                            C00C6900
      IF(N1)410,410,420                                                  C00C7000
  410 AVO=C.                                                             CCCC7100
      GO TO 430                                                          C0007200
  420 AVO=AVOX                                                           C0C07300
      GO TO 430                                                          CCC07310
  425 CALL VALFCL(PAC,PEXF,TAC,TEXF,TDEL,VFCL,AVC)                       CCCC7320
```

```
  430 IF(T-TAU)440,435,435                                          CCOC7330
  435 CONTINUE                                                      C00C7340
      CALL FUNGEN(2,ATC,FREQTC,0.,T,CCTC,WDCO)                      CCCC7350
  440 CONTINUE                                                      CCCC7370
      WGO2=WGO2-(XMRCAT/(XMRCAT+1.))*WDGGC*TDEL                     CCCC7500
      WGF=WGF-WDGGO*TDEL/(XMRCAT+1.)                                C0CC7600
      WGGO=WGGC-WDEXC*TDEL                                          C00C7650
      WGEXO=WGEXC-WDXO*TDEL                                         CCCC7700
      WAO=WAO-(WDCC+WDRO+WDGO1+WDGC2)*TDEL                          CCCC7800
      WGO2=MAX1F(0.,WGC2)                                           CCCC7900
      WGF=MAX1F(0.,WGF)                                             0CCC7910
      WGGO=MAX1F(0.,WGGO)                                           CCCC7920
      WGEXO=MAX1F(0.,WGEXO)                                         CCCC7930
      WAO=MAX1F(0.,WAC)                                             CCCC7940
C                 OUTPUT                                          CC020000
 1000 IPR=IPR+1                                                     C0020100
      IF(IPR-IPRT)1040,1020,1020                                    CC02C200
 1020 XT(I)=T                                                       C0020300
      XPEXO(I)=PEXC                                                 C0020400
      XPAO(I)=PAC                                                   00020410
      XPGO(I)=PGC                                                   C0020415
      XPGGO(I)=PGGC                                                 CC020420
      XPGEXO(I)=PGEXO                                               CC02C430
      PEXFX(I)=PEXF/100.                                            C0020435
      XTWO(I)=TWC                                                   CC020440
      XTEXO(I)=TEXC                                                 C0020450
      XTAO(I)=TAC                                                   C002C460
      XTGGC(I)=TGGO/10.                                             C0020470
      XTCATC(I)=TCATC/10.                                           C0020480
      XTGEXO(I)=TGEXO                                               CC02C490
      XAVO(I)=AVC                                                   0002C500
      XAGO(I)=AGC                                                   C0020510
      AGFX(I)=AGF                                                   00020520
      XWDCO(I)=WDCC                                                 C002C530
      XPTO(I)=PTC/100.                                              00020540
      IF(PLT-.5)1030,1030,1025                                      CCC2C600
 1025 XWDLO(I)=WDLC/10.                                             C0020610
      XWDAO(I)=WDAC/10.                                             C0020620
```

```
      XWDGO1(I)=WDGO1                                                    C0020630
      XWDGO2(I)=WDGO2                                                    C0020640
      WDGEX(I)=WDGE                                                      C0020650
      XWDGGO(I)=WDGGO                                                    C0020660
      XWDGXO(I)=WDEXO                                                    C0020670
      XWDXO(I) =WDXO                                                     C0020680
 1030 I=I+1                                                              C0020800
      IPR=0                                                              C0020810
 1040 T=T+TDEL                                                           C0022100
      IF(I-202)1060,2000,2000                                            C0022200
 1060 IF(T-TMAX)10,10,2000                                               C0022300
 2000 NPT=I-1                                                            C0022400
      NAPRT=1                                                            C0022450
      NBPRT=NPT                                                          C0022451
 2100 WRITE OUTPUT TAPE 6,111,(XT(I),XTEXO(I),XTWO(I),XTGGO(I),XTCATO(I)C0022500
     1,XTGEXO(I),XTAO(I),XPEXO(I),XPGO(I),XPGEXO(I),XPAO(I),XPGGO(I),XWDO0022600
     2GO(I),XAVO(I),XAGO(I),AGEX(I),XPTO(I),PEXEX(I),I=NAPRT,NBPRT)      C0022700
  111 FORMAT(9F12.4)                                                     C0022800
 2500 CALL SCPLTV(NPT,XT,1,48,IR,6,XTEXO,XTWO,XTGGO,XTCATO,XTGEXO,XTAO)  C0022900
      CALL LINPTV(NPT,XT,XTEXO,0,IR)                                     C0023000
      CALL LINPTV(NPT,XT,XTWO,0,IR)                                      C0023100
      CALL LINPTV(NPT,XT,XTGGO,0,IR)                                     C0023200
      CALL LINPTV(NPT,XT,XTCATO,0,IR)                                    C0023300
      CALL LINPTV(NPT,XT,XTGEXO,0,IR)                                    C0023400
      CALL LINPTV(NPT,XT,XTAO,0,IR)                                      C0023500
      CALL SCPLTV(NPT,XT,1,48,IR,5,XPEXO,XPGGO,XPGEXO,XPAO,XPGO)         C0023600
      CALL LINPTV(NPT,XT,XPEXO,0,IR)                                     C0023700
      CALL LINPTV(NPT,XT,XPGGO,0,IR)                                     C0023800
      CALL LINPTV(NPT,XT,XPGEXO,0,IR)                                    C0023900
      CALL LINPTV(NPT,XT,XPAO,0,IR)                                      C0024000
      CALL LINPTV(NPT,XT,XPGO,0,IR)                                      C0024100
      CALL SCPLTV(NPT,XT,1,48,IR,6,XWDOO,XAVO,XAGO,AGEX,XPTO,PEXEX)      C0024200
      CALL LINPTV(NPT,XT,XWDOO,0,IR)                                     C0024300
      CALL LINPTV(NPT,XT,XAVO,0,IR)                                      C0024400
      CALL LINPTV(NPT,XT,XAGO,0,IR)                                      C0024500
      CALL LINPTV(NPT,XT,XPTO,0,IR)                                      C0024520
      CALL LINPTV(NPT,XT,AGEX,0,IR)                                      C0024530
      CALL LINPTV(NPT,XT,PEXEX,0,IR)                                     C0024540
```

THE FOLLOWING IS A LISTING OF THE INPUT DECK DECK 1

```
      IF(PLT-.5)2700,2700,2550                                                  C0024543
 2550 WRITE OUTPUT TAPE 6,111,(XT(I),XWDLO(I),XWDAO(I),XWDGO1(I),XWDGO2(CCC24545
     1I),WDGFX(I),XWDGGO(I),XWDGXO(I),XWDXO(I),I=NAPRT,NBPRT)                   CC024546
 2600 CALL SCPLTV(NPT,XT,1,48,IR,4,XWDLO,XWDAO,XWDGO1,XWDGO2)                   C0024550
      CALL LINPTV(NPT,XT,XWDLO,0,IR)                                            C0024551
      CALL LINPTV(NPT,XT,XWDAO,0,IR)                                            CC024552
      CALL LINPTV(NPT,XT,XWDGO1,0,IR)                                           C0024553
      CALL LINPTV(NPT,XT,XWDGO2,0,IR)                                           CC024554
      CALL SCPLTV(NPT,XT,1,48,IR,-4,WDGFX,XWDGGO,XWDGXO,XWDXO)                  C0024555
      CALL LINPTV(NPT,XT,WDGFX,0,IR)                                            CC024556
      CALL LINPTV(NPT,XT,XWDGGO,0,IR)                                           C0024557
      CALL LINPTV(NPT,XT,XWDGXO,0,IR)                                           CC024558
      CALL LINPTV(NPT,XT,XWDXO,0,IR)                                            C0024559
 2700 CONTINUE                                                                  C0024605
      IF(T-TMAX)3000,1,1                                                        C0024610
 3000 XT(1)=XT(201)                                                             CC024612
      XTEXO(1)=XTEXO(201)                                                       CC024614
      XTWO(1)=XTWO(201)                                                         CC024616
      XTGGO(1)=XTGGO(201)                                                       C0024618
      XTCATO(1)=XTCATO(201)                                                     C0024620
      XTGEXO(1)=XTGEXO(201)                                                     C0024622
      XTAO(1)=XTAO(201)                                                         C0024624
      XPEXO(1)=XPEXO(201)                                                       C0024626
      XPGO(1)=XPGO(201)                                                         CC024628
      XPGEXO(1)=XPGEXO(201)                                                     C0024630
      XPAO(1)=XPAO(201)                                                         C0024632
      XPGGO(1)=XPGGO(201)                                                       C0024634
      XWDCO(1)=XWDCO(201)                                                       C0024636
      XAVO(1)=XAVO(201)                                                         C0024638
      XAGO(1)=XAGO(201)                                                         C0024640
      AGFX(1)=AGFX(201)                                                         C0024642
      XPTO(1)=XPTO(201)                                                         CC024644
      PEXFX(1)=PEXFX(201)                                                       CCC24646
      IF(PLT-.5)3100,3100,3050                                                  CCC24650
 3050 XWDLO(1)=XWDLO(201)                                                       C0024652
      XWDAO(1)=XWDAO(201)                                                       00C24654
      XWDGO1(1)=XWDGO1(201)                                                     00024656
      XWDGO2(1)=XWDGO2(201)                                                     C0024658
```

THE FOLLOWING IS A LISTING OF THE INPUT DECK DECK 1

```
      WDGFX(1)=WDGFX(201)                                          C0024660
      XWDGGC(1)=XWDGGD(201)                                        CC024662
      XWDGXC(1)=XWDGXD(201)                                        00024664
      XWDXD(1)=XWDXC(201)                                          C0024666
3100  I=2                                                          C0024700
      GO TO 10                                                     CC024710
      END                                                          C1000000
```

THE FOLLOWING IS A LISTING OF THE INPUT DECK DECK 2

```
C                AL LIEBMAN  VA-2  X-6095                                  C0029000
C                FUEL PROPELLANT CONDITIONER MODEL                          C0029010
      DIMENSION XT(250) ,XTWH(250), XTEXH(250), XTAH(250), XTGGH(250), X0029020
     1TCATH(250), XTGEXH(250), XPEXH(250), XPAH(250), XPGH(250), XPGGH(2C0029030
     25C), XPGEXH(250), XAVH(250), XAGH(250), XAGC(250), XWDGH(25C), XPTCC29040
     3H(250), XPAC(250), XWDLH(250), XWDAH(250), XWDGG1(250), XWDGG2(25000029050
     4),XWDGH(25C),XWDGGH(250),XWDGXH(250),XWDXH(250),XWDRH(250)           C0029060
      COMMON TDEL,PRT,TMAX,                                                 C0029070
     1DB1H,DB3H,DB3PH,DB4H,DB5H,                                            C0029080
     2QLH,QHXH,TDXVH,TDXGH,ARATC,                                           C0029090
C                ARATO=AGC1/AGC2  WHEREAGC1 IS BYPASS AREA                  C0029092
C                MAKE ZERO FOR NO BYPASS                                    C0029093
     3VLHX,VGH,VGGH,VGEXH,VAH,                                              C0029100
     4AGG,FREQGG,TAL,                                                       C0029110
     5ATC,FREQTC,DCTC,                                                      C0029120
     6ATH,FREQTH,THH1,                                                      C0029130
     7TH1,TH2,TH3,TH4,TH5,                                                  C0029140
     8RLH,RGH1,RWH,CWH,PLT,XLTC                                             C0029150
     9,TVO,TVC                                                              C0029155
    1 CALL DRWR(TDEL,1)                                                     C0029160
C                CONSTANTS                                                  C0029170
      IPRT=PRT+.1                                                           C0029180
      PH3=17.                                                               C0029190
      PARH=17.5                                                             C0029200
      RHOLH=4.42/1728.                                                      C0029210
      DTH=.114/1728.                                                        C0029220
      QVH=190.55                                                            C0029230
      CPH=2.9                                                               C0029240
      RGH=920.                                                              C0029250
      RGO=58C.                                                              C0029260
      TLH=37.                                                               C0029270
      SIGH=1.                                                               C0029280
      ZH=.95                                                                C0029290
      CALL AREA(20.,19.,37.,9200.,.01785,AVHX)                              C0029300
      AEXH=AVHX                                                             C0029310
      CALL AREA(12.,11.,200.,4635.,.003580,AGGH)                            C0029330
      CALL AREA(11.,6.,2500.,3700.,.00358,AGEXH)                            C0029340
      CALL AREA(18.,17.,200.,9200.,.01785,AAH)                              C0029350
```

THE FOLLOWING IS A LISTING OF THE INPUT DECK DECK 2

```
      AXH=(.00358*SQRTF(3700.*600.))/(224.*6.)                          C0029360
      ARH=(.01785*SQRTF(9200.*200.))/(224.*17.5)                        C0029370
      IF(ARATC)2,2,3                                                    C0029372
    2 WDOGG=.CC2C44                                                     C0029373
      WDHGG=.CC2C44                                                     C0029374
      WDOHGG=WDOGG+WDHGG                                                C0029375
      CALL AREA(12.,11.,200.,4914.,WDCHCG,AGGH)                         C0029376
      CALL AREA(11.,6.,2000.,4914.,WDCHGG,AGEXH)                        C0029377
      AXH=(WDCHGG*SQRTF(4914.*600.))/(224.*6.)                          C0029378
      GO TO 4                                                           C0029381
    3 WDOGG=.CC2C44                                                     C0029383
      WDHGG=.0C1536                                                     C0029385
    4 CALL AREA(17.,12.,200.,578.,WDCGG,AGCX)                           C0029387
      CALL AREA(17.,12.,200.,9200.,WDHGG,AGHX)                          C0029388
      XRH=1./((AVHX**2)*772.*RHCLH)                                     C0029390
      XLH=VLHX/((3.14**2)*386.)                                         C0029400
      WLHX=RHCLH*VLHX                                                   C0029410
      WRITE OUTPUT TAPE 6,5,AVHX,AGGH,AGEXH,AAH,AXH,ARH,AGHX,AGCX       C0029420
    5 FORMAT(3X,8E10.6)                                                 C0029430
C                    INITIAL CONDITIONS                                 C0029440
      T=0.                                                              C0029450
      IPR=IPRT-1                                                        C0029460
      I=1                                                               C0029470
      WDTH=C.                                                           C0029480
      WDLH=C.                                                           C0029490
      WDDH=C.                                                           C0029500
      WDEXH=C.                                                          C0029510
      WDGO1=C.                                                          C0029520
      WDGO2=C.                                                          C0029540
      WDGH=C.                                                           C0029550
      WDGGH=0.                                                          C0029560
      WDGEXH=C.                                                         C0029570
      WDXH=C.                                                           C0029580
      WDAH=C.                                                           C0029590
      WDRH=0.                                                           C0029600
      WDCH=C.                                                           C0029610
      WLH=C.                                                            C0029620
      WLEXH=C.                                                          C0029630
```

THE FOLLOWING IS A LISTING OF THE INPUT DECK DECK 2

```
C                AL LIEBMAN  VA-2  X-6095                                  C0029C00
C                FUEL PROPELLANT CONDITIONER MODEL                          C0029010
      DIMENSION XT(250) ,XTWH(250), XTEXH(250), XTAH(250), XTGGH(250), X00029020
     1TCATH(250), XTGEXH(250), XPEXH(250), XPAH(250), XPGH(250), XPGGH(2C0029030
     250), XPGEXH(250), XAVH(250), XAGH(250), XAGC(250), XWDCH(25C), XPTCC29040
     3H(250), XPAC(250), XWDLH(250), XWCAH(250), XWDGC1(250), XWDGC2(25000029050
     4),XWDGH(25C),XWDGGH(250),XWDGXH(250),XWDXH(250),XWDRH(250)          CC029060
      COMMON TDEL,PRT,TMAX,                                                C0029070
     1DB1H,DB3H,DB3PH,DB4H,DB5H,                                           C0029080
     2QLH,QHXH,TDXVH,TDXGH,ARATC,                                          00029090
C                ARATO=AGC1/AGC2  WHEREAGC1 IS BYPASS AREA                  C0029092
C                MAKE ZERO FOR NO BYPASS                                    CC029093
     3VLHX,VGH,VGGH,VGEXH,VAH,                                             C0029100
     4AGG,FREQGG,TAL,                                                      C0029110
     5ATC,FREQTC,DCTC,                                                     C0029120
     6ATH,FREQTH,TWH1,                                                     C0029130
     7TH1,TH2,TH3,TH4,TH5,                                                 C0C29140
     8RLH,RGH1,RWH,CWH,FLT,XLTC                                            C0029150
     9,TVO,TVC                                                             CC029155
    1 CALL DRWR(TDEL,1)                                                    C002916C
C                CONSTANTS                                                 00029170
      IPRT=PRT+.1                                                          C0029180
      PH3=17.                                                              C0029190
      PARH=17.5                                                            C0029200
      RHOLH=4.42/1728.                                                     C0029210
      DTH=.114/1728.                                                       C0029220
      QVH=19C.55                                                           C0029230
      CPH=2.9                                                              00029240
      RGH=920C.                                                            C0029250
      RGO=58C.                                                             C0029260
      TLH=37.                                                              C0029270
      SIGH=1.                                                              00029280
      ZH=.95                                                               CC029290
      CALL AREA(20.,19.,37.,9200.,.01785,AVHX)                             CC029300
      AEXH=AVHX                                                            C0029310
      CALL AREA(12.,11.,200.,4635.,.003580,AGGH)                           C0029330
      CALL AREA(11.,6.,2500.,3700.,.00358,AGEXH)                           C0029340
      CALL AREA(18.,17.,200.,9200.,.01785,AAH)                             C0029350
```

THE FOLLOWING IS A LISTING OF THE INPUT DECK DECK 2

```
      AXH=(.00358*SQRTF(3700.*600.))/(224.*6.)                          C0029360
      ARH=(.01785*SQRTF(9200.*200.))/(224.*17.5)                        C0029370
      IF(ARATC)2,2,3                                                    C0029372
    2 WDOGG=.CC2C44                                                     C0029373
      WDHGG=.CC2C44                                                     C0029374
      WDOHGG=WDOGG+WDHGG                                                C0029375
      CALL AREA(12.,11.,200.,4914.,WDCHCG,AGGH)                         C0029376
      CALL AREA(11.,6.,2000.,4914.,WDCHGG,AGEXH)                        C0029377
      AXH=(WDCHGG*SQRTF(4914.*600.))/(224.*6.)                          C0029378
      GO TO 4                                                           C0029381
    3 WDOGG=.CC2C44                                                     C0029383
      WDHGG=.0C1536                                                     C0029385
    4 CALL AREA(17.,12.,200.,578.,WDCGG,AGCX)                           C0029387
      CALL AREA(17.,12.,200.,9200.,WDHGG,AGHX)                          C0029388
      XRH=1./((AVHX**2)*772.*RHCLH)                                     C0029390
      XLH=VLHX/((3.14**2)*386.)                                         C0029400
      WLHX=RHCLH*VLHX                                                   C0029410
      WRITE OUTPUT TAPE 6,5,AVHX,AGGH,AGEXH,AAH,AXH,ARH,AGHX,AGCX       C0029420
    5 FORMAT(3X,8E10.6)                                                 C0029430
C                   INITIAL CONDITIONS                                  C0029440
      T=0.                                                              C0029450
      IPR=IPRT-1                                                        C0029460
      I=1                                                               C0029470
      WDTH=C.                                                           C0029480
      WDLH=C.                                                           C0029490
      WDDH=C.                                                           C0029500
      WDEXH=C.                                                          C0029510
      WDG01=C.                                                          C0029520
      WDG02=C.                                                          C0029540
      WDGH=C.                                                           C0029550
      WDGGH=0.                                                          C0029560
      WDGEXH=C.                                                         C0029570
      WDXH=C.                                                           C0029580
      WDAH=C.                                                           C0029590
      WDRH=0.                                                           C0029600
      WDCH=C.                                                           C0029610
      WLH=C.                                                            C0029620
      WLEXH=C.                                                          C0029630
```

THE FOLLOWING IS A LISTING OF THE INPUT DECK DECK 2

```
      WEXH=15.*6./(RGH*TWH1)                                    00029640
      WGH=0.                                                    00029650
      WGO2=0.                                                   00029660
      WGGH=0.                                                   00029670
      WGEXH=0.                                                  00029680
      TEXH=TWH1                                                 00029690
      TEXH1=TEXH                                                00029700
      TGH=TLH                                                   00029720
      TAH=200.                                                  00029730
      TTH=TLH                                                   00029740
      TGGH=TLH                                                  00029750
      TCATH=TLH                                                 00029760
      TGEXH=TLH                                                 00029770
      TWLH=TWH1                                                 00029774
      TWGH=TWH1                                                 00029775
      TWH=TWH1                                                  00029780
      ER1H=0.                                                   00029790
      ER2H=0.                                                   00029800
      ER3H=0.                                                   00029810
      N1H=0                                                     00029820
      N2H=0                                                     00029830
      N3H=0                                                     00029840
      PLH=0.                                                    00029850
      PEXH=15.                                                  00029860
      PGH=0.                                                    00029880
      PGGH=0.                                                   00029890
      PAH=15.                                                   00029900
      DAH=PAH/(RGH*TAH)                                         00029902
      PGEXH=0.                                                  00029904
      QHH=0.                                                    00029908
      TDO1H=0.                                                  00029912
      TDO2H=0.                                                  00029916
      TDO3H=0.                                                  00029920
      TDC1H=0.                                                  00029924
      TDC2H=0.                                                  00029928
      TDC3H=0.                                                  00029932
      AVH=0.                                                    00029936
      AGH=0.                                                    00029940
```

```
THE FOLLOWING IS A LISTING OF THE INPUT DECK                    DECK    2

      AGO=0.                                                                C0029944
      XH=C.                                                                 C0029946
      WAH=PAH*VAH/(RGH*TAH*ZH)                                              00029948
      JSTART=C.                                                             C0029952
      MSTART=C.                                                             C0029956
      MPRIME=C.                                                             C0029960
 5010 CONTINUE                                                              00029964
      CALL FUNGEN(1,ATH,FREQTH,20.,T,1.,PTH)                                CC030000
      IF(XLIQH-.5)5011,5011,5500                                            C0030100
 5500 IF(AVH)551C,5510,5520                                                 CC030200
 5510 WDLH=C.                                                               00030300
      GO TO 555C                                                            00030400
 5520 MSTART=MSTART+1                                                       00030500
      IF(PTH-PEXH)5530,5530,5540                                            C0030600
 5530 WDLH=C.                                                               C0030700
      GO TO 555C                                                            00030800
 5540 CALL FLCL(TDEL,XRH,XLH,PTH,PEXH,WDLH,WLH)                             CC030900
      IF(WLH-WLHX)5550,5550,5560                                            0C031000
 5550 IF(MPRIME)5120,5120,5580                                              C0031100
 5560 MPRIME=MPRIME+1                                                       C0031200
 5580 WDLH1=MAX1F(.C1,WDLH)                                                 CC031300
      WDAH1=MAX1F(.01,WDAH)                                                 C0031320
      RWLH=RGH1*((.021/WDLH1)**.8)                                          00031340
      RWGH=RGH1*((200./TEXH)**.12)*((.021/WDAH1)**.8)                       CC031360
      CALL FLEX(SIGH,TDEL,RWLH,RWGH,XH,XDELH,PEXH,TWLH,TWGH,TLH,TEXH,DEX00031380
     1H,WLXH,WEXH,VLHX,WLH,CWH,WLAH,WGAH)                                   00031400
      TWH=XH*TWLH+(1.-XH)*TWGH                                              CC031420
      IF(WLAH)5035,5C35,5590                                                C0031500
 555C TAH=(WAH*TAH+WLAH*(TLH-CVH/CPH)+WGAH*TEXH1)/(WAH+WLAH+WGAH)           CC031600
      TEXH1=TEXH                                                            CC031700
      WAH=WAH+WLAH+WGAH                                                     C0031800
      GO TO 5C35                                                            00031900
 5011 CCNTINUE                                                              0C032000
      IF(AVH)5012,5012,5020                                                 C0032100
 5012 WDTH=C.                                                               CC032200
      GO TO 5C25                                                            00032300
 5020 MSTART=MSTART+1                                                       C0032400
      CALL FLOG(PTH,PLH,AVH,DTH,WDTH)                                       00032500
```

```
5025 IF(MSTART)5120,5120,5026                                          CC032600
5026 CONTINUE                                                          CC032700
     CALL ACCLM(SIGH,TDEL,WLH,TLH,WDTH,TTH,0.,0.,PLH,VLHX,DLH)         C0032800
     CALL FLOG(PLH,PEXH,AEXH,DLH,WDLH)                                 C0032900
     WLH=WLH-WDLH*TDEL                                                 C0033000
     WLH=MAX1F(C.,WLH)                                                 00033100
5030 CONTINUE                                                          C0033200
     WDLH1=MAX1F(.01,WDLH)                                             C0033280
     RWGH=RGH1*((200./TEXH)**.12)*((.021/WDLH1)**.8)                   C0033290
     CALL HEX(SIGH,TDEL,WDLH,RWGH,PEXH,TWH,TLH,TEXH,CEXH,WEXH,CWH)     CC033300
     TWGH=TWH                                                          C0033310
5035 CONTINUE                                                          CC033400
     IF(TAH-(TH3+DB3H))5050,5050,5080                                  00033500
5050 IF(TAH-(TH3-DB3H))5100,5120,5120                                  C0033600
5080 ER2H=1.                                                           00033700
     ER3H=1.                                                           CC033800
     GO TO 5120                                                        00033900
5100 ER2H=-1.                                                          C0034000
     ER3H=-1.                                                          00034100
5120 IF(JSTART)525C,525C,5125                                          CC034200
5125 AGO2=AGO/(1.+ARATO)                                               00034300
     AGO1=AGO*ARATO/(1.+ARATO)                                         C0034400
5130 CALL FUNGEN(1,AGG,FREQGG,PAH,T,1.,PAC)                            00034500
     TAO=TAH                                                           C0034600
     DAO = PAC/(RGC*TAC)                                               CC034700
     CALL FLOG(PAC,PGH,AGO2,DAC,WDGC2)                                 C0034800
     CALL FLOG(PAO,PGGH,AGC),DAC,WDGC1)                                CC034900
     CALL FLOG (PAH,PGH,AGH,DAH,WDGH)                                  CC035000
     CALL GMIX(TDEL,WGC2,WGH,WDGC2,WDGH,TAC,TAH,TGH,PGH,RCATH,VGH,DGH) CC035100
     CALL FLOG(PGH,PGGH,AGGH,DGH,WDGGH)                                CC035200
     CALL GGEN(WDGGH,WDGC1,RCATH,TDEL,TGGH,PGGH,VGGH,TCATH,WGGH,DGGH)  CC035300
     CALL FLOG(PGGH,PGEXH,AGEXH,DGGH,WDEXH)                            00035400
     IF(TAH-(TH3+DB5H))5140,5140,5220                                  CC035500
5140 CONTINUE                                                          CC035600
     IF(TGGH-(TH1+DB1H))5150,5150,5180                                 CC035700
5150 IF(TGGH-(TH1-DB1H))5160,5190,5190                                 CC035800
5160 ER2H=-1.                                                          CC035900
     GO TO 5200                                                        CC036000
```

```
      5180 ER2H=1.                                                                  00036100
           GO TO 5200                                                               00036200
      5190 CONTINUE                                                                 00036300
      5200 IF(TCATH-TH2)5220,5220,5210                                              00036400
      5210 ER2H=1.                                                                  00036500
      5220 CALL GGBEX(XH,TDEL,WGEXH,TGEXH,WDEXH,TGCH,TWLH,TWGH,RWH,CWH,VGEXH,      00036600
          1PGEXH)                                                                   00036601
           TWH=XH*TWLH+(1.-XH)*TWGH                                                 00036610
           IF(AVH)5250,5250,5270                                                    00036800
      5250 IF(TWH-(TH4+DB4H))5260,5260,5270                                         00036900
      5260 IF(TWH-(TH4-DB4H))5270,5270,5270                                         00037000
      5270 ER2H=-1.                                                                 00037100
           ER3H=-1.                                                                 00037200
           IF(TCATH-TH2)5270,5272,5272                                              00037300
      5272 ER2H=1.                                                                  00037400
           GO TO 5270                                                               00037500
      5274 ER2H=1.                                                                  00037600
           ER3H=1.                                                                  00037700
      5270 CALL DELAY(ER2H,N2H,TDO2H,TDC2H,TDXGH,TDEL)                              00037800
           IF(N2H)5280,5280,5284                                                    00037900
      5280 AGO=0.                                                                   00038000
           GO TO 5288                                                               00038100
      5284 AGO=AGOX                                                                 00038200
           JSTART=JSTART+1                                                          00038300
      5288 CALL DELAY(ER3H,N3H,TDO3H,TDC3H,TDXGH,TDEL)                              00038400
           IF(N3H)5292,5292,5296                                                    00038500
      5292 AGH=0.                                                                   00038600
           GO TO 5300                                                               00038700
      5296 AGH=AGHX                                                                 00038800
      5300 WDXH=224.*PGEXH*AXH/SQRTF(4914.*TGEXH)                                   00038900
           IF(PEXH-PAH)5305,5305,5310                                               00039000
      5305 WDAH=0.                                                                  00039100
           GO TO 5315                                                               00039200
      5310 CALL FLOG(PEXH,PAH,AAH,DEXH,WDAH)                                        00039300
           WEXH=WEXH-WDAH*TDEL                                                      00039400
           WEXH=MAXIF(0.,WEXH)                                                      00039500
      5315 CALL ACCUM(SIGH,TDEL,WAH,TAH,WEAH,TEXH,CHH,QLH,PAH,VAH,DAH)             00039600
           IF(PAH-(PH3+DB3PH))5320,5320,5330                                        00039700
```

THE FOLLOWING IS A LISTING OF THE INPUT DECK DECK ?

```
      5320 IF(PAH-(PH3-DB3PH))5350,5360,5360                          C0039800
      5330 ER1H=1.                                                    C0039900
           IF(PAH-PARH)5360,5360,5340                                 CC04C000
      5340 WDRH=224.*PAH*ARH/SQRTF(9200.*TAH)                         C0040100
           GO TO 5365                                                 CC040200
      5350 ER1H=-1.                                                   C0040300
      5360 WDRH=C.                                                    C0040400
      5365 IF(ER1H)537C,537C,5366                                     CC04045C
      5366 IF(TAH-(TH3+DB3H))5380,5370,5370                           0004C500
      537C QHH=C.                                                     00040600
           GO TO 54CC                                                 00040700
      5380 IF(TAH-(TH3-DB3H))539C,5400,5400                           CCC4C800
      539C QHH=QHXH                                                   CCC4C900
      5400 CALL DELAY(ER1H,N1H,TDC1H,TCC1H,TCXVH,TDEL)                CC041000
           IF(N1H)541C,541C,5420                                      CC041100
      541C CALL OPEN(N1H,AVH,TDEL,TVC,AVHX)                           C0041200
           GO TO 543C                                                 00041300
      5420 CALL OPEN(N1H,AVH,TDEL,TVC,AVHX)                           CCC41400
      543C IF(T-TAL)544C,5435,5435                                    CCC41500
      5435 CONTINUE                                                   C0C41600
           CALL FUNGEN(2,ATC,FREQTC,C.,T,DCTC,WDCH)                   C0041700
      5440 CONTINUE                                                   CC041800
           WGO2=WGC2-(RCATH/(RCATH+1.))*WDGGH*TDEL                    C0041900
           WGH=WGH-WDGGH*TDEL/(RCATH+1.)                              CC042000
           WGGH=WGGH-WDEXH*TDEL                                       CCC42100
           WGEXH=WGEXH-WCXH*TDEL                                      00042200
           WAH=WAH-(WDCH+WDRH+WDGH)*TDEL                              CC042300
           WGO2=MAX1F(C.,WGC2)                                        00042400
           WGH=MAX1F(C.,WGH)                                          00042500
           WGGH=MAX1F(C.,WGGH)                                        CC042600
           WGEXH=MAX1F(C.,WGEXH)                                      C0042700
           WAH=MAX1F(C.,WAH)                                          C0042800
C                    OUTPUT                                         CC050000
       60CC IPR=IPR+1                                                CCC50100
           IF(IPR-IPRT)6C40,6020,6020                                 CCC50200
       6020 XT(I)=T                                                  CCC50300
           XPEXH(I)=PEXH                                              CCC50400
           XPAH(I)=PAH                                                CC050500
```

```
      XPGH(I)=PGH                                                          C0050600
      XPGGH(I)=PGGH                                                        CCC5C700
      XPGEXH(I)=PGEXH                                                      CC050800
      XPAC(I)=PAC/1CC.                                                     CCC5C900
      XTWH(I)=TWH                                                          CCC51000
      XTEXH(I)=TEXH                                                        C0051100
      XTAH(I)=TAH                                                          00051200
      XTGGH(I)=TGGH/10.                                                    00051300
      XTCATH(I)=TCATH/10.                                                  CC051400
      XTGEXH(I)=TGEXH                                                      00051500
      XAVH(I)=AVH                                                          CC051600
      XAGH(I)=AGH                                                          C0051700
      XAGC(I)=AGC                                                          CCC51800
      XWDCH(I)=WDCH                                                        C0051900
      XPTH(I)=PTH/100.                                                     C0052000
      IF(PLT-.5)6030,6030,6025                                             CC052100
 6025 XWDLH(I)=WDLH/10.                                                    C0052200
      XWDAH(I)=WDAH/10.                                                    CCC52300
      XWDGC1(I)=WDGC1                                                      CCC52400
      XWDGC2(I)=WDGC2                                                      CC052500
      XWDGH(I)=WDGH                                                        CC052600
      XWDGGH(I)=WDGGH                                                      C0052700
      XWDGXH(I)=WDEXH                                                      C0052800
      XWDXH(I)=WDXH                                                        CC052900
      XWDRH(I)=WDRH/10.                                                    CCC52910
 6030 I=I+1                                                                CCC53000
      IPR=0                                                                CC053100
 6040 T=T+TDEL                                                             C0053200
      IF(I-200)6060,7000,7000                                              C0053300
 6060 IF(T-TMAX)5010,5010,7000                                             CC053400
 7000 NPT=I-1                                                              CCC53500
 7100 WRITE OUTPUT TAPE 6,112,(XT(I),XTEXH(I),XTWH(I),XTGGH(I),XTCATH(I)CCC53600
     1,XTGEXH(I),XTAH(I),XPEXH(I),XPGH(I),XPGEXH(I),XPAH(I),XPGGH(I),XWD00053700
     2CH(I),XAVH(I),XAGH(I),XAGC(I),XPTH(I),XPAC(I),I=1,NPT)               CCC53800
  112 FORMAT(3X,9E11.4)                                                    00053900
      CALL SCPLTV(NPT,XT,1,48,IP,6,XTEXH,XTWH,XTGGH,XTCATH,XTGEXH,XTAH)    CC054000
      CALL LINPTV(NPT,XT,XTEXH,0,IP)                                       CCC54100
      CALL LINPTV(NPT,XT,XTWH,0,IP)                                        CCC54200
```

THE FOLLOWING IS A LISTING OF THE INPUT DECK DECK 2

```
      CALL LINPTV(NPT,XT,XTGGH,0,IR)                                          CCC54300
      CALL LINPTV(NPT,XT,XTCATH,0,IR)                                         CCC54400
      CALL LINPTV(NPT,XT,XTGEXH,0,IR)                                         CC054500
      CALL LINPTV(NPT,XT,XTAH,0,IR)                                           C0054600
      CALL SCPLTV(NPT,XT,1,48,IR,5,XPEXH,XPGGH,XPGEXH,XPAH,XPGH)              CCC54700
      CALL LINPTV(NPT,XT,XPEXH,0,IR)                                          CCC548CC
      CALL LINPTV(NPT,XT,XPGGH,0,IR)                                          CCC54900
      CALL LINPTV(NPT,XT,XPGEXH,0,IR)                                         CC055000
      CALL LINPTV(NPT,XT,XPAH,0,IR)                                           CCC55100
      CALL LINPTV(NPT,XT,XPGH,0,IR)                                           CCC55200
      CALL SCPLTV(NPT,XT,1,48,IR,6,XWDCH,XAVH,XAGH,XPTH,XAGC,XPAO)            CC055300
      CALL LINPTV(NPT,XT,XWDCH,C,IR)                                          CCC55400
      CALL LINPTV(NPT,XT,XAVH,0,IR)                                           C0055500
      CALL LINPTV(NPT,XT,XAGH,0,IR)                                           CCC55600
      CALL LINPTV(NPT,XT,XPTH,0,IR)                                           CCC5570C
      CALL LINPTV(NPT,XT,XAGO,0,IR)                                           CCC5580C
      CALL LINPTV(NPT,XT,XPAO,0,IR)                                           CCC55900
      IF(PLT-.5)77CC,7700,7600                                                CCC56000
760C WRITE CLTPLT TAPE  6,112,(XT(I),XWDLH(I),XWDAH(I),XWDGC1(I),XWDCO2CCC56C50
     1(I),XWDGH(I),XWDGGH(I),XWDGXH(I),XWDXH(I),I=1,NPT)                      CC056051
      CALL SCPLTV(NPT,XT,1,48,IR,5,XWDLH,XWDGGH,XWDGC1,XWDCO2,XWDRH)          C0056100
      CALL LINPTV(NPT,XT,XWDLH,0,IR)                                          C0056200
      CALL LINPTV(NPT,XT,XWDGGH,0,IR)                                         CCC5630C
      CALL LINPTV(NPT,XT,XWDGO1,0,IR)                                         C0056400
      CALL LINPTV(NPT,XT,XWDGC2,0,IR)                                         CCC565CC
      CALL LINPTV(NPT,XT,XWDRH,0,IR)                                          CC056510
      CALL SCPLTV(NPT,XT,1,48,IR,-4,XWDGH,XWDAH,XWDGXH,XWDXH)                 CCC56600
      CALL LINPTV(NPT,XT,XWDGH,0,IR)                                          C0056700
      CALL LINPTV(NPT,XT,XWDAH,0,IR)                                          CCC56800
      CALL LINPTV(NPT,XT,XWDGXH,0,IR)                                         CCC56900
      CALL LINPTV(NPT,XT,XWDXH,0,IR)                                          CCC57000
7700 CONTINUE                                                                 CCC57100
      IF(T-TMAX)8CCC,1,1                                                      CCC57200
8000 XT(1)=XT(2C1)                                                            CCC57300
      XTEXH(1)=XTEXH(2C1)                                                     C0057400
      XTWH(1)=XTWH(2C1)                                                       CCC57500
      XTGGH(1)=XTGGH(2C1)                                                     CCC57600
      XTCATH(1)=XTCATH(201)                                                   CCC57700
```

THE FOLLOWING IS A LISTING OF THE INPUT DECK DECK 2

```
      XTGEXH(1)=XTGEXH(201)                                          C0C57800
      XTAH(1)=XTAH(201)                                              C0C57900
      XPEXH(1)=XPEXH(201)                                            C0C58000
      XPGH(1)=XPGH(201)                                              C0C58100
      XPGEXH(1)=XPGEXH(201)                                          C0C58200
      XPAH(1)=XPAH(201)                                              C0C58300
      XPGGH(1)=XPGGH(201)                                            C0C58400
      XWDCH(1)=XWDCH(201)                                            C0C58500
      XAVH(1)=XAVH(201)                                              C0C58600
      XAGH(1)=XAGH(201)                                              C0C58700
      XAGC(1)=XAGC(201)                                              00C58800
      XPTH(1)=XPTH(201)                                              C0C58900
      XPAC(1)=XPAC(201)                                              C0C59000
      IF(PLT-.5)8100,8100,8050                                       C0C59100
 8050 XWDLH(1)=XWDLH(201)                                            00C59200
      XWDAH(1)=XWDAH(201)                                            C0C59300
      XWDGC1(1)=XWDGC1(201)                                          C0C59400
      XWDG02(1)=XWDG02(201)                                          C0C59500
      XWDGH(1)=XWDGH(201)                                            00C59600
      XWDGGH(1)=XWDGGH(201)                                          C0C59700
      XWDGXH(1)=XWDGXH(201)                                          C0C59800
      XWDXH(1)=XWDXH(201)                                            C0C59900
 8100 I=2                                                            C0C60000
      GO TO 5010                                                     C0C60100
      END                                                            C0C60500
```

APPENDIX C

Computer Deck Listing of Subprograms for Thrustor and Conditioner Simulation

THE FOLLOWING IS A LISTING OF THE INPUT DECK DECK 21

```
      SUBROUTINE ACCUM(SIG,TDEL,WG,TGO,WDG,TG,QH,QL,PG,VOL,RHOG)      50000001
      IF(SIG)10,10,20                                                 50000003
C     CX                                                              50000004
   10 CP=.24                                                          50000007
      R=48.25*12.                                                     50000010
      Z=.927                                                          50000013
      GO TO 30                                                        50000016
C     FUEL                                                            50000017
   20 CP=2.9                                                          50000020
      R=767.*12.                                                      50000023
      Z=.95                                                           50000026
   30 CONTINUE                                                        50000028
      TGO=(WG*TGO+WDG*TDEL*TG)/(WG+WDG*TDEL)                          50000029
      WG=WG+WDG*TDEL                                                  50000030
      TGO=TGO+((QH-QL)/(CP*WG))*TDEL                                  50000040
      PG=Z*WG*R*TGO/VOL                                               50000050
      RHOG=WG/VOL                                                     50000055
      RETURN                                                          50000060
      END                                                             50000070
```

THE FOLLOWING IS A LISTING OF THE INPUT DECK DECK 13

```
      SUBROUTINE AREA(P1,P22,T,R,WDOT,A)                              12000010
      P2MIN=.53*P1                                                    12000015
      P2=AMAX1F(P22,P2MIN)                                            12000016
      B=.71+.29*P2/P1                                                 12000020
      RAD=(772.*(1.-P2/P1))/(R*T))                                    12000025
      RAD=AMAX1F(0.,RAD)                                              12000030
      C=SQRTF(RAD)                                                    12000035
      A=WDOT/((B*P1*C)*.73)                                           12000040
      RETURN                                                          12000050
      END                                                             12000060
```

THE FOLLOWING IS A LISTING OF THE INPUT DECK DECK 10

```
      SUBROUTINE ASJN(XK,R,T,WDOT,P,A)                                  13000010
      G=386.                                                            13000020
      EX=(XK+1.)/(XK-1.)                                                13000030
      EX=MAX1F(0.,EX)                                                   13000035
      RAD=(2./(XK+1.))**EX                                              13000040
      RAD=MAX1F(0.,EX)                                                  13000045
      SON=SQRTF(XK*G*R*T)                                               13000050
      A=WDOT/(P*G*XK*SQRTF(RAD)/SON)                                    13000060
      RETURN                                                            13000070
      END                                                               13000080
```

```
      SUBROUTINE COMB(TDEL,AT,VC,WDOH,WDO,WDH,RCAT,TC,PC,XMR,Q,WDOTN,TC531000100
     1,WC,TO,WO)                                                      31000101
      IF(RCAT)2,2,4                                                   31000200
    2 TC=200.                                                         31000220
      WDOT=WDOH+WDO+WDH
      CALL FLOSON(1.,AT,TC,PC,WDOTN)                                  31000260
      PCDOT=(9200.*TC/VC)*(WDOT-WDOTN)                                31000280
      PC=PC+PCDOT*TDEL                                                31000290
      WC=WC+(WDOT-WDOTN)*TDEL                                         31000300
      GO TO 40                                                        31000320
    4 CONTINUE                                                        31000700
      WDO1=(RCAT/(RCAT+1.))*WDOH                                      31000800
      WDH1=WDOH-WDO1                                                  31000900
      WC1=WC/2.                                                       31000945
      WC=WC+(WDOH+WDO-WDOTN)*TDEL                                     31000950
      WC=MAX1F(WC,WC1)                                                31000951
      WC=MAX1F(WC,0.)                                                 31000952
      PC=WC*R*TC/VC                                                   31000955
      WO=WO+((WDO1+WDO)-(XMR/(XMR+1.))*WDOTN)*TDEL                    31000960
      WO=MAX1F(WO,0.)                                                 31000965
      WH=WC-WO                                                        31000970
      WH=MAX1F(WH,.000001)                                            31000972
      XMR=WO/WH                                                       31000980
      R=18540./(1.71*XMR+2.3)                                         31001150
      R=MAX1F(R,0.)                                                   31001151
      CPM=(XMR*.24+2.9)/(XMR+1.)                                      31001200
      CP=(RCAT*.24+2.9)/(RCAT+1.)                                     31001220
      IF(WDO)6,6,7                                                    31001300
    6 TC=TC5                                                          31001305
      GO TO 39                                                        31001310
    7 IF(TC5-1500.)10,10,20                                           31001320
   10 QR=0.                                                           31001340
      GO TO 30                                                        31001360
   20 XMRR=WDO/(WDH1-WDO1/8.)                                         31001370
      XMRR=MAX1F(XMRR,0.)                                             31001375
      WDR=WDO+WDH1-WDO1/8.                                            31001380
      CPR=(WDO*.24+(WDR-WDO)*2.9)/WDR                                 31001385
      CALL RMIX(XMRR,TCR)                                             31001390
      QR=(TCR-TO)*CPR                                                 31001400
```

```
   30 IF(WC)33,33,36                                                              31001440
   33 TC=TC                                                                       31001445
      GO TO 39                                                                    31001450
   36 TDC=(WDOH*CP*TC5+WDO*.24*TO+QR*WDR-WDOTN*CPM*TC)/(WC*CPM/1.4)               31001455
      TDC=MINIF(TDC,150000.)                                                      31001457
      TDC=MAXIF(TDC,-150000.)                                                     31001458
      TC=TC+TDC*TDEL                                                              31001460
      TC=MAXIF(TC,TO)                                                             31001480
   39 CONTINUE                                                                    31002299
      WDOT=WDOH+WDH+WDO                                                           31002300
      CON1=PC*AT*386.*.8102                                                       31002500
      CON2=SQRTF(1.4*386.*R*TC)                                                   31002510
      WDOTN=CON1/CON2                                                             31002520
   40 CONTINUE                                                                    31002650
      PC=MAXIF(0.,PC)                                                             31002700
      RETURN                                                                      31002800
      END(1,0,0,0,0,0,1,0,0,1,0,0,0,0,0)
```

THE FOLLOWING IS A LISTING OF THE INPUT DECK DECK 15

```
      SUBROUTINE VALFOL(P1,P2,T1,T2,TDEL,VFOL,A)                        00000100
C     P1-O2 , P2-H2                                                     00000110
      IF(VFOL)10,10,20                                                  00000200
   10 P11=P1                                                            00000300
      P22=P2                                                            00000400
      W1=P1/(58O.*T1)                                                   00000500
      W2=P2/(92CO.*T2)                                                  00000600
      DX=0.                                                             00000640
      X=C.                                                              00000642
      A1 =.7854*(.03)**2                                                00000644
      A1=16.*A1                                                         00000645
      A2 =.7854*(.03)**2                                                00000646
      A2=16.*A2                                                         00000647
      V1 =1.                                                            00000648
      V2 =1.                                                            00000650
      A11=1.49                                                          00000652
      A22=1.125                                                         00000654
      XK=40.                                                            00000656
      FS0=6.25                                                          00000658
      XMAX=.02                                                          00000660
      WPOP=.40                                                          00000662
      AS=.14                                                            00000664
   2C RHO1=P1/(58O.*T1)                                                 00000700
      RHO2=P2/(92CO.*T2)                                                00000800
      IF(P1-P11)30,40,50                                                00000900
   3C CALL FLOG(P11,P1,A1,RHO1,WD1)                                     00001000
      WD1=-WD1                                                          00001100
      GO TO 60                                                          00001200
   4C WD1=0.                                                            00001300
      GO TO 60                                                          00001400
   5C CALL FLOG(P1,P11,A1,RHO1,WD1)                                     00001500
   6C W1=W1+WD1*TDEL                                                    00001600
      P11=W1*58O.*T1/V1                                                 00001700
      IF(P2-P22)70,80,90                                                00001800
   7C CALL FLOG(P22,P2,A2,RHO2,WD2)                                     00001900
      WD2=-WD2                                                          00002000
      GO TO 100                                                         00002100
   8C WD2=C.                                                            00002200
```

THE FOLLOWING IS A LISTING OF THE INPUT DECK DECK 15

```
      GO TO 100                                                          00002300
   90 CALL FLOG(P2,P22,A2,RHO2,WD2)                                      00002400
  100 W2=W2+WD2*TDEL                                                     00002500
      P22=W2*9200.*T2/V2                                                 00002600
      DDX=(P22*A22-P11*A11+(FS1-XK*X))/(WPOP/386.)                       00002700
      DX=DX+DDX*TDEL                                                     00002800
      X=X+DX*TDEL                                                        00002900
      X=MAX1F(X,0.)                                                      00003000
      X=MIN1F(XMAX,X)                                                    00003100
      A=X*AS/XMAX                                                        00003200
      VFOL=VFOL+1.                                                       00003300
      IF(X)220,220,210                                                   00003310
  210 IF(X-XMAX)230,220,220                                              00003320
  220 DX=0.                                                              00003330
  230 CONTINUE                                                           00003340
      RETURN                                                             00003400
      END                                                                00003500
```

THE FOLLOWING IS A LISTING OF THE INPUT DECK DECK 18

```
      SUBROUTINE  RMIX(R,Y)                                          33000010
      X=R/(R+1.)                                                     33000020
      IF(X-.45)10,10,20                                              33000030
   10 Y=200.+2690. * X                                               33000040
      GO TO 100                                                      33000050
   20 IF(X-.88)40,30,30                                              33000060
   30 Y=-41250.*(X-1.)+200.                                          33000070
      GO TO 100                                                      33000080
   40 IF(X-.82)50,50,60                                              33000090
   50 Y=9860.*(X-.45)+1500.                                          33000100
      GO TO 100                                                      33000110
   60 Y=(1.03+.01*SQRTF(9.-(100.*X-85.)**2))*5000.                   33000120
  100 CONTINUE                                                       33000130
      RETURN                                                         33000140
      END                                                            33000150
```

THE FOLLOWING IS A LISTING OF THE INPUT DECK DECK 20

```
      SUBROUTINE DELAY(ER,N,TD1,TDC,TDX,TDEL)                    80000100
      IF(ER)210,110,10                                           80000200
   10 IF(N)110,110,20                                            80000300
   20 TD0=0.                                                     80000400
      TDC=TDC+TDEL                                               80000500
      IF(TDC-TDX)500,30,30                                       80000600
   30 N=0                                                        80000700
      TDC=0.                                                     80000800
      GO TO 500                                                  80000900
  110 TD0=0.                                                     80001000
      TDC=0.                                                     80001100
      GO TO 500                                                  80001200
  210 IF(N)220,220,110                                           80001300
  220 TDC=0.                                                     80001400
      TD1=TD0+TDEL                                               80001500
      IF(TD0-TDX)500,230,230                                     80001600
  230 N=1                                                        80001700
      TDC=0.                                                     80001800
  500 CONTINUE                                                   80001900
      RETURN                                                     80002000
      END                                                        80002100
```

THE FOLLOWING IS A LISTING OF THE INPUT DECK DECK 5

```
      SUBROUTINE FLEX(SIG,TDEL,RL,RG,X,XDEL,PG,TWL,TWG,TL,TG,RHOG,WL,WG,20000100
     1VLX,VLL,C,WLA,WGA)                                                20000101
      X0=X                                                              20000140
      WR=.C49*(Tw/1800.)**4                                             20000150
      IF(SIG)10,10,20                                                   20000200
C     OXIDIZER                                                          20000300
   10 GV=91.78                                                          20000400
      RHOL=71.15/1728.                                                  20000500
      CP=.24                                                            20000600
      R=48.25*12.                                                       20000700
      VOL=29.                                                           20000800
      Z=.927                                                            20000900
      GO TO 30                                                          20001000
C     FUEL                                                              20001100
   20 GV=190.55                                                         20001200
      RHOL=4.43/1728.                                                   20001300
      CP=2.9                                                            20001400
      R=767.*12.                                                        20001500
      VOL=38.                                                           20001600
      Z=.95                                                             20001700
   30 WL=WLL-VLX*RHOL                                                   20001720
   40 IF(WL)45,45,50                                                    20001728
   45 X=0.                                                              20001732
      VOL1=VOL-WL/RHOL                                                  20001734
      Q=(Tw-TG)/RG                                                      20001736
      TG=(Q/(CP*WG))*TDEL+TG                                            20001738
      TG=MINIF(TG,Tw)                                                   20001739
      PG=Z*WG*R*TG/VOL1                                                 20001740
      GO TO 80                                                          20001744
   50 CONTINUE                                                          20001800
      IF(X-1.)60,54,54                                                  20001840
   54 WRITE OUTPUT TAPE 6,55                                            20001845
   55 FORMAT(12HX IS TOO BIG)                                           20001850
      WLA=(X-1.)*VOL*RHOL                                               20001860
      WGA=WG                                                            20001862
      WL=VOL*RHOL                                                       20001863
      WG=0.                                                             20001864
      X=1.                                                              20001866
```

```
      GO TO 70                                                          20001870
EC    WLA=0.                                                            20001874
      WGA=0.                                                            20001878
70    CONTINUE                                                          20001899
      XMAX=MAX1F(0.,XDEL)                                               20001900
      XMIN=MIN1F(XDEL,0.)                                               20002000
71    WL=X * (TWL-TL)/RL + XMAX * C*(TWG-TWL)                           20002100
72    QG=(1.-X)*(TWG-TG)/RG                                             20002200
73    WGDEL=QL*TDEL/QV                                                  20002300
      WL=WL-WGDEL                                                       20002400
      WL=MAX1F(0.,WL)                                                   20002500
      WLL=WL+VLX*RHOL                                                   20002600
74    X=WL/(RHOL*VOL)                                                   20002700
      XDEL=X-X0                                                         20002800
75    TWL=TWL-QL*TDEL/(X*C)                                             20002900
      TWL=MAX1F(TL,TWL)                                                 20002950
76    TG=TG+(QG/(CP*WG))*TDEL                                           20003000
77    TG=(WG*TG+WGDEL*TL)/(WG+WGDEL)                                    20003100
      TG=MIN1F(TG,TWG)                                                  20003200
      TG=MAX1F(TL,TG)                                                   20003300
      WG=WG+WGDEL                                                       20003400
      WG=MAX1F(0.,WG)                                                   20003450
78    PG=Z*WG*R*TG/((1.-X)*VOL)                                         20003500
79    RHOG=WG/((1.-X)*VOL)                                              20003600
EC    QG=QG + (1.-X) * QR                                               20003700
      TWG=(TWG * (1.-X+XMIN) -TWL*XMIN)/(1.-X)                          20003800
      TWG=TWG-QG * TDEL/((1.-X)*C)                                      20003900
      TWG=MAX1F(TWL,TWG)                                                20004000
      RETURN                                                            20004300
      END                                                               20004400
```

THE FOLLOWING IS A LISTING OF THE INPUT DECK DECK 19

```
      SUBROUTINE FLOG(P1,P2,A,RHOG,WDG)                          30000010
      IF(P1)10,10,20                                             30000011
   10 WDG=0.                                                     30000012
      GO TO 100                                                  30000013
   20 P2MIN=.53*P1                                               30000014
      P2=AMAX1F(P2,P2MIN)                                        30000016
      Y=.71+.29*P2/P1                                            30000020
      RAD=(772.*RHOG*(P1-P2))                                    30000025
      RAD=AMAX1F(0.,RAD)                                         30000030
      WDG=.73*A*Y*SQRTF(RAD)                                     30000035
  100 CONTINUE                                                   30000039
      RETURN                                                     30000040
      END                                                        30000045
```

THE FOLLOWING IS A LISTING OF THE INPUT DECK DECK 11

```
      SUBROUTINE FLOL(TDEL,XR,XL,P1,P2,WOUT,W)                  10000010
      W=W+WOUT*TDEL                                             10000020
      A=TDEL*XR                                                 10000030
      B=XL                                                      10000040
      C=TDEL*P2-XL*WOUT-TDEL*P1                                 10000050
      RAD=B**2-4.*A*C                                           10000060
      IF(RAD)10,20,20                                           10000070
   10 WRITE OUTPUT TAPE 6,15                                    10000080
   15 FORMAT(20HFLOL RAD IS NEGATIVE)                           10000090
      GO TO 100                                                 10000100
   20 WOUT=(-B+SQRTF(RAD))/(2.*A)                               10000110
  100 RETURN                                                    10000120
      END                                                       10000130
```

THE FOLLOWING IS A LISTING OF THE INPUT DECK DECK 22

```
      SUBROUTINE FLOSON(SIG,A,T,P,WDOT)                          70000100
      G=386.                                                     70000200
      IF(SIG)10,10,20                                            70000300
C     GX                                                         70000400
   10 XK=1.394                                                   70000500
      R=48.25*12.                                                70000600
      GO TO 30                                                   70000700
C     FUEL                                                       70000800
   20 XK=1.398                                                   70000900
      R=767.*12.                                                 70001000
   30 EX=(XK+1.)/(XK-1.)                                         70001100
      EX=MAX1F(0.,EX)                                            70001150
      RAD=(2./(XK+1.))**EX                                       70001200
      RAD=MAX1F(0.,RAD)                                          70001250
      T=MAX1F(T,0.)                                              70001270
      SON=SQRTF(XK*G*R*T)                                        70001300
      WDOT=A*P*G*XK*SQRTF(RAD)/SON                               70001400
      RETURN                                                     70001500
      END                                                        70001600
```

THE FOLLOWING IS A LISTING OF THE INPUT DECK DECK 16

```
      SUBROUTINE FUNGEN(J,A,F,B,T,X,Y)                              90000100
      GO TO(10,20,30),N                                             90000200
   10 Y=A*SINF(6.28*F*T) + B                                        90000300
      GO TO 100                                                     90000400
   20 P=1./F                                                        90000500
      NT=T/P                                                        90000600
      TT=T/P-FLOATF(NT)                                             90000700
      IF(TT-X)30,30,40                                              90000800
   30 Y=A+B                                                         90000900
      GO TO 100                                                     90001000
   40 Y=B                                                           90001100
      GO TO 100                                                     90001200
C                    FREQ-TIME CONSTANT                            90001201
   50 Y=B*(1.-1./EXPF(T/F))                                         90001220
  100 CONTINUE                                                      90001240
      RETURN                                                        90001300
      END                                                           90001400
```

THE FOLLOWING IS A LISTING OF THE INPUT DECK DECK 8

```
      SUBROUTINE GGEN(WDOF,WDO,XMR,TDEL,TG,PG,VOL,TCAT,WG,DG)          40000100
      WG1=WG+(WDOF+WDO)*TDEL                                           40000200
      IF(WG1)10,10,20                                                  40000300
   10 PG=0.                                                            40000400
      WG=0.                                                            40000500
      GO TO 100                                                        40000600
   20 IF(WDOF)23,23,27                                                 40000650
   23 TG1=200.                                                         40000655
      XMR1=17.36                                                       40000660
      GO TO 45                                                         40000665
   27 CP=(XMR*.24+2.9)/(XMR+1.)                                        40000700
      CCAT=.001                                                        40000800
      CALL RMIX(XMR,TCAT1)                                             40000900
      TCDEL=(TCAT1-TCAT)/(1.+CCAT/(WDOF*CP*TDEL))                      40001000
      TCAT=TCAT+TCDEL                                                  40001100
      IF(WDO)30,30,40                                                  40001200
   30 TG=TCAT                                                          40001300
      XMR1=XMR                                                         40001400
      GO TO 50                                                         40001500
   40 WDF1=WDOF/(XMR+1.)                                               40001600
      XMR1=((WDOF-WDF1)+WDO)/WDF1                                      40001700
      CALL RMIX(XMR1,TG1)                                              40001800
   45 CONTINUE                                                         40001890
      TG=(WG*TG+(WG1-WG)*TG1-WDOF*TDEL*(TCAT1-TCAT))/WG1               40001900
   50 WG=WG1                                                           40002000
      XMW=1.71*XMR1+2.3                                                40002100
      RG=1545.*12./XMW                                                 40002200
      PG=WG*RG*TG/VOL                                                  40002300
  100 DG=WG/VOL                                                        40002400
      RETURN                                                           40002500
      END                                                              40002600
```

THE FOLLOWING IS A LISTING OF THE INPUT DECK DECK 14

```
      SUBROUTINE GSHELX(X,TDEL,WG,TGJ,WDG,TG,TWL,TWG,R,C,VOL,PG)          60000100
      CP=4.9/5.                                                           60000200
      IF(WG+WDG)50,50,10                                                  60000255
   10 TGO=(WG*TGJ+WDG*TDEL*TG)/(WG+WDG*TDEL)                              60000300
      WG=WG+WDG*TDEL                                                      60000400
      WGL=X*WG                                                            60000500
      WGG=WG-WGL                                                          60000600
   20 DO 40 I=1,10                                                        60000700
      QL=X * (TGO-TWL)/R                                                  60000800
      QG=(1.-X) * (TGO-TWG)/R                                             60000900
      IF(X)25,25,30                                                       60000950
   25 TWLO=C.                                                             60000960
      GO TO 35                                                            60000970
   30 TWL=TWL+(QL/(X * C))*TDEL/10.                                       60001000
   35 TWG=TWG+(QG/((1.-X)*C))*TDEL/10.                                    60001100
      TGO=TGO-((QL+QG)/((WGL+WGG)*CP))*TDEL/10.                           60001200
   40 CONTINUE                                                            60001400
      TW=X*TWL+(1.-X)*TWG                                                 60001420
      IF(TW-TG)44,44,46                                                   60001425
   44 TGO=MAX1F(TW,TGO)                                                   60001430
      GO TO 50                                                            60001435
   46 TGO=MAX1F(TG,TGO)                                                   60001440
   50 CONTINUE                                                            60001450
      PG=WG*3700.*TGO/VOL                                                 60001500
      RETURN                                                              60001600
      END                                                                 60001700
```

THE FOLLOWING IS A LISTING OF THE INPUT DECK DECK 17

```
      SUBROUTINE GMIX(TDEL,W0,WF,WD0,WDF,T0,TF,TMIX,PMIX,XMR,VOL,DMIX)   11000100
      W01=W0                                                             11000200
      WF1=WF                                                             11000300
      W0=W01+WD0*TDEL                                                    11000400
      WF=WF1+WDF*TDEL                                                    11000500
      TMIX =(WD0*.24*T0+WDF*2.9*TF)*TDEL/(W0*.24+WF*2.9)                 11000600
      PMIX=(W0/32.+WF/2.)*18540.*TMIX/VOL                                11000700
      XMR=W0/WF                                                          11000800
      DMIX=(W0+WF)/VOL                                                   11000900
      RETURN                                                             11001000
      END                                                                11001100
```

THE FOLLOWING IS A LISTING OF THE INPUT DECK DECK 6

```
      SUBROUTINE HEX(SIG,TDEL,WDL,RG,PG,TW,TL,TG,RHOG,WG,C)          21000100
      IF(SIG)10,10,20                                                21000200
C     OXIDIZER                                                       21000300
   10 CP=.24                                                         21000400
      R=48.25*12.                                                    21000500
      VOL=29.                                                        21000600
      Z=.927                                                         21000700
      T1=163.                                                        21000710
      GO TO 30                                                       21000800
C     FUEL                                                           21000900
   20 CP=2.9                                                         21001000
      R=767.*12.                                                     21001100
      VOL=38.                                                        21001200
      Z=.95                                                          21001300
      T1=37.                                                         21001310
   30 WDL=MAX1F(0.,WDL)                                              21001350
   60 TG=(WG*TG+WDL*TDEL*TL)/(WG+WDL*TDEL)                           21001400
      Q=(TW-TG)/RG                                                   21001500
      WG=WDL*TDEL+WG                                                 21001600
      TG=(Q/(CP*WG))*TDEL+TG                                         21001700
      TG=MAX1F(T1,TG)                                                21001710
      PG=Z*WG*R*TG/VOL                                               21001800
      RHOG=WG/VOL                                                    21001900
      QR=.C49                                                        21001950
      TW=-(Q+QR*(TW/1870.)**4)*TDEL/C+TW                             21002000
      TW=MAX1F(0.,TW)                                                21002100
      RETURN                                                         21002200
      END                                                            21002300
```

THE FOLLOWING IS A LISTING OF THE INPUT DECK DECK 1

```
      SUBROUTINE OPEN(N,AV,TDEL,TVC,AVX)                              81000100
C                N-POS,OPEN    N=0,NEG,CLOSE                        81000150
      IF(N)10,10,20                                                   81000200
   10 AV=AV-(TDEL/TVC)*AVX                                            81000300
      AV=MAX1F(0.,AV)                                                 81000400
      GO TO 40                                                        81000500
   20 AV=AV+(TDEL/TVC)*AVX                                            81000600
      AV=MIN1F(AV,AVX)                                                81000700
   40 CONTINUE                                                        81000800
      RETURN                                                          81000900
      END                                                             81001000
```

```
      SUBROUTINE QCAT(NCAT,TG,TC1,TC2,TC3,TC4,TC5,TC,C,WDOT,TDEL,Q,RC,P1 34000010
     1,P2,P3,P4,P5,PC,RHO)                                               34000011
      IF(NCAT)4,4,20                                                     34000020
C                 GRADIENT IS ALWAYS TC3IS GT TC2 IS GT TC1              34000021
    4 IF(TC4-TC3)6,8,8                                                   34000024
    6 DELT=TC3-TG                                                        34000028
      GO TO 14                                                           34000032
    8 IF(TC5-TC4)10,12,12                                                34000036
   10 DELT=TC4-TG                                                        34000040
      GO TO 14                                                           34000044
   12 DELT=TC5-TG                                                        34000048
   14 XN1=(TC1-TG)/DELT                                                  34000052
      XN2=(TC2-TC1)/DELT                                                 34000056
      XN3=(TC3-TC2)/DELT                                                 34000060
      XN4=(TC4-TC3)/DELT                                                 34000064
      XN5=(TC5-TC4)/DELT                                                 34000068
      NRC=0                                                              34000070
      NCAT=1                                                             34000080
      GO TO 1000                                                         34000090
   20 IF(RC)30,30,40                                                     34000094
   30 TC=TG                                                              34000098
      TCG=0.                                                             34000102
      T4=TG                                                              34000103
      T5=TG                                                              34000104
      GO TO 50                                                           34000106
   40 CALL RMIX(RC,TC)                                                   34000110
      TCG=TC-TG                                                          34000111
      NRC=NRC+1                                                          34000112
      IF(NRC-1)50,45,50                                                  34000113
   45 T4=TC4                                                             34000114
      T5=TC5                                                             34000115
   50 TG1=TG+XN1*TCG                                                     34000116
      TG2=TC1+XN2*TCG                                                    34000120
      TG3=TC2+XN3*TCG                                                    34000130
      TG4=TC3+XN4*TCG                                                    34000140
      TG5=TC4+XN5*TCG                                                    34000150
      CP=(RC*.24 + 2.9)/(RC +1.)                                         34000154
      CC=C/CP                                                            34000155
      IF(WDOT)70,70,60                                                   34000157
```

```
   60 CONTINUE                                                          34000158
      CW=CC/(WDOT*TDEL*5.)+1.                                           34000160
C     CC=CAT HEAT CAPACITY/GAS SPECIFIC HEAT(SOME AV VALUE FOR BOTH)    34000161
      TC1=TC1+(TG1-TC1)/CW                                              34000170
      TC2=TC2+(TG2-TC2)/CW                                              34000180
      TC3=TC3+(TG3-TC3)/CW                                              34000190
      TC4=TC4+(TG4-TC4)/CW                                              34000200
      TC4=MAX1F(T4,TC4)                                                 34000201
      TC5=TC5+(TG5-TC5)/CW                                              34000210
      TC5=MAX1F(T5,TC5)                                                 34000211
   70 CONTINUE                                                          34000215
      Q=WDOT*(TC-TC5)*CP                                                34000220
      XMW=(RC+1.)/(RC/32.+.5)                                           34000300
      RR=1545.*12./XMW                                                  34000310
      RHO1=(P1+P2)/(RR*(TG1+TC1))                                       34000320
      RHO2=(P2+P3)/(RR*(TG2+TC2))                                       34000330
      RHO3=(P3+P4)/(RR*(TG3+TC3))                                       34000340
      RHO4=(P4+P5)/(RR*(TG4+TC4))                                       34000350
      RHO5=(P5+PC)/(RR*(TG5+TC5))                                       34000360
      RHO=(RHO1+RHO2+RHO3+RHO4+RHO5)/5.                                 34000370
      DP1=1./RHO1                                                       34000375
      DP2=1./RHO2                                                       34000380
      DP3=1./RHO3                                                       34000390
      DP4=1./RHO4                                                       34000400
      DP5=1./RHO5                                                       34000410
      DPRAT=(P1-PC)/(DP1+DP2+DP3+DP4+DP5)                               34000420
      P2=P1-DP1*DPRAT                                                   34000430
      P3=P2-DP2*DPRAT                                                   34000440
      P4=P3-DP3*DPRAT                                                   34000450
      P5=P4-DP4*DPRAT                                                   34000460
      IF(NRC)1000,1000,900                                              34000500
  900 RC=MAX1F(RC,.000001)                                              34000502
 1000 CONTINUE                                                          34000600
      RETURN                                                            34000610
      END(1,0,0,0,0,0,1,0,0,1,0,0,0,0,0)
```

The following program subroutines for data input and output are utilized in the simulation model. These subroutines are part of the Rocketdyne computer library and may not be compatible with all computer installations. The functions of each subroutine are defined.

SUBROUTINE SCPLTV

This program subroutine receives arrays of data and produces graphical output via a cathode ray tube/camera. The input variables to the subroutine are: the number of points to be plotted, the abscissa, the ordinates, and certain control parameters.

SUBROUTINE LINPTV

This program subroutine is subordinated to SCPLTV and is used to specify the manner in which the data points are to be connected, i.e., solid line, dotted line, etc.

SUBROUTINE DRWR

This subroutine provides for the reading in of data and the printing out of the same data for reference purposes. A unique feature of this subroutine is its ability to handle multiple input cases. For subsequent cases, only those input variables being changed need to be inputed.

CONTRACTUAL DISTRIBUTION

RECIPIENT	COPIES
NASA - Lewis Research Center 21000 Brookpark Road Cleveland, Ohio 44135	
Attn: Contracting Officer, MS 500-210	1
Liquid Rocket Technology Branch MS 500-209	12
Technical Report Control Office, MS 5-5	1
Technology Utilization Office, MS 3-16	1
AFSC Liaison Office, MS 4-1	2
Library	2
Office of Reliability & Quality Assurance, MS 500-203	1
E. W. Conrad, MS 500-1	1
D. L. Nored, MS 500-209	1
NASA Headquarters Washington, D. C. 20546	
Attn: Code MT	1
RPX	4
RPL	2
SV	1
Scientific and Technical Information Facility P. O. Box 33 College Park, Maryland 20740	
Attn: NASA Representative Code CRT	6
NASA - Ames Research Center Moffett Field, California 94035	
Attn: Library	1
C. A. Syvertson	1
Leonard Roberts, Code MAD	1
NASA - Flight Research Center P. O. Box 273 Edwards, California 93523	
Attn: Library	1

RECIPIENT	COPIES
NASA - Goddard Space Flight Center Greenbelt, Maryland 20771 Attn: Library	1
NASA - Kennedy Space Center Kennedy Space Center, Florida 32899 Attn: Library	1
NASA - Langley Research Center Langley Station Hampton, Virginia 23365 Attn: Library John M. Riebe	1 1
NASA - Manned Spacecraft Center Houston, Texas 77001 Attn: Library Norman H. Chaffee, Code PPD	1 1
NASA - George C. Marshall Space Flight Center Huntsville, Alabama 35812 Attn: Library Keith Chandler, R-P&VE-PA Keith Coates, R-P&VE-PAS	1 1 1
NASA - Western Support Office 150 Pico Boulevard Santa Monica, California 90406 Attn: Library	1
Jet Propulsion Laboratory 4800 Oak Grove Drive Pasadena, California 91103 Attn: Library Dave Evans, Liquid Propulsion	1 1
Office of the Director of Defense Research & Engineering Washington, D. C. 20301 Attn: Dr. H. W. Schulz, Office of Asst. Dir. (Chem. Technology)	1
Defense Documentation Center Cameron Station Alexandria, Virginia 22314	1

RECIPIENT	COPIES
RTD (RTNP) Bolling Air Force Base Washington, D. C. 20332	1
Arnold Engineering Development Center Air Force Systems Command Tullahoma, Tennessee 37389 Attn: AEOIM	1
Advanced Research Projects Agency Washington, D. C. 20525 Attn: D. E. Mock	1
Aeronautical Systems Division Air Force Systems Command Wright-Patterson Air Force Base Dayton, Ohio Attn: D. L. Schmidt, Code ASRCNC-2	1
Air Force Systems Command (SCLT/ Capt. S. W. Bowen) Andrews Air Force Base Washington, D. C. 20332	1 1
Air Force Rocket Propulsion Laboratory (RPR) Edwards, California 93523 Attn: K. Rimer	1 1
Air Force Rocket Propulsion Laboratory (RPM) Edwards, California 93523	1
Air Force Office of Scientific Research Washington, D. C. 30333 Attn: SREP, Dr. J. F. Masi	1
U. S. Air Force Washington 25, D. C. Attn: Col. C. K. Stambaugh, Code AFRST	1
U. S. Army Missile Command Redstone Scientific Information Center Redstone Arsenal, Alabama 35808 Attn: Chief, Document Section Dr. W. Wharton	1 1

RECIPIENT	COPIES
Air Force Aero Propulsion Laboratory Research and Technology Division Air Force Systems Command United States Air Force Wright-Patterson AFB, Ohio 45433 Attn: APRP (C. M. Donaldson)	1
Aerojet-General Corporation P. O. Box 296 Azusa, California 91703 Attn: Librarian	1
Aerojet-General Corporation 11711 South Woodruff Avenue Downey, California 90241 Attn: F. M. West, Chief Librarian	1
Aerojet-General Corporation P. O. Box 1947 Sacramento, California 95809 Attn: Technical Library 2484-2015A Dr. C. M. Beighley D. T. Bedsole	1 1 1
Aeronutronic Division of Philco Corporation Ford Road Newport Beach, California 92600 Attn: Dr. L. H. Linder, Manager D. A. Carrison Technical Information Department	1 1 1
Aerospace Corporation P. O. Box 95085 Los Angeles, California 90045 Attn: J. G. Wilder, MS-2293 Library-Documents	1 1
Arthur D. Little, Inc. Acorn Park Cambridge 40, Massachusetts Attn: A. C. Tobey	1

RECIPIENT	COPIES
Astropower, Incorporated Subs. of Douglas Aircraft Company 2968 Randolph Avenue Costa Mesa, California Attn: Dr. George Moc Director, Research	1
Astrosystems, Incorporated 1275 Bloomfield Avenue Caldwell Township, New Jersey Attn: A. Mendenhall	1
ARO, Incorporated Arnold Engineering Development Center Arnold AF Station, Tennessee 37389 Attn: Dr. B. H. Goethert Chief Scientist	1
Atlantic Research Corporation Shirley Highway & Edsall Road Alexandria, Virginia 22314 Attn: A. Scurlock Security Office for Library	1 1
Battelle Memorial Institute 505 King Avenue Columbus, Ohio 43201 Attn: Report Library, Room 6A	1
Beech Aircraft Corporation Boulder Facility Box 631 Boulder, Colorado Attn: J. H. Rodgers	1
Bell Aerosystems, Inc. Box 1 Buffalo, New York 14205 Attn: T. Reinhardt W. M. Smith F. R. Herud	1 1 2

RECIPIENT	COPIES
Bendix Systems Division Bendix Corporation Ann Arbor, Michigan Attn: John M. Bureger	1
The Boeing Company Aero Space Division P. O. Box 3707 Seattle, Washington 98124 Attn: Ruth E. Peerenboom (1190) J. . Alexander	1 1
Chemical Propulsion Information Agency Applied Physics Laboratory 8621 Georgia Avenue Silver Spring, Maryland 20910	1
Chrysler Corporation Missile Division Warren, Michigan Attn: John Gates	1
Chrysler Corporation Space Division New Orleans, Louisiania Attn: Librarian	1
Curtiss-Wright Corporation Wright Aeronautical Division Woodridge, New Jersey Attn: G. Kelley	1
Engelhard Industries 113 Astor Street Newark, New Jersey 07114 Attn: Tech. Librarian	1
Douglas Aircraft Company, Inc. Santa Monica Division 3000 Ocean Park Blvd., Santa Monica, California 90405 Attn: J. L. Waisman R. W. Hallet G. W. Burge	1 1 1

RECIPIENT	COPIES
Fairchild Stratos Corporation Aircraft Missiles Division Hagerstown, Maryland Attn: J. S. Kerr	1
General Dynamics/Astronautics P. O. Box 1128 San Diego, California 92112 Attn: F. Dore Library & Information Services (128-00)	1 1
Convair Division General Dynamics Corporation P. O. Box 1128 San Diego, California 92112 Attn: Mr. W. Fenning Centaur Resident Project Office	1
General Electric Company Re-Entry Systems Department P. O. Box 8555 Philadelphia, Pennsylvania 19101 Attn: F. E. Schultz Dr. E. S. Gantz	1 1
General Electric Company Flight Propulsion Lab. Department Cincinnati 15, Ohio Attn: D. Suichu	1
Grumman Aircraft Engineering Corporation Bethpage, Long Island, New York Attn: Joseph Gavin	1
Hughes Aircraft Company Aerospace Group 1950 East Imperial Highway El Segundo, California 90009 Attn: D. D. Newman	1

RECIPIENT	COPIES
Kidde Aero-Space Division Walter Kidde & Company, Inc. 675 Main Street Belleville 9, New Jersey Attn: R. J. Hanville, Director of Research Engineering	1
Lockheed Missiles & Space Company P. O. Box 504 Sunnyvale, California Attn: Y. C. Lee, Power Systems R&D Technical Information Center	1 1
Lockheed Propulsion Company P. O. Box 111 Redlands, California 92374 Attn: Miss Belle Berlad, Librarian H L. Thackwell	 1 1
Lockheed Missiles & Space Company Propulsion Engineering Division (D.55-11) 1111 Lockheed Way Sunnyvale, California 94087	1
Marquardt Corporation 16555 Saticoy Street Box 2013 - South Annex Van Nuys, California 91404 Attn: Librarian W. H. Lien, Advanced Systems	 1 2
Martin-Marietta Corporation Martin Division Baltimore 3, Maryland Attn: John Calathes (3214)	 1
McDonnell Aircraft Corporation P. O. Box 6101 Lambert Field, Missouri Attn: R. A. Herzmark F. D. McVey	 1 1

RECIPIENT	COPIES
North American Aviation, Inc. Space & Information Systems Division 12214 Lakewood Boulevard Downey, California 90242	
Attn: Technical Information Center, D/096-722 (AJ01)	1
H. Storms	1
Northrop Space Laboratories 1001 East Broadway Hawthorne, California	
Attn: Dr. William Howard	1
Radio Corporation of America Astro-Electornics Division Defense Electronic Products Princeton, New Jersey	
Attn: S. Fairweather	1
Republic Aviation Corporation Farmingdale, Long Island, New York	
Attn: Dr. Wm. O'Donnell	1
Rocket Research Corporation 520 South Portland Street Seattle, Washington 98108	
Attn: M. E. Maes	1
Rocketdyne, Division of North American Aviation, Inc. 6633 Canoga Avenue Canoga Park, California 91304	
Attn: Library, Department 496-306	1
Space-General Corporation 777 Flower Street Glendale, California	
Attn: C. E. Roth	1
Sunstrand-Denver Division of Sundstrand Corporation 2480 West 70th Avenue Denver, Colorado 80221	
Attn: R. N. Bailey	1

RECIPIENT	COPIES
Thiokol Chemical Corporation Reaction Motors Division Denville, New Jersey 07834	
Attn: A. Sherman	1
Librarian	1
TRW Systems, Incorporated One Space Park Redondo Beach, California 90200	
Attn: G. W. Elverum	1
STL Tech. Lib. Doc. Acquisitions	1
D. H. Lee	2
TRW, Incorporated TAPCO Division 23555 Euclid Avenue Cleveland, Ohio	
Attn: P. T. Angell	1
United Aircraft Corporation Corporation Library 400 Main Street East Hartford, Connecticut 06118	
Attn: Dr. David Rix	1
Erle Martin	1
United Aircraft Corporation Pratt and Whitney Aircraft Division Florida Research and Development Center Post Office Box 2691 West Palm Beach, Florida 33402	
Attn: R. J. Coar	1
Librarian	1
United Aircraft Corporation United Technology Center Post Office Box 358 Sunnyvale, California 94088	
Attn: Librarian	1

RECIPIENT	COPIES
United Aircraft Corporation Hamilton Standard Division Winsor Locks, Connecticut Attn: M. Marcus	1
Vought Astronautics Post Office Box 5907 Dallas 22, Texas Attn: Warren C. Trent	1
TRW Systems Group Technical Information One Space Park Redondo Beach, California 90278 Attn: Acquisitions	1

NOMENCLATURE

A	-	area, foot^2 or inch^2
C_F	-	thrust coefficient
C_o	-	discharge coefficient
D	-	diameter, feet
E	-	activation energy, BTU/pound nole
G_o	-	superficial mass flux, pound/feet^2-sec
I_{sp}	-	specific impulse, seconds
K	-	ratio of specific heats
K	-	constant
L	-	inertance, second^2/inch^2
L	-	length, feet
Lp	-	length of poppet travel, feet
L*	-	characteristic length, inch
M	-	mass, pound
M	-	molecular weight, pound/pound mole
M	-	momentum flux, foot-pound/second^2
MR	-	mixture ratio (O/F)
Nu	-	Nusselt number
Ns	-	number of components of type x
P	-	pressure, pounds/inch^2
Pr	-	Prandtl number
Px	-	probability of failure in component type x
R	-	gas constant
R	-	effective flow resistance, second^2/inch^2 pound
R	-	gas constant, BTU/pound mole - R
R	-	reliability index
Re	-	Reynolds number
S	-	poppet travel distance, inches
T	-	temperature, R
Te	-	valve temperature, R

U	-	overall heat transfer coefficient, BTU/inch^2-sec-R
V	-	velocity, feet/second
V	-	volume, feet^3
$\dot{W}$	-	flowrate, pound/second
X_{tt}	-	Martinelli parameter
Yo	-	orifice approach factor
a	-	specific catalyst area, feet^{-1}
a_h, a_o	-	complex time constant
c	-	specific heat, BTU/pound-R
c*	-	characteristic velocity, feet/second
f	-	friction factor
f*	-	modified friction factor
f_o	-	frequency, cycle/second
g	-	gap thickness, inch
g	-	gravitional constant, feet/second^2
h	-	heat transfer coefficient, BTU/inch^2 second-R
q	-	heat transfer rate, BTU/second
r	-	radius, inch
r_c		critical pressure ratio
t	-	thickness, inch
t	-	time, second
x	-	length, feet
x	-	quality
ΔP	-	pressure difference, pound/inch^2
ΔT_m	-	log mean temperature difference, R
θ	-	time, seconds
θ_F	-	full time, seconds
θ_p	-	poppet opening time, seconds
α	-	ratio of specific heats
α	-	chemical reactivity
ϵ	-	porosity

η - efficiency
λ - heat of vaporization, BTU/pound
μ - viscosity, pound/feet-second
ρ - density, pound/feet^3
τ - time constant, second
ψ - sphericity

REFERENCES

1. Franciscus, L. D. and E. A. Lezberg, "Effects of Exhaust Nozzle Recombination on Hypersonic Ramjet Performance: Part II--Analytical Investigation, " AIAA Journal, Vol. 1, No. 9, 2077, September 1961.

2. CR-54657, Investigation of Catalytic Ignition of Oxygen/Hydrogen Systems, R. W. Roberts, H. L. Burge, and M. Ladacki, NASA, December 1965.

3. CR-54086, Investigation of Catalytic Ignition of Oxygen/Hydrogen Systems, R. Roberts, NASA, September 1965.

4. Megdal, D. and R. Kosson, "Shock Predictions in Conical Nozzles," AIAA Journal, Vol. 3, No. 8, 1554, August 1965.

5. NAS7-136-F, Volume 2, Study of High Effective Area Ratio Nozzles for Spacecraft Engines, Aerojet-General Corp., Sacramento, Calif., June 1964.

6. TR-65-107, Performance Characteristics of Compound A/Hydrazine Propellant Combination, Volume I, prepared under Contract No. AF04(611)-9573 by Rocketdyne, a Division of North American Aviation, Inc., Canoga Park, California, May 1965, CONFIDENTIAL.

7. Arbit, H. A. and S. D. Clapp, Development of Injector Design Criteria Applicable to the Lance Missile Booster Engine: Unlike-Impinging Doublet Injectors, RR64-51, Rocketdyne, a Division of North American Aviation, Inc., Canoga Park, California, November 1965, CONFIDENTIAL.

8. Clapp, S. D. and G. W. Cawood, Development of Injector Design Criteria Applicable to the Booster and Sustainer Engines of the Lance Missile, RR63-40, Rocketdyne, a Division of North American Aviation, Inc., Canoga Park, California, December 1963.

9. TR-66-152, Study of Droplet Effects on Steady-State Combustion, Volume I--Measured Spray Parameter Analysis and Performance Correlation, by Rocketdyne, a Division of North American Aviation, Inc., Canoga Park, California, January 1966.

10. Rupe, J. H., "A Correlation Between the Dynamic Properties of a Pair of Impinging Streams and the Uniformity of Mixture Ratio Distribution in the Resulting Spray," JPL Progress Report No. 20-209, March 1956.

11. Elverum, G. W. and T. F. Morley, "Criteria for Optimum Mixture Ratio Distribution Using Several Types of Impinging Stream Injector Elements," JPL Memo No. 30-5, February 1965.

12. Rupe, J. H., "The Liquid-Phase Mixing of a Pair of Impinging Streams," JPL Progress Report No. 20-195, August 1953.

13. Roberts, R. W., Hydrogen-Oxygen Catalytic Ignition Studies for Application in the J-2 Engine, Rocketdyne Research Report No. 64-2, Rocketdyne, A Division of North American Aviation, Inc., Canoga Park, California, January 1964.

14. Bendersky, C., Hydrogen/Oxygen Catalytic Ignition, Rocketdyne Research Report No. 63-9, Rocketdyne, a Division of North American Aviation, Inc., Canoga Park, California, January 1963.

15. CR-72118, Development of Hydrogen/Oxygen Catalysts," T. J. Jennings, W. E. Armstrong, and H. H. Voge, Shell Development Co., Emeryville, California, July 1966.

16. Hilario, M. and R. Roberts, An Investigation of Catalytically-Ignited Oxygen/Hydrogen Attitude Control Engines, Rocketdyne Research Report No. 64-61, Rocketdyne, a Division of North American Aviation, Inc., Canoga Park, California.

17. Elliott, D. G., D. R. Bartz, and S. Silver, Calculation of Turbulent Boundary-Layer Growth and Heat Transfer in Axi-Symmetric Nozzles, Jet Propulsion Laboratory Report No. 32-387, Pasadena, California, February 1963.

18. Bailey, R. N., "Development of Catalytic Hydrogen-Oxygen Reaction Chambers for Space Power Systems," American Rocket Society Paper No. 2516-62.

19. McAdams, W. H., Heat Transmission, McGraw-Hill Book Company, Inc., New York, 1954.

20. Hendricks, R. C., R. W. Graham, Y. Y. Hsu, and A. A. Mederos, "Correlation of Hydrogen Heat Transfer in Boiling and Supercritical Pressure Stages," ARS Journal, February 1962.

21. Graham, R. W., R. C. Hendricks, Y. Y. Hau, and R. Fredrison, Experimental Heat Transfer and Pressure Drop of Film Boiling Liquid Hydrogen Flowing Through a Heated Tube, presented at the 1960 Cryogenic Engineering Conference, Boulder, Colorado, August 1960.

22. Grimson, E. D., ASME Transactions, No. 59, 583-594 (1937) and No. 60, 381-391 (1938).

23. Hunter, B. J., J. E. Bell, and J. E. Penner, "Expulsion Bladders for Cryogenic Fluids," Adv. in Cryogenic Engineering, 7 (1961).

24. Pope, D. H., "Expulsion Bladders for Cryogenic Liquids," Adv. in Cryogenic Engineering, 10 (1964).

25. Harnett, R. T., F. J. Sanson, and L. M. Warshowsky, "Midas- an Analog Approach to Digital Computation," Simulation, September 1964.

26. Pelchman, G. E., "An Enlarged Version of Midas," Simulation, October 1964.

27. Bell Aerosystems Company, "Feasibility Demonstration of Advanced Attitude Control Systems," AFRPL-TR-62-251, November 1965, CONFIDENTIAL.

28. Bell Aerosystems Company, "Feasibility Demonstration of Advanced Attitude Control Systems," AFRPL-TR-66-55, March 1966, CONFIDENTIAL.

Security Classification

DOCUMENT CONTROL DATA - R&D

(Security classification of title, body of abstract and indexing annotation must be entered when the overall report is classified)

1. ORIGINATING ACTIVITY (Corporate author) Rocketdyne, a Division of North American Aviation, Inc., 6633 Canoga Avenue, Canoga Park, California	2a. REPORT SECURITY CLASSIFICATION Unclassified 2b. GROUP

3. REPORT TITLE EVALUATION AND DEMONSTRATION OF THE USE OF CRYOGENIC PROPELLANTS (O_2-H_2) FOR REACTION CONTROL SYSTEMS--VOLUME I - CONCEPTUAL DESIGN AND ANALYTICAL EVALUATION

4. DESCRIPTIVE NOTES (Type of report and inclusive dates)
Final Report June 1967

5. AUTHOR(S) (Last name, first name, initial)
Falkenstein, Gary L. Grubman, Donald, Liebman, Allen, Rodewald, Newell R.

6. REPORT DATE June 1967	7a. TOTAL NO. OF PAGES 388	7b. NO. OF REFS 250
8a. CONTRACT OR GRANT NO. NAS3-7941 NAS3-7941 b. PROJECT NO. c. d.	9a. ORIGINATOR'S REPORT NUMBER(S) R-6838-1 9b. OTHER REPORT NO(S) (Any other numbers that may be assigned this report) CR-72176	

10. AVAILABILITY/LIMITATION NOTICES

11. SUPPLEMENTARY NOTES	12. SPONSORING MILITARY ACTIVITY

13. ABSTRACT

The results and evaluations of an investigation of the feasibility of a cryogenic (O_2-H_2) reaction control system are presented. This volume presents the analytical, conceptual design, and system analysis results from the program. Possible applications of such a reaction control system include propellant settling engines, attitude control, and secondary propulsion for upper stages, spacecraft, and orbital tankers. Two types of systems representative of a system integrated with the tankage for a pump-fed main propulsion system (chamber pressure of 10 psia) and a system fed from separate tankage (chamber pressure of 100 psia) were investigated. Candidate system design concepts were evaluated from the standpoints of weight, volume, reliability, technical state-of-the-art, etc., and one concept selected for further investigation. Experimental evaluation of the system is reported in Volume II of this report.

DD FORM 1 JAN 64 1473

Security Classification

14. KEY WORDS	LINK A		LINK B		LINK C	
	ROLE	WT	ROLE	WT	ROLE	WT
reaction control system						
catalytic ignition						
oxygen						
hydrogen						
cryogenic propellants						
cryogenic reaction control system						

INSTRUCTIONS

1. **ORIGINATING ACTIVITY:** Enter the name and address of the contractor, subcontractor, grantee, Department of Defense activity or other organization *(corporate author)* issuing the report.

2a. **REPORT SECURITY CLASSIFICATION:** Enter the overall security classification of the report. Indicate whether "Restricted Data" is included. Marking is to be in accordance with appropriate security regulations.

2b. **GROUP:** Automatic downgrading is specified in DoD Directive 5200.10 and Armed Forces Industrial Manual. Enter the group number. Also, when applicable, show that optional markings have been used for Group 3 and Group 4 as authorized.

3. **REPORT TITLE:** Enter the complete report title in all capital letters. Titles in all cases should be unclassified. If a meaningful title cannot be selected without classification, show title classification in all capitals in parenthesis immediately following the title.

4. **DESCRIPTIVE NOTES:** If appropriate, enter the type of report, e.g., interim, progress, summary, annual, or final. Give the inclusive dates when a specific reporting period is covered.

5. **AUTHOR(S):** Enter the name(s) of author(s) as shown on or in the report. Enter last name, first name, middle initial. If military, show rank and branch of service. The name of the principal author is an absolute minimum requirement.

6. **REPORT DATE:** Enter the date of the report as day, month, year; or month, year. If more than one date appears on the report, use date of publication.

7a. **TOTAL NUMBER OF PAGES:** The total page count should follow normal pagination procedures, i.e., enter the number of pages containing information.

7b. **NUMBER OF REFERENCES:** Enter the total number of references cited in the report.

8a. **CONTRACT OR GRANT NUMBER:** If appropriate, enter the applicable number of the contract or grant under which the report was written.

8b, 8c, & 8d. **PROJECT NUMBER:** Enter the appropriate military department identification, such as project number, subproject number, system numbers, task number, etc.

9a. **ORIGINATOR'S REPORT NUMBER(S):** Enter the official report number by which the document will be identified and controlled by the originating activity. This number must be unique to this report.

9b. **OTHER REPORT NUMBER(S):** If the report has been assigned any other report numbers *(either by the originator or by the sponsor)*, also enter this number(s).

10. **AVAILABILITY/LIMITATION NOTICES:** Enter any limitations on further dissemination of the report, other than those imposed by security classification, using standard statements such as:

(1) "Qualified requesters may obtain copies of this report from DDC."

(2) "Foreign announcement and dissemination of this report by DDC is not authorized."

(3) "U. S. Government agencies may obtain copies of this report directly from DDC. Other qualified DDC users shall request through

_____."

(4) "U. S. military agencies may obtain copies of this report directly from DDC. Other qualified users shall request through

_____."

(5) "All distribution of this report is controlled. Qualified DDC users shall request through

_____."

If the report has been furnished to the Office of Technical Services, Department of Commerce, for sale to the public, indicate this fact and enter the price, if known.

11. **SUPPLEMENTARY NOTES:** Use for additional explanatory notes.

12. **SPONSORING MILITARY ACTIVITY:** Enter the name of the departmental project office or laboratory sponsoring *(paying for)* the research and development. Include address.

13. **ABSTRACT:** Enter an abstract giving a brief and factual summary of the document indicative of the report, even though it may also appear elsewhere in the body of the technical report. If additional space is required, a continuation sheet shall be attached.

It is highly desirable that the abstract of classified reports be unclassified. Each paragraph of the abstract shall end with an indication of the military security classification of the information in the paragraph, represented as *(TS)*, *(S)*, *(C)*, or *(U)*.

There is no limitation on the length of the abstract. However, the suggested length is from 150 to 225 words.

14. **KEY WORDS:** Key words are technically meaningful terms or short phrases that characterize a report and may be used as index entries for cataloging the report. Key words must be selected so that no security classification is required. Identifiers, such as equipment model designation, trade name, military project code name, geographic location, may be used as key words but will be followed by an indication of technical context. The assignment of links, rules, and weights is optional.